Flight Testing of Advanced RNP to ILS Autoland with DLR's A320 Test Aircraft

Flugversuche zu erweiterten automatischen Landungen mittels RNP auf ILS mit dem A320-Testflugzeug des DLR

Tobias Blase

IB-Nummer 112-2015/33
Zugänglichkeitsstufe A/I

DLR Institut für Flugführung

Dokumenteigenschaften

Titel	Flight Testing of Advanced RNP to ILS Autoland with DLR's A320 Test Aircraft Flugversuche zu erweiterten automatischen Landungen mittels RNP auf ILS mit dem A320-Testflugzeug des DLR
Betreff	The following report was created during the master thesis of Mr. Tobias Blase at the Institute of Flight Guidance at the DLR. Der folgende Bericht entstand im Rahmen der Masterarbeit von Herrn Tobias Blase am Institut für Flugführung des DLR.
Autor	Tobias Blase
Betreuer	Thomas Dautermann Thomas Ludwig
Institut	Institute of Flight Guidance / Institut für Flugführung
Zugänglichkeitsstufe	A/I
Speicherdatum	13. Oktober 2015
Version	1.0
Freigabe	Die Freigabe erfolgt im gesonderten Freigabeprozess

Kurzfassung

Diese Arbeit behandelt die Betriebseigenschaften des DLR-Testflugzeugs A320-ATRA während Flugversuchen zu experimentellen RNP to ILS-Anflügen auf den Flughafen Braunschweig-Wolfsburg. Der Zweck dieser Flugversuchskampagne war es, die Durchführbarkeit von erweiterten Prozeduren mit automatischer Landung zu demonstrieren, die eine Kurve mit konstantem Radius auf einen ILS-Präzisionsendanflug mit Längen zwischen einer und fünf nautischen Meilen beinhalten. Ermöglicht durch Flächennavigationssysteme basierend auf Satellitennavigation, erlauben diese Prozeduren die Einbeziehung von Kurven mit einem vorhersagbaren Flugweg über Grund in die Anflugphase und somit die Konstruktion von flexibleren Routen in Gegenden mit hohem Verkehrsaufkommen oder schwierigem Terrain. Weiterhin können aufgrund kürzerer Anflugwege und der Möglichkeit, lärmempfindliche Gebiete zu umfliegen, umweltfreundlichere Prozeduren geschaffen werden.

Während der Flugversuche wurden drei Interessenschwerpunkte untersucht: Die Leistung des ATRA bei automatischen Landungen wurde in Anflügen mit unterschiedlichen Längen des Endanflugs ausgewertet, um eine Mindestlänge für die Selbstlandefähigkeit des Testflugzeugs zu ermitteln. Darüber hinaus wurde der vom Flugmanagementsystem generierte vertikale Flugweg hinsichtlich seiner Übereinstimmung mit dem beabsichtigten Flugweg für einen schnellen Übergang zum ILS am Ende der Kurve vor dem Endanflug bewertet. Zusätzlich wurde das Einhalten des lateralen Flugwegs während des Übergangs zum Landekurssender auf ein Verlassen des RNP-Korridors untersucht.

Die Ergebnisse der Flugversuche zeigen, dass es in allen experimentellen Anflügen unabhängig von der Länge des Endanflugs möglich ist, eine automatische Landung durchzuführen. Die laterale Navigationsleistung ist ausreichend für Verfahren mit hohen Anforderung wie RNP 0.1, auch wenn die Aktivierung des Anflugmodus zu größeren Abweichungen führen kann, sobald das Flugzeug in den Empfangsbereich des Landekurssenders einfliegt. Während der Flugversuche wurde außerdem festgestellt, dass RNP to ILS-Anflüge mit einem vertikalen Bahnwinkel kodiert werden sollten, um einen frühzeitigen Sinkflug zu verhindern. Auch wenn Anflüge ohne einen vertikalen Bahnwinkel ebenfalls erfolgreich waren, führten sie zu einem unerwünschten Horizontalflug, der die Vorteile hinsichtlich Lärmbelastung und Treibstoffverbrauch reduziert oder sogar aufhebt. Dennoch ist es bei Berücksichtigung der Ergebnisse dieser Flugversuchskampagne möglich, sichere RNP to ILS-Anflüge zu fliegen und dabei die Vorteile dieser Prozeduren aufrechtzuerhalten.

Abstract

This thesis shows the performance of DLR's test aircraft A320-ATRA during flight tests of experimental RNP to ILS approaches to Braunschweig-Wolfsburg airport. The purpose of the flight test campaign was to demonstrate the feasibility of advanced procedures including a fixed radius turn onto ILS precision final segments with lengths between one and five nautical miles for autoland operations. Enabled by precise area navigation systems based on satellite navigation, these procedures allow the inclusion of turns with a predictable ground track into the approach phase, thus allowing the construction of more flexible routes in areas with a high traffic density or difficult terrain. Furthermore, more environment-friendly procedures can be created due to shorter approach tracks and the possibility to circumnavigate areas sensitive to noise.

During the flight tests, three main areas of interest were investigated: The autoland performance of the ATRA was evaluated in approaches with varying lengths of the final approach segment in order to identify a minimum required length for the autoland capability of the test aircraft. Beyond that, the vertical path generated by the flight management system was assessed with regard to its compliance with the intended flight path for a successful transition to ILS guidance at the end of the turn before the final approach. Additionally, the lateral path following during the transition to localizer guidance was investigated for possible violations of the RNP corridor.

The results of the flight tests show that it is possible to perform an automatic landing during all experimental approaches, regardless of the length of the final approach segment. Lateral navigation is precise enough to support operations with high accuracy requirements such as RNP 0.1, although the activation of the approach mode can cause larger deviations as soon as the aircraft enters the localizer service volume. During the flight tests, it was also found that RNP to ILS approaches should be coded with a flight path angle in the navigation database in order to prevent an early descent to the ILS intercept height. Although procedures coded without a flight path angle were successful as well, an undesirable level segment was included into the approach by the flight management system, reducing or neutralizing the benefits with regard to noise pollution and fuel efficiency. However, in consideration of the findings of this flight test campaign, it is possible to safely fly RNP to ILS approaches while maintaining the advantages inherent to these procedures.

Table of Contents

Kurzfassung **4**

Abstract **5**

1. Introduction **8**
1.1. Purpose and Motivation 9
1.2. Overview 10

2. Fundamentals **11**
2.1. RNP to ILS Concept 11
2.2. RNP Navigation Error Components 13
2.3. Global Navigation Satellite Systems (GNSS) 14
2.3.1. Code Range Positioning 15
2.3.2. Carrier Phase Positioning 16
2.3.3. Differential Positioning 18
2.4. World Geodetic System 21
2.4.1. Ellipsoidal Coordinates 23
2.4.2. Cartesian Coordinates 25
2.5. ARINC 429 Avionics Data Bus Standard 25
2.6. ARINC 424 Navigation System Database Standard 29

3. Preparation of the Flight Test Campaign **34**
3.1. Objectives 34
3.2. Experimental Approaches 36
3.2.1. Structure 37
3.2.2. ARINC 424 Coding 39
3.3. Simulator Test 44
3.3.1. Findings 44
3.3.2. Consequences for Flight Test Preparation 46
3.4. Required Data 47
3.4.1. Parameter List 49

4. Execution of the Flight Tests **52**
4.1. Test Aircraft and Auto Flight System 52
4.1.1. Flight Planning and Performance Predictions 53
4.1.2. Autopilot Modes 56
4.1.3. Automatic Landing Capabilities 61
4.2. In-Flight Data Recording 62
4.3. Flight Test Procedure 63

5. Data Analysis and Results 68
5.1. Navigation Accuracy 68
5.1.1. Lateral Navigation Accuracy 71
5.1.2. Vertical Navigation Accuracy 77
5.2. ILS Intercept Performance 82
5.3. Automatic Landing Performance 84
5.4. Pilot Feedback 86

6. Conclusion 90
6.1. Conflicts with Existing Regulations and Standards 90
6.1.1. ICAO 90
6.1.2. ARINC 424 93
6.2. Summary 94
6.3. Further Work 95

7. Bibliography 97

Abbreviations 99

List of Figures 102

List of Tables 103

Appendix A – ARINC 424 Navigation Database 104

Appendix B – Lateral Trajectory and Atmospheric Conditions 121

Appendix C – Lateral and Vertical Flight Technical Error 139

Appendix D – Lateral Navigation System Error 157

Appendix E – Flight Path Angle 175

Appendix F – Localizer and Glideslope Deviations 193

1. Introduction

With the introduction of the radius to fix leg as part of the performance-based navigation concept, procedure designers obtained a means for the inclusion of turns with a predictable and repeatable ground track into the approach segments. Without the dispersion of ground tracks inherent in previous turn constructions as a result of varying speeds, bank angles and roll rates between different aircraft and flight management systems, new possibilities emerge for the creation of shorter, more flexible approach procedures. Additionally, curved segments can now be used to reliably circumnavigate populated areas in the vicinity of highly frequented airports, thus providing a relief to the direct environment of airports with regard to noise pollution.

However, approach procedures based solely on the performance-based navigation concept do not offer the possibility of automatic landings due to the lack of highly precise lateral and vertical guidance during the final approach phase. The instrument landing system is widely used for this purpose and allows approaching aircraft to manually or automatically follow ground-based radio signals that provide both lateral and vertical guidance using a complex array of antennas installed in the vicinity of the runway. As a result of the functional principle of the instrument landing system, aircraft must follow a straight approach path, which limits the flexibility of conventional approaches using this technology.

The Institute of Flight Guidance of the German Aerospace Center (DLR) investigates the potential of novel approach procedures that combine the flexibility of curved approach paths with the reliable guidance of the instrument landing system during the final approach segment. In the new concept, the initial and intermediate phases of the approach utilize the performance-based navigation concept to include curved segments into the approach in order to reduce the overall track-mileage and place the approach path in areas that are less sensitive to noise pollution. At the end of the intermediate approach segment, the straight final approach path provided by the instrument landing system is intercepted and the auto flight system of the approaching aircraft couples onto the lateral and vertical guidance signals.

Regarding the transition to the guidance signals of the instrument landing system, several requirements must be met during procedure design in order to deliver the aircraft to a position that allows a swift engagement of the corresponding autopilot guidance modes. This is crucial as

the straight final approach segment shall be as short as possible so as to maintain a high level of flexibility during procedure design and allow for shorter approach tracks. An earlier requirement analysis presented in [1] has shown that the length of the final approach segment is the critical design parameter for these approaches, as a lengthy final approach will reduce the benefits of the novel concept, whereas a final approach that is too short will not provide enough time for the engagement of the necessary autopilot modes to approaching aircraft.

Aiming to test the feasibility of several approaches with varying final approach lengths, the Institute of Flight Guidance designed a set of experimental approaches for Braunschweig-Wolfsburg airport. These approaches were tested in flight trials with the Advanced Technology Research Aircraft (ATRA), an Airbus 320 operated by the DLR, in order to gain further insight into the possibilities and restrictions of the test aircraft regarding the new approach concept.

1.1. Purpose and Motivation

The aim of this work is the analysis of the data recorded during the flight test campaign with regard to the navigation accuracy, transition to the instrument landing system and automatic landing performance of the test aircraft. To that end, the preparation and conduct of the flight tests including definition of objectives and parameters as well as data recording are also part of this work. This includes the necessary computations for the determination of the navigation errors and the creation of scripts for data analysis and visualization.

With the data gathered in the flight trails, a practical length for the final segment of approaches that combine curved segments with a transition to the instrument landing system is to be determined. Beyond that, the capability of the test aircraft to perform an automatic landing after such an approach is a key area of interest during the experiments. As part of the flight test preparation, the experimental approaches are also tested in an Airbus 320 full flight simulator equipped with the original avionics systems so as to identify possible system-related issues that need to be resolved before the actual flight tests. Additionally, feedback from the test pilots is to be obtained after the flight test campaign and implications for further standardizations by the regulating authorities are presented.

1.2. Overview

In chapter 2, a general introduction into the fundamental principles and technologies that are applied in the scope of the flight test campaign is given. This includes a summary of the RNP to ILS concept and its advantages over conventional ILS approaches as well as an explanation of the navigation error components defined in the PBN concept. Furthermore, the essential operating principles of satellite navigation systems and different methods for satellite signal measurement are described. The World Geodetic System from 1984, which serves as the underlying representation of the earth for all computations during data analysis, and its application in different coordinate systems are also discussed in this chapter. Finally, a short introduction into the ARINC standards for avionics data buses and navigation system databases is given.

Chapter 3 covers the preparation of the flight test campaign and details the objectives of the experiments with the ATRA. The experimental approaches that were designed for the flight tests and the coding of the approaches for the navigation database of the ATRA are presented as well. Beyond that, the initial tests of the experimental approaches in an Airbus 320 full flight simulator and their implications for the actual flight tests are discussed. A list and description of the parameters recorded during the flight tests concludes this chapter.

In chapter 4, the execution of the flight tests and the test aircraft are discussed. For this purpose, the ATRA and especially its auto flight system are presented in greater detail. This includes a description of the autopilot modes involved in the RNP to ILS approaches and the prerequisites for an automatic landing. The in-flight data recording and the experimental procedure during the flight test campaign are further topics of this chapter.

Methods for data analysis and the results of the flight tests with the ATRA are presented in chapter 5. Besides the navigation accuracy of the ATRA during the approaches, the ILS intercept and automatic landing performance are important aspects of the experiments. The chapter is rounded off by feedback regarding the viability of the approaches in their current form from an operational point of view.

Chapter 6 concludes this report with a discussion of the conflicts with existing regulations and standards that would need to be overcome in the future. Beyond that, an outlook at prospects for further work on the topic of RNP to ILS approaches is given.

2. Fundamentals

In the following chapter, the fundamental principles of the technologies and concepts applied during the preparation, execution and evaluation of the flight test campaign are presented. It provides basic information regarding the different topics that are revisited in later chapters of this report when they become relevant for the individual steps of the project.

2.1. RNP to ILS Concept

Required navigation performance (RNP) refers to a navigation specification that can be applied to procedures in all phases of flight. A procedure denoted as a RNP procedure is associated with a certain minimum navigation accuracy that must be provided by the navigation systems of all aircraft that wish to operate on this particular route. In addition, the navigation system must be capable of monitoring its own performance and display its actual navigation performance (ANP) to the crew. As part of the performance-based navigation (PBN) concept, RNP allows airspace users to adhere to the demanded navigation accuracy by any means available, thus simplifying the approval process for aircraft equipped with different sets of navigation sensors [1]. After the introduction of the Global Positioning System (GPS), satellite navigation has become the primary means of navigation for civil aviation as it offers high navigation accuracy and is available around the globe.

The PBN concept also offers the possibility to include curved segments defined by a fixed radius into navigation procedures, thus introducing a means of designing a precise curved ground track. Although most flight management systems (FMS) were able to create curved segments for a smooth transition between two straight segments before, the shape of these segments depends on the computing FMS and can thus vary from aircraft to aircraft. The introduction of fixed-radius turns featuring a repeatable ground track allowed for more flexible procedures and created new possibilities for procedure designers. Together with the navigation specifications RNP approach and advanced RNP that allow fixed-radius turns in the approach phase, new approach procedures with high navigation accuracy can be designed [2]. In comparison to conventional approach procedures, this results in shorter approaches with a more flexible ground track, allowing the circumnavigation of noise-sensitive areas. In addition, the reduction of track mileage leads to an improved environmental fingerprint as less fuel is required.

In order to further improve the availability of RNP approaches, the possibility of a transition to a ground-based landing aid in the final phase of the approach is envisaged [3]. As non-precision approaches, RNP approaches cannot be terminated with an automatic landing, reducing the usefulness of the approach in adverse weather conditions. By including a transition to a precision landing aid such as the Instrument Landing System (ILS) in the final part of the approach, a "hybrid" procedure is created, combining the advantages of both flexible RNP guidance and automatic landing capability provided by a precision approach [4]. Ideally, the initial and intermediate approach sections would be designed in such a way as to provide a preferably short curved approach path that avoids noise-sensitive areas before transitioning onto the straight precision final approach. Since the ILS is the most commonly used landing aid in civil aviation, an RNP to ILS approach would be the usual application of this concept, although future implementations could also include variations using a GNSS landing system (GLS).

The implementation of RNP to ILS approaches is based solely on available technologies that are already in use. Both RNP non-precision approaches and ILS precision approaches are in wide use at airports around the world. As a result, most modern flight guidance systems (FGS) are capable of flying both kinds of approach procedures automatically and are able to perform an automatic landing if a precision approach is selected which provides lateral and vertical guidance to the control loops of the respective autopilot landing modes.

However, the established methods in which FMS handle conventional RNP and ILS approaches can also cause issues when a combination of both RNP and ILS guidance is used in a single approach procedure. ILS approaches, for example, typically feature a relatively long straight final approach during which the aircraft is aligned with the runway course and established on the lateral and vertical guidance beams of the ILS. In an RNP to ILS approach, the aircraft would turn onto the final approach course much later than usual, thus significantly reducing the time available to the avionics to capture the lateral and vertical guidance beams. Moreover, the current navigation database standard does not include a combination of non-precision and precision approaches, thus requiring the complete approach to be coded as a precision approach, resulting in further implications. For more information regarding the technical difficulties encountered with RNP to ILS approaches, refer to an earlier requirement analysis [5] and section 3 of this report.

2.2. RNP Navigation Error Components

As RNP specifications require the airspace user to employ on-board performance monitoring and alerting, the total system error (TSE) must be smaller than the RNP value associated with this particular airway for the airspace user to be allowed to operate on it. The three main error sources for RNP systems are the path definition error (PDE), the flight technical error (FTE) and the navigation system error (NSE) as shown in Figure 2.1 [1].

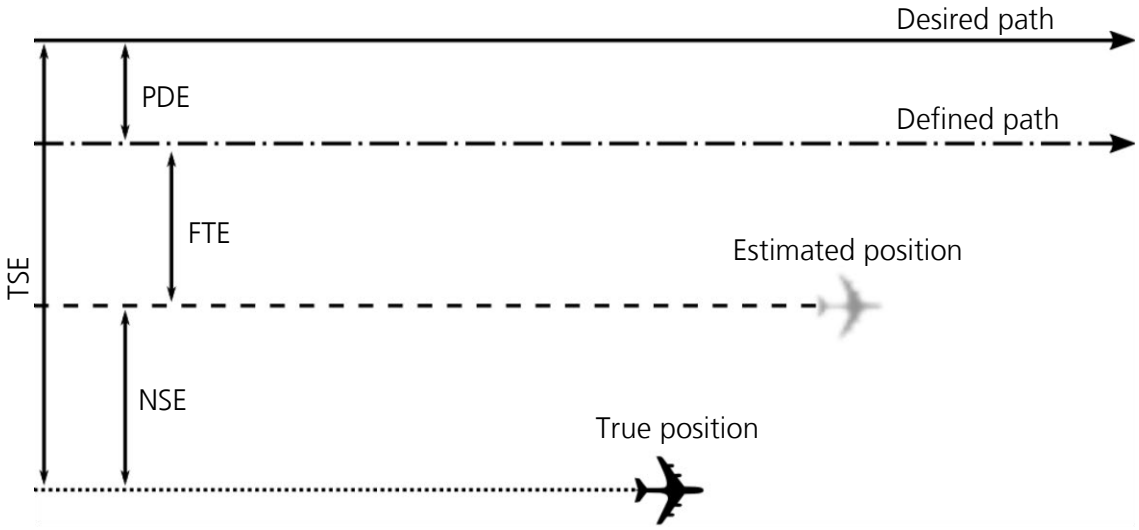

Figure 2.1: RNP navigation error components <own figure after [1]>

The three error components are defined as follows [1]:

- **PDE** is a discrepancy between the path defined in the navigation database and the path that is defined to be flown over ground by the procedure designer. The definition of a repeatable path over ground requires the utilization of a FMS with a navigation database containing unambiguously defined waypoints and path terminators. Repeatable ground tracks cannot be realized with fly-by and fly-over turns, altitude terminators or paths based on heading. Radius to fix legs or fixed radius transitions must be used for unambiguously defined turns in RNP applications, as only these turns allow the definition of a ground path and thus the determination of FTE and NSE. The WGS 84 must be used as the earth reference model for error determination; any differences between other models used for path definition or errors resulting from data resolution are considered to be part of the PDE.

- **FTE** refers to the deviation of the estimated position of the aircraft from the path defined in the navigation database and thus depends on the ability of the crew or autopilot to follow the intended path. In-flight monitoring of the FTE can occur either manually per crew procedure or automatically by the autopilot. Deviations induced by display errors are part of the FTE.

- **NSE** is the difference between the actual position of the aircraft and the position indicated by the navigation system. It depends on the navigation sensors involved in the calculation of the position solution. In most modern aircraft, navigation is performed based on a combination of inertial and satellite navigation.

The vector sum of the three error components is the total system error:

$$TSE = \sqrt{PDE^2 + FTE^2 + NSE^2} \quad \textbf{(2.1)}$$

2.3. Global Navigation Satellite Systems (GNSS)

Satellite-based positioning uses the signals of multiple artificial satellites orbiting earth to determine the position of a receiver by means of trilateration. This requires knowledge about the positions of the sending satellites as the unknown receiver position is calculated from the measured ranges to the individual satellites. Each measured range defines the surface of a sphere centered on the satellite on which the receiver position could be located [6]. For this reason, at least three range measurements must be available for an unambiguous identification of the receiver position. However, as the range to each satellite is computed from the run time of the signal, both the satellite and the receiver clock would need to be perfectly synchronized with the system time in order to obtain a correct range measurement. Otherwise even smallest deviations from system time would lead to significant measurement errors as the radio signal emitted by the satellites travels with the speed of light. Yet perfect synchronization of all satellite and receiver clocks with system time is nearly impossible and would require highly accurate equipment to be deployed, thus creating excessive cost and rendering satellite-based positioning unaffordable for most users. The problem is circumvented by including a fourth measurement which is used to determine the clock offset from system time. This allows the utilization of inexpensive clocks in the receiver equipment, which are set approximately to system time. Due to the time offset, the measured range varies from the actual geometric range and is therefore named pseudorange.

The pseudorange R consists of the geometric range ϱ and a range correction $\Delta\varrho$, which is a function of clock bias δ and speed of light c [7].

$$\boldsymbol{R = \varrho + \Delta\varrho = \varrho + c\delta} \tag{2.2}$$

Using an earth-fixed Cartesian coordinate system and the Pythagorean theorem, equation 2.2 can be rewritten to include the coordinates of both the receiver and satellite positions:

$$\boldsymbol{R = \sqrt{(x_s - x_r)^2 + (y_s - y_r)^2 + (z_s - z_r)^2} + c\delta} \tag{2.3}$$

The components x_s, y_s and z_s of the position vector of the satellite are known as they are broadcasted via the navigation signal transmitted by the satellite. Equation 2.3 thus contains four unknown variables: the three components of the receiver position vector x_r, y_r, z_r and the clock bias δ. The four unknown variables can be determined with four simultaneous equations; hence at least four satellites need to be available to a receiver to obtain a position fix. Pseudorange measurement can be realized by measuring either time or phase differences of received satellite signals and reproduced receiver signals [7]. The two methods are described in the following sections.

2.3.1. Code Range Positioning

The time difference between emission and reception of the satellite signal is determined based on the reading of the satellite clock as included in the navigation message and the reading of the receiver clock upon reception. Although satellite clocks are highly accurate atomic clocks, both timestamps can vary from the common system time of the GNSS. So both emission time t_s^{sat} as determined by the satellite and reception time t_r^{rec} as determined by the receiver can be affected by a bias with respect to the common time system. The satellite clock bias δ_s is usually much smaller than the receiver clock bias δ_r, but has to be considered if accurate position fixes are to be obtained. By expressing emission time t_s and reception time t_r in the common system time in relation to the biased values of the different time systems, one obtains

$$\boldsymbol{t_r^{rec} - t_s^{sat} = (t_r + \delta_r) - (t_s + \delta_s) = \Delta t + \delta} \tag{2.4}$$

with the actual signal run time Δt and the combined clock biases of satellite and receiver δ [7]. The code pseudorange results from the multiplication of the left-hand side of equation 2.4 with the speed of light.

$$\boldsymbol{R = c(t_r^{rec} - t_s^{sat}) = c\Delta t + c\delta = \varrho + c\delta} \quad \textbf{(2.5)}$$

It can be seen that the result is identical to the general form of the pseudorange equation 2.2.

In the case of GPS, all satellites emit the navigation signal on the same frequency. In order to provide the receiver with a means of distinguishing the received signals, each satellite has a unique Pseudorandom Noise (PRN) code which is used for the modulation of its individual navigation message onto the carrier frequency. Each receiver reproduces the PRN codes used by the satellites and uses autocorrelation to compare reproduced and received signals. By shifting the reproduced signal until full correlation is achieved, the receiver can track the navigation signal and decode the included navigation message in order to gain information about the position of the sending satellite and time of signal emission [8].

2.3.2. Carrier Phase Positioning

Another possible way of obtaining the pseudoranges is measurement of the navigation signal carrier phase. Analogous to equation 2.2, the phase pseudorange Φ can be written as

$$\boldsymbol{\Phi = \varrho + c\delta + \lambda N} \quad \textbf{(2.6)}$$

The additional term in equation 2.6 results from the unknown initial integer number $\boldsymbol{N}$ of cycles between the satellite and receiver [7]. Again, the time offset from system time that affects both the satellite and receiver clocks has to be considered. The phase φ_s of the received carrier with the frequency f_s and the phase φ_r of the reference carrier emulated in the receiver with the frequency f_r can be expressed for any epoch t in the common system time using the following equations:

$$\boldsymbol{\varphi_s(t) = f_s t - f_s \frac{\varrho}{c} - \varphi_{s0}} \quad \textbf{(2.7)}$$

$$\boldsymbol{\varphi_r(t) = f_r t - \varphi_{r0}} \quad \textbf{(2.8)}$$

φ_{s0} and φ_{r0} are the initial phases caused by the satellite and receiver clock errors. Using the clock biases δ_s and δ_r, they can be rewritten as

$$\varphi_{s0} = -f_s \delta_s \tag{2.9}$$

$$\varphi_{r0} = -f_r \delta_r \tag{2.10}$$

Combining equations 2.7 to 2.10 in order to obtain the phase difference between received and emulated carrier in a common time system yields

$$\varphi_s(t) - \varphi_r(t) = -f_s \frac{\varrho}{c} + f_s \delta_s - f_r \delta_r + (f_s - f_r)t \tag{2.11}$$

With regard to the very small frequency deviations f_s and f_r from the nominal frequency f and the short signal propagation times, the last term in equation 2.11 produces only minimal deviations in the phase difference which are below the noise level and can thus be neglected. Using the combined clock bias with respect to the common time system and rewriting the phase difference as φ, equation 2.11 can be simplified to become

$$\varphi = -f \frac{\varrho}{c} - f\delta \tag{2.12}$$

After a receiver is turned on at the initial epoch t_0, the fractional phase difference is instantaneously available [7]. However, the initial integer number N of cycles between satellite and receiver is unknown. If the received signal can be tracked continuously without loss of lock, the integer ambiguity remains constant, and the phase difference at any epoch is a function of the measurable fractional phase $\Delta\varphi$.

$$\varphi = \Delta\varphi + N \tag{2.13}$$

By substituting equation 2.13 into equation 2.12 and replacing the frequency according to the relation

$$c = \lambda f \Leftrightarrow f = \frac{c}{\lambda} \tag{2.14}$$

the equation for the phase pseudoranges can be obtained:

$$\Delta\varphi = -\frac{\varrho}{\lambda} - \frac{c}{\lambda}\delta - N \tag{2.15}$$

Note that equation 2.15 describes the phase pseudorange as a dimensionless quantity due to the measurement of phase cycles. In order to obtain a range measurement between satellite and receiver, equation 2.15 is multiplied by λ and the dimensional quantity Φ is introduced [7]:

$$\boldsymbol{\Phi = -\Delta\varphi\lambda = \varrho + c\delta + \lambda N} \tag{2.16}$$

Measuring phase pseudoranges offers a higher precision than code pseodoranges, but also places higher requirements on the receiving equipment. Determination of the initial integer ambiguity and the necessity for a phase lock loop result in a more sophisticated receiver. The advantage of this method results from the highly accurate measurement of the phase, which can be better than 0.01 cycles. For an electromagnetic wave with a frequency in the gigahertz range, this corresponds to millimeter precision [7].

2.3.3. Differential Positioning

The accuracy of both code range and carrier phase positioning can be increased if a second receiver is available at a reference position whose exact coordinates are known. Typically, the reference receiver is designated as the base, while the other receiver at an unknown position is called the rover. For measurements based on code range, the measured pseudoranges at the reference station are compared to the actual distances to the satellites. These are computed from the satellite position as contained in the navigation message and the coordinates of the reference station. Pseudorange corrections (PRC) and range rate corrections (RRC) are computed for each pseudorange measurement and transmitted to the rover, which applies the corrections to its own pseudorange measurements, thus eliminating systematic errors that affect both receivers in the same way such as satellite clock bias or atmospheric delay of the signal. However, the true error at the position of the rover will differ from the error at the base, but due to the relatively long distance to the satellites in comparison to the base-rover distance, the pseudorange corrections computed from the measurements at the base will generally be valid and improve the position accuracy [8].

By generalizing equation 2.5, the code range at base station A to satellite s can be modeled for epoch t_0 as follows:

$$\boldsymbol{R_A^s(t_0) = \varrho_A^s(t_0) + \Delta\varrho_A^s(t_0) + \Delta\varrho^s(t_0) + \Delta\varrho_A(t_0)} \tag{2.17}$$

Here, $\varrho_A^s(t_0)$ is the geometric range from station A to satellite s. The term $\Delta\varrho_A^s(t_0)$ denotes all range biases that are influenced by both the receiver and satellite positions such as the atmospheric delay of the signal. All range biases influenced only by the satellite such as the effect of the satellite clock error are summarized in $\Delta\varrho^s(t_0)$, whereas $\Delta\varrho_A(t_0)$ contains all purely receiver-related biases such as the effect of the receiver clock error.

The pseudorange correction PRC computed at reference station A to satellite s for epoch t_0 is defined as the difference between the geometric range and the measured pseudorange:

$$\boldsymbol{PRC^s(t_0) = \varrho_A^s(t_0) - R_A^s(t_0)} \quad \textbf{(2.18)}$$

Substituting equation 2.17 into equation 2.18 yields:

$$\boldsymbol{PRC^s(t_0) = -\Delta\varrho_A^s(t_0) - \Delta\varrho^s(t_0) - \Delta\varrho_A(t_0)} \quad \textbf{(2.19)}$$

Since everything on the right-hand side of equation 2.19 is known, $PRC^s(t_0)$ can be computed. Together with its time derivate, the range rate correction $RRC^s(t_0)$, it is transmitted to the rover B, where the pseudorange correction for any observation epoch t is determined based on the following relation:

$$\boldsymbol{PRC^s(t) = PRC^s(t_0) + RRC^s(t_0)(t - t_0)} \quad \textbf{(2.20)}$$

The term $(t - t_0)$ is also denoted as latency. In order to achieve a high accuracy, the RRC and latency need to be sufficiently small [7].

At the position of the rover B, the equivalent to equation 2.17 at epoch t is:

$$\boldsymbol{R_B^s(t) = \varrho_B^s(t) + \Delta\varrho_B^s(t) + \Delta\varrho^s(t) + \Delta\varrho_B(t)} \quad \textbf{(2.21)}$$

Applying the predicted pseudorange correction $PRC^s(t)$ yields the corrected pseudorange measurement $R_B^s(t)_{corr}$:

$$\boldsymbol{R_B^s(t)_{corr} = R_B^s(t) + PRC^s(t)} \quad \textbf{(2.22)}$$

$$\boldsymbol{R_B^s(t)_{corr} = \varrho_B^s(t) + [\Delta\varrho_B^s(t) - \Delta\varrho_A^s(t)] + [\Delta\varrho_B(t) - \Delta\varrho_A(t)]} \quad \textbf{(2.23)}$$

Note that the satellite-dependent bias $\varrho^s(t)$ is canceled out in equation 2.23. For short distances between base and rover, the biases depending on both the receiver and satellite position are highly correlated, significantly reducing the influence of atmospheric delay [7]. The corrected pseudorange measurements are used for positioning of the rover, increasing the accuracy in comparison to standalone operation of the rover receiver.

For differential positioning using carrier phase measurements, pseudorange corrections are computed analogously to the previously described method. Equation 2.24 is generalized in order to contain the individual biases with regard to their origin:

$$\boldsymbol{\Phi_A^s(t_0) = \varrho_A^s(t_0) + \Delta\varrho_A^s(t_0) + \Delta\varrho^s(t_0) + \Delta\varrho_A(t_0) + \lambda N_A^s} \quad \textbf{(2.24)}$$

The pseudorange correction $PRC^s(t_0)$ for differential positioning with carrier phases is consequently given by:

$$\boldsymbol{PRC^s(t_0) = \varrho_A^s(t_0) - \Phi_A^s(t_0)} \quad \textbf{(2.25)}$$

From equations 2.24 and 2.25 results:

$$\boldsymbol{PRC^s(t_0) = -\Delta\varrho_A^s(t_0) - \Delta\varrho^s(t_0) - \Delta\varrho_A(t_0) - \lambda N_A^s} \quad \textbf{(2.26)}$$

Again, PRC and RRC are transmitted to the rover and applied to the pseudorange measurements. The procedure for the application of the phase pseudorange corrections is equivalent to the previously described method for code pseudorange corrections.

$$\boldsymbol{\Phi_B^s(t)_{corr} = \Phi_B^s(t) + PRC^s(t)} \quad \textbf{(2.27)}$$

$$\boldsymbol{\Phi_B^s(t)_{corr} = \varrho_B^s(t) + [\Delta\varrho_B^s(t) - \Delta\varrho_A^s(t)] + [\Delta\varrho_B(t) - \Delta\varrho_A(t)] + \lambda[N_B^s - N_A^s]} \quad \textbf{(2.28)}$$

Again, the satellite-related biases cancel each other out, leaving only the receiver-related biases and the biases that depend on both the receiver and satellite positions. For sufficiently small baselines, these biases can also be neglected. The main difference between code range differential positioning and carrier phase differential positioning is the last term in equation 2.28 which results from the integer ambiguities that have to be considered for all carrier phase measurements. Differential GPS (DGPS) with carrier phases is often used for precise kinematic applications [7].

The distance between base and rover is an important factor for the accuracy of the corrections and the precision of the rover position. It is thus desirable to keep the length of the baseline vector as short as possible while maintaining the reference station in a position that is protected from possible further biases such as multipath. Any error in the base measurement will have a direct influence on the position solution at the rover position. A typical precision that can be achieved with differential positioning is in the order of one to two meters for code range positioning and 20 centimeters for carrier phase positioning [8].

2.4. World Geodetic System

A geodetic system is a mathematical representation of the earth or parts of it and is required to assign unique coordinates to a particular position. The simplest reference system is the approximation of the earth as a sphere, which neglects the flattening at the poles. While the accuracy of positioning using a spherical model of the earth might be sufficient for many purposes, there are also several areas of application that require a higher accuracy, for example geodesy. For this reason, a series of local or regional reference systems has been created over time that better represent the actual surface of the earth in the specific areas in which they are used [7]. However, some applications such as cartography or navigation require an internationally unified reference system in order to be applicable everywhere on the planet.

The World Geodetic System (WGS) was introduced as a result of this requirement. It models the earth as a spheroid, which is a more accurate representation of the actual form of the earth than a sphere. The WGS includes three components: A standard coordinate system for the earth, a standard spheroidal reference surface as a datum for altitude data and a gravitational equipotential surface that defines the nominal sea level [9].

A standardized coordinate system is the basis for all position information on the surface of the earth. The WGS defines its prime meridian, i.e. the meridian of zero longitude, to coincide with the International Reference Meridian (IRM) as maintained by the International Earth Rotation and Reference Systems Service (IERS) [10]. The equator defines all positions with zero latitude; a combination of latitude and longitude can be used to unambiguously describe every position on the surface of the earth. Altitude information, however, cannot be expressed using latitude and longitude only and necessitates the introduction of a spheroidal reference surface.

The datum surface used by WGS is formed by an oblate spheroid with a semi-major axis a and the reciprocal of the flattening f. Two additional defining parameters are the angular velocity of the earth ω and the gravitational constant of the earth GM. All other geometric or physical constants of the WGS are derived from these four defining parameters. For navigation purposes and the conversion between earth-fixed coordinate systems only the length of the semi-major axis and the reciprocal of the flattening are required. Their values are defined as follows [9]:

$$a = 6378137.0\ \mathrm{m}$$

$$\frac{1}{f} = 298.257223563$$

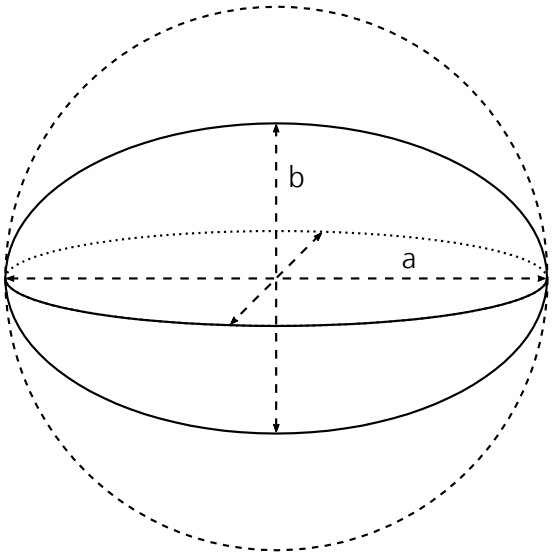

Figure 2.2: Spheroid geometry <own figure>

Figure 2.2 illustrates the difference between a circle and a spheroid. Instead of a constant radius, the spheroid is defined by its semi-major axis and flattening. These parameters can be used to compute the length of the semi-minor axis b from the following equation:

$$f = \frac{a - b}{a} \Leftrightarrow b = a\,(1 - f) \tag{2.29}$$

Another geometric constant used to describe a spheroid is the eccentricity e:

$$e = \sqrt{1 - \frac{b^2}{a^2}} \tag{2.30}$$

In addition to the definition of a coordinate system and a reference spheroid, the WGS also contains a geoid in order to approximate the irregular gravitational field of the earth. When compared to the datum surface, which is an idealized mathematical model of the physical form of the earth, the geoid is much more irregular as it describes an equipotential surface, i.e. the form the earth would have if it was completely covered by water [7]. The irregularities in the gravity field of the earth are caused by the uneven distribution of the mass on the surface and within the earth. This means that in areas with a mass excess, the geoid is higher than the reference spheroid, whereas it is lower in areas with a mass deficit [11]. The height of a specific

point above the geoid is called the orthometric height H, whereas the height above the reference datum is defined as the ellipsoidal height h. The difference between the two heights varies significantly in sign and magnitude depending on the position of measurement. The geoidal height or undulation N can be used to approximate the relationship between the geoid and the reference datum by using the following equation [7]:

$$h = H + N \tag{2.31}$$

2.4.1. Ellipsoidal Coordinates

In most applications, the position of an object relative to the earth is expressed using the ellipsoidal coordinates latitude, longitude and height. The latitude φ is an angular measurement that specifies the north-south position of a point on the surface of the earth. Its magnitude ranges from 0° at the equator to 90° at the respective poles. Whether a point is located on the northern or southern hemisphere is indicated by the sign of the latitude, with positive values for points north of the equator and negative values for points south of the equator. All lines with constant latitude are circles parallel to the equator in east-west direction [12].

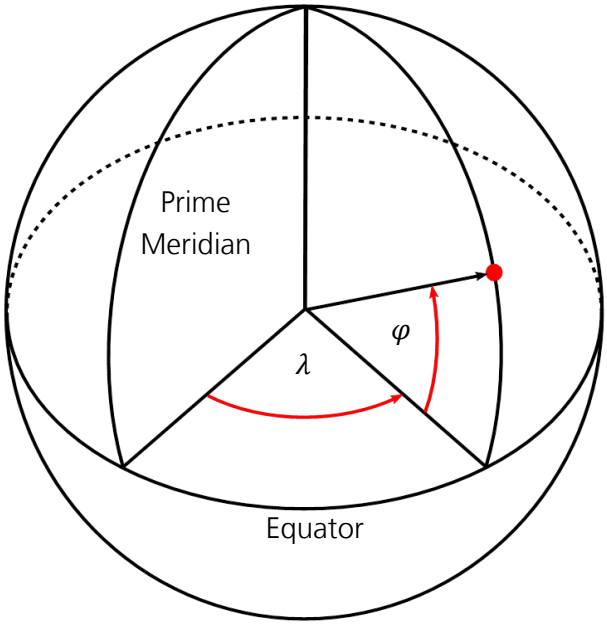

Figure 2.3: Latitude and longitude <own figure>

The second coordinate used to describe a position on the surface of the earth is the longitude λ. It is also an angular measurement, but denotes the east-west position of a point and ranges from 0° to 180° in magnitude. Since there is no natural characteristic that could serve as a zero point

like the equator in latitude measurement, an international prime meridian of zero longitude was defined. Positive longitudes denote positions east of this line, while negative longitudes denote positions west of the prime meridian. All lines of constant longitude are great ellipses and connect the north and south pole. Due to this fact, the distance between two lines of constant longitude changes with latitude. Unlike with latitude, there is a discontinuity at the antipodal meridian of the prime meridian, and all positions on this line can be described with +180° and -180° [12]. Figure 2.3 shows how all points on the surface of the earth can be described in terms of latitude and longitude.

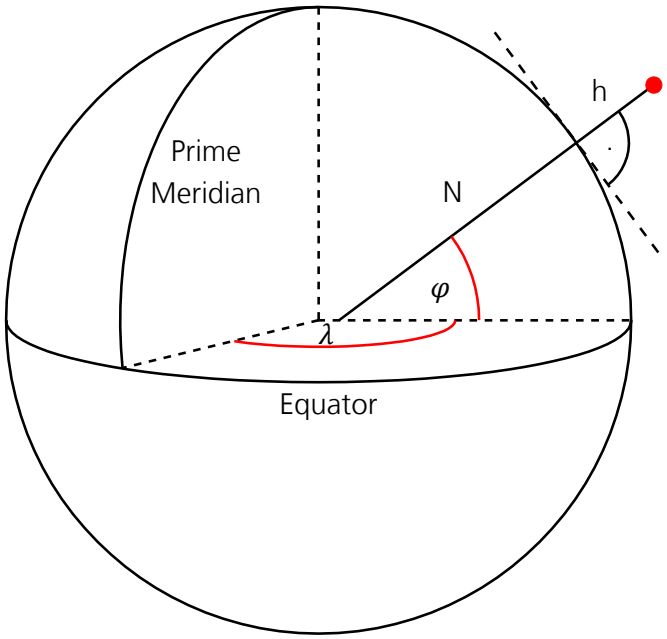

Figure 2.4: Ellipsoidal height and radius of curvature of the prime vertical <own figure>

While all positions on the surface of the reference datum can be described using latitude and longitude, a third coordinate is required if a specific point is located above or below this surface. The ellipsoidal height h is the height above or below a plane normal to the spheroid at the associated position indicated by latitude and longitude as shown in Figure 2.4. It should also be noted that many applications such as cartography and navigation use the Mean Sea Level (MSL) as the vertical datum instead of the ellipsoidal height. MSL is better represented by the geoid, although influences such as currents, air pressure variations and others create a location-dependent offset between MSL and the geoid. However, MSL is not defined consistently and can thus vary depending on the field of application. In aviation, however, the WGS has been adopted as the standard geodetic reference system for navigation [13].

2.4.2. Cartesian Coordinates

While ellipsoidal coordinates provide an adequate means of indicating a position, they are rather inconvenient when calculations are to be performed. Distances and directions can be expressed much better using a standard Cartesian coordinate system with its origin in the center of the spheroid. The Z-axis is aligned with the International Reference Pole (IRP) as defined by the IERS, while the X-axis passes through the IRM and forms an angle of 90° with the Z-axis. The Y-axis is located so as to complete a right-handed orthogonal coordinate system that is fixed with respect to the surface of the spheroid. Using standard vector operations, the Cartesian coordinate system allows relatively simple computation of direct distances between positions without the disadvantage of becoming inaccurate close the poles. Using unit vectors, the distance between two points can be split into components along certain directions, for example to determine the vertical and lateral deviation of a trajectory from the planned path.

In order to be able to apply these operations, position information must be available in Cartesian coordinates. However, navigation systems usually output ellipsoidal coordinates as they are more intuitive for the operator, thus necessitating a conversion from ellipsoidal to Cartesian coordinates. This can be done using the following formulae [7]:

$$\boldsymbol{X = (N + h)\cos\varphi\cos\lambda} \tag{2.32}$$

$$\boldsymbol{Y = (N + h)\cos\varphi\sin\lambda} \tag{2.33}$$

$$\boldsymbol{Z = \left(\frac{b^2}{a^2}N + h\right)\sin\varphi} \tag{2.34}$$

Here, N refers to the radius of curvature of the prime vertical as shown in Figure 2.4. It depends on latitude and can be computed from equation 2.35.

$$\boldsymbol{N = \frac{a^2}{\sqrt{a^2\cos^2\varphi + b^2\sin^2\varphi}}} \tag{2.35}$$

2.5. ARINC 429 Avionics Data Bus Standard

The overall avionics system of any aircraft is a result of the combination of several smaller sub-systems such as radio navigation sensors, air data computers, attitude heading reference systems, inertial navigation systems and many more. Integration of these sub-systems into the overall

system is essential for the operability of an aircraft and its capability of carrying out its individual tasks effectively. In order to facilitate the interconnection and control of the sub-systems, specifications and requirements for avionics systems and equipment were introduced as the electrical equipment of both military and civil aircraft became more complex after World War II [14].

Aeronautical Radio, Incorporated (ARINC) organizes and provides technical standards for airborne electrical equipment. While all standards published by ARINC are consensus-based and voluntary, most equipment manufacturers follow these standards, resulting in consistent form, fit, function and interfaces for many avionics and other airline electrical equipment. Therefore all equipment made to an ARINC standard should be completely interchangeable with equipment from other manufacturers, thus allowing for relatively fast and cheap replacement of individual systems without affecting other components of the overall avionics system.

Generally, ARINC standards can be divided into three classes. An ARINC characteristic defines the physical properties of a sub-system in terms of size, form, input and output interfaces as well as environmental and functional requirements. ARINC specifications detail data communication standards or high-level computer languages. Thirdly, ARINC reports provide guidelines and general information related to avionics maintenance and support that is regarded as good practice by airlines [15].

The ARINC specification 429 defines standards for the air transport industry with regard to the transfer of digital information between avionics sub-systems. Each avionics system transmits its data to all other systems requiring this information via a single twisted shielded pair of wires. Data transfer is one-directional and from designated output ports only. In case a system both transmits and receives data, multiple connections are necessary as bi-directional data flow is not permitted in the ARINC specification 429 [15].

ARINC 429 includes numeric data transmission in either two's complement fractional binary (BNR) or binary coded decimal (BCD) notation. Source systems supply data in an open-loop transmission, i.e. sinks do not confirm that information has been received. Furthermore, data transmission occurs at high rates to ensure only small changes between updates, thus reducing the effect of eventual dropouts. A parity bit included in each ARINC 429 data word allows simple error checks after reception of an update, which – together with data plausibility checks –

prevents the utilization or display of data from an erroneous word. Other data formats that can be handled by ARINC 429 are alpha and numeric data encoded using the ISO alphabet 5 and graphic data such as standardized symbols on maps and similar displays [15].

Each ARINC 429 digital word contains 32 bits in five different fields. Typically, the bits within an ARINC 429 word are identified by their bit number which ranges from one to 32. However, it is common to illustrate ARINC 429 words in the order from bit 32 to bit one, i.e. starting with bit 32 on the left. The five fields of each word differ in size depending on their contents. Using the typical notation and starting on the left, an ARINC 429 digital word is composed as follows:

- Bit 32 serves as the parity bit that is used to verify the integrity of the received data word, i.e. whether the word was damaged or garbled during transmission. The parity bit should be encoded so that word parity is rendered odd, i.e. an odd number of positive bits are contained in the word. Depending on the state of the other 31 bits, the parity bit can be set to either zero or one to ensure a correct number of positive bits in the word.

- Bits 30 and 31 contain the sign/status matrix (SSM). The encoding of these two bits depends on the data representation of the particular word, but typically contains information regarding the hardware status of the sending equipment such as normal operation, failure warning, functional test or no computed data. For words containing BCD numeric data, the SSM is also used to indicate the sign of the corresponding values according to Table 2.1.

Bit Number		**Meaning**
31	30	
0	0	Plus, North, East, Right, To, Above
0	1	No Computed Data
1	0	Functional Test
1	1	Minus, South, West, Left, From, Below

Table 2.1: BCD sign/status matrix [15]

For BNR encoded data, bit 29 is used in addition to bits 30 and 31 for a separate sign matrix. The BNR status matrix remains on bits 30 and 31 and contains additional states for failure warning and normal operation as shown in Table 2.2.

Bit Number		Meaning
31	30	
0	0	Failure Warning
0	1	No Computed Data
1	0	Functional Test
1	1	Normal Operation

Table 2.2: BNR status matrix [15]

The new sign matrix for BNR encoded data on bit 29 is illustrated in Table 2.3.

Bit Number	Meaning
29	
0	Plus, North, East, Right, To, Above
1	Minus, South, West, Left, From, Below

Table 2.3: BNR sign matrix [15]

For all discrete data words, the SSM is similar to the BNR status matrix in Table 2.2, with the exception that the positions of "Failure Warning" and "Normal Operation" are interchanged.

- Bits 11 to 29 contain the data field of each word with information encoded in an appropriate data representation. Standards for the units, ranges, resolutions, refresh rates and number of significant bits of the information items to be transmitted via the ARINC 429 bus can be found in [15].

- Bits 9 and 10 contain the source/destination identifier (SDI). The SDI is only used in case a specific word needs to be directed to a single system within a multi-system installation or if the source system needs to be determined from the word content. Otherwise, the SDI bits can be used to increase the resolution available for numeric data.

- Bits 1 to 8 are used to encode a label for each ARINC 429 word which identifies the data type contained in the data field. The eight bits of the word label are three binary coded octal characters that are assigned to a specific information item. In combination with a three character hexadecimal equipment identification code, distinction between information with the same label but different origin is enabled. Each system with one or

more ARINC 429 ports is identified by a unique triplet of hexadecimal characters and can have up to 255 eight bit labels assigned to it for data transmission to other systems.

2.6. ARINC 424 Navigation System Database Standard

The ARINC specification 424 defines a recommended standard for airborne navigation system reference data files. As the operational software used in flight planning systems, flight simulators and other applications is not standardized and thus dependent on the system manufacturer, a common file format for the navigation database used by these systems is required to enable procedure designers and air navigation service providers to publish navigation data. Navigation databases contain aeronautical information about airports, runways, waypoints, navigation aids, airways as well as arrival and departure routes and are used by the flight management system (FMS) of modern aircraft for flight planning. Aircraft operators can purchase navigation databases tailored to their individual route network and destination airports from an aeronautical information service provider. Each individual navigation database consists of entries from both a set of standard data published by official institutions and a set of customer-specific data. The application of the ARINC 424 standard for database encoding ensures that the flight management systems of all aircraft can read the navigation database, regardless of their manufacturer and update status. Updates for navigation databases need to be released on a fixed 28 day aeronautical information regulation and control cycle.

Within a navigation database, navigation information is organized in sectors and subsectors according to Table 2.4. In this way, entries to a navigation database can be referenced across sectors and used in multiple applications. For example, a navigation aid entered in the VHF subsector of the navaid sector can be referenced in enroute airways as well as in airport standard instrument departures (SID) or standard terminal arrival routes (STAR).

Section	Subsections
Navaids	VHF navaids NDB navaids
Enroute	Enroute waypoint Enroute airway marker Holding patterns Enroute airways Enroute airways restrictions Enroute communications
Airports	Airport reference points Airport gates Airport terminal waypoints Airport SIDs Airport STARs Airport approaches Airport runway Airport and heliport localizer/glide slope Airport and heliport MLS Airport and heliport marker/localizer MSA Airport communications Airport and heliport terminal NDB Airport SBAS path point Flight planning arrival/departure data record GNSS landing system Airport terminal arrival altitude
Company routes and alternate destinations	Company routes Alternate records
Special use airspace	Restrictive airspace FIR/UIR Controlled airspace
Cruising tables	Cruising tables Geographical reference table MORA Preferred routes GBAS path point

Table 2.4: Definition of ARINC 424 sections and subsections [16]

ARINC 424 uses a record format with a fixed length of 132 characters. Each record is composed of a combination of fields with varying length that contain information specific to the navigation item that is described. For example, a waypoint record includes - among others - fields for the waypoint identifier, the waypoint type and its latitude and longitude. Airways are then created by sequencing waypoints and specifying additional information for each waypoint such as path

terminators or altitude constraints, thus creating the individual legs of an airway or terminal procedure. As each leg is detailed in one ARINC 424 record, the overall procedure is composed of several records whose number depends on the amount of waypoints included in the procedure. With regard to the record fields, the ARINC 424 specification differentiates between enroute airways and airport-related approaches, SIDs and STARs. Approach records, for example, include the type of approach and the corresponding runway, whereas enroute records contain maximum and minimum altitudes as well as a reference to a published cruising level table. Other information such as the RNP value associated with each leg is found in both entry types, but might be located on different characters of the individual 132 character records [16].

In addition to the general encoding standards for navigation information, the ARINC 424 specification also includes rules and standards for the coding of terminal procedures into the navigation database format. In order to prevent an excessive number of named waypoints in terminal airspace, the path and terminator concept is used to reduce the number of waypoints that is required to support these procedures. A set of path terminator codes for waypoints in terminal procedures is defined, allowing the use of the same waypoint for multiple procedures without reducing the flexibility of the individual flight path. By coding a waypoint with a specific path terminator code for a particular procedure, the flight path to this waypoint as well as the termination of this flight path are defined. However, the same waypoint can be coded with another path terminator code for other procedures, thus enabling the creation of different flight paths with a limited set of named waypoints. A total number of 23 different path terminator codes are detailed in the ARINC 424 specification. For the sake of brevity only a subset of leg types that is commonly used in the approach phase is presented in Table 2.5.

Path terminator	Description
IF	**Initial fix leg** A database waypoint is defined as the starting point of a terminal procedure
TF	**Track to fix leg** Great circle track over ground between two database waypoints
RF	**Radius to fix leg** Constant radius turn between two database waypoints
CF	**Course to fix leg** Specified course to a database waypoint
FA	**Fix to altitude leg** Specified track over ground from a database waypoint to a specified altitude
DF	**Direct to fix leg** Unspecified track over ground from an unspecified position to a database waypoint
CR	**Course to radial termination leg** Specified course to a specified radial from a database VOR navaid

Table 2.5: Subset of ARINC 424 path terminators [16]

Similar to the path terminator concept that enables multiple uses of waypoints for lateral navigation, different altitude information can be assigned to a single waypoint in each ARINC 424 approach record it is included in. This decoupling of horizontal and vertical position information allows for a less complex waypoint structure in the airport environment. For example, a waypoint that is part of the approach path to a runway can also be part of a departure or missed approach path of the opposite runway direction. While the horizontal position of the waypoint is fixed by its waypoint record in the navigation database, its altitude information is contained in the respective ARINC 424 record of each individual procedure and can thus be adapted to the different requirements.

Altitude information is specified by altitude constraints associated with a waypoint. The altitude constraint is composed of a numerical value that indicates the waypoint altitude in feet and a waypoint crossing description. The latter indicates to the FMS whether the waypoint should be passed at the specified altitude or can also be passed higher or lower than the declared altitude at the discretion of the FMS. Less restrictive altitude constraints that allow deviations from the specified altitude are often used when no precisely defined vertical path is required and enable the FMS to calculate a more efficient gradient based on the current flight performance

parameters. The three commonly used crossing descriptions are the "at", "at or above" and "at or below" constraints, which are coded in the ARINC 424 navigation database according to Table 2.6.

Field content	Constraint type	Description
(blank)	At	Waypoint must be passed at the altitude specified in the altitude field of the record
+ (plus)	At or above	Waypoint must be passed at or above the altitude specified in the altitude field of the record
- (minus)	At or below	Waypoint must be passed at or below the altitude specified in the altitude field of the record

Table 2.6: Constraint types [16]

3. Preparation of the Flight Test Campaign

In this chapter, the objectives of the flight test campaign are summarized. Beyond that, the structure of the experimental approaches as well as their coding into the navigation database of the ATRA is discussed. The findings of preliminary simulator tests and their implications for the preparation of the actual flight tests are also part of this chapter. Finally, the data required for the subsequent evaluation of the flight tests and the final parameter list is explained.

3.1. Objectives

An earlier requirement analysis [5] for RNP to ILS approaches identified the length of the straight final approach segment to be the crucial parameter for successful automatic landings. Hence, one of the main areas of interests during the flight tests is the autoland performance of the ATRA during the experimental procedures with a relatively short final approach. As no information is available from official sources regarding the internal control laws of the auto flight system, the flight tests are necessary to identify a possibly required minimum length of the final approach segment for automatic landings.

As the initial and intermediate segments of the approach are based on RNP guidance, the navigation accuracy of the ATRA during this part of the procedure is also of interest. Especially the vertical path following during the RNP part of the approach is important for safe and successful RNP to ILS approaches as the aircraft must be at the correct altitude at the end of the RF leg to allow seamless transition to glideslope guidance. If the ILS intercept point is reached with a significant deviation from the associated target altitude, engagement of the glideslope track mode of the autopilot might take too long to allow subsequent engagement of the land mode before the runway is reached. This aspect becomes more critical as the remaining distance on the final approach is reduced and is thus most important for the experimental approaches with a very low ILS intercept height. Both possible cases of deviation from the target altitude entail specific problems for the transition to glideslope guidance as shown in Figure 3.1: If the aircraft is too high at the ILS intercept point, a descent with a vertical path angle higher than the nominal glideslope angle is required to capture the glideslope. This contradicts the principle of a stabilized approach and might cause discomfort to the crew, especially in procedures with an already very low ILS intercept height. In the other case, i.e. the aircraft is too low when reaching the ILS intercept point, the glideslope can be captured from below as in conventional ILS

approaches. However, this would require a horizontal flight path until the glideslope is captured, thus exposing the environment to extensive noise due to the increased amount of thrust required for level flight. It can be seen that passing of the ILS intercept point either too high or too low is in contrary to the aims of implementing RNP to ILS approaches and therefore needs to be avoided. For this reason, adherence to the design vertical profile is one of the key areas of interest for the flight tests with the ATRA.

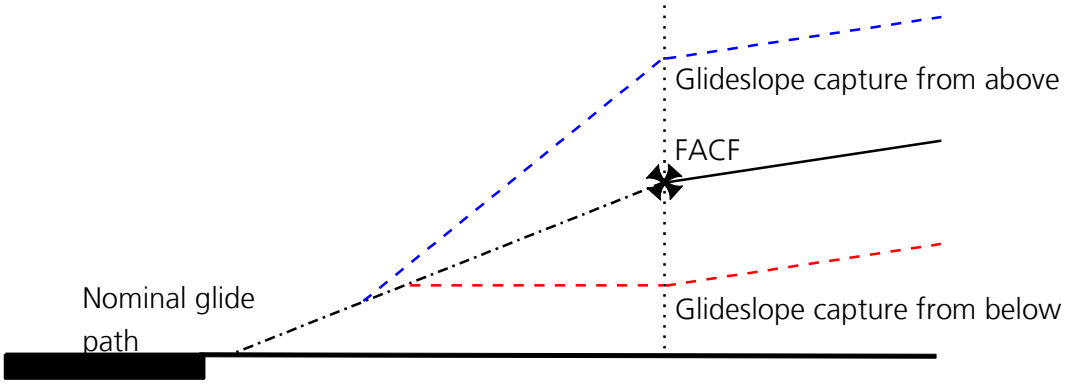

Figure 3.1: Glideslope capture after reaching the ILS intercept point too high or too low <own figure>

While not being as crucial as the vertical path, the lateral navigation accuracy of the ATRA during the RNP part of the approach is also an important aspect of the flight tests. As for the vertical path, the aircraft needs to pass the designated ILS intercept point as precisely as possible for a quick transition to localizer guidance. Again, the time available to the auto flight system for the transition from the localizer capture mode to the localizer track mode is highly dependent on the length of the final approach segment, rendering this problem more critical for approaches with low ILS intercept heights. Poor lateral navigation accuracy and thus high lateral deviation from the intended flight path at the ILS intercept point causes the auto flight system to remain in the localizer capture mode for a prolonged amount of time and thus might prevent the timely engagement of the land mode.

An issue specific to RNP to ILS approaches arises due to the lateral transition from RNP guidance to the localizer signal at the end of the RF leg. If the approach mode is armed prior to reaching the ILS intercept point, the auto flight system might switch to the localizer mode immediately, causing a deviation from the RNP path that was intended to be flown until the end of the curved segment. Due to the angular characteristic of the localizer signal, this problem is of higher significance for approaches that intercept the ILS guidance beam at higher altitudes and thus greater distances from the runway threshold. For approaches with a low RNP value such as 0.1 or

0.3 nautical miles, an early activation of the approach mode might cause a violation of the RNP corridor if the designated ILS intercept point is located far enough from the runway threshold as shown in Figure 3.2.

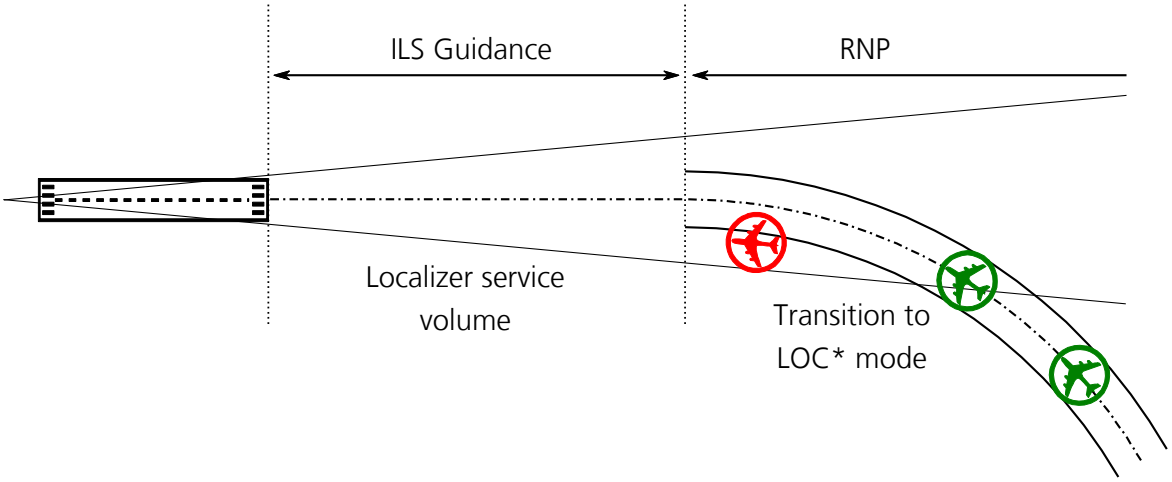

Figure 3.2: Early transition to LOC* mode with active approach mode <own figure>

All in all, three key aspects of RNP to ILS approaches are to be investigated in the flight tests:

- **Autoland performance** (minimum required final approach length, autoland capability indicated by the auto flight system)
- **Vertical path following** (adherence to design vertical path, time required for transition to glideslope guidance after engagement of the approach mode)
- **Lateral navigation accuracy** (actual navigation performance, time required for transition to localizer guidance after engagement of the approach mode, deviations from lateral flight path and possible RNP corridor violation for early approach mode activation)

3.2. Experimental Approaches

A set of five experimental RNP to ILS approaches was designed for runway 26 of Braunschweig-Wolfsburg airport. Each approach includes a RF leg terminating on the ILS intercept point at different heights between 550 and 2,000 feet above ground level, resulting in a final approach length between 1.73 and 6.28 nautical miles. The individual approaches are named ILS S through ILS W and feature greater ILS intercept heights with ascending alphabetical order. For more information regarding the design of the experimental approaches, refer to [5].

Designation	ILS Intercept Height	Final Segment Length	Time on Final Segment (IAS = 140 kt)
ILS S RWY26	550 ft AGL	1.73 NM	~ 45 s
ILS T RWY26	750 ft AGL	2.36 NM	~ 61 s
ILS U RWY26	1,000 ft AGL	3.14 NM	~ 81 s
ILS V RWY26	1,500 ft AGL	4.71 NM	~ 121 s
ILS W RWY26	2,000 ft AGL	6.28 NM	~ 161 s

Table 3.1: Experimental approach design parameters

3.2.1. Structure

Each approach includes two initial approach fixes (IAF) that are connected to the entry point of the RF leg with a TF leg. The IAFs are placed so as to result in a track angle change in the RF leg of either 90 or 180 degrees. During the RNP part of the approach, i.e. up to the ILS intercept point, the vertical profile is designed to feature a constant descent with a flight path angle of minus two degrees starting at the IAF. The approaches ILS S through ILS V start in an altitude of 4,000 feet above sea level, whereas ILS W starts in 5,000 feet above sea level in order to provide a straight leg with a length sufficient for alignment prior to the entry point of the RF leg. Figure 3.3 and Figure 3.4 show the possible approach paths for the five experimental approaches.

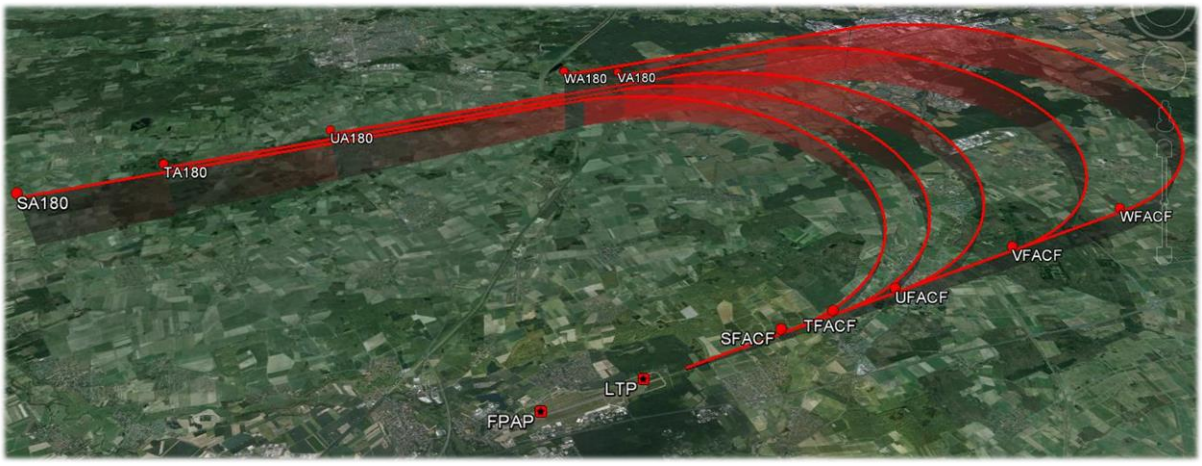

Figure 3.3: Approach paths with track angle change of 180 degrees <Google Earth>

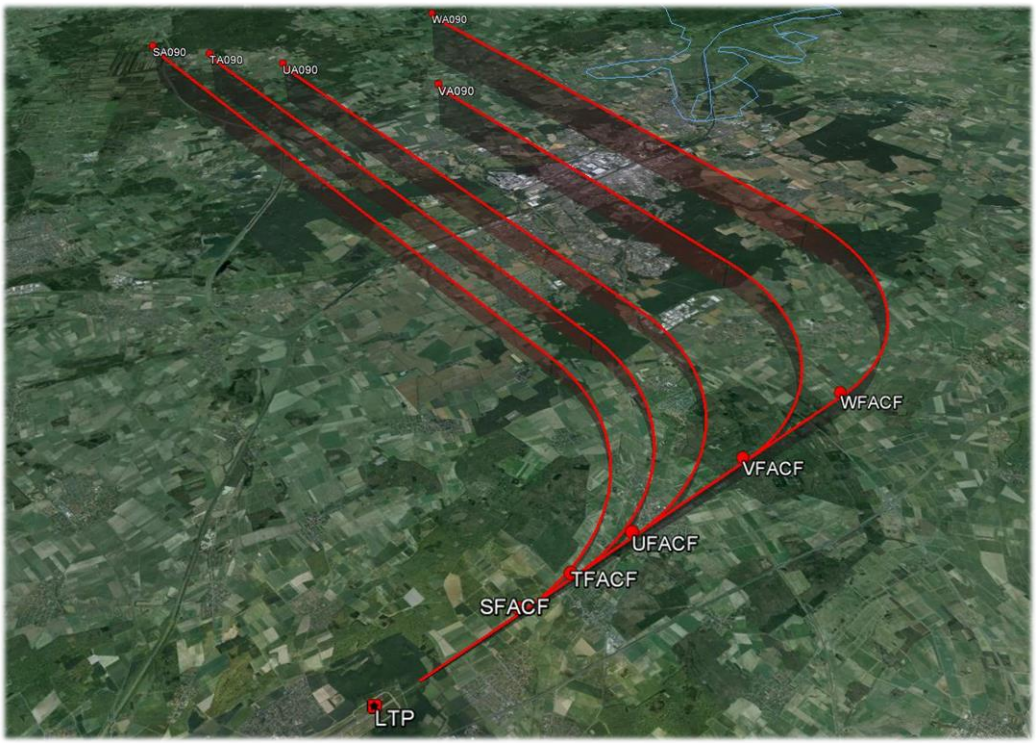

Figure 3.4: Approach paths with track angle change of 90 degrees <Google Earth>

The five-digit waypoint identifiers were chosen so as to allow a clear identification of both the approach and the individual path that the waypoint belongs to. As shown in Table 3.2, they are composed of two alphabetical and three numeric characters identifying the approach, the placement in the waypoint sequence and the track angle change during the RF leg. The final approach point (FAP) for each approach was originally named "xFAP0", where "x" refers to the name of the respective approach, e.g. "SFAP0". However, due to the way ILS approaches are coded in the ARINC 424 standard, the FAP had to be replaced with a Final Approach Course Fix (FACF) and an additional waypoint had to be inserted on the final approach. The ARINC 424 coding of the experimental approaches is described in greater detail in the next section.

Digit	Example	Description
1	S	Part of "ILS **S** RWY26"
2	A	First waypoint in the individual approach path
3-5	090	90° track angle change during the RF leg of the individual approach path

Table 3.2: Composition of the ARINC 424 waypoint identifier

3.2.2. ARINC 424 Coding

The set of experimental approaches was prepared for insertion into the navigation database of the ATRA by Lufthansa Systems FlightNav. A certified information technology service provider has to be tasked with the code conversion of the approaches for reasons of approval.

The ARINC 424 database obtained from Lufthansa FlightNav is a tailored database for the DLR, containing several other experimental approaches besides the RNP to ILS approaches. The first part contains the individual identifiers and positions of the waypoints as in the waypoint list in [5], while the second part consists of the approach records. Table 3.3 shows the layout for one 132 character waypoint record in the ARINC 424 standard and gives an example for the encoding of waypoint "SA090", one of the IAFs for the approach "ILS S RWY26". The records for all other waypoints are similar to the one exemplified in Table 3.3 and differ mainly in the contents of the fields for waypoint identifier and type as well as latitude and longitude.

ARINC 424 approach records are organized in a different layout as outlined in the example in Table 3.4. However, each experimental approach consists of several records that detail the available IAFs and the corresponding approach trajectories. Each record represents one leg of the approach, i.e. the flight path between two waypoints. Table 3.4 exemplifies the coding of the RF leg with a track angle change of 180 degrees leading to the ILS intercept point for the approach "ILS T RWY26". The complete ARINC 424 waypoint and approach records for the experimental RNP to ILS approaches can be found in appendix A.

Character	Example	Field Content	Description
1	T	Record type	T – Tailored data
2-4	DR1	Customer code	DLR
5	P	Section code	P – Airport section
6	(Blank)	Subsection code	Subsection code occupies character 13 for terminal waypoints
7-10	EDVE	Region code	ICAO identification code for Braunschweig-Wolfsburg airport
11-12	ED	ICAO code	E – Europe D – Germany
13	C	Subsection code	C – Terminal waypoint
14-18	SA090	Waypoint identifier	Waypoint "SA090"
19	(Blank)	Spacing	-
20-21	ED	ICAO code	See characters 11-12
22	0	Continuation record no.	Primary record
23-26	(Blank)	Spacing	-
27-29	WIF	Waypoint type	W – RNAV Waypoint I – Initial Approach Fix F – Published for use in approach procedures
30-31	(Blank)	Waypoint usage	Blank if terminal use only
32	(Blank)	Spacing	-
33-41	N52325622	Waypoint latitude	52° 32′ 56.22′′ North
42-51	E010391857	Waypoint longitude	010° 39′ 18.57′′ East
52-74	(Blank)	Spacing	-
75-79	E0025	Dynamic magnetic variation	2.5° East
80-84	(Blank)	Reserved	-
85-87	WGE	Datum code	WGS 84
88-95	(Blank)	Reserved	-
96-98	(Blank)	Name format indicator	Not applicable
99-123	SA090	Waypoint name/description	Waypoint name without further description
124-128	00082	File record no.	Entry no. 82 to the database
129-132	1506	Cycle date	Cycle 6 in 2015

Table 3.3: Exemplary ARINC 424 waypoint record

Character	Example	Field Content	Description
1	T	Record type	T – Tailored data
2-4	DR1	Customer code	DLR
5	P	Section code	P – Airport section
6	(Blank)	Spacing	-
7-10	EDVE	Airport identifier	ICAO identification code for Braunschweig-Wolfsburg airport
11-12	ED	ICAO code	E – Europe D – Germany
13	F	Subsection code	F – Approach procedure
14-19	I26–T	SID/STAR/approach identifier	I – ILS approach 26 – Runway identification – (dash) – Placeholder T – Approach indicator
20	A	Route type	A – Approach transition
21-25	TA180	Transition identifier	Waypoint "TA180"
26	(Blank)	Procedure design aircraft category or type	Not specified
27-29	030	Sequence no.	3rd waypoint in route sequence
30-34	TFACF	Fix identifier	Waypoint "TFACF"
35-36	ED	ICAO code	See characters 11-12
37	P	Section code	P – Airport section
38	C	Subsection code	C – Terminal waypoint
39	0	Continuation record no.	Primary record
40-43	EE B	Waypoint description code	E – Essential waypoint E – End of continuous segment (Blank) B – Intermediate approach fix
44	R	Turn direction	Right
45-47	031	RNP	RNP 0.3
48-49	RF	Path and termination	Radius to fix
50	(Blank)	Turn direction valid	Not applicable
51-54	BWG	Recommended navaid	Navaid identification for ILS/DME runway 26
55-56	ED	ICAO code	See characters 11-12
57-62	002600	ARC radius	Turn radius of 2.6 NM
63-66	0830	Theta	Magnetic bearing to the waypoint: 83°

67-70	(Blank)	Rho	Not specified
71-74	2630	Magnetic course	Outbound magnetic course from the waypoint: 263°
75-78	0026	Distance	Here: Turn radius instead of distance
79	P	Recommended navaid section code	P – Airport section
80	I	Recommended navaid subsection code	I – Localizer/Glide Slope
81	(Blank)	Leg inbound/outbound indicator	Not applicable
82	(Blank)	Reserved	-
83	(Blank)	Altitude description	"At" altitude constraint
84	(Blank)	ATC indicator	
85-89	01038	Altitude field 1	Waypoint altitude : 1038 feet
90-94	(Blank)	Altitude field 2	Not applicable
95-99	(Blank)	Transition altitude	Not applicable
100-102	(Blank)	Speed limit	Not applicable
103-106	(Blank)	Vertical angle	Not applicable
107-111	CFX02	Center fix	Reference to turn center fix "CFX02"
112	(Blank)	Multiple code	Not applicable
113-114	ED	ICAO code	See characters 11-12
115	P	Section code	P – Airport section
116	C	Subsection code	C – Terminal waypoint
117	(Blank)	GNSS/FMS indication	Not applicable
118	(Blank)	Speed limit description	Not applicable
119	D	Route qualifier 1	D – DME required for procedure
120	S	Route qualifier 2	S – Procedure with straight-in minimums
121-123	(Blank)	Vertical scale factor	Not applicable
124-128	00233	File record no.	Entry no. 233 to the database
129-132	1508	Cycle date	Cycle 8 in 2015

Table 3.4: Exemplary ARINC 424 approach record

Before the experimental approaches could be included in the navigation database of the ATRA, a small change to the approach structure was necessary. ARINC 424 coding of ILS approaches requires three consecutive waypoints on the final approach: a final approach course fix, a final approach fix (FAF) and the runway threshold. For conventional ILS approaches, the FACF is used

for initial alignment with the runway course before the transition to ILS guidance occurs at the FAF. However, as RNP to ILS approaches feature a curved segment prior to the ILS intercept point, no FACF can be placed on the extended runway centerline as required for ARINC 424 coding. This issue was circumvented by inserting an additional waypoint into the final approach between the ILS intercept point and the runway threshold. In order to adhere to the ARINC 424 nomenclature, the original ILS intercept point "xFAP0" was renamed to "xFACF" for each of the individual approaches. The additional waypoint was then designated as the new "xFAP0" waypoint and placed on the final approach about 0.7 nautical miles from the runway threshold for all five procedures. Although its coordinates and altitude are identical in all approaches, it was coded individually for each procedure so as to follow the naming scheme applied to the other waypoints. Figure 3.5 shows a comparison of the original layout of the final approach and the new layout adjusted for ARINC 424 coding.

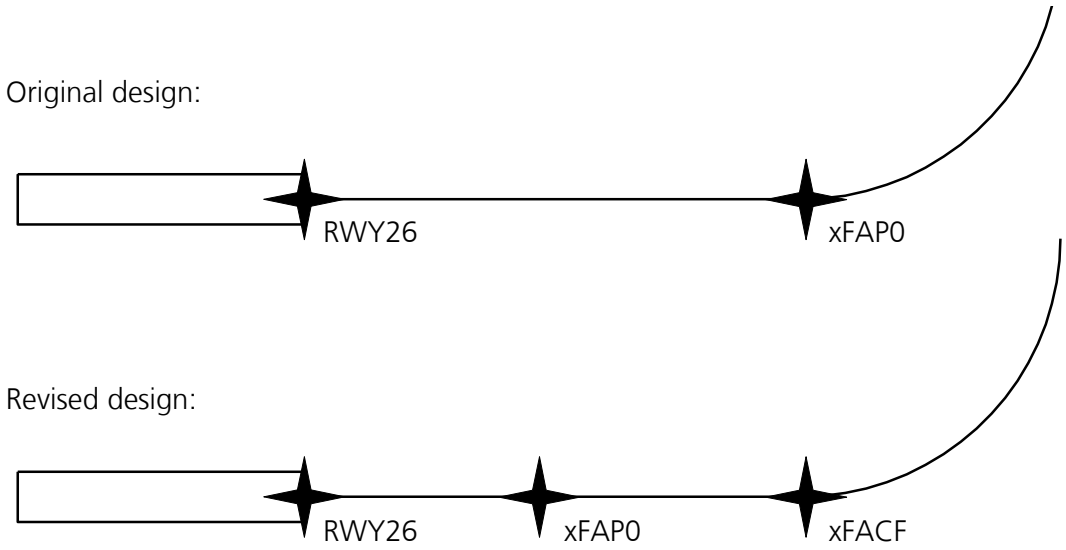

Figure 3.5: Original final approach layout and ARINC 424-compliant layout <own figure>

The vertical part of the approaches was coded with minimum altitude constraints in order to examine the vertical path generated by the FMS on the RNP part of the procedure. Only the IAF and the ILS intercept point received an "at" altitude constraint so as to ensure consistent start and end altitudes of the RNP trajectory. Beyond that, an "at" altitude is required at the ILS intercept point as the aircraft needs to be positioned as close to the glideslope as possible at the end of the turn to allow for a seamless transition to ILS guidance. As a result of this coding, the FMS is able to determine the vertical path prior the ILS intercept variably based on the current flight conditions.

3.3. Simulator Test

Prior to the flight tests with the ATRA, the experimental approaches were tested in an A320 full flight simulator in order to verify the correct functionality of the navigation database with the FMGS and identify possible system-related issues. Of peculiar interest was the vertical path generated by the FMS as no vertical path angle was coded for the procedures and the only altitude constraints were placed at the IAFs and ILS intercept points. The simulator tests were planned to gain an insight into the vertical path generation by the FMS and the requirements for the correct coding of the vertical path, as several possibilities exist for the inclusion of altitude information in the navigation database as described in section 2.6. Additionally, the height dependency of the ILS intercept performance was to be assessed in order to identify any problems with the planned schedule for the actual flight tests, which envisaged a gradual reduction of the intercept height, starting with an intercept height of 2,000 feet AGL in the approach "ILS W RWY26". Unfortunately, no ARINC 429 interface for data recording was available in the simulator, thus limiting the findings of the simulator tests to qualitative observations of the system behavior during the approaches.

3.3.1. Findings

During the simulator tests of the experimental approaches, the altitude constraints used in the ARINC 424 coding of the navigation database did not result in the intended vertical path. Instead, after passing the IAF, the FMS created a vertical path that included an idle descent down to the next altitude constraint and then continued with a level segment until the corresponding waypoint was reached. The intermediate level-off was placed shortly prior to the apex of the curve for the approaches with a track angle change of 180 degrees, which were tested primarily during the simulator session. As a result, the aircraft continued in level flight for the rest of the RF leg before the approach mode was armed at the end of curve and the passing of the associated altitude constraint allowed a further descent. Figure 3.6 shows the predicted level-off position marked by a magenta arrow on the navigation display (ND) of the simulator cockpit.

Figure 3.6: Early level-off as indicated on the simulator ND <own photograph>

This behavior, often called "dive and drive", is consistent with conventional "step-down" approach patterns that include a gradual descent. However, this method is contradicting the aims of RNP to ILS approaches as it is inefficient with regard to fuel consumption and noise abatement due to the relatively high thrust setting during the level segments when compared to an approach with a continuous descent. Although a very good glideslope capture performance can be achieved with the "dive and drive" technique, the drawbacks of extended horizontal flight are too severe for operational use in RNP to ILS approaches. Especially in the envisaged approaches with low ILS intercept heights, "dive and drive" would result in prolonged level flight in altitudes that are too low for safe operation in instrument meteorological conditions. Figure 3.7 illustrates the design vertical path and the vertical path generated by the FMS during the simulator tests.

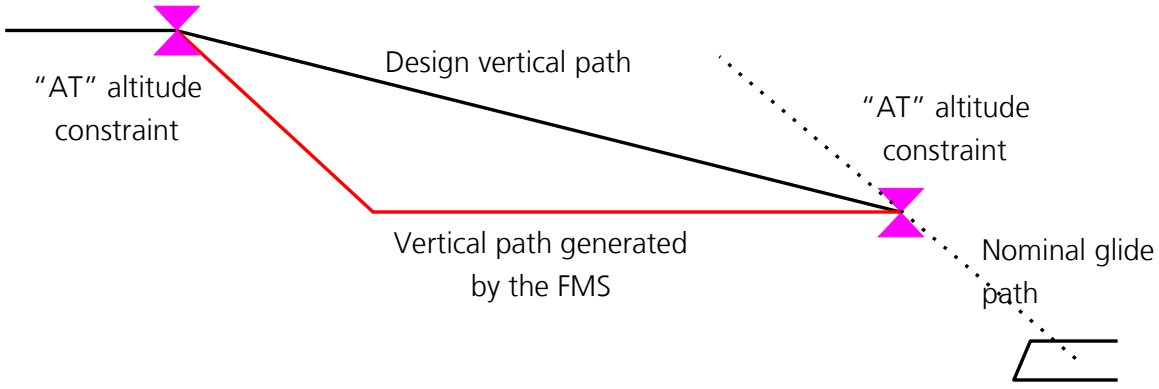

Figure 3.7: Design vertical path and „dive and drive" behavior of the aircraft <own figure>

The lateral navigation accuracy was, as expected, more than sufficient for immediate localizer capture at the end of the RF leg. In combination with the steeper descent followed by level flight, a very good overall ILS capture performance could be achieved and the aircraft was able to land automatically in all of the tested approaches.

In an attempt to recreate the design vertical path with a constant descent, the approaches were repeated with a manually selected flight path angle. In this case, lateral navigation and thrust setting were left in the managed autopilot mode and thus under the control of the FMS, while the vertical path was controlled via the selected autopilot mode. Starting at the IAF, a vertical path angle of minus two degrees was selected, resulting in a shallower descent. Using this method, the design vertical path was followed much more precisely, although multiple corrections to the selected flight path angle were necessary to reach the end of the RF leg at the target altitude. Without the corrections, the aircraft was too high when reaching the ILS intercept point, which increased the time required for glideslope capture. While automatic landing was still possible in all tested cases, the land mode engaged not until 150 feet AGL was reached for the lowest of the experimental approaches.

3.3.2. Consequences for Flight Test Preparation

The idle descent and resulting higher flight path angle observed during the simulator tests led to the conclusion that the database coding of the experimental approaches at that time was not adequate for the actual flight tests. Due to the large deviations from the design vertical path, the gathering of insightful data regarding the glideslope capture performance would be impossible. For this reason, a part of the experimental approaches was revised in the navigation database and supplemented with an additional altitude constraint at the beginning of the RF leg and a vertical path angle for the RNP part of the approach. The alternative coding was applied to the approaches with a track angle change of 90 degrees and added to the navigation database in the next ARINC cycle. As a result, the waypoint "xB090" of each approach now features an "at or above" constraint at its design altitude and a vertical path angle of minus two degrees is coded in the characters 103 through 106 for the approach records prior to the ILS intercept point "xFACF". The different realizations of the vertical path coding are compared in Figure 3.8.

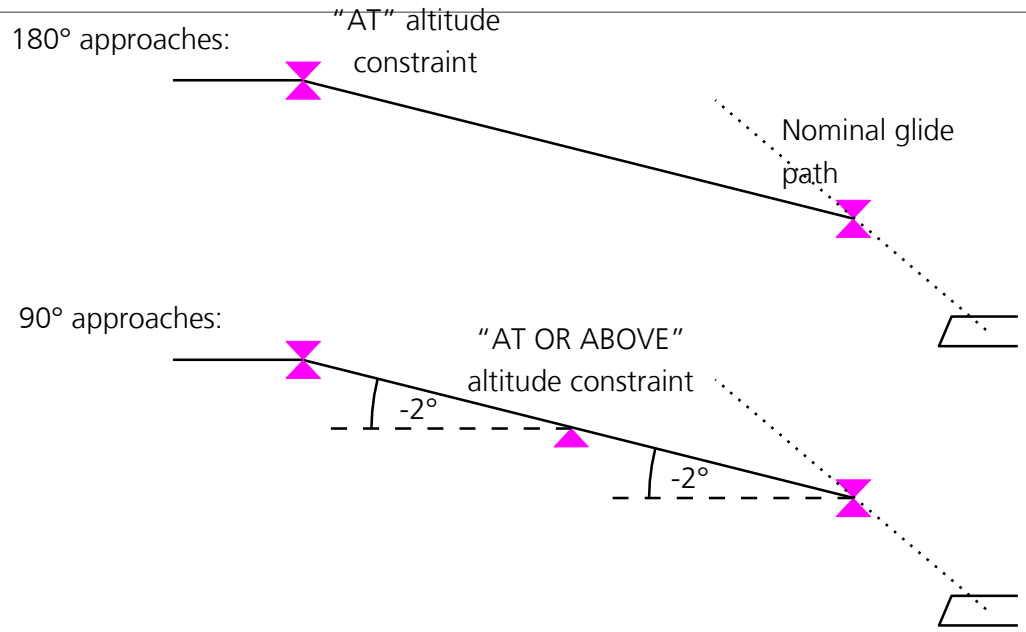

Figure 3.8: Vertical path coding with and without flight path angle <own figure>

Prior to the actual flight tests, it was unknown whether the FMS of the ATRA would respect the newly coded vertical path angle in an ILS approach before the approach mode is armed. Hence an "at or above" altitude constraint was included at the entry point of the curved segment to limit the "dive and drive" behavior in case the vertical path angle is disregarded by the FMS. The different coding of the two possible approach trajectories, i.e. either with a 90 degree or a 180 degree track angle change, allows the comparison of the vertical paths flown by the FMS for each variant. In order to assess the effects of the activation of the approach mode on the vertical path, the approaches with a track angle change of 90 degrees will be flown twice. During one of the approaches, the approach mode will be engaged when reaching the end of the RF leg as envisaged in the RNP to ILS concept described in [5], whereas it will be activated already at the IAF in the second approach. By comparing both approaches, conclusions can be drawn about the adherence to the design vertical path and whether it is necessary to activate the approach mode for the FMS to regard the vertical path angle coded in the navigation database.

3.4. Required Data

In order to be able to analyze the performance of the ATRA with regard to the objectives listed in section 3.1, the relevant data has to be identified and recorded during the flight tests. The most important parameters that need to be extracted from the on-board data stream for the evaluation of the flight tests are:

- System time for data sorting and synchronization
- Aircraft latitude and longitude as indicated by the integrated navigation systems, i.e. the hybrid position calculated from a coupled inertial navigation and satellite navigation system
- Aircraft altitude above sea level as computed by the air data computer from barometric height measurement
- Aircraft height above ground level as measured by the radar altimeter
- Glideslope and localizer deviations as computed by the FMGC
- Selected QNH and outside air temperature from the air data computer
- Aircraft speed, including true airspeed (TAS) and ground speed
- Active autopilot modes and autoland capabilities
- State of the "Approach" pushbutton

The hybrid position that is used for navigation by the FMGC is required for the calculation of the FTE. However, the calculation of the NSE requires the actual position of the aircraft to be known and is thus not realizable without additional measurements. An additional position reference is obtained from an additional GPS antenna and receiver installed in the ATRA. Using post-processed differential carrier phase data, a highly accurate measurement of the actual aircraft position can be calculated after the flight tests and used as a reference for the calculation of the NSE. These calculations require the recording of several additional parameters during the flight tests:

- GPS system time for data sorting and synchronization as well as application of post-processing corrections
- GPS latitude and longitude
- GPS height above the WGS 84 reference ellipsoid

With the exception of the autopilot modes and the state of the "Approach" pushbutton, all parameters were already part of the standard set of data that is recorded in each flight test. As part of the flight test preparation, the ARINC 429 labels containing the relevant autopilot modes and the pushbutton state were identified and added to the list of standard recordings. All

standard data can be easily extracted from the flight recording and converted into an ASCII text file for further processing. A complete list of the data available in the standard recording is presented in the next section.

3.4.1. Parameter List

A brief description of all standard data recorded during the flight tests with the ATRA is given in Table 3.5. All parameters are coded in either BNR or BCD notation and thus can be directly converted to decimal numbers in the ASCII text file. The only exceptions are the seven digital words from the flight guidance computer (FGC), the display management computer (DMC) and flight control unit (FCU), which contain – among other information – the active autopilot modes, automatic landing capabilities and the state of the "Approach" pushbutton. The respective 32-bit ARINC 429 digital words are stripped of their label, which is contained in the first eight bits, and then coded as a decimal value in the ASCII text file. In order to evaluate the word contents, this decimal value is converted back to binary notation. The state of the individual bits can then be interpreted according to the Airbus flight data interface management unit (FDIMU) parameter list for the ATRA.

Parameter name	Description
exo_time	UTC time since midnight in milliseconds
ATRA_Long	Longitude calculated by the on-board navigation system
ATRA_Lat	Current latitude calculated by the on-board navigation system
JAVAD_Long	Current longitude calculated by the external GPS receiver
JAVAD_Lat	Current latitude calculated by the external GPS receiver
JAVAD_Height	Current ellipsoidal height calculated by the external GPS receiver
exoGS_DEV	Angular deviation from the glideslope center in degrees
exoLOC_DEV	Angular deviation from the localizer center in degrees
mag_HDG	Magnetic heading in degrees
True_HDG	True heading in degrees
mag_TRC	Magnetic track in degrees
gnd_SPD	Ground speed in knots
x_ACCEL	Acceleration along the aircraft x-axis as multiple of g
y_ACCEL	Acceleration along the aircraft y-axis as multiple of g
z_ACCEL	Acceleration along the aircraft z-axis as multiple of g
ew_SPD	East-west velocity in knots
ns_SPD	North-south velocity in knots
pitch_Ang	Pitch angle in degrees
roll_Ang	Roll angle in degrees
fpa_Ang	Vertical flight path angle in degrees
vert_SPD	Vertical speed in feet per minute
Alfa	Angle of attack α in degrees
Beta	Sideslip angle β in degrees
wnd_Ang	Wind direction in degrees
wnd_SPD	Wind speed in knots
gear	State of the landing gear (0 = up, 1 = down)
slats	Slat position in degrees
flaps	Flap position (0 to 4)
spoiler	Spoiler position in degrees
Eta	Elevator deflection in degrees
Xi	Aileron deflection in degrees
Xeta	Rudder deflection in degrees
nose_whl	Nose wheel steering angle in degrees

re_QNH	Selected QNH in hectopascal
pressAlt	Altitude with respect to selected QNH in feet
std_qnh_Alt	Altitude with respect to standard QNH in feet
radar_Alt	Radar altitude in feet
TAS	True airspeed in knots
SAT	Static air temperature in degrees Celsius
CAS	Calibrated airspeed in knots
m_Mach	Mach number
stat_Press	Static pressure in hectopascal
max_ASPD	Maximum airspeed in knots
min_ASPD	Minimum airspeed in knots
dem_CAS	Demanded calibrated airspeed in knots
dem_HDG	Demanded heading in knots
dem_ALT	Demanded altitude in feet
dem_ALTR	Demanded altitude rate in feet per minute
dem_Roll	Demanded roll angle in degrees
n1_l	N1 left engine in percentage of maximum RPM
n1_r	N1 right engine in percentage of maximum RPM
ff_l	Fuel flow left engine in kilograms per hour
ff_r	Fuel flow right engine in kilograms per hour
EGT_l	Exhaust gas temperature left engine in degrees Celsius
EGT_r	Exhaust gas temperature right engine in degrees Celsius
Throtl1	Throttle lever angle engine 1 in degrees
Throtl2	Throttle lever angle engine 2 in degrees
DW276_31D	ARINC 429 label 276 from the DMC
DW274_22G	ARINC 429 label 274 from the FGC
DW275_22G	ARINC 429 label 275 from the FGC
DW146_22G	ARINC 429 label 146 from the FGC
DW273_22G	ARINC 429 label 273 from the FGC
DW270_22G	ARINC 429 label 270 from the FGC
DW274_22C	ARINC 429 label 274 from the FCU

Table 3.5: Standard parameters recorded during ATRA flight tests

4. Execution of the Flight Tests

In the following chapter, the test aircraft A320-ATRA and its auto flight system are described with a focus on the autopilot modes and automatic landing capabilities that apply to ILS approaches followed by an automatic landing. Additionally, the flight test installation used for data recording during the flight tests and the flight test procedure are presented.

4.1. Test Aircraft and Auto Flight System

The ATRA is an A320-232 that has been modified with experimental equipment for the various research tasks of the DLR. As the largest member of the fleet of research aircraft operated by the DLR and as one of the most commonly used aircraft types in civil aviation, it offers several possibilities for the trial of new technologies and procedures in the field of flight guidance. To fulfill its role as a research aircraft, the ATRA is equipped with modular experimental equipment as well as data interfaces that allow the monitoring and recording of all flight parameters, including the inter-system communication of the various sub-systems [17].

Besides the evaluation and testing of new displays, the Department of Pilot Assistance of the DLR Institute of Flight Guidance is involved in the development of new procedures that aim to reduce the track mileage and noise pollution of the terminal flight phases. In the flight testing of the experimental RNP to ILS approaches, the ATRA is used to investigate the behavior and autoland performance of the auto flight system with regard to RF legs ending on a short ILS final segment. As mentioned in section 3.1, the vertical path generation and ILS intercept performance of the FMGS are of particular interest for this investigation. For this reason, the individual autopilot modes that are active during the RNP to ILS approaches are recorded and evaluated to gain an insight into possible limitations that result from the system functionality.

The ATRA is equipped with a Thales FMS2 that contains two flight management and guidance computers (FMGC), two multipurpose control and display units (MCDU), a flight control unit (FCU) and two flight augmentation computers (FAC). The combination of these subsystems is the flight management and guidance system (FMGS), which performs many routine flight planning operations and gives predictions of flight time, mileage, speed and altitude. Estimations are based on routes selected from the navigation database, which are inserted into the active flight plan via the MCDU during flight preparation. The FMGS also calculates altitude and speed profiles for the

desired route and takes into account aircraft performance criteria and air traffic control (ATC) requirements [18].

In managed mode, the FMGS steers the aircraft along the preplanned lateral route in accordance with the calculated altitude and speed profiles based on navigation and aircraft performance data. Temporary modifications to flight parameters such as speed, heading, altitude or vertical speed can be entered manually via the FCU. In this case, the FMGS disregards the preplanned route and guides the aircraft according to the manually selected values. This so-called selected mode always has priority over managed mode and remains active until the crew reactivates the managed mode manually.

During normal operation, the FMGS is in dual mode and both FMGCs are synchronized, i.e. they compare their individual computations and exchange data. Inputs can be made to both MCDUs and are transferred to both FMGCs and all peripherals. In case any abnormal conditions are detected, the FMGS automatically reverts to independent mode. In this degraded mode, both FMGCs work independently and are only linked to peripherals on their respective side of the flight deck. FMGC single mode becomes active if one of the two FMGCs fails. In such an event, the MCDU on the side of the failed FMGC can be connected to the remaining operative FMGC, causing all peripherals to operate based on the outputs of this system.

4.1.1. Flight Planning and Performance Predictions

The navigational functions of the FMGS are based on the aircraft position as computed by the two FMGCs. In Airbus terminology, this position is designated as the flight management (FM) position and is computed from a combination of an inertial reference system (IRS) position and a radio or GPS position. The selection of the positioning equipment is based on the estimated accuracy and integrity of each system. When GPS data is available and successfully tested, the FMGC operates in mixed navigation mode using IRS and GPS position. In case reliable GPS data is not available, the system reverts to the use of a combination of IRS position and any available navaids or IRS position only.

IRS position is computed by the FMGCs based on a mean-weighted average of the three IRSs onboard the aircraft and is thus named the "MIX IRS" position. If one of the three IRSs drifts abnormally or fails, its influence on the "MIX IRS" position is either decreased or it is rejected completely. When GPS data is available, each IRS computes a mixed position based on IRS and

GPS, the so-called "GPIRS" position. One of the three "GPIRS" positions received by each FMGC is selected based on a figure of merit and priority. If the "GPIRS" data fails to comply with an integrity criterion, GPS mode is rejected and radio positioning is used instead to complement the IRS position data.

As long as either a GPS or a radio position is available in addition to the "MIX IRS" position, a bias vector is computed from the "MIX IRS" to the GPS or radio position and updated continuously. If the GPS or radio position is lost, the last bias vector is memorized and used for the computation of the FM position in IRS only mode. When additional navigation systems are available again, the system resumes a mixed navigation mode and continues updating the bias vector with the new position information. In decreasing order of priority, the four navigation modes for enroute navigation are [18]:

- IRS-GPS
- IRS-DME/DME
- IRS-VOR/DME
- IRS only

The FMGS also computes an estimated position uncertainty (EPU) in order to give an indication of the available navigation accuracy. Depending on the navigation mode in use, the EPU varies between 0.05 nautical miles for IRS-GPS mode and 0.42 nautical miles in IRS-VOR/DME mode. In IRS only mode, the EPU cannot be specified as a threshold value due to the drift of the IRS and is instead given as the current drift rate in nautical miles per hour. Navigation accuracy is classified as either high or low, depending on whether the EPU exceeds the current RNP value. In IRS-GPS mode, an additional integrity requirement for failure detection and warning is included in the estimate of the navigation accuracy.

In addition to its navigation functionality, the FMGS also computes predictions for events such as reaching the top of climb or top of descent for the active flight plan and displays them to the crew on the ND. The computations are based on the current state of the aircraft and environmental conditions, i.e. weight, center of gravity, altitude, speed, engaged autopilot modes, wind and air temperature. Predictions are based on the assumption that the aircraft will continue to operate in the currently active managed or selected autopilot modes. If any deviations from the planned lateral and vertical profile occur or the active flight plan is revised by the crew,

the FMGC updates its predictions and the corresponding indications to match the new circumstances. Indications on the ND are known as pseudo waypoints and are depicted with the symbols from Table 4.1.

Symbol	Definition
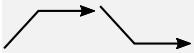	Top of climb or level-off at the position where the aircraft will reach the altitude selected in the FCU (blue) or the current altitude constraint if it is more restrictive than the FCU altitude (magenta)
	Top of descent (white) or continue descent (blue if descent mode is armed, white if it is not)
	Start of climb (blue if climb mode is armed, white if it is not)
	Predicted intercept of the descent path if there is a vertical deviation in descent mode (blue if descent mode is armed, white if it is not)
	Speed change at the position where the aircraft will automatically accelerate or decelerate to a new speed to meet a speed limit or constraint (magenta)
	Decelerate point at the position where the aircraft is predicted to decelerate for approach (magenta if in managed speed mode and navigation mode or approach mode is engaged, white if in selected speed mode or heading/track mode)
	Altitude constraint symbol at the corresponding waypoint (magenta if the constraint is predicted to be met, amber if it is predicted to be missed and white if the constraint is not taken into account by the FMGS and navigation mode is engaged)
 (10  (ETP)	Time or equitime point marker at the position where the aircraft reaches a time marker or equitime point (green)
	Energy circle symbol representing the required distance to land (green). Centered on the aircraft position and oriented to the current track line. Only displayed in descent and approach phases and in selected heading/track mode.

Table 4.1: Pseudo waypoint symbols and definitions [18]

In addition to the pseudo waypoints, the FMGC also computes the predicted time of arrival at the next waypoint in the flight plan and shows this information in the upper right corner of the ND. For this calculation, the direct distance to the waypoint is used and the current ground speed is assumed to remain constant.

4.1.2. Autopilot Modes

The tasks of the autopilot are stabilization of the aircraft around its center of gravity, acquiring and tracking of a flight path and controlling the aircraft during automatic landings or go-arounds. For this purpose, it commands the positions of the control surfaces for pitch, roll and yaw as well as the nose wheel position when the aircraft is on the ground. Only one of the two autopilots of the A320 can be engaged at any time except when the localizer and glideslope or go-around mode is active, which allows the second autopilot to be engaged in standby mode to take over control if the first autopilot fails. In addition to the two autopilots, the autothrust function of the FMGS is available to control the aircraft speed or thrust setting of the engines. While the autopilot can control either a target speed or a vertical trajectory using its pitch modes, the autothrust can control either a target speed or a fixed thrust setting. However, it is not possible for both systems to control the target speed simultaneously. Hence the selection of the autopilot mode determines the autothrust mode as follows [18]:

- When the autopilot pitch mode controls a vertical trajectory, the autothrust is in control of the target speed.
- When the autopilot pitch mode controls a target speed, the autothrust controls the thrust setting.
- When no autopilot pitch mode is engaged, the autothrust controls the target speed.

The modes of the A320 autopilot can be categorized into three groups, depending on whether they are used for control in lateral or vertical navigation or for speed control. Each of these groups can be further divided into managed and selected guidance modes as illustrated in Table 4.2

Guidance	Managed modes	Selected modes
Lateral	NAV, APP NAV LOC*, LOC RWY RWY TRK GA TRK ROLL OUT	HDG-TRK
Vertical	SRS (TO and GA) CLB, DES ALT CST, ALT CST* ALT CRZ G/S*, G/S FINAL, FINAL APP FLARE	OP CLB, OP DES V/S, FPA ALT*, ALT EXPEDITE
Speed	FMGC REFERENCE (ECON, Auto SPD, SPD LIM) EXPEDITE	FCU REFERENCE

Table 4.2: A320 autopilot guidance modes [18]

Managed guidance modes can be engaged in different ways depending on their purpose. In general, managed modes are armed by pushing the appropriate knob on the FCU. However, managed modes also engage automatically after take-off when the thrust levers are positioned accordingly, a "direct to" leg is inserted in the MCDU or the approach or localizer pushbuttons are pushed. As opposed to this, the selected modes can only be engaged by pulling the appropriate knob on the FCU.

Lateral and vertical modes are explained in greater detail in Table 4.3 and Table 4.4.

Mode	Guidance	Remark
RWY	Takeoff guidance along the runway centerline using LOC	Activated by thrust levers in takeoff/go-around position
RWY TRK	Guidance along the track followed at mode engagement	Automatically armed at takeoff if HDG-TRK is preselected
NAV	Guidance along the lateral flight plan	Automatically armed at takeoff unless HDG-TRK is preselected
HDG-TRK	Aircraft follows the heading or track selected by the flight crew on the FCU	Basic mode to which the FMGS reverts in case of a flight plan discontinuity or loss of flight plan
LOC*	Localizer capture mode, i.e. aircraft automatically intercepts the localizer signal	Engaged by pressing the "LOC" or "APPR" pushbuttons on the FCU
LOC	Localizer track mode, i.e. aircraft follows the localizer signal	Engages subsequently to LOC* mode after the aircraft is established on the localizer
APP NAV	Guidance along the lateral approach path	Engaged by pressing the "APPR" pushbutton with a non-precision approach selected in the flight plan
LAND	Common mode used below 400 feet radio altitude during automatic ILS approaches	Engages only if both LOC and G/S modes are already engaged
GA TRK	Go-around guidance along the track followed at mode engagement	Triggered by moving the thrust levers to go-around position
ROLL OUT	After-landing guidance along the runway centerline	Engages automatically after an automatic landing

Table 4.3: A320 autopilot lateral modes [18]

Mode	Guidance	Remark
SRS	Takeoff and go-around guidance to maintain a safe speed provided by the speed reference system (SRS)	Activated by thrust levers in takeoff/go-around position. Automatic disengagement when reaching the acceleration altitude or engaging another vertical mode.
CLB	Climb towards the altitude selected in the FCU along the vertical flight plan with consideration of altitude constraints	Only available if lateral NAV mode is engaged. The autothrust system manages thrust.
DES	Descent towards the altitude selected in the FCU along the vertical flight plan with consideration of altitude constraints	Only available if lateral NAV mode is engaged. The autothrust system can manage either speed or thrust.
OP CLB OP DES	Direct climb or descent towards altitude selected in the FCU without consideration of altitude constraints	The autothrust system manages thrust
EXPEDITE	Increased vertical speed during climb or descent with either maximum lift to drag ratio in climb or Mach 0.8/340 knots in descent	Selected mode for faster climb or descent towards new altitude
ALT CST* ALT CST	Altitude constraint capture and altitude constraint track modes, i.e. consideration of altitude constraint from the vertical flight plan	CLB or DES mode is armed to engage after altitude constraint is passed
ALT* ALT ALT CRZ	Altitude acquire, altitude and cruise altitude modes to maintain level flight at the altitude selected in the FCU	ALT CRZ is part of the managed guidance and engages if the altitude selected in the FCU equals the cruise altitude
V/S-FPA	Vertical guidance according to a selected vertical speed or vertical flight path angle	Basic mode. The selected target altitude is displayed in blue on the PFD.
G/S* G/S FINAL	Glideslope capture, glideslope track and final approach modes, i.e. the aircraft captures and follows the glideslope or the vertical path of a non-precision approach	Engaged by pressing the "APPR" pushbutton with a precision approach (G/S*, G/S) or a non-precision approach (FINAL) selected in the flight plan
FLARE	Common mode used for flare on the pitch axis during automatic	Engages below 50 feet radio altitude, taking into account the current vertical speed

	landings

Table 4.4: A320 autopilot vertical modes [18]

The current status of the autothrust system, the lateral and vertical modes of the autopilot, the approach capabilities and the engagement status of the autopilot and autothrust systems is displayed on the Flight Mode Annunciator (FMA), which is located directly above the Primary Flight Display (PFD) in front of each pilot. It has a tabular structure and is composed of five columns and three rows, in which information about the various subsystems of the auto flight system is displayed as shown in Figure 4.1.

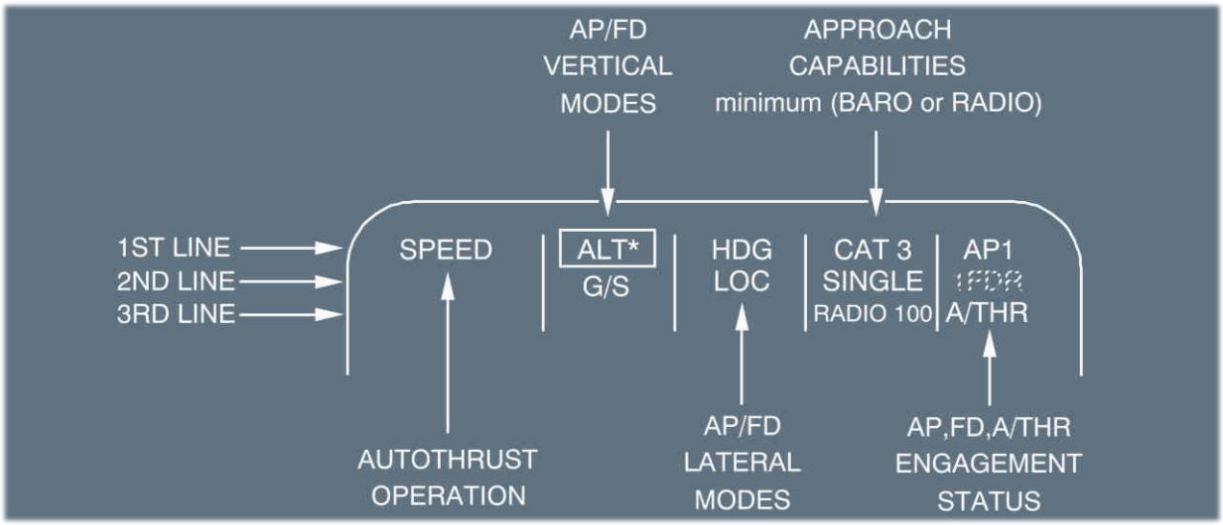

Figure 4.1: A320 flight mode annunciator [18]

The first column shows the engaged mode of the autothrust system in the first row and the armed mode in the second row. The same structure is used in the second and third row, but with regard to the vertical and lateral modes of the autopilot respectively. All engaged modes, i.e. the first row of the first three columns, are displayed in green, while the armed modes, i.e. the second row, are displayed either in blue or magenta. Following each mode change, the FMA displays a white box around the newly engaged mode for ten seconds. If an armed mode is displayed in magenta, this indicates that the mode was armed due to an FMGS constraint. The third row of the first three columns is used for special messages regarding the flight controls and the FMGS. Messages related to the flight controls such as the instruction to use manual pitch trim have priority over messages related to the FMGS.

In the fourth column, messages regarding the approach capabilities of the aircraft are displayed in rows one and two using white color. More information about the approach capabilities of the

A320 and their application for autoland operations can be found in section 4.1.3. The current minimum altitude for the approach is displayed in blue in the third row and can be expressed either as a barometric or a radio altitude, depending on the type of approach that is flown.

Information about the engagement status of the two autopilots and the autothrust system is displayed in the fifth column. The first row shows the currently active autopilot in white, which can be either autopilot one, autopilot two or simultaneous operation of both autopilots during approaches with ILS guidance. On the second row, the flight director engagement status on the two PFDs in the cockpit is displayed in white. The third row contains either a white indication when the autothrust system is active, a blue indication when it is armed or nothing in case it is not active. All autothrust and autopilot modes as well as approach capabilities of the two FMGCs are synchronized by the FMGS to provide identical information on the two individual FMAs.

4.1.3. Automatic Landing Capabilities

Automatic landing with the A320 requires the availability of a ground-based navigation system that provides guidance to the auto flight system during the final approach. In case of an ILS approach, the autopilot modes involved in an automatic landing are:

Vertical Modes	Lateral Modes
G/S* (capture) G/S (track)	LOC* (capture) LOC (track)
Common Modes LAND, FLARE, ROLL OUT	

Table 4.5: A320 autopilot modes for ILS-based automatic landing [18]

An ILS-based automatic landing can be initiated by pressing the "Approach" pushbutton on the FCU with an ILS approach selected in the active flight plan. As a result, the G/S and LOC modes are armed and appear in blue in the second row of the appropriate columns of the FMA. Besides the selection of an ILS approach, this requires ILS and radio altitude signals to be available and the aircraft to be above 400 feet radio altitude. Given these requirements, the G/S and LOC modes will engage automatically once the capture conditions are met. Furthermore, the second autopilot may be engaged in approach mode in order to obtain fail-operational autoland capability.

Depending on parameters such as ILS signal quality and availability of radio altimeter data, each FMGC computes its automatic landing capability, which is displayed in the fourth column of the

FMA. For an automatic landing, at least "CAT2" capability needs to be indicated by the FMGCs. "CAT3 SINGLE" is indicated when full autoland capability is available with one active autopilot, i.e. the auto flight system is fail-passive. In normal operation, however, the second autopilot is engaged after activation of the approach mode and "CAT3 DUAL" is announced on the FMA, indicating that the auto flight system is fail-operational.

When the aircraft reaches a position where ILS capture conditions are fulfilled, the G/S* and LOC* modes engage automatically. Engagement of the G/S* mode does not require valid radio altimeter data, but only "CAT1" autoland capability will be displayed on the FMA until radio altimetry becomes available. However, the G/S* mode cannot engage until LOC* mode is engaged or when the aircraft is above the glide path and its planned trajectory does not cross the glideslope. After engagement of the G/S* and LOC* modes, the auto flight system establishes the aircraft on the glideslope and localizer axes. When established on the axes, the respective G/S and LOC modes engage and the aircraft is guided horizontally and vertically along the ILS until a radio altitude of 30 feet is reached.

After passing 400 feet radio altitude, the common LAND mode engages automatically if G/S and LOC modes were engaged previously. In LAND mode, G/S and LOC modes are locked and cannot be changed or disengaged via the FCU. The auto flight system continues the approach and triggers the successive engagement of the FLARE and ROLL OUT modes. LAND mode can only be disengaged after landing, by initiating a go-around or by disengaging both autopilots. When reaching approximately 40 feet radio altitude, the FLARE mode engages. In this mode, the yaw axis of the aircraft is aligned with the runway centerline while the aircraft flares on the pitch axis to reduce its vertical speed for landing. If the autothrust system is active, both engines are automatically reduced to idle thrust. After touchdown, ROLL OUT mode engages for guidance along the runway centerline until the aircraft leaves the runway or comes to a stop.

4.2. In-Flight Data Recording

In order to provide real-time data during flight tests, the ATRA is equipped with a Flight Test Installation (FTI) that manages the acquisition and transmission of data from the various sensors and equipment used in the aircraft. The ATRA-FTI is a modular unit consisting of eight logical measurement systems that are allocated to four chassis and are interconnected via Ethernet. Sensor values and ARINC 429 words are gathered and processed by several signal processors in

each chassis and then provided to the measurement systems via the Ethernet connection. Computers connected to the FTI network can access and process the base data as desired via a Component Object Model (COM) interface. However, utilization of the COM interface requires proprietary libraries and the use of the Windows operating system, thus limiting the possible applications. For this reason, a more flexible interface is provided by the IENA format developed by Airbus. Two IENA converters generate a data stream from the received network packages and archive the measured data within the FTI data recorder [19].

The IENA format summarizes all data recorded during a flight and the individual timestamps and thus enables the consistent processing and storage of data acquired in different flight tests. Each IENA frame consists of a header containing an identifier as well as the size, timestamp and status information of the data transmitted in the frame. It is followed by the user data area containing the measured values that are to be transmitted and a field signaling the end of the IENA frame. Due to its platform independence and the possibility to reproduce recorded IENA frames independently from the measurement system, the IENA format is ideally suited for the preparation and evaluation of flight tests.

Flight test data is written to the IENA data stream according to a XidML specification. XidML is an open standard extensible markup language developed for the aerospace industry and is used to describe how digital information is acquired, processed, transmitted and stored. The IENA data stream is decoded by a program called "IenaDecoder", which was developed at the Institute of Flight Guidance. It can be used for online decoding of the IENA data stream during flight tests and for post-processing of recorded IENA frames. Data recorded during flight tests can be reproduced in real time or in fractions and multiples of the original recording speed. Since the IENA data stream contains a large amount of information, the user can select the parameters of interest before starting the playback of the record. All selected parameters are then written to an ASCII file at the selected sampling rate. A typical sampling rate for data recorded during flight tests is 20 hertz.

4.3. Flight Test Procedure

As mentioned in section 3.3.2, the simulator tests of the experimental RNP to ILS approaches resulted in a change of the ARINC 424 coding of the approach paths with a track angle change of 90 degrees, which now include an additional altitude constraint and a vertical path angle.

Consequently, this approach path is planned to be flown twice per ILS intercept height in order to assess the implications of pressing the "Approach" pushbutton at different times, i.e. when passing either the IAF or the ILS intercept point. Including the single approach with a track angle change of 180 degrees, there are three planned approaches per ILS intercept height. Given that there are five experimental approaches with different ILS intercept heights, an overall number of 15 approaches are to be flown with the ATRA during the flight test campaign. In order to be able to verify correct data recording and perform a preliminary data analysis, the approaches are scheduled to be flown in three groups of five approaches each over a time period of three weeks. Within the individual groups, the approaches are mixed with regard to ILS intercept height, track angle change and time of pressing the "Approach" pushbutton. Within Table 4.6, the flight test schedule for the experimental RNP to ILS approaches is shown with the identification letter of the respective approach and the track angle change during the RF leg. In case the approach is to be flown with the "Approach" pushbutton pressed at the IAF, this is stated as well in order to be able to distinguish between the two approaches with a track angle change of 90 degrees. Note that within each group, the first approach intercepts the ILS at 2,000 feet above ground (ILS W RWY26). The intercept height is then gradually decreased until the lowest experimental approach is reached (ILS S RWY26).

Approach No.	Week 1	Week 2	Week 3
1	W 90°	W 90° APPR	W 180°
2	V 180°	V 90°	V 90° APPR
3	U 90° APPR	U 180°	U 90°
4	T 90°	T 90° APPR	T 180°
5	S 180°	S 90°	S 90° APPR

Table 4.6: Flight test schedule

However, due to unforeseen problems with the flight test permit, the experimental approaches could not be flown in compliance with the original schedule and had to be postponed for several weeks. For this reason, the original concept of testing one group of approaches per week was dismissed. Instead, the 15 approaches were flown on three different days within the same week, although this reduced the available time for data checks. While the sequence of approaches as envisaged in Table 4.6 was kept, the grouping of the approaches had to be adjusted due to weather conditions. The first approach, ILS W RWY26 with a track angle change of 90 degrees,

was flown on July 16, 2015, when the ATRA returned to Braunschweig-Wolfsburg airport from another flight test. Data recorded during this approach was analyzed for completeness before the remaining approaches were flown in the following week between July 20 and July 23, 2015.

Each approach was flown up to a full stop or touch and go landing, i.e. all autopilot modes that are part of an automatic landing engaged successively as described in section 4.1.3. After takeoff, the flight crew contacted the appropriate radar controller and informed them about the starting position and altitude of the next approach. The flight crew then climbed to the altitude of the IAF of the respective approach, i.e. 4,000 feet MSL for the approaches ILS S, T, U and V and 5,000 feet MSL for the approach ILS W, and aligned the aircraft with the initial track to be flown after passing the IAF. For the approach paths with a track angle change of 180 degrees, this was an extended traffic pattern with the IAF positioned in the downwind leg. As the approaches with a track angle change of 90 degrees start with a southern track, the flight crew set a northern course after takeoff and aligned the aircraft with the initial track by turning about 180 degrees to the right. Initially, ATC was only able to issue a descent clearance to the Minimum Vectoring Altitude (MVA) of 3,500 feet MSL as the experimental RNP to ILS approaches are no officially published approach procedures. Thus the remaining part of the descent could only be cleared by ATC after the flight crew reported the field in sight and a visual approach was possible. This entails a requirement for good weather conditions that provide sufficient visibility and cloud ceilings.

After reporting the field in sight and receiving clearance from ATC for further descent at the discretion of the flight crew, the altitude of the ILS intercept point of the respective approach is entered in the FCU, indicating to the auto flight system that it is cleared to descent down to this altitude. At this stage, the only remaining tasks for the flight crew are the configuration of the flaps and landing gear, monitoring of the flight parameters and activation of the approach mode at the end of the curved segment or the IAF according to the flight test schedule. After the transition to ILS guidance and engagement of the G/S and LOC modes, the flight crew monitors the descent and subsequent engagement of the LAND mode. In case of a touch and go landing, the aircraft is configured for takeoff immediately after touchdown. After takeoff, the previously described flight test procedure is repeated for the next approach.

All in all, the flight tests could be conducted as scheduled. However, due to emerging clouds in the altitude of the IAF, the second test run had to be aborted as ATC clearance for a visual

approach could no longer be obtained. As a result, only three of the five planned approaches could be tested on this day, leaving the remaining two approaches for the third test run, which then included seven approaches. In addition, the first test of the approach "ILS S RWY26", which was conducted with a track angle change of 180 degrees during the RF leg and thus without a vertical path angle coded in the navigation database, had to be aborted due to the "dive and drive" behavior of the aircraft, as this would have led to a horizontal segment in a very low altitude. The flight crew decided to abort this approach due to reasons of safety. The aborted approach was not repeated in a later test run but instead replaced with an approach with an identical ILS intercept height and a coded vertical path angle. An overview of the actually conducted flight tests is given in Table 4.7. Appendix B shows plots of the lateral trajectory for each approach and details the atmospheric conditions during the individual flight tests.

During the flight test of approach "ILS U RWY26" with a track angle change of 90° and engagement of the approach mode at the IAF, an early engagement of the LOC* mode could be observed due to a side lope of the localizer signal. The approach was continued normally after a brief intervention of the flight crew to realign the aircraft with the intended flight path. However, as a result of this observation, it was decided to omit the activation of the approach mode at the IAF for the approaches "ILS T RWY26" and "ILS S RWY26", as these approaches intercept the ILS even closer to the runway and were thus expected to create the same issue. The approaches "ILS W RWY26" and "ILS V RWY26" were tested as intended in the schedule to determine whether they would be affected by the localizer side lope as well. Due to the greater distance between the localizer antenna and the ILS intercept point in these approaches, the effect of the localizer side lope was not observed and the auto flight system followed the flight path without early engagement of the LOC* mode.

Approach No.	Date	Approach	Remarks
1	16 July 2015	ILS W 90°	
2	20 July 2015	ILS V 180°	
3	20 July 2015	ILS U 90°	"APPR" at IAF Early engagement of LOC* mode due to localizer side lobe
4	20 July 2015	ILS T 90°	
5	20 July 2015	ILS S 180°	Aborted due to prolonged level flight in ILS intercept altitude as a result of "dive and drive"
6	20 July 2015	ILS W 90°	"APPR" at IAF
7	21 July 2015	ILS V 90°	
8	21 July 2015	ILS U 180°	
9	21 July 2015	ILS T 90°	"APPR" at IAF planned but canceled due to expected localizer side lobe
10	23 July 2015	ILS W 180°	Manual at or above altitude constraint at WB180
11	23 July 2015	ILS T 90°	Late approach mode engagement
12	23 July 2015	ILS S 90°	Above glideslope at ILS intercept point
13	23 July 2015	ILS V 90°	"APPR" at IAF Temporary autopilot disconnect due to VFR traffic
14	23 July 2015	ILS U 90°	Late descent clearance out of 3,500 feet
15	23 July 2015	ILS V 180°	"APPR" at IAF Short level segment due to ATC
16	23 July 2015	ILS S 90°	

Table 4.7: Flight test procedure for RNP to ILS approaches at Braunschweig-Wolfsburg airport

5. Data Analysis and Results

The necessary calculations for the determination of the navigation errors during the experimental approaches as well as the results with regard to navigation accuracy, ILS intercept capability and autoland performance are described in this chapter. Furthermore, feedback regarding the viability of the procedures that was received from the flight crew of the ATRA after the RNP to ILS approaches is presented.

5.1. Navigation Accuracy

Adherence to the intended lateral and vertical paths of the experimental approaches is evaluated by computing the lateral and vertical components of the FTE for each approach flown with the ATRA. The position information recorded during the flight tests is compared against the respective design trajectory on the basis of the methods described in [20] and [21]. However, since the deviations are to be computed for the whole approach including the curved RF leg, the procedure had to be modified since it is originally only used for straight final approach segments. The original method uses unit vectors to split the overall difference between the measured aircraft position and the design trajectory into its longitudinal, lateral and vertical components. For straight final approaches, only one set of unit vectors is required as the orientation of the design trajectory does not change. This set of unit vectors is determined in an earth-centered, earth-fixed Cartesian coordinate system using the known position of the runway threshold as a reference point. Using the equations presented in section 2.4.2, the published ellipsoidal coordinates and elevation of the runway threshold are converted to the Cartesian components of the position vector r_{LTP} of the Landing Threshold Point (LTP) with regard to the origin of the coordinate system, i.e. the center of the earth. A second vector r_{FPAP} points to the Flight Path Alignment Point (FPAP), which is used to define the approach direction and is typically represented by the opposite runway threshold. The along-track or longitudinal unit vector u_{long} can then be computed as follows:

$$\boldsymbol{u_{long} = \frac{r_{FPAP} - r_{LTP}}{|r_{FPAP} - r_{LTP}|}} \qquad \textbf{(5.1)}$$

A vertical unit vector u_{vert} can be computed by defining a Threshold Crossing Point (TCP), which is located above the LTP:

$$\boldsymbol{u_{vert}} = \frac{\boldsymbol{r_{TCP}} - \boldsymbol{r_{LTP}}}{|\boldsymbol{r_{TCP}} - \boldsymbol{r_{LTP}}|} \tag{5.2}$$

The lateral unit vector u_{lat} is rectangular to the approach trajectory and can be found by computing the cross product of the previously computed unit vectors:

$$\boldsymbol{u_{lat}} = \boldsymbol{u_{vert}} \times \boldsymbol{u_{long}} \tag{5.3}$$

Using this set of unit vectors, any deviation from the straight final approach path can be split into its respective components in an earth-centered, earth-fixed Cartesian coordinate system. Figure 5.1 illustrates the geometry for the computation of the unit vectors.

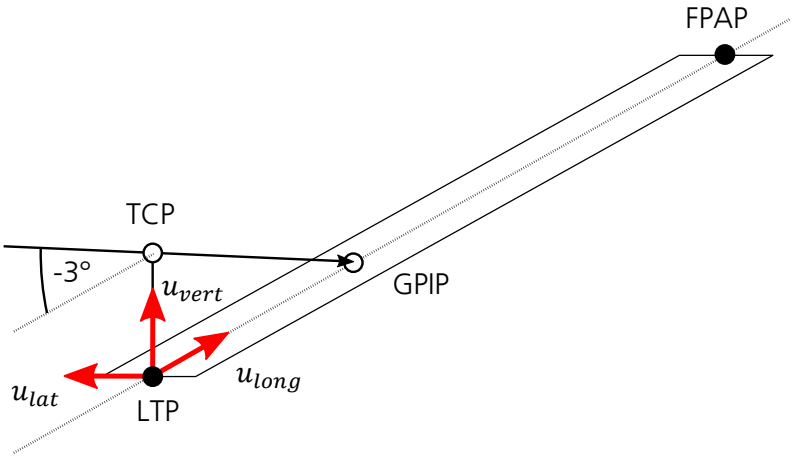

Figure 5.1: Unit vectors defining the final approach segment <own figure after [20]>

In order to apply this method to the experimental RNP to ILS approaches that contain a curved segment, multiple sets of unit vectors are required. A numerical solution for this problem was realized using MATLAB: An array containing a sequence of points representing the approach trajectory was created for each experimental approach. Besides the latitude, longitude and altitude of each point, the array also contains the along-track distance of the individual point, starting at the designated intersection of the runway and the glidepath, i.e. the intended touchdown point or Glide Path Intercept Point (GPIP). Furthermore, the three components of the unit vectors along the trajectory as well as vertical and rectangular to it are stored in the array, resulting in an overall number of 13 entries per point. Depending on the length of the approach, the ten arrays containing the design approach paths have a length between 600 and 900 entries.

The measured position of the aircraft during the flight tests is also stored in array format, but with a much higher resolution. As the two asynchronous sets of data cannot be directly compared due to the lack of a common timestamp, the trajectories are compared iteratively using

a simple MATLAB script. The existing arrays containing the design trajectory and its unit vectors for each individual point and the flight test data are loaded into the MATLAB workspace. In the first step, the single points of both arrays are converted from ellipsoidal coordinates to earth-centered, earth-fixed Cartesian coordinates, resulting in two new arrays that contain the x-, y- and z-components of the vectors pointing from the center of the earth to the respective point. Due to the sampling rate of the flight test data, the array containing the aircraft trajectory is much larger. Depending on the length of the approach path, these arrays have a typical length between 5,000 and 12,000 entries.

In the next step, the program iterates through the flight data array r^f of length m and computes the distance d to all points of the design path array r^d of length n. For the two arrays the following applies:

$$\boldsymbol{r_i^f} = \begin{pmatrix} \boldsymbol{x_i} \\ \boldsymbol{y_i} \\ \boldsymbol{z_i} \end{pmatrix}^{\boldsymbol{f}} \forall \{\boldsymbol{i} \in \mathbb{N} \mid \boldsymbol{i} = \boldsymbol{1}, \dots, \boldsymbol{m}\} \tag{5.4}$$

$$\boldsymbol{r_j^d} = \begin{pmatrix} \boldsymbol{x_j} \\ \boldsymbol{y_j} \\ \boldsymbol{z_j} \end{pmatrix}^{\boldsymbol{d}} \forall \{\boldsymbol{j} \in \mathbb{N} \mid \boldsymbol{j} = \boldsymbol{1}, \dots, \boldsymbol{n}\} \tag{5.5}$$

The vector pointing from the point j of the design path array to the point i of the flight data array then results from vector subtraction:

$$\boldsymbol{d_{i,j}} = \boldsymbol{r_i^f} - \boldsymbol{r_j^d} \tag{5.6}$$

As a result of this operation, a three-dimensional $(m \times n \times 4)$ matrix is formed, containing the x-, y- and z-component of $d_{i,j}$ in the entries $(m \times n \times 1)$ through $(m \times n \times 3)$. The fourth entry contains the length of the respective vector, i.e. the total deviation of the flight trajectory from the design trajectory for this specific combination of points. It results from the norm of the vector $d_{i,j}$.

$$|\boldsymbol{d_{i,j}}| = \sqrt{\left(\boldsymbol{x_i^f} - \boldsymbol{x_j^d}\right)^2 + \left(\boldsymbol{y_i^f} - \boldsymbol{y_j^d}\right)^2 + \left(\boldsymbol{z_i^f} - \boldsymbol{z_j^d}\right)^2} = \sqrt{\boldsymbol{x_{i,j}^2} + \boldsymbol{y_{i,j}^2} + \boldsymbol{z_{i,j}^2}} \tag{5.7}$$

The matrix resulting from this step thus contains the components and lengths of the vectors from all points of the design path array to all points of the flight data array. Its structure is shown in Figure 5.2.

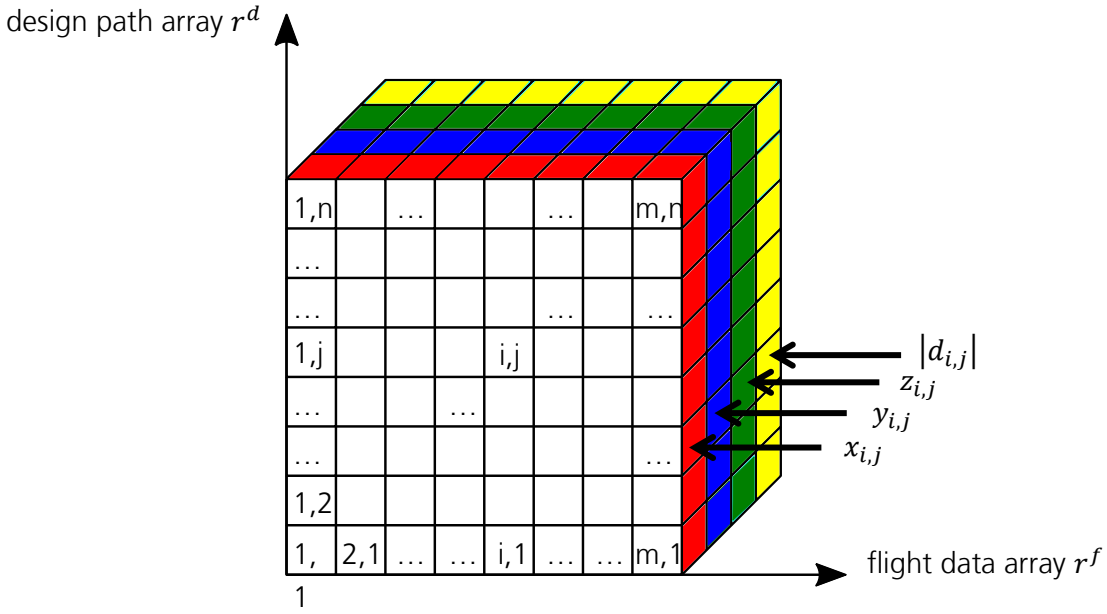

Figure 5.2: Structure of the deviation matrix <own figure>

For the computation of the lateral and vertical deviations, the program iterates along the first dimension of the matrix. During each step, it searches for the minimum vector length along the second dimension. The result is the closest point of the design path for the currently evaluated point of the flight trajectory. By reference to the index of the minimum vector length found during each iteration, the appropriate unit vectors and along-track distance of the corresponding point of the design path are extracted from the design path array. The lateral and vertical deviations Δ^{lat} and Δ^{vert} from the design path can then be computed as follows:

$$\boldsymbol{\Delta_i^{lat}} = \begin{pmatrix} \boldsymbol{x_{i,j}} \\ \boldsymbol{y_{i,j}} \\ \boldsymbol{z_{i,j}} \end{pmatrix} \times \boldsymbol{u_j^{lat}} \tag{5.8}$$

$$\boldsymbol{\Delta_i^{vert}} = \begin{pmatrix} \boldsymbol{x_{i,j}} \\ \boldsymbol{y_{i,j}} \\ \boldsymbol{z_{i,j}} \end{pmatrix} \times \boldsymbol{u_j^{vert}} \tag{5.9}$$

The output of the program is a new array with the same length as the flight data array, containing the lateral and vertical deviations for each point in the flight data array as well as its along-track distance.

5.1.1. Lateral Navigation Accuracy

Figure 5.3 shows the range of the lateral FTE in the crucial part of the 16 approaches to Braunschweig-Wolfsburg airport, i.e. after passing the entry point of the RF leg. A positive FTE

denotes a deviation to the right side of the design trajectory; a negative FTE indicates a deviation to the left.

Figure 5.3: Lateral FTE after the RF leg entry point per approach

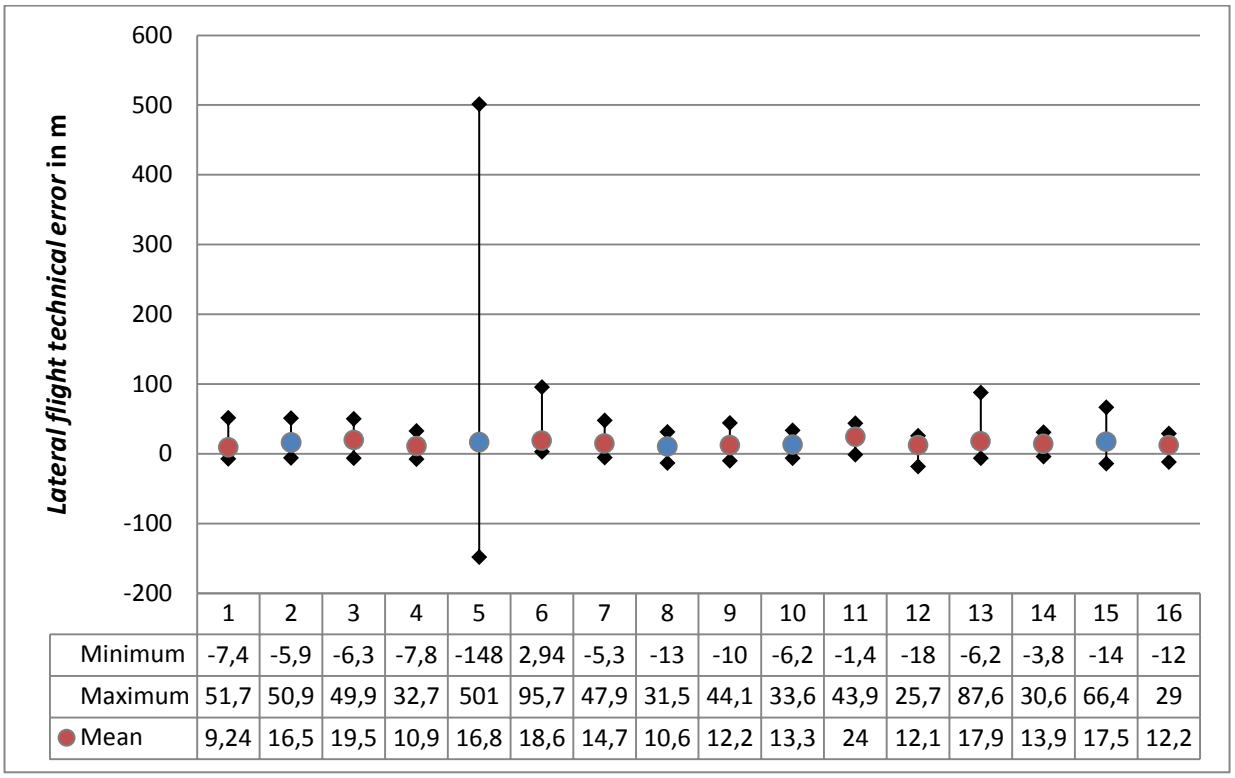

	1	2	3	4	5	6	7	8	9	10	11	12	13	14	15	16
Minimum	-7,4	-5,9	-6,3	-7,8	-148	2,94	-5,3	-13	-10	-6,2	-1,4	-18	-6,2	-3,8	-14	-12
Maximum	51,7	50,9	49,9	32,7	501	95,7	47,9	31,5	44,1	33,6	43,9	25,7	87,6	30,6	66,4	29
Mean	9,24	16,5	19,5	10,9	16,8	18,6	14,7	10,6	12,2	13,3	24	12,1	17,9	13,9	17,5	12,2

Note: All approaches show a small mean lateral FTE that is well within the acceptable range for both RNP 0.1 and RNP 0.3 operations. No significant difference can be noticed between 90° approaches (red) and 180° approaches (blue). Approach #5 was aborted and thus shows a higher lateral FTE.

It can be seen that all approaches feature very low lateral FTEs with mean values below 25 meters, with the exception of the fifth approach which had to be discontinued due to the early descent. In the resulting go-around, the autopilot was disengaged, causing the high lateral deviations as a result of manual flight. Except for approach number eleven, the mean lateral FTE remained below 20 meters and thus well within the acceptable RNP limits even for procedures that require RNP 0.1, for which it equals to a tenth of a nautical mile, i.e. 185.2 meters. Even when considering the maximum lateral FTE for each approach, a value of 100 meters is never exceeded for all approaches except the aborted one. A more detailed plot of the lateral and vertical FTEs for each of the experimental approaches can be found in appendix C.

Out of the four approaches that were flown with approach mode engagement at the IAF, three show a slightly higher standard deviation in the lateral FTE after the RF leg entry point. During the first of these approaches (approach #3), the LOC* mode engaged early due to a localizer side lobe. The resulting deviation from the intended flight path was significant, but happened prior to the RF leg entry point and is thus not included in Figure 5.3. As a result of the localizer side lobe, the flight crew switched to the selected guidance mode of the autopilot in order to realign the aircraft with the intended flight path. The approach mode was only re-engaged at the end of the RF leg, which explains the lower lateral deviations prior to localizer capture in comparison to the other approaches with approach mode engagement at the IAF. These approaches (approaches #6, #13 and #15) show a higher range of lateral deviations, although the mean value remains similar to those of the remaining approaches with later approach mode engagement.

Figure 5.4: Combined plot of lateral deviations during 90° approaches

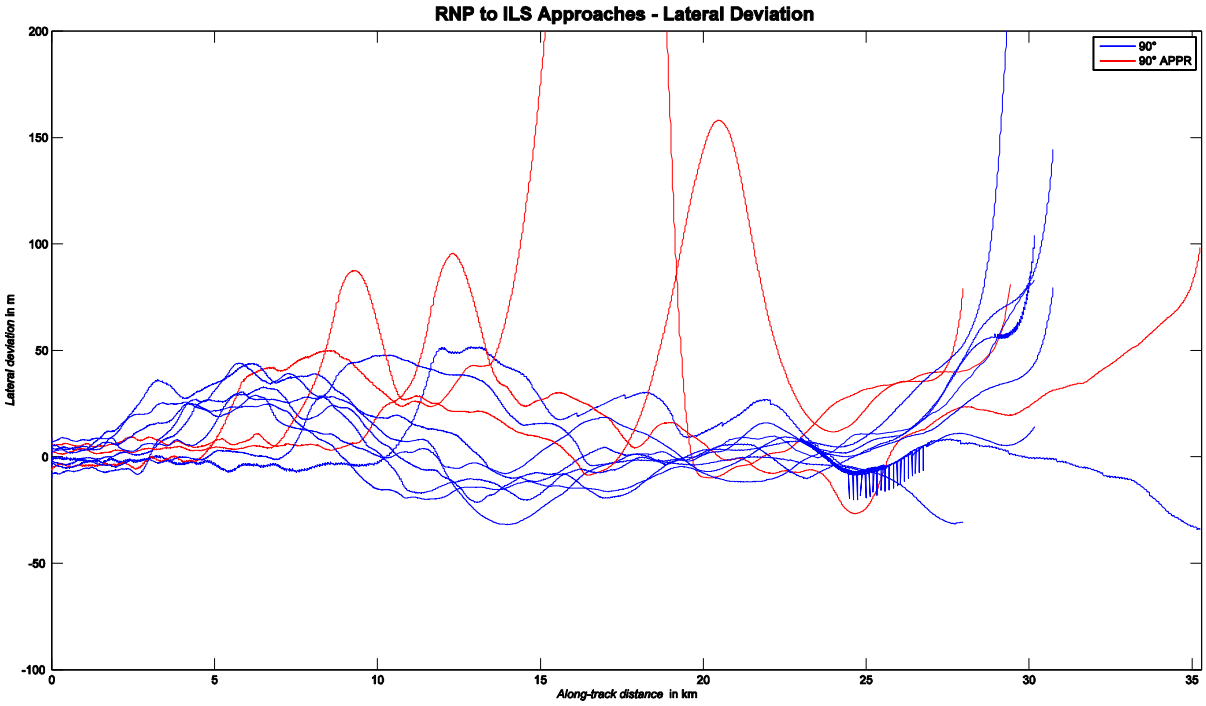

Note: It can be seen that approach mode activation at the IAF (red) causes higher lateral deviations than approach mode activation at the ILS intercept point (blue). This is due to the early engagement of LOC* mode when the aircraft enters the localizer service volume and the subsequent deviation from the RNP path.

The higher maximum lateral deviation during these approaches can be traced back to the system behavior described in section 3.1: As the approach mode is engaged during the whole approach,

the auto flight system is free to switch to the LOC* mode as soon as the localizer signal becomes available, even though the end of the RF leg is not yet reached. As a result of the early LOC* engagement, the aircraft intercepts the localizer on a direct course instead of following the RF leg until its end, thus creating the observed lateral deviations from the design flight path.

Figure 5.4 shows a combined plot of the lateral deviation for all approaches with a track angle change of 90 degrees. Each of the three approaches with approach mode engagement at the IAF shows a peak in the lateral deviation shortly prior to the position of the respective ILS intercept point. This deviation to the right side is the result of the switch to LOC* mode prior to the end of the RF leg and the following intercept course chosen by the FMGS. It is noteworthy that even with the higher lateral deviations that result from the early localizer intercept, the lateral FTE remains within acceptable limits and might still be sufficient for procedures that require high accuracies such as RNP 0.1.

Figure 5.5: Standard deviation of the lateral FTE

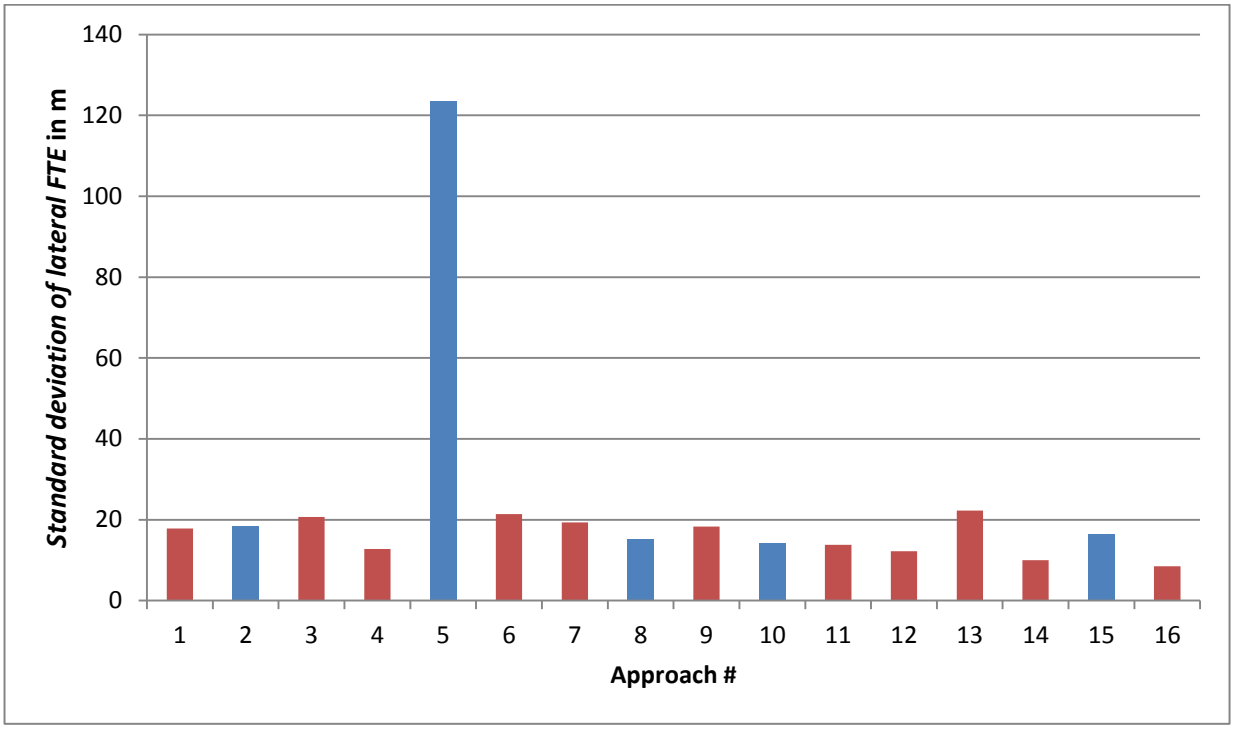

Note: The standard deviation of the lateral FTE is similar for all approaches, regardless of the track angle change during the RF leg. Red bars are 90° approaches; blue bars represent 180° approaches.

With regard to the standard deviation of the lateral FTE shown in Figure 5.5, no significant influence of the approach mode activation can be observed. Although slightly higher for the

approaches with early approach mode activation, the standard deviation of the lateral FTE is similarly low for all approaches with the exception of approach #5, which had to be aborted. This speaks for the navigation accuracy of the auto flight system, which is able to maintain a high correlation of the indicated position of the aircraft and the intended lateral flight path.

Figure 5.6: Lateral NSE per approach

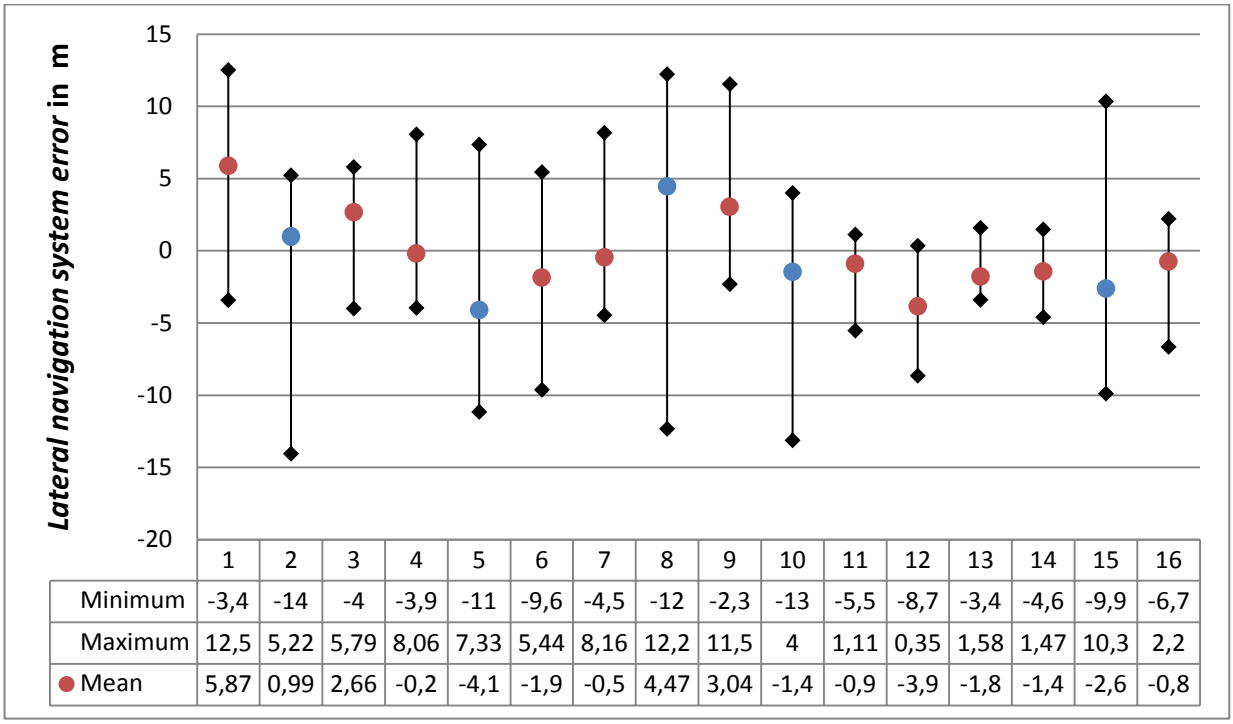

	1	2	3	4	5	6	7	8	9	10	11	12	13	14	15	16
Minimum	-3,4	-14	-4	-3,9	-11	-9,6	-4,5	-12	-2,3	-13	-5,5	-8,7	-3,4	-4,6	-9,9	-6,7
Maximum	12,5	5,22	5,79	8,06	7,33	5,44	8,16	12,2	11,5	4	1,11	0,35	1,58	1,47	10,3	2,2
● Mean	5,87	0,99	2,66	-0,2	-4,1	-1,9	-0,5	4,47	3,04	-1,4	-0,9	-3,9	-1,8	-1,4	-2,6	-0,8

Note: A very small mean lateral NSE was observed during all approaches. Although the values for 180° approaches (blue) are spread slightly wider than in 90° approaches (red), the lateral NSE remains below 15 meters in all cases.

In order to access the compliance to an RNP limit, the lateral TSE has to be examined. Assuming that the PDE is negligible, the NSE is the second component that contributes to the TSE besides the FTE. As computation of the NSE requires knowledge of the actual position of the aircraft, post-processed differential GPS data is used for the determination of the actual flight path during the flight tests. NSE computation is performed similarly to the computation of the FTE, only instead of the design path array, the array containing the post-processed differential GPS data is compared to the flight data array. Figure 5.6 shows the lateral component of the NSE during the experimental RNP to ILS approaches.

It can be seen that the lateral NSE is much smaller than the lateral FTE, ranging between -15 and 15 meters. Again, a negative NSE indicates that the indicated position of the aircraft is located to the left of the actual position, whereas a positive NSE indicates a deviation to the right. The magnitude of the mean lateral NSE exceeds five meters only during one of the approaches, allowing the conclusion that the contribution of the NSE to the TSE is small. Even in the worst possible case, i.e. that both the maximum FTE and NSE occur at the same time and in the same direction, the navigation accuracy is still sufficiently high to meet the requirements of approach procedures based on RNP 0.3 or RNP 0.1 in 95 per cent of the time.

Figure 5.7: Standard deviation of the lateral NSE

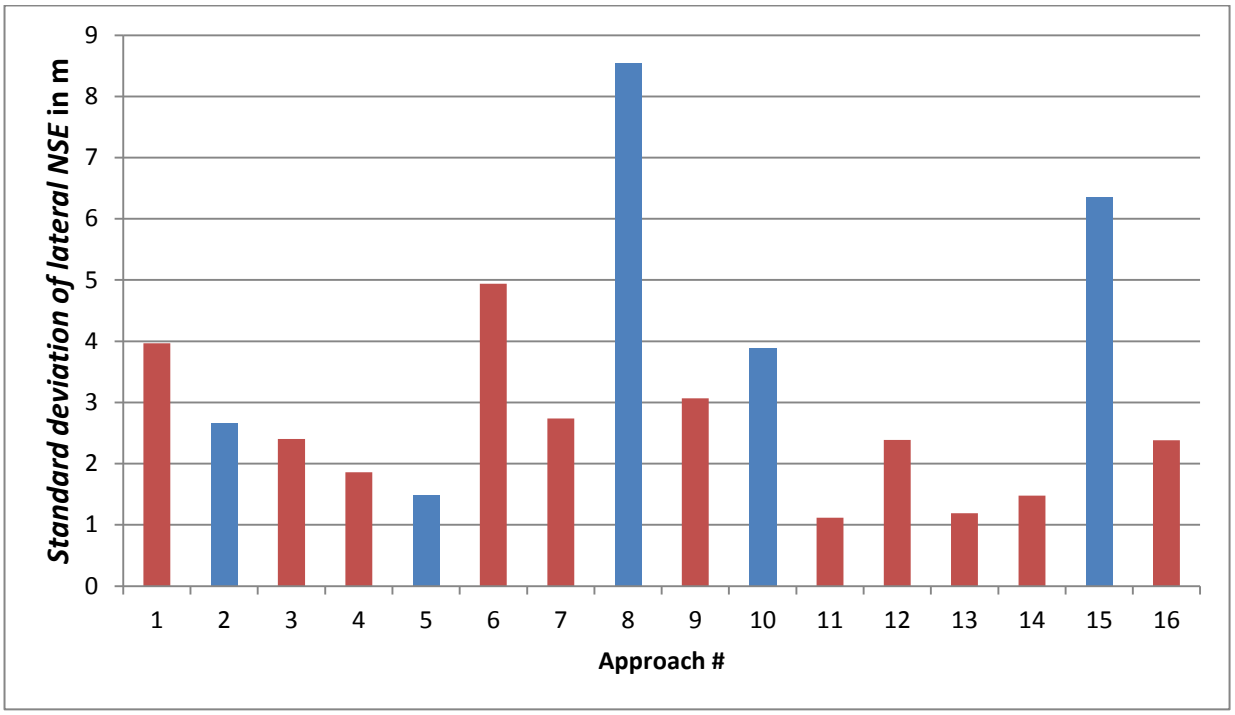

Note: The standard deviation of the lateral NSE is similarly low for all approaches. Again, no obvious influence of the track angle change during the RF leg is noticeable, as the results from 180° approaches (blue) and 90° approaches (red) are located within the same range.

While being less uniform than the standard deviation of the lateral FTE, the standard deviation of the lateral NSE is also much smaller. As can be seen in Figure 5.7, the standard deviation remains below ten meters for all approaches and does not exceed five meters in the majority of the flight tests. Variations in the standard deviation of the lateral NSE can be attributed to changing GPS signal quality, which can be caused by a varying number of available satellites, less favorable satellite constellations or signal shading caused by the wings or stabilizers of the aircraft.

However, the overall influence of the NSE on the lateral navigation accuracy during the RNP to ILS approaches can be neglected as its contribution to the TSE is only a fraction of that of the FTE.

It can be concluded that the lateral navigation accuracy is not crucial for RNP to ILS approaches with the ATRA, as the observed lateral FTEs and NSEs are small enough to ensure adherence to the RNP corridor during the first part of the approach. When the approach mode is activated at the start of the approach, higher lateral deviations occur when the localizer signal becomes available and the LOC* mode engages. However, the impact of this circumstance on the adherence to the RNP corridor is smaller as expected, thus leaving both options for the activation of the approach mode viable. Nevertheless localizer side lobes could become a problem for RNP to ILS approaches that intercept the localizer and glideslope very close to the runway threshold if the approach mode is already activated at the IAF.

5.1.2. Vertical Navigation Accuracy

The vertical FTE during the experimental RNP to ILS approaches is shown in Figure 5.8. Again, the respective maximum, minimum and mean values have been determined only from data recorded after the entry point of the RF leg in order to exclude deviations from the planned vertical path caused by late ATC clearances during the initial part of the approach. A positive vertical FTE implies that the aircraft was above the design path, whereas a negative vertical FTE occurs when the aircraft is lower than intended at the corresponding along-track position.

In general, the vertical FTE is greater than the lateral FTE, which is to be expected due to the inaccuracies entailed by barometric altimetry. As with the lateral FTE, the vertical FTE is much larger for the fifth approach due to the go-around manoeuver after the abort of the approach during the RF leg. However, even with a higher range of values, the vertical FTE is still small enough for compliance with the criteria for navigation accuracy in approach procedures and remains within the boundaries of RNP 0.1 applications in most of the approaches. Refer to appendix C for more detailed plots of the lateral and vertical FTEs of the individual approaches.

Figure 5.8: Vertical FTE after the RF leg entry point per approach

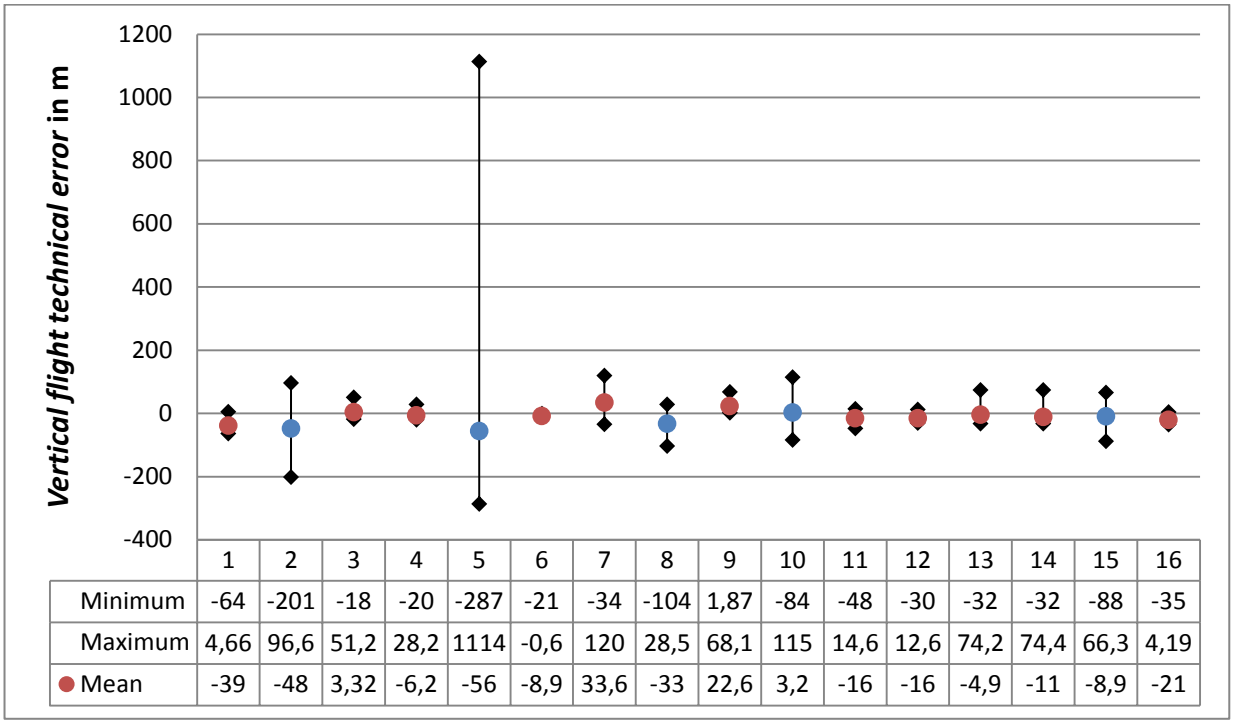

	1	2	3	4	5	6	7	8	9	10	11	12	13	14	15	16
Minimum	-64	-201	-18	-20	-287	-21	-34	-104	1,87	-84	-48	-30	-32	-32	-88	-35
Maximum	4,66	96,6	51,2	28,2	1114	-0,6	120	28,5	68,1	115	14,6	12,6	74,2	74,4	66,3	4,19
● Mean	-39	-48	3,32	-6,2	-56	-8,9	33,6	-33	22,6	3,2	-16	-16	-4,9	-11	-8,9	-21

Note: For the vertical FTE, a more distinct difference between the approaches coded with and without a flight path angle can be noticed. The 180° approaches (blue), which were coded without a flight path angle, show a higher variation in the vertical FTE due to the "dive and drive" behavior of the FMS. However, the mean vertical FTE remains within the acceptable limits for all RNP operations most of the time. For RNP 0.1 operations, a flight path angle should be included in the navigation database to improve vertical navigation accuracy.

The analysis of the vertical FTE also shows clear differences between approaches with a track angle change of 180 degrees that were coded without a vertical path angle and the approaches with a track angle change of 90 degrees, which include a vertical path angle in the ARINC 424 coding of the navigation database. In the five approaches that did not include a fixed flight path angle (approaches #2, #5, #8, #10 and #15), the vertical FTE shows much higher negative values than in the other approaches, which is a result of the previously mentioned "dive and drive" characteristic. The effect is most visible in approaches #2 and #5. In approach #10, an additional altitude constraint was entered manually for the entry point of the RF leg, thus limiting the "dive and drive" effect as the FMS was not allowed to descend to the final ILS intercept altitude immediately after passing the IAF. During approach #15 a short level segment had to be included due to a missing descent clearance from ATC, which also reduced the effects of "dive and drive" on the vertical FTE.

Figure 5.9: Standard deviation of the vertical FTE

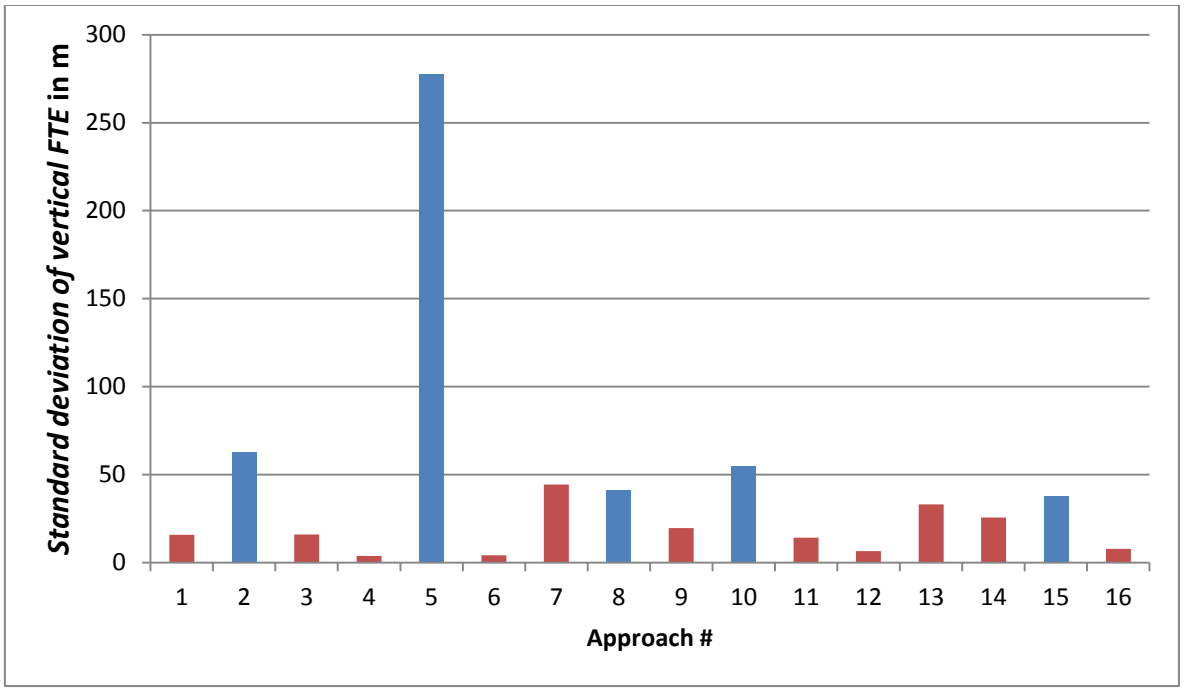

Note: The standard deviation of the vertical FTE clearly shows the influence of the missing flight path angle for the 180° approaches (blue). All 90° approaches (red) that could be completed without incidents such as late clearances display a smaller standard deviation of the vertical FTE.

In comparison to the standard deviation of the lateral FTE, the vertical FTE shows a much higher spread of values for its standard deviation between the individual approaches as can be seen in Figure 5.9. Especially the approaches without a coded flight path angle show comparatively high standard deviations, although some of the approaches that do feature a fixed flight path angle also show relatively high standard deviations due to unplanned events such as late ATC clearances. Examples are approaches #13 and #14, during which the autopilot had to be briefly disconnected due to crossing VFR traffic and a late descent clearance out of the MVA was obtained from ATC. However, most of the approaches with a track angle change of 90 degrees have very low standard deviations, which allow the conclusion that the FMGS is able to follow the desired vertical profile much more precisely when a flight path angle is included in the navigation database. Especially approaches #4, #6, # 12 and #16 feature very low standard deviations and a mean vertical FTE near zero, indicating that the aircraft followed the design path very closely.

Figure 5.10: Comparison of vertical deviations during 90° and 180° approaches

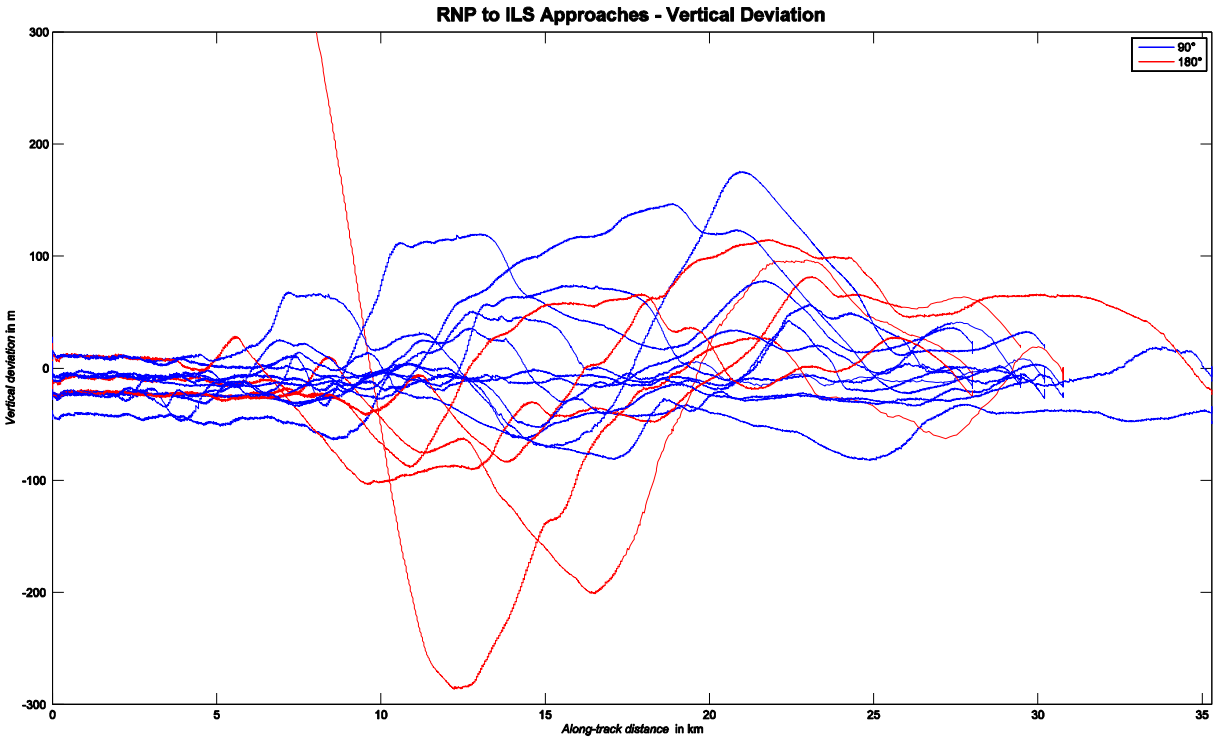

Note: The "dive and drive" behavior observed during approaches without a coded flight path angle (red) is clearly recognizable. In comparison to the approaches that include a flight path angle (blue), the vertical path flown by the aircraft is much lower than the intended path during the RF leg if no flight path angle is coded in the navigation database.

Figure 5.10 shows a combined plot of the vertical deviations from the intended flight path and displays the values for the approaches with a track angle change of 90 degrees in blue, while the values for the approaches with a track angle change of 180° are represented in red. In direct comparison it becomes obvious that the aircraft has a tendency to fly below the design vertical trajectory during approaches without a coded flight path angle, although the vertical navigation performance is not necessarily worse as long as enough altitude constraints are available to prevent a long idle descent.

The improved vertical path following during the approaches with a coded flight path angle also becomes clear when analyzing the flight path angles measured during the experimental approaches. Detailed plots of the measured flight path angle for each approach can be found in appendix E. Although the flight path angle does not remain constant in any of the approaches due to permanent corrections of the trajectory, e.g. after extension of the flaps, the target values of minus two degrees during the RNP part and minus three degrees during the ILS part of the

approach are met more often on average if a flight path angle is included in the navigation database. An exemplary comparison of the measured flight path angles during an approach without coded flight path angle and an approach with coded flight path angle is shown in Figure 5.11.

Figure 5.11: Measured flight path angles during approaches #2 and #16

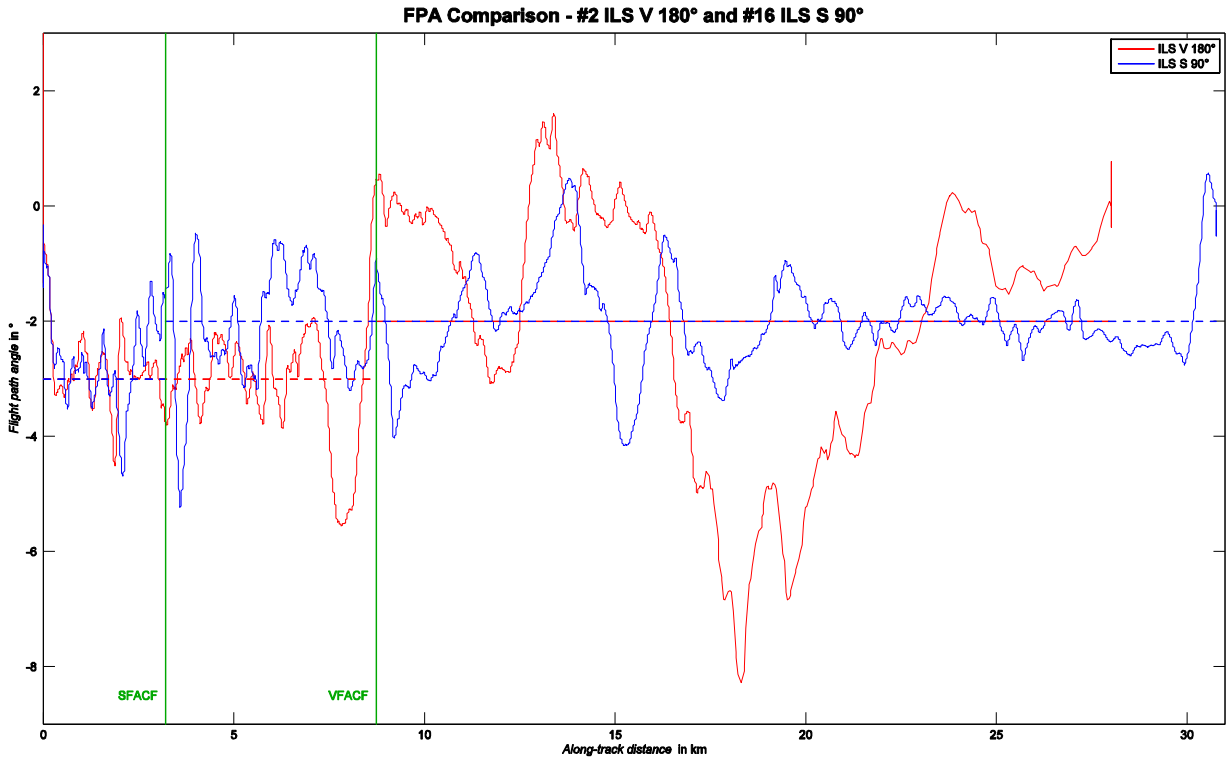

Note: The aircraft is able to maintain the intended flight path angle during the RNP part of the approach much better during the 90° approach (blue). During the 180° approach (red), the flown flight path angle deviates more strongly from the intended value for the respective approach segment (dashed line).

During the approach with a track angle change of 180° that is depicted in red, the aircraft performs a steeper descent than envisaged in the design trajectory during the RF leg until it reaches the altitude constraint of the next waypoint. After reaching the altitude constraint, it continues the approach in level flight and thus with a flight path angle around zero. In the course of the approach plotted in blue that includes a flight path angle in the navigation database, however, the measured flight path angle fluctuates around the target value of minus two degrees for the whole RNP part of the procedure, although relatively large deviations can occur for short amounts of time, e.g. as a result of flap extension. Only after the glideslope signal is captured a relatively constant flight path of three degrees is flown in all of the experimental approaches. It

should be noted that improved flight path following can be observed in all procedures that include a coded flight path angle, regardless of the activation of the approach mode. The approaches with a track angle change of 180 degrees, however, can deviate more strongly from the design vertical profile depending on the amount and spacing of altitude constraints in the approach path. In general the vertical navigation performance is less predictable and reliable for approaches that do not have a flight path angle coded into the navigation database.

5.2. ILS Intercept Performance

In all experimental approaches except for approach #5 which had to be aborted, a successful transition from RNP to ILS guidance could be achieved, although the required time for localizer and glideslope capture after activation of the approach mode varied widely in some cases. Naturally, the time required for engagement of the LOC and GS modes was much higher for the approaches with approach mode engagement at the IAF. In this case, the required time depends directly on the remaining length of the approach trajectory after the IAF. During approach #3, the approach mode was also activated at the IAF, but was temporarily disengaged due to a localizer side lobe. As a result, the approach mode was reactivated at the designated ILS intercept point at the end of the RF leg, rendering this approach effectively as one of the normal approaches with regard to the ILS intercept performance. Figure 5.12 shows the required times for both localizer and glideslope capture for each of the approaches.

It is noticeable that the respective minimum times of 13.8 and 18.9 seconds that were observed for LOC and GS mode engagement occurred several times during the experimental approaches. This encourages the assumption that these are the respective software-related minimum times required by the auto flight system to verify signal integrity between the redundant FMGCs. Nevertheless, even in cases where the observed minimum times were exceeded, the localizer mode engaged in less than 20 seconds after approach mode activation for nine out of twelve approaches with approach mode engagement after the RF leg. GS mode engagement also requires less than 20 seconds in nine out of twelve approaches, although not from the same subset as for LOC mode engagement. During nine of the 15 approaches, the LOC mode engaged prior to the GS mode as in conventional ILS approaches.

Figure 5.12: Time between approach mode activation and localizer/glideslope capture

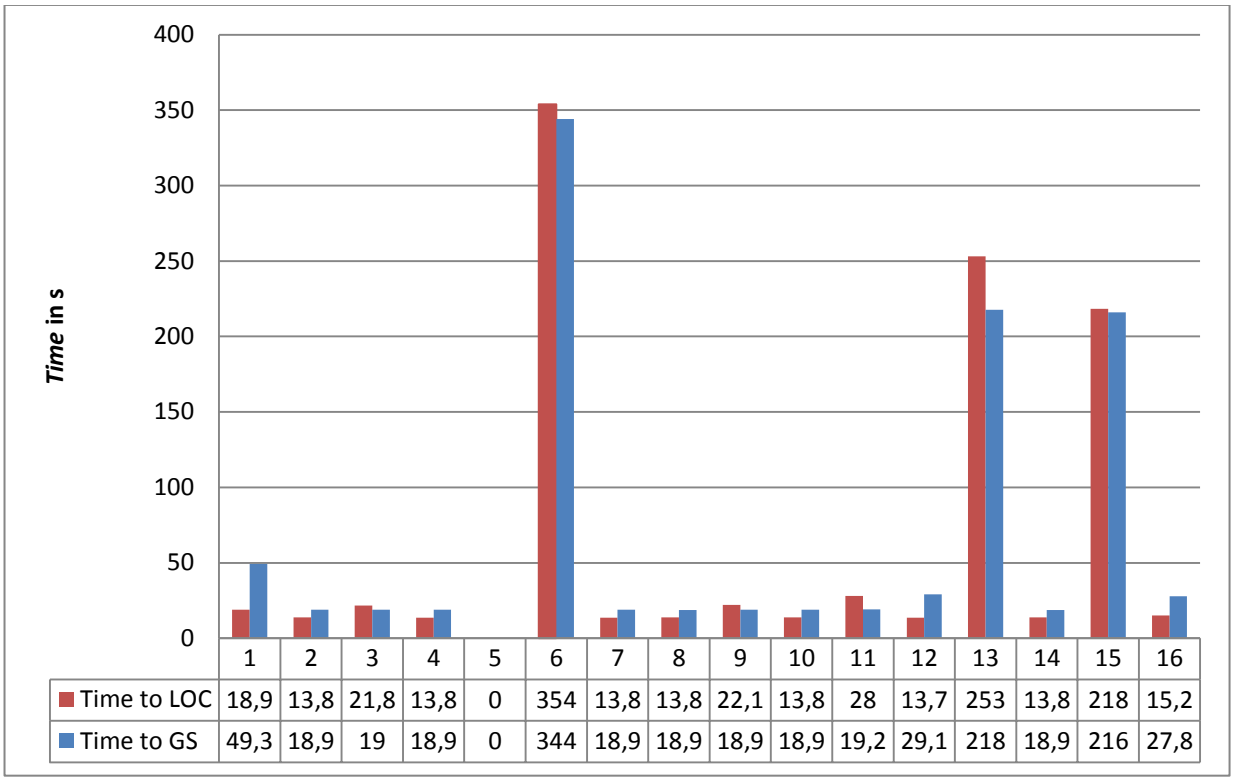

	1	2	3	4	5	6	7	8	9	10	11	12	13	14	15	16
Time to LOC	18,9	13,8	21,8	13,8	0	354	13,8	13,8	22,1	13,8	28	13,7	253	13,8	218	15,2
Time to GS	49,3	18,9	19	18,9	0	344	18,9	18,9	18,9	18,9	19,2	29,1	218	18,9	216	27,8

Note: The required time for localizer (red) and glideslope (blue) capture is equally low for all approaches with approach mode activation at the ILS intercept point. However, for all approaches with approach mode activation at the IAF, the required time depends on the length of the RNP part of the approach. In general, the vertical navigation accuracy is the most important factor for a quick transition to ILS guidance as glideslope capture from above is more time-consuming than glideslope capture from below or corrections to the lateral flight path.

With localizer and glideslope capture times well below 30 seconds for the majority of the approaches, a successful transition from RNP to ILS guidance does not seem to be an issue. The angular localizer and glideslope deviations for each of the approaches are presented in appendix F. The plots show the deviations starting at the entry point of the RF leg for the approaches with a track angle change of 90 degrees and at the apex of the curve for the approaches with a track angle change of 180 degrees. Except for approach #5, only minor deviations from both the localizer and the glideslope center remain at the ILS intercept point for all approaches, thus facilitating a fast transition to ILS guidance.

5.3. Automatic Landing Performance

A successful automatic landing could be performed in all approaches with a successful transition to ILS guidance, i.e. all experimental approaches except approach #5. Surprisingly, the overall automatic landing performance during the flight trials surpassed the observed performance during the simulator tests as the LAND mode engaged shortly after passing a radio altitude of 400 feet in all approaches, even with an ILS intercept point as low as 550 feet above ground in the approach "ILS S RWY26". As a result of the short ILS intercept times discussed in section 5.2, the aircraft was almost always established on localizer and glideslope with engaged LOC and GS modes prior to 400 feet above ground, which is the activation threshold for the LAND mode [18]. Given the small range of radio altitudes at which LAND mode engaged during the flight tests, it can be concluded that the LAND mode usually engages around 370 feet radio altitude, even if the aircraft flies with engaged LOC and GS modes long before reaching 400 feet above ground level.

Figure 5.13: Radio altitude at LAND mode engagement per approach

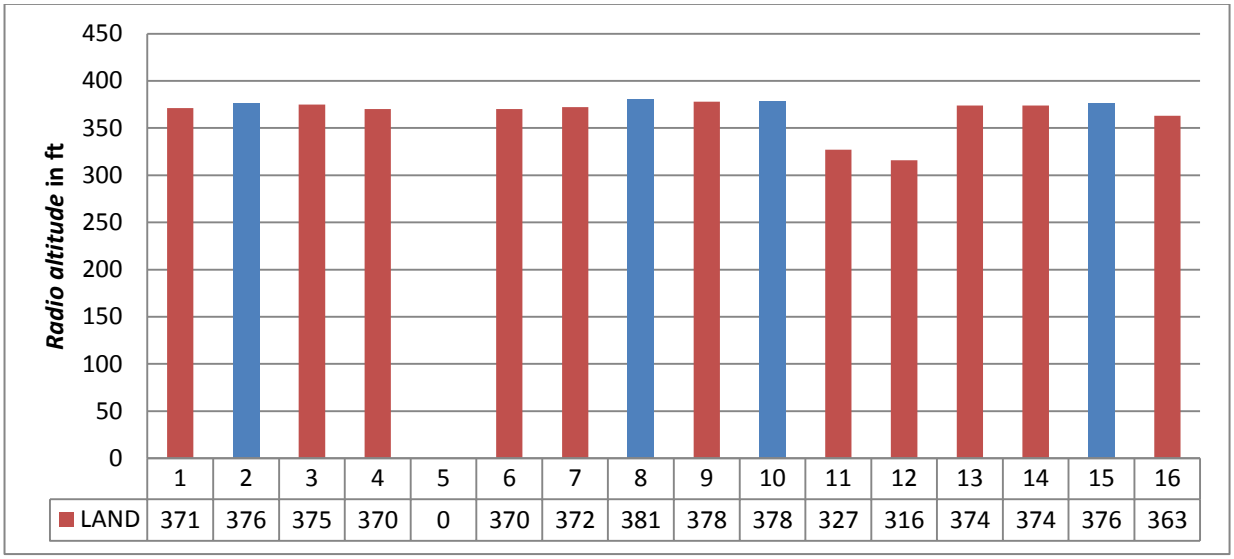

	1	2	3	4	5	6	7	8	9	10	11	12	13	14	15	16
LAND	371	376	375	370	0	370	372	381	378	378	327	316	374	374	376	363

Note: The radio altitude of the aircraft at LAND mode engagement is nearly identical for both the 180° approaches (blue) and the 90° approaches (red). With the exception of approach #5, which had to be aborted, LAND mode usually engaged between 360 and 380 feet above ground level. In approaches #11 and #12, during which the ILS intercept point was reached slightly high, LAND mode engagement required slightly longer. However, engagement still occurred above 300 feet radio altitude and thus early enough for an automatic landing.

Figure 5.13 shows the individual radio altitudes at which the LAND mode engaged during the experimental approaches. It can be seen that the engagement altitudes are nearly identical and range between 363 and 381 feet above ground. Only approaches #11 and #12 have slightly lower LAND mode engagement altitudes of 327 and 316 feet respectively. During approach #11 of type "ILS T RWY26" with an ILS intercept altitude of 750 feet above ground level, the approach mode was activated late, i.e. several seconds after passing the ILS intercept point. This led to short level flight as the aircraft continued on RNP guidance, thus maintaining the altitude currently cleared for descent on the FCU, which was set to the altitude constraint of the ILS intercept point. Before the inactive approach mode was noticed and subsequently armed, the aircraft continued in ALT mode for a short amount of time, thus prolonging the glideslope capture after approach mode activation. Approach #12 of type "ILS S RWY26" with an ILS intercept altitude of 550 feet above ground level was flown slightly above the design vertical profile and thus positioned the aircraft above the glideslope at the end of the RF leg. During the necessary glideslope intercept from above, the aircraft overshot the glideslope center once, which contributed to the prolonged time for LAND mode engagement. However, when the glideslope was captured, the auto flight system immediately switched to LAND mode in 316 feet above ground level and a standard automatic landing could be performed.

The autoland capability indicated on the FMA was CAT 3 for all approaches and was available only seconds after activation of the approach mode. Both CAT 3 SINGLE and CAT 3 DUAL automatic landings were successfully performed during the experimental RNP to ILS approaches. The CAT 1 ILS facilities at Braunschweig-Wolfsburg airport did not affect the autoland capability of the ATRA in any way; hence automatic landing after RNP to ILS approaches is not limited to certain types of ILS ground installations.

Nonetheless the experimental approaches to Braunschweig-Wolfsburg airport have shown that correct vertical path following is crucial for a quick transition to ILS guidance and a subsequent automatic landing. Especially for approaches with very short final segments, the LOC and GS modes need to engage soon after approach mode activation in order to ensure a timely engagement of the LAND mode. A positive vertical deviation from the design trajectory affects the glideslope capture performance more strongly as the resulting glideslope capture from above takes more time and requires greater corrections, whereas a standard glideslope capture from below is much less critical. Nevertheless, all deviations from the design trajectory encountered in the flight trials were small enough to deliver the aircraft to a position out of which localizer and

glideslope capture was possible fast enough for a successful automatic landing, regardless of the length of the final approach.

5.4. Pilot Feedback

After the completion of the RNP to ILS flight trials with the ATRA, the two test pilots were interviewed in order to obtain an assessment of the feasibility of the experimental approaches from an operational point of view. Their opinions, comments and criticism regarding the realization of the RNP to ILS approaches and the handling of the aircraft are presented in the following section.

- Expected and actual behavior during approaches coded without a vertical path angle.

The pilots stated that the "dive and drive" behavior observed during the preliminary simulator tests and during the approaches with a track angle change of 180 degrees in the actual flight tests was unexpected, but might have been predictable with more intensive research with regard to the functionality of the FMS. Without a previous briefing that included the results of the simulator tests, they would have expected a "fitting" vertical profile on the basis of the altitude constraints included in the approach coding. However, they also stated that airline pilots might be more familiar with the vertical path generation of the A320 FMS due to their experience with numerous approaches to different airports.

- Differences between conventional ILS approaches and RNP to ILS approaches and their acceptability for the flight crew.

RNP to ILS approaches deviate from the order of events in conventional ILS approaches mainly in the time of the approach mode activation. Normally, pilots push the "Approach" pushbutton after receiving clearance for the selected approach from ATC. The position-dependent activation of the approach mode as envisaged for RNP to ILS approaches is perceived as a "weak point" by the test pilots as the risk of failed approach is relatively high due to the requirement for manual activation at the end of the RF leg, which could easily be missed. An automatic activation of the approach mode is recommended to improve the reliability of the procedure and remove the risk of missing the right moment for activation.

- Configuration of the aircraft for landing during the RF leg.

In general, the aircraft can be configured for landing during a turning segment without any problems. However, regulations require approaching aircraft to be configured for landing and stabilized on the approach track in at least 1,000 feet above ground level for instrument approaches. The pilots would like to maintain this procedure for RNP to ILS approaches as well since a prediction of the correct moment for reducing the thrust, setting the flaps and extending the landing gear is complicated by the inclusion of curved segments into the approach. This is due to the change of the wind direction relative to the aircraft during the curve and the changed energy budget of the aircraft in turning flight. Presuming more experience with this kind of approach, the pilots could imagine reducing the minimum height for a configured and stabilized approach, but not below 800 feet above ground level.

- Sufficiency of the approach information provided by the cockpit instruments.

Sufficient information regarding the lateral and vertical trajectory of the approach is available from the ND and the altitude constraints associated with the waypoints. In combination with the approach charts, the pilots can visualize the intended flight path and are capable of detecting deviations from the design trajectory. However, the current characterization of RNP to ILS approaches as ILS approaches in the navigation database is misleading and should be replaced with a unique label which clearly identifies the approach type. This is emphasized even more by the requirement for later approach mode activation in comparison to conventional ILS approaches. The pilots would favor a solution that allows approach mode activation immediately after clearance is received, but prohibits engagement of the LOC* and GS* modes until the end of the RF leg is reached.

- Approach mode activation at the end of the turn per crew procedure.

According to the pilots, manual approach mode activation at the end of the RF leg per crew procedure is conceivable but unpleasant due to the risk of missing the right moment. In case this is implemented nonetheless, an "attention getter" display should be introduced that reduces the amount of attention the pilots need to pay to this task.

- Mode awareness and annunciation.

All autopilot modes and functions that are used during RNP to ILS approaches are also part of existing procedures, hence the mode awareness and annunciation is not affected by the RNP to ILS concept. However, the pilots lament a general tendency to neglect or overlook certain displays that are not crucial to the safety of the flight such as the FMA. Although the relevant information is available at all times, it is sometimes not perceived because other tasks require the attention of the pilots. The risk of missing an event such as the transition to localizer guidance is present, but is not necessarily higher for RNP to ILS approaches as long as the pilot workload is not increased in comparison to other approach types.

- Acceptable heights for ILS intercept.

As mentioned before, the inclusion of a curved segment complicates the assessment of the current thrust setting and configuration status. For this reason, the pilots think that the ILS intercept height should depend on the track angle change during the RF leg. Additionally, they would not recommend placing the ILS intercept below 1,000 feet above ground level. Until more experiences with RNP to ILS approaches have been made, an ILS intercept height of 1,500 feet above ground level might be more promising for new implementations of the concept.

- Workload during RNP to ILS approaches in comparison to conventional ILS approaches.

The opinion of the test pilots is that the workload during RNP to ILS approaches strongly depends upon the technical realization of the concept. In case the approach mode has to be activated manually, the workload is increased as one pilot needs to focus on the right moment for pushing the "Approach" pushbutton, thus reducing the attention for other displays and messages significantly. Beyond that, the workload is more or less identical to other approaches and includes the configuration of the aircraft for landing and monitoring of the autopilot modes. RNP to ILS approaches also offer the potential for a reduction of pilot workload, as the predefined approach track reduces the need for ATC instructions and thus the amount of interactions with ATC via radio.

- Additional information useful or required for RNP to ILS approaches.

In order to facilitate the assessment of the current settings, the pilots would like to add an indication of the remaining along-track distance to the ND. In conventional ILS approaches, this information is often provided by a DME, which cannot be used in RNP to ILS approaches due to the curved segments in the intermediate approach phase. Additionally, knowledge about the expected wind in different altitudes during the approach would be useful to estimate the head- or tailwind components, which would contribute to the assessment of the right moment for setting the flaps or extending the landing gear.

6. Conclusion

Conflicts with the current official regulations and coding procedures that would need to be resolved for the implementation are discussed in the following chapter. Beyond that, this chapter concludes this report by summarizing the findings of the flight tests and presenting an outlook to possible further work on the topic of RNP to ILS approaches.

6.1. Conflicts with Existing Regulations and Standards

Due to the "hybrid" character of RNP to ILS approaches, which are part non-precision and part precision approaches, no official regulations exist for the design of such procedures. Although they were coded as ILS approaches for the RNP to ILS flight trials, the existing ICAO regulations regarding ILS precision approaches and RNP non-precision approaches cover all aspects of RNP to ILS procedure design. Moreover, the requirements for effective RNP to ILS procedure design contradict in parts the individual guidelines published for the construction of ILS and RNP approach procedures by ICAO in [22]. Additionally, the current ARINC 424 standard for navigation system databases as published in [16] does not include a means to code "hybrid" procedures that feature a transition from RNP to ILS guidance without the approach structure of conventional ILS approaches. The following sections point out the conflicts with current regulations and standards and propose possible changes that would facilitate the introduction of RNP to ILS approaches for commercial aviation.

6.1.1. ICAO

Volume II of [22] provides the basic guidelines for procedure design according to international safety standards defined by ICAO. Recommendations are given for different approach categories, including ILS and RNP approaches, and are ordered by the single segments of the respective procedure, i.e. the initial, intermediate and final approach segments. As RNP to ILS approaches only differ from conventional ILS approaches in the design of the intermediate and final segments, the existing ICAO guidelines regarding these segments are screened for conflicts with the design criteria for effective RNP to ILS approaches as presented in [5].

The intermediate approach segment connects the initial approach segment to the FAF for non-precision approaches and the FAP for precision approaches. On this segment, the aircraft configuration, speed and position shall be adjusted for entry into the final approach segment.

According to ICAO, the track of the intermediate approach segment shall be aligned with the localizer course for all ILS approaches. Segment length shall be sufficient for alignment with both the localizer and glideslope, taking into account the angle of interception of the initial approach segment and the localizer course. ICAO defines an optimum segment length of the intermediate approach of five nautical miles with the requirement for the whole segment to be located within the service volume of the localizer signal.

For all PBN procedures such as RNP approaches, similar guidelines apply for the intermediate approach segment. According to ICAO, the intermediate approach segment shall be aligned with the final approach course whenever possible. If this is not the case and a turn at the FAF is required, a maximum track angle change of 15 degrees for fly-by turns and 45 degrees for RF legs is not to be exceeded for procedures with barometric vertical guidance. For SBAS procedures, the same rules apply, but only RF legs can be used for turns at the FAF. If an RF leg is part of the intermediate approach, its minimum radius shall be 2.55 nautical miles. The minimum length of the intermediate approach for PBN procedures is two nautical miles for straight intermediate segments or when a RF leg is used for curves prior to the FAF. If a fly-by turn is part of the intermediate approach, a straight segment with a minimum length of 2 nautical miles has to be included in the approach between the fly-by turn and the FAF.

On the final approach segment, the approaching aircraft performs a precise alignment with the runway centerline and descends for landing. It begins at the FAF for non-precision approaches respectively at the FAP for precision approaches and ends at the missed approach point (MAPt), at which the missed approach procedure begins in case the approach has to be aborted. The final approach segment is aligned with the runway centerline for both ILS and PBN procedures, although some new RNP specifications allow the use of RF legs in the final approach segment. For ILS approaches, an optimum length of five nautical miles and a minimum length of three nautical miles are defined by ICAO. Furthermore, a position fix such as the outer marker or a DME must be available to approaching aircraft to verify the correct glide path. The recommended length for the final approach segment of PBN procedures is very similar and ranges from a minimum value of three nautical miles to a maximum value of nine nautical miles.

The most obvious discrepancy between existing regulations and aims for efficient RNP to ILS procedure design arises from the regulations regarding the intermediate approach segment. Neither ILS nor PBN procedure guidelines allow RF legs with a track angle change greater than 45

degrees prior to the FAF, thus limiting the flexibility of possible RNP to ILS approaches significantly. If RNP to ILS approaches were to be created under the current regulation, they would most likely be categorized as ILS approaches, which would further reduce the possibilities for more efficient procedure design as the intermediate and final approach segments would have to be aligned. In order to realize RNP to ILS approaches as envisaged, the use of RF legs in the intermediate approach of ILS approaches prior to the ILS intercept would have to be allowed, which necessitates a removal of the requirement for the alignment of intermediate and final approach. With the currently permissible minimum length for ILS final approach segments of three nautical miles, approaches with a nominal intercept height of approximately 1,000 feet above ground level could be realized. If utilized in combination with RF legs in the intermediate approach, this final approach length would be sufficient for the creation of more flexible procedures that offer a reduction in track mileage compared to conventional ILS approaches.

Another topic that would need to be evaluated is the requirement for an outer marker or a DME in order to obtain information about the remaining distance to the threshold. In RNP to ILS approaches with curved segments, a DME cannot be used to determine the remaining distance as the along-track distance to the threshold does not coincide with the direct distance measured by the DME. However, due to the repeatable ground track provided by RF legs, the remaining along-track distance could be included at certain points in the approach chart or directly associated with the waypoints in the navigation database. That way, every waypoint that is part of the approach procedure could serve as an artificial marker that allows cross-checking of the current altitude. However, compared to the current system that employs physical markers emitting a radio signal that is received by the aircraft when it passes over the marker, an artificial marker associated with a waypoint in the navigation database would lack an external reference and thus increases the dependency on the on-board navigation systems. Since all waypoints in RNP to ILS approaches are combined with an altitude constraint and a vertical path angle can be included in the navigation database, the vertical path of the approach is predefined and can be monitored by the FMGS during approach. As long as reliable altitude information is available from the air data computer, no DME or physical marker is required to verify that the aircraft is at the correct altitude for a particular position during the approach.

In possible changes to existing regulations, the focus should thus be on the requirements for the intermediate approach segment under consideration of the capabilities of navigation systems suitable for PBN procedures. The flight trials with the ATRA have shown that existing avionics

systems are capable of intercepting ILS guidance without an early alignment with the final approach course if the intermediate approach is designed in a way that positions the aircraft directly on the localizer and glideslope.

6.1.2. ARINC 424

Similar to the ICAO guidelines, the established approach categories in the ARINC 424 navigation database standard do not cover all aspects of RNP to ILS approaches. While the flight trials could be executed successfully with the experimental approaches coded as conventional ILS approaches, this required a specific workaround due to the existing representation of ILS approaches in the current version of the ARINC 424 standard. As mentioned in section 3.2.2, the coding of ILS approaches requires three consecutive waypoints on the final approach segment. The FACF, which is used for initial alignment with the localizer course in conventional ILS approaches, must be placed on the extended runway centerline prior to the actual FAP. However, due to the placement of an RF leg directly prior to the FAP in RNP to ILS approaches, no FACF can be positioned on the extended runway centerline. Although this problem could be circumvented by simply designating the actual FAP as the FACF and inserting an additional point on the final approach segment which serves as the FAP for coding purposes, this solution is not particularly elegant.

According to [16], the FACF is located at a distance of two to eight nautical miles from the coded FAP to designate the beginning of the final approach coding. For the coding of RNP to ILS approaches, this function could be transferred to the FAP in order to remove the necessity of a FACF, as the requirement for a separate FACF and FAP on the final approach segment is redundant if the intermediate approach is not aligned with the final approach. Beyond that, the current version of the ARINC 424 standard does not contain any obstacles for the coding of RNP to ILS procedures. However, it might be desirable to include a separate approach category for RNP to ILS approaches in order to clearly distinguish between conventional ILS approaches and ILS approaches with curved segments and a shortened final approach as well as to provide a unique identifier for the selection of approaches from the navigation database.

In case the idea of automatic approach mode activation is pursued, this event might be coupled with the overflight of the FAP. In this scenario, the ARINC 424 standard would need to include a clear definition of the corresponding point that might differ from the representation of the FAP or FAF in other approaches since the approach mode is usually armed much earlier than in RNP to

ILS approaches. However, this would entail far reaching changes exceeding the scope of the ARINC 424 standard, as the involved avionics systems currently do not support this function either.

6.2. Summary

In this report, the results of a flight test campaign on experimental RNP to ILS approaches with the A320-ATRA of the DLR are presented. During the flight tests, the main focus of the experiments was on the autoland performance of the ATRA in approaches with varying ILS intercept heights and track angle changes during the RF leg leading to the final approach. An overall number of 16 approaches to Braunschweig-Wolfsburg airport were flown with ILS intercept heights between 550 and 2,000 feet above ground level and track angle changes of either 90 or 180 degrees during the turn. The data recorded during the flight tests was analyzed with regard to the lateral and vertical navigation accuracy, the ILS intercept performance and the autoland capability of the ATRA.

During the preparation of the flight tests, it was noticed that the original database coding causes the FMS of the ATRA to create a vertical profile for the approach that deviates strongly from the intended path and includes an early descent to the ILS intercept height. As a result of this observation, a subset of the prepared approaches was changed to include a vertical path angle, thus allowing a comparison of the original design with altitude constraints only and the revised design which features a coded vertical path angle in the RNP part of the approach.

With the exception of one approach that was aborted due to an early descent to 550 feet above ground level, all approaches could be completed with a successful transition to ILS guidance and a subsequent automatic landing. The length of the straight final approach had no influence on the autoland capability of the aircraft, which was available immediately after localizer and glideslope capture at all times. RNP guidance during the initial and intermediate approach was accurate enough to deliver the aircraft to an intercept position out of which localizer and glideslope capture were possible within 20 seconds of approach mode activation for most of the approaches. Especially the correct altitude of the aircraft at the intended ILS intercept point is crucial for a quick transition to ILS guidance, which is required mostly for the approaches with ILS intercept heights below 1,000 feet above ground level.

The flight trials also showed that it is recommendable to include a vertical path angle in the coding of the approach, as the vertical path following is generally more accurate than in approaches that are based on altitude constraints only. In particular, the "dive and drive" behavior observed in the simulator tests and the approaches without a coded vertical path angle can be avoided by including a fixed vertical path angle into the approach coding.

In summary, it can be stated that the findings of the flight test campaign confirm the viability of the RNP to ILS concept. The most important design parameter, i.e. the length of the final approach segment, is much less critical than expected as automatic landings are possible with ILS intercept heights as low as 550 feet above ground level. Moreover, the definition of the vertical approach path in the navigation database is important for correct vertical path following during the RNP part of the approach. Although operational and approval-related aspects remain to be cleared, the technical requirements for successful RNP to ILS operations are already available in modern aircraft such as the A320.

6.3. Further Work

With the completion of the flight test campaign, the first part of the research activity regarding automatic landings after RNP to ILS approaches is concluded. However, the findings presented in this report and in [5] are strongly connected to the A320 aircraft family, which raises the question how other types of aircraft and flight management systems handle the specific challenges of RNP to ILS approaches. The abilities and potential restrictions of the Boeing 737 are of particular interest, as it is another aircraft that is widely used by airlines on short and medium-haul routes. In order to evaluate the practicability of RNP to ILS approaches on a larger scale, simulator tests or even flight tests with an actual aircraft could be performed. Moreover, different avionics systems should be tested with experimental RNP to ILS approaches so as to ascertain that there are no unforeseen problems with systems produced by other manufacturers.

Beyond that, there are many opportunities for further research on the RNP to ILS concept in the field of air traffic control. The advantages of RNP to ILS procedures such as shorter and more flexible approach paths should be analyzed from the point of view of an air traffic controller, paying special attention to aspects such as compatibility with other approaches, lateral and vertical separation of approaching and departing aircraft as well as controller workload. In addition, the effect of the usage of RF legs in approaches to airports with parallel runways would

need to be evaluated with regard to possible problems with the Traffic Alert and Collision Avoidance System (TCAS) that could emerge as a result of aircraft turning onto the final approach later than in existing procedures. Multiple RNP to ILS approaches to the same runway that start at different IAFs and thus include turning segments of different length could also lead to confusion and create difficulties for the adherence to lateral separation minimums.

Finally, the continued development and application of the GLS as an alternative or even replacement for the ILS offers the possibility of new RNP to GLS procedures. A set of experimental RNP to GLS procedures for runway 08 of Braunschweig-Wolfsburg airport has already been included in the navigation database of the ATRA and can be used in future flight tests. Although basically identical to the RNP to ILS approaches for runway 26, the different avionics systems involved during GLS approaches might have an effect on the GLS intercept or autoland performance of the ATRA. Further investigation of this topic would complement the previous research on RNP to ILS approaches and might result in additional procedures suited for a more flexible and environment-friendly approach phase.

7. Bibliography

[1] T. Blase, *Anforderungsanalyse und Entwurf von xLS-Autoland-Operationen mit gekurvten RNP für das Versuchsflugzeug A320-ATRA des DLR,* Braunschweig: DLR Institut für Flugführung, 2015.

[2] International Civil Aviation Organization, *Performance-based Navigation (PBN) Manual,* Montréal: ICAO, 2012.

[3] International Civil Aviation Organization, *Required Navigation Performance Authorization Required (RNP AR) Procedure Design Manual,* Montréal: ICAO, 2009.

[4] SESAR Joint Undertaking, *The VINGA Project Final Report,* Brussels: SESAR Joint Undertaking, 2011.

[5] SESAR Project 9.9, *Deliverable D1 - Operational Concept Description,* Brussels: SESAR Joint Undertaking, 2012.

[6] H. Dodel and D. Häupler, *Satellitennavigation*, Berlin: Springer, 2010.

[7] B. Hofmann-Wellenhof, H. Lichtenegger and E. Wasle, *GNSS - Global Navigation Satellite Systems*, Vienna: Springer, 2008.

[8] C. A. Ogaja, *Applied GPS for Engineers and Project Managers*, Reston, VA: American Society of Civil Engineers, 2011.

[9] National Imagery and Mapping Agency, *Department of Defense World Geodetic System 1984,* Springfield, VA: NIMA, 2000.

[10] D. D. McCarthy, *IERS Conventions (IERS Technical Note 21),* Paris: Central Bureau of IERS - Observatoire de Paris, 1996.

[11] C. M. R. Fowler, *The Solid Earth: An Introduction to Global Geophysics*, Cambridge: Cambridge University Press, 2007.

[12] B. Hofmann-Wellenhof and H. Moritz, *Physical Geodesy*, Vienna: Springer, 2006.

[13] International Civil Aviation Organization, *World Geodetic System - 1984 (WGS-84) Manual*, Montréal: ICAO, 2002.

[14] R. Collinson, *Introduction to Avionics Systems*, Dordrecht: Springer, 2011.

[15] Aeronautical Radio, Incorporated, *ARINC Specification 429P1-18,* Annapolis, MD: ARINC, 2012.

[16] Aeronautical Radio, Incorporated, *ARINC Specification 424-20,* Annapolis, MD: ARINC, 2011.

[17] Deutsches Zentrum für Luft- und Raumfahrt, Airbus A320-232 D-ATRA, 2012. [Online]. Available: http://www.dlr.de/dlr/desktopdefault.aspx/tabid-10203/339_read-277#/gallery/110. [Accessed 23 February 2015].

[18] Airbus, *A318/A319/A320/A321 Flight Crew Operating Manual,* Toulouse: Airbus, 2013.

[19] K. Giese, *IenaDecoder - Dokumentation des Programms,* Braunschweig: DLR Institut für Flugführung, 2010.

[20] RTCA, Inc., *Minimum Operational Performance Standards for GPS Local Area Augmentation System Airborne Equipment,* Washington, D.C.: RTCA, 2008.

[21] M. Felux, T. Dautermann and H. Becker, *GBAS Landing System - Precision Approach Guidance After ILS*, Aircraft Engineering and Aerospace Technology: An International Journal, vol. 85, no. 5, pp. 382-388, 2013.

[22] International Civil Aviation Organization, *Procedures for Air Navigation Services - Aircraft Operations,* Montréal: ICAO, 2014.

Abbreviations

AGL ..... Above Ground Level
ANP ..... Actual Navigation Performance
ARINC ..... Aeronautical Radio, Incorporated
ASCII ..... American Standard Code for Information Interchange
ATC ..... Air Traffic Control
ATRA ..... Advanced Technology Research Aircraft
BCD ..... Binary Coded Decimal
BNR ..... Binary
COM ..... Component Object Model
DGPS ..... Differential GPS
DLR ..... *(German)* Deutsches Zentrum für Luft- und Raumfahrt
DME ..... Distance Measuring Equipment
EPU ..... Estimated Position Uncertainty
FAC ..... Flight Augmentation Computer
FAF ..... Final Approach Fix
FAP ..... Final Approach Point
FCU ..... Flight Control Unit
FDIMU ..... Flight Data Interface Management Unit
FGS ..... Flight Guidance System
FIR ..... Flight Information Region
FM ..... Flight Management
FMA ..... Flight Mode Annunciator
FMGC ..... Flight Management and Guidance Computer
FMGS ..... Flight Management and Guidance System
FMS ..... Flight Management System
FPA ..... Flight Path Angle
FPAP ..... Flight Path Alignment Point
FTE ..... Flight Technical Error

FTI ..... Flight Test Installation
GBAS ..... Ground-Based Augmentation System
GLS ..... GNSS Landing System
GNSS ..... Global Navigation Satellite System
GPIP ..... Glide Path Intercept Point
GPS ..... Global Positioning System
IAF ..... Initial Approach Fix
ICAO ..... International Civil Aviation Organization
IENA ..... *(French)* Installation d'Essais Nouveaux Avions
IERS ..... International Earth Rotation and Reference Systems Service
ILS ..... Instrument Landing System
IRM ..... International Reference Meridian
IRP ..... International Reference Pole
IRS ..... Inertial Reference System
LTP ..... Landing Threshold Point
MAPt ..... Missed Approach Point
MCDU ..... Multipurpose Control and Display Unit
MLS ..... Microwave Landing System
MORA ..... Minimum Off Route Altitude
MSA ..... Minimum Sector Altitude
MSL ..... Mean Sea Level
MVA ..... Minimum Vectoring Altitude
ND ..... Navigation Display
NDB ..... Non-Directional Beacon
NM ..... Nautical Mile
NSE ..... Navigation System Error
PBN ..... Performance-based Navigation
PDE ..... Path Definition Error
PFD ..... Primary Flight Display

PRC ..... Pseudorange Correction
RNP ..... Required Navigation Performance
RRC ..... Range Rate Correction
SBAS ..... Space-Based Augmentation System
SDI ..... Source/Destination Identifier
SID ..... Standard Instrument Departure
SRS ..... Speed Reference System
SSM ..... Sign/Status Matrix
STAR ..... Standard Terminal Arrival Route
TAS ..... True Airspeed
TCAS ..... Traffic Alert and Collision Avoidance System
TSE ..... Total System Error
UIR ..... Upper Flight Information Region
VFR ..... Visual Flight Rules
VHF ..... Very High Frequency
WGS ..... World Geodetic System
XidML ..... eXtensible Instrumentation Data exchange Mark-up Language

List of Figures

Figure 2.1: RNP navigation error components 13
Figure 2.2: Spheroid geometry 22
Figure 2.3: Latitude and longitude 23
Figure 2.4: Ellipsoidal height and radius of curvature of the prime vertical 24
Figure 3.1: Glideslope capture after reaching the ILS intercept point too high or too low 35
Figure 3.2: Early transition to LOC* mode with active approach mode 36
Figure 3.3: Approach paths with track angle change of 180 degrees 37
Figure 3.4: Approach paths with track angle change of 90 degrees 38
Figure 3.5: Original final approach layout and ARINC 424-compliant layout 43
Figure 3.6: Early level-off as indicated on the simulator ND 45
Figure 3.7: Design vertical path and „dive and drive" behavior of the aircraft 45
Figure 3.8: Vertical path coding with and without flight path angle 47
Figure 4.1: A320 flight mode annunciator 60
Figure 5.1: Unit vectors defining the final approach segment 69
Figure 5.2: Structure of the deviation matrix 71
Figure 5.3: Lateral FTE after the RF leg entry point per approach 72
Figure 5.4: Combined plot of lateral deviations during 90° approaches 73
Figure 5.5: Standard deviation of the lateral FTE 74
Figure 5.6: Lateral NSE per approach 75
Figure 5.7: Standard deviation of the lateral NSE 76
Figure 5.8: Vertical FTE after the RF leg entry point per approach 78
Figure 5.9: Standard deviation of the vertical FTE 79
Figure 5.10: Comparison of vertical deviations during 90° and 180° approaches 80
Figure 5.11: Measured flight path angles during approaches #2 and #16 81
Figure 5.12: Time between approach mode activation and localizer/glideslope capture 83
Figure 5.13: Radio altitude at LAND mode engagement per approach 84

List of Tables

Table 2.1: BCD sign/status matrix 27
Table 2.2: BNR status matrix 28
Table 2.3: BNR sign matrix 28
Table 2.4: Definition of ARINC 424 sections and subsections 30
Table 2.5: Subset of ARINC 424 path terminators 32
Table 2.6: Constraint types 33
Table 3.1: Experimental approach design parameters 37
Table 3.2: Composition of the ARINC 424 waypoint identifier 38
Table 3.3: Exemplary ARINC 424 waypoint record 40
Table 3.4: Exemplary ARINC 424 approach record 42
Table 3.5: Standard parameters recorded during ATRA flight tests 51
Table 4.1: Pseudo waypoint symbols and definitions 55
Table 4.2: A320 autopilot guidance modes 57
Table 4.3: A320 autopilot lateral modes 58
Table 4.4: A320 autopilot vertical modes 60
Table 4.5: A320 autopilot modes for ILS-based automatic landing 61
Table 4.6: Flight test schedule 64
Table 4.7: Flight test procedure for RNP to ILS approaches at Braunschweig-Wolfsburg airport . 67

Appendix A – ARINC 424 Navigation Database

Property of LIDO. Please contact:
Lufthansa Systems Flight Nav Inc.
P. O. Box 202
CH- 8058 Zurich-Airport
fms.support@lhsystems.com

Appendix B – Lateral Trajectory and Atmospheric Conditions

#1 ILS W 90°

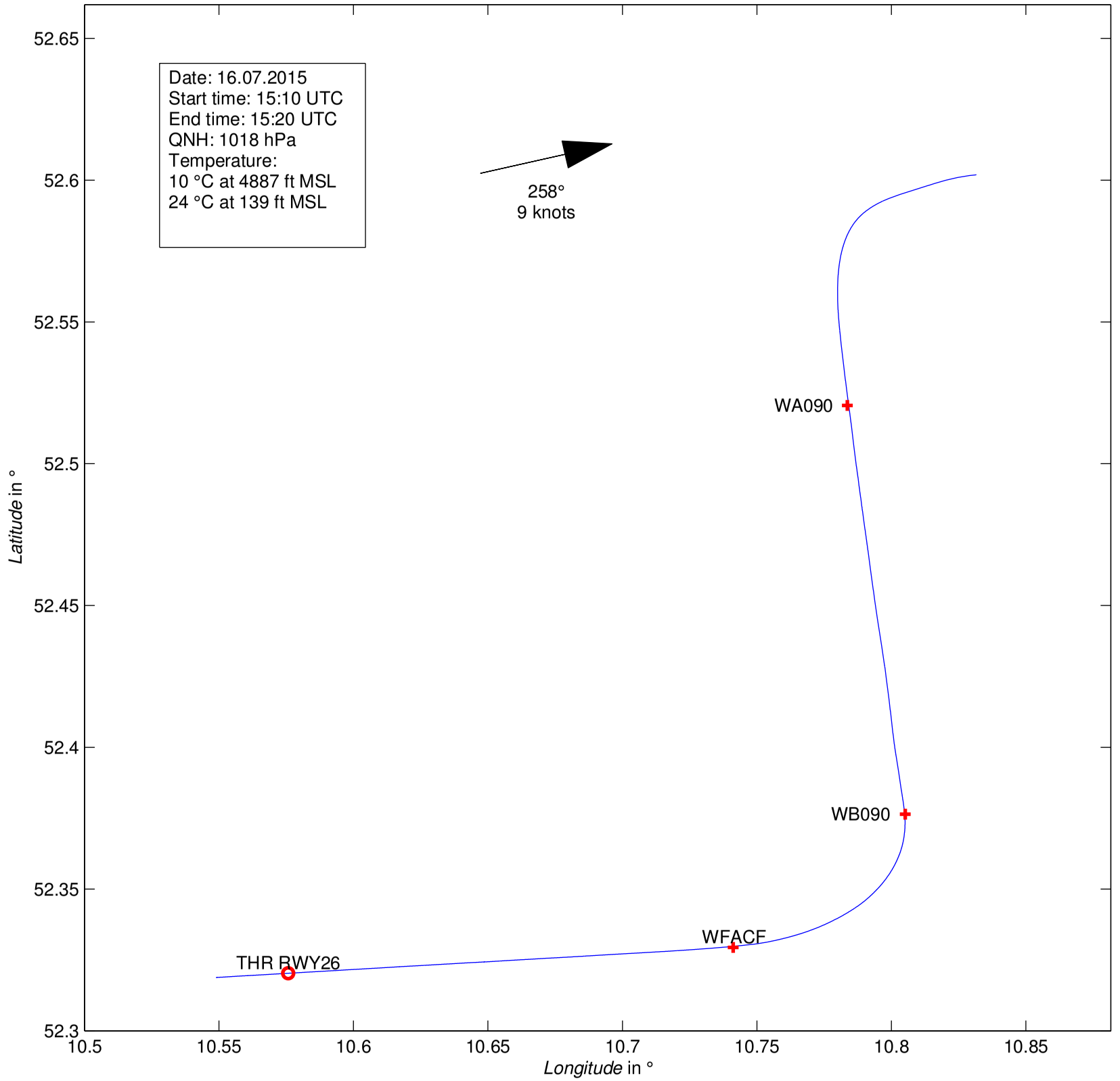

DLR Institut für Flugführung

#2 ILS V 180°

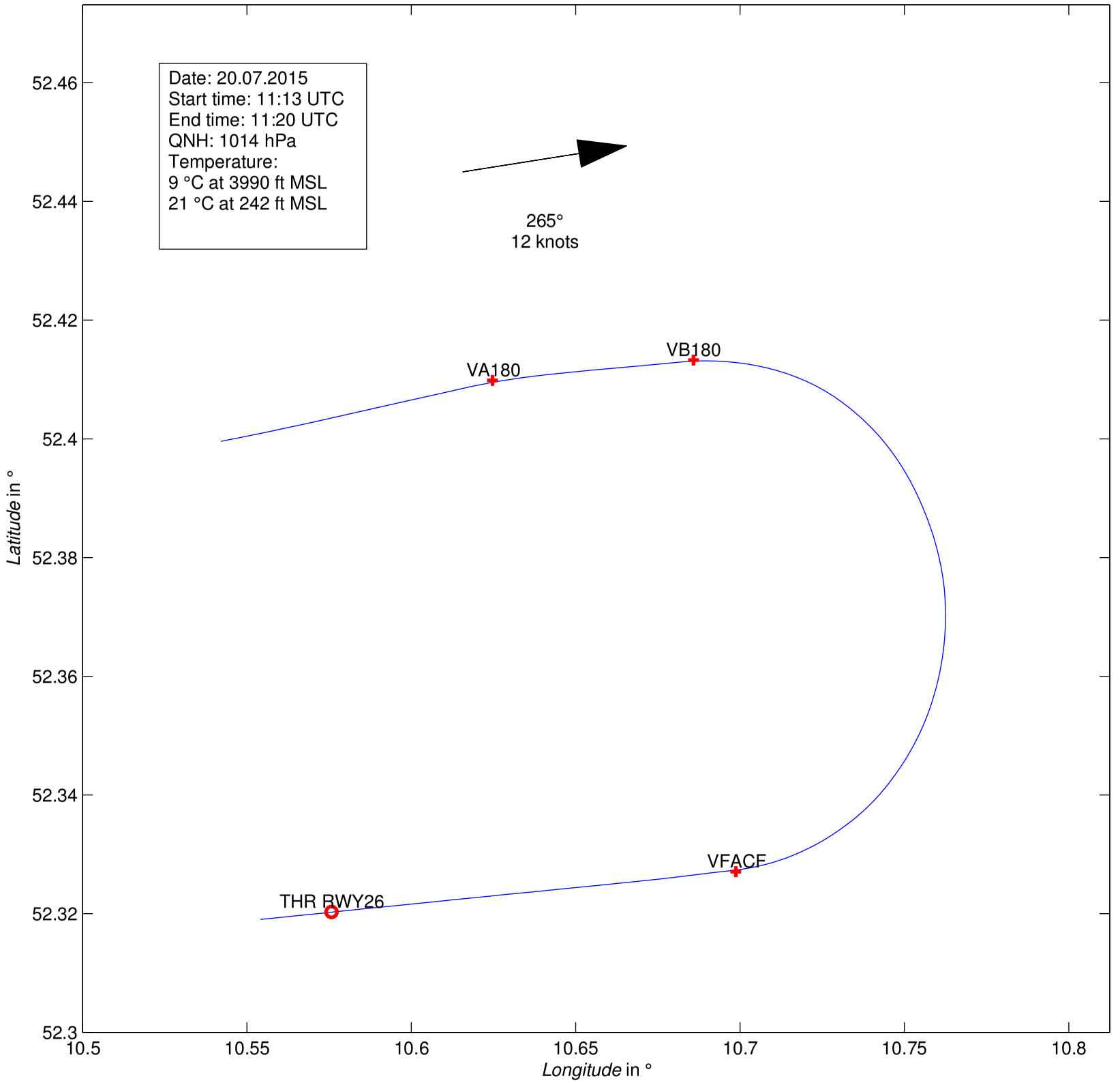

DLR Institut für Flugführung

#3 ILS U 90° APPR

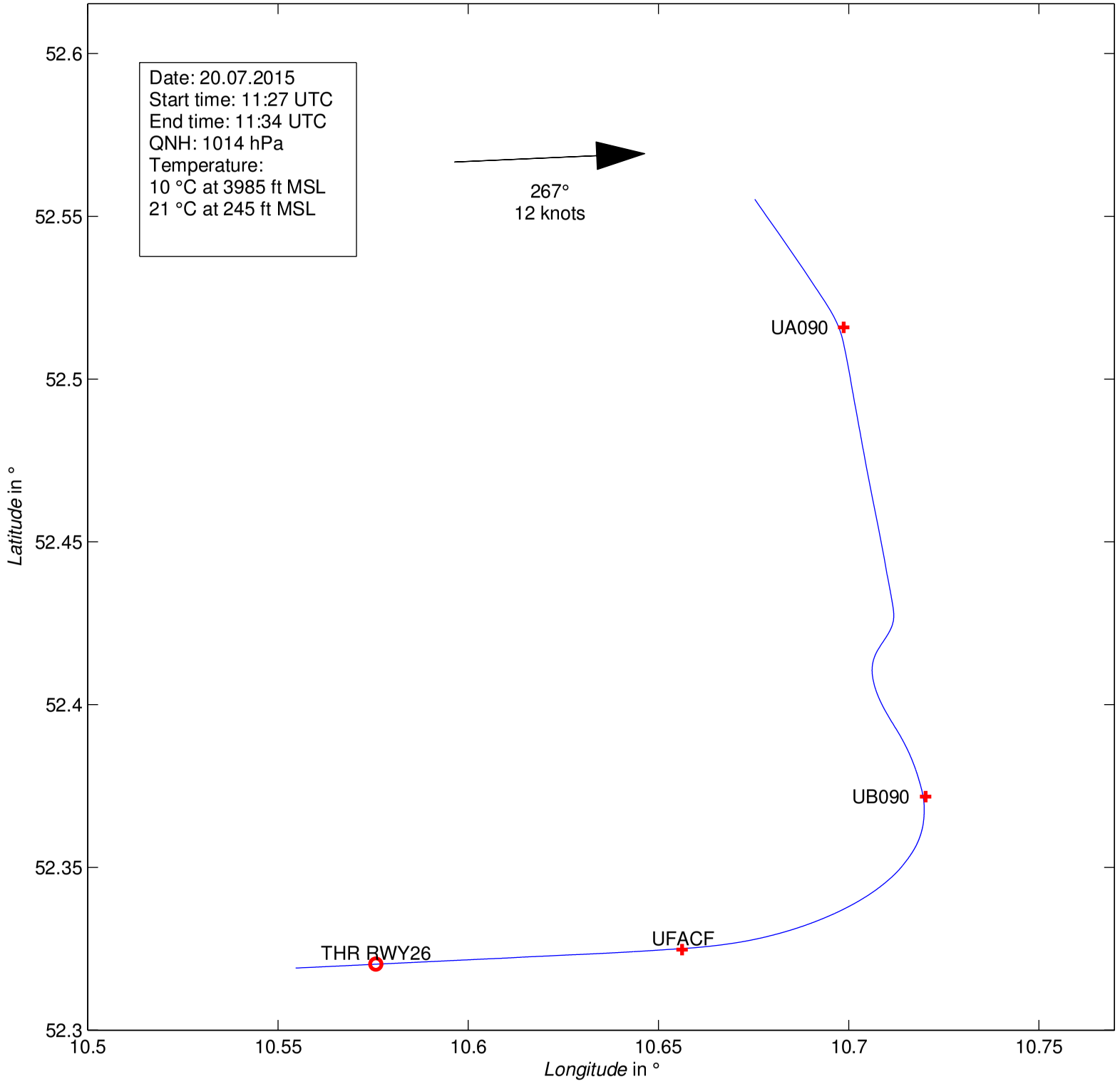

DLR Institut für Flugführung

#4 ILS T 90°

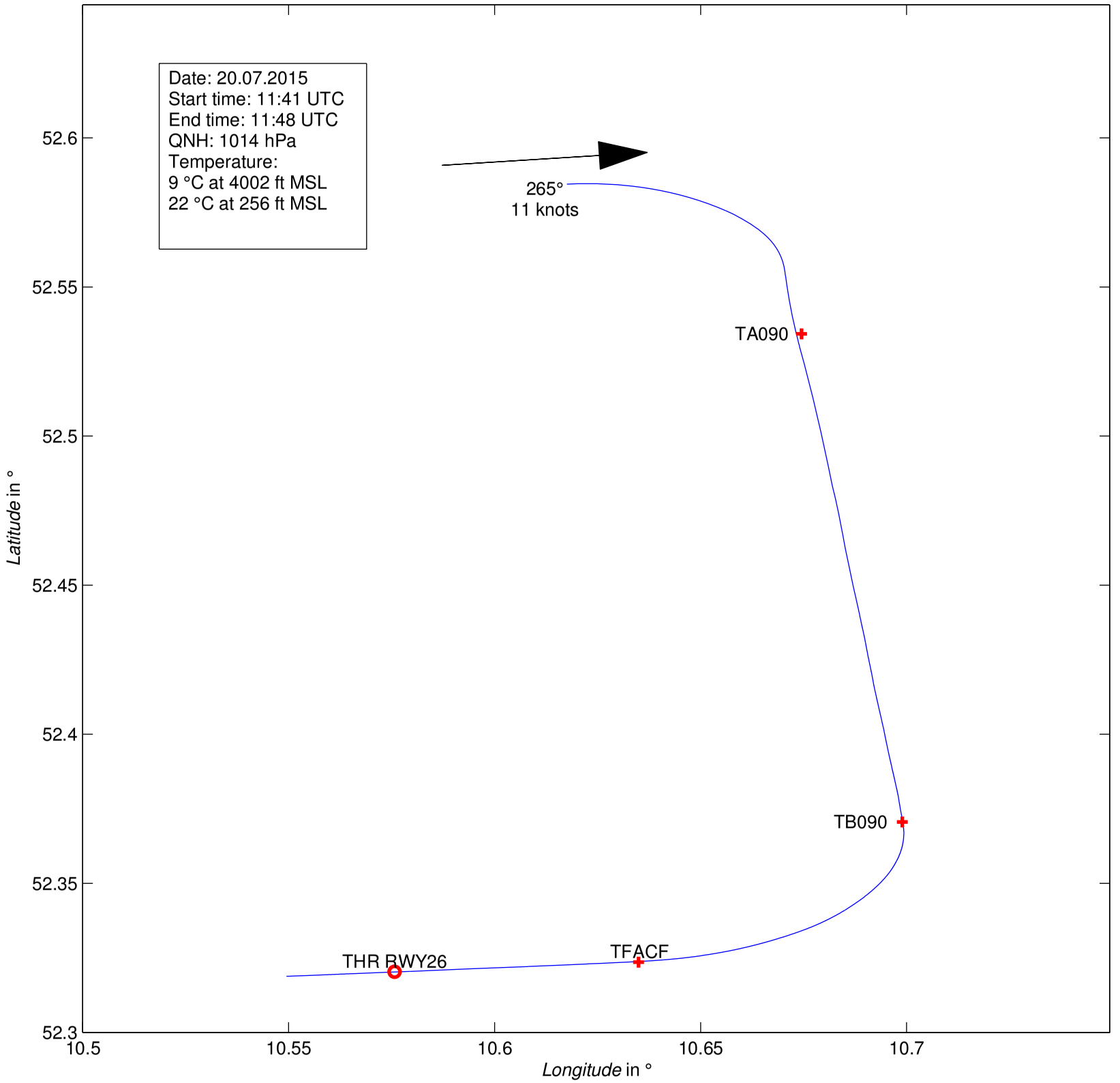

DLR Institut für Flugführung

#5 ILS S 180°

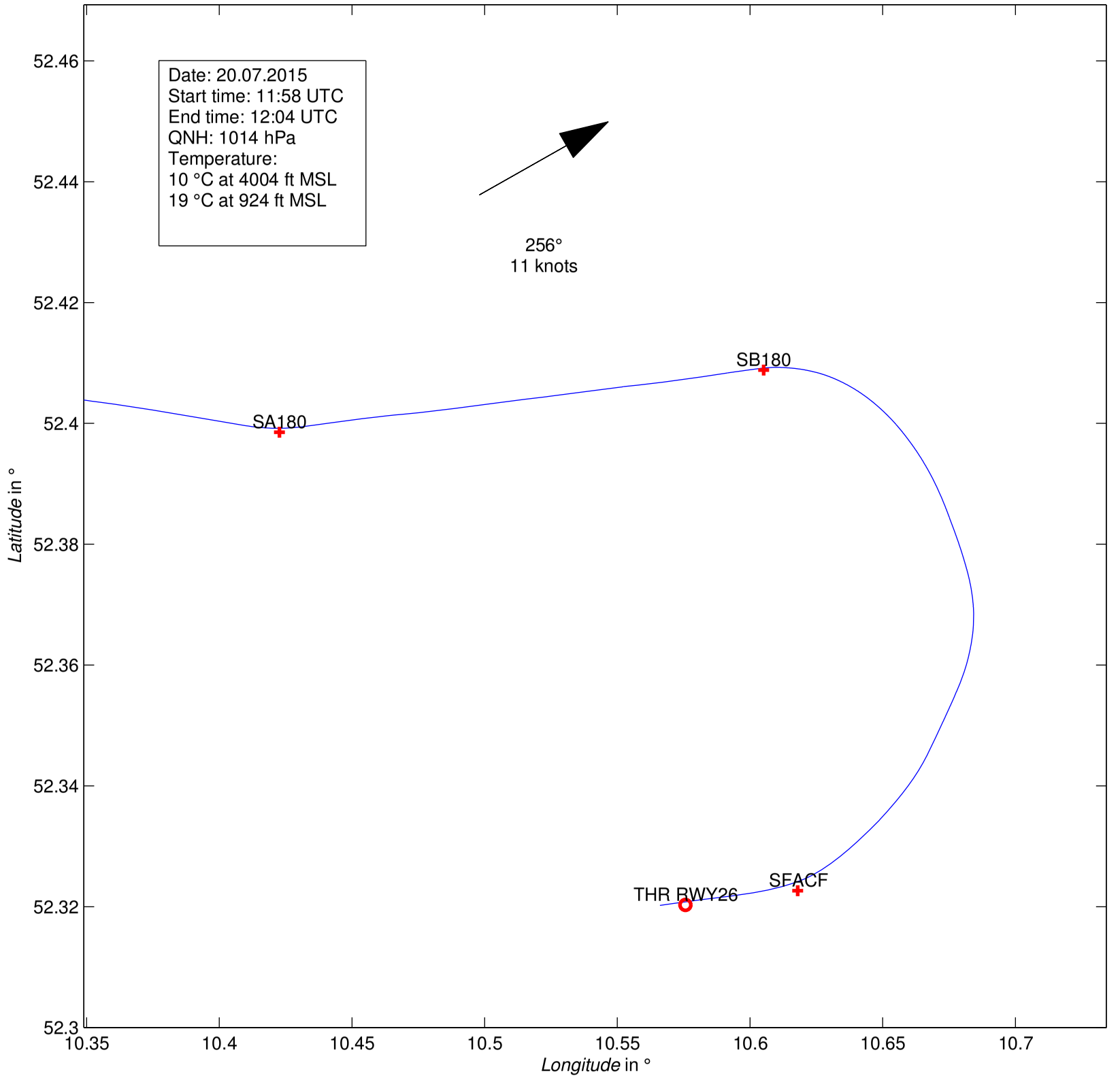

DLR Institut für Flugführung

#6 ILS W 90° APPR

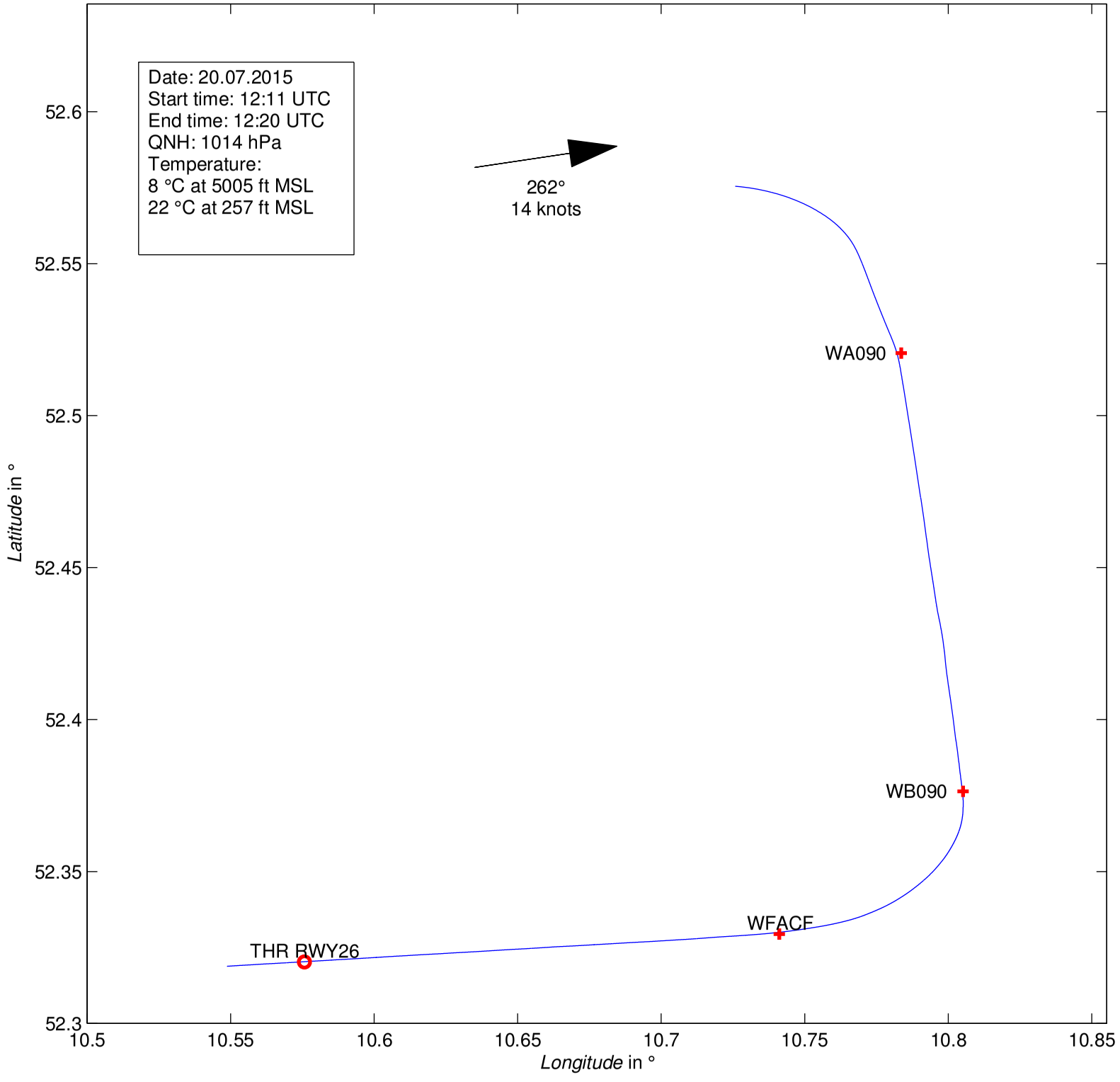

DLR Institut für Flugführung

#7 ILS V 90°

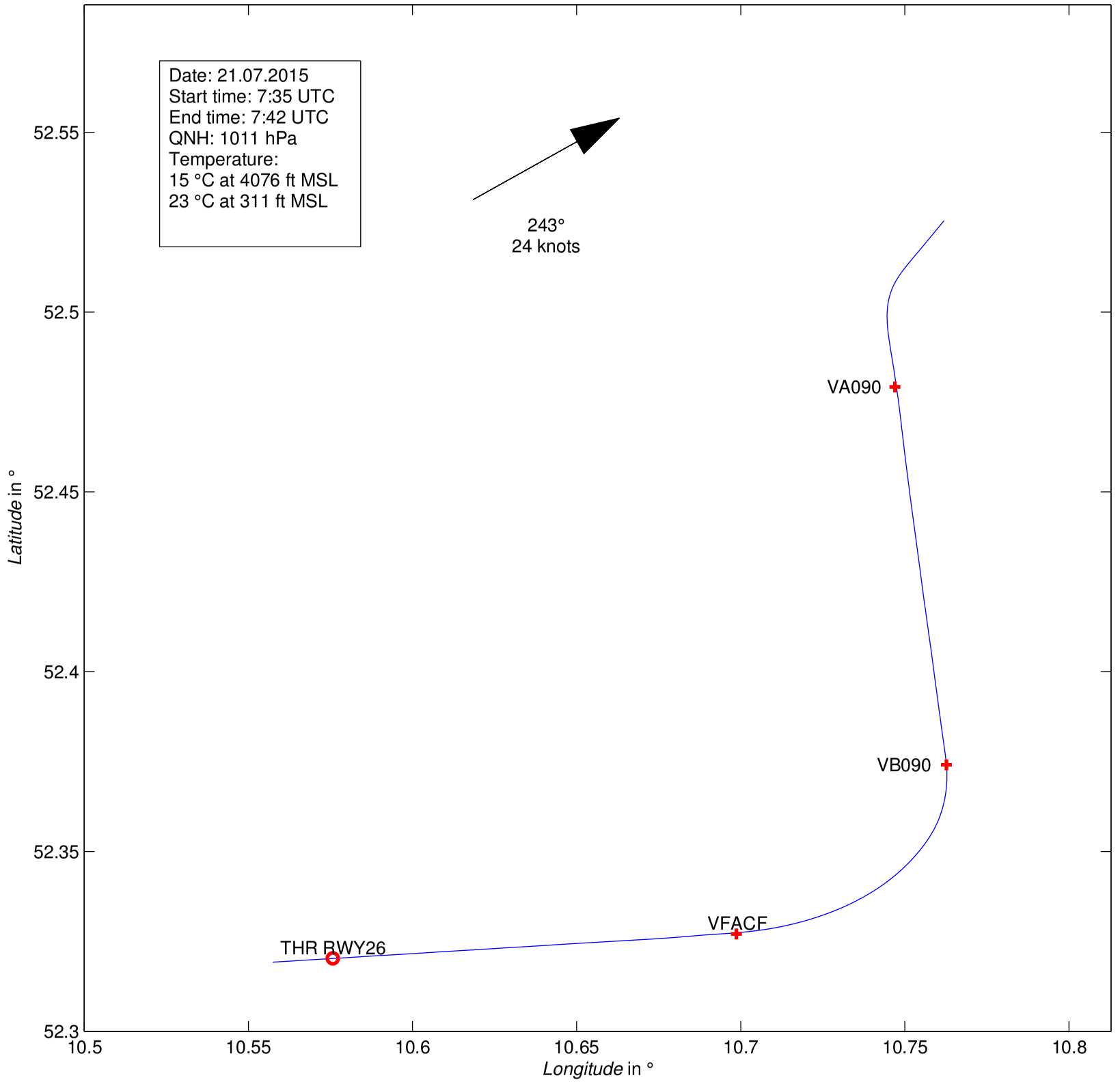

DLR Institut für Flugführung

#8 ILS U 180°

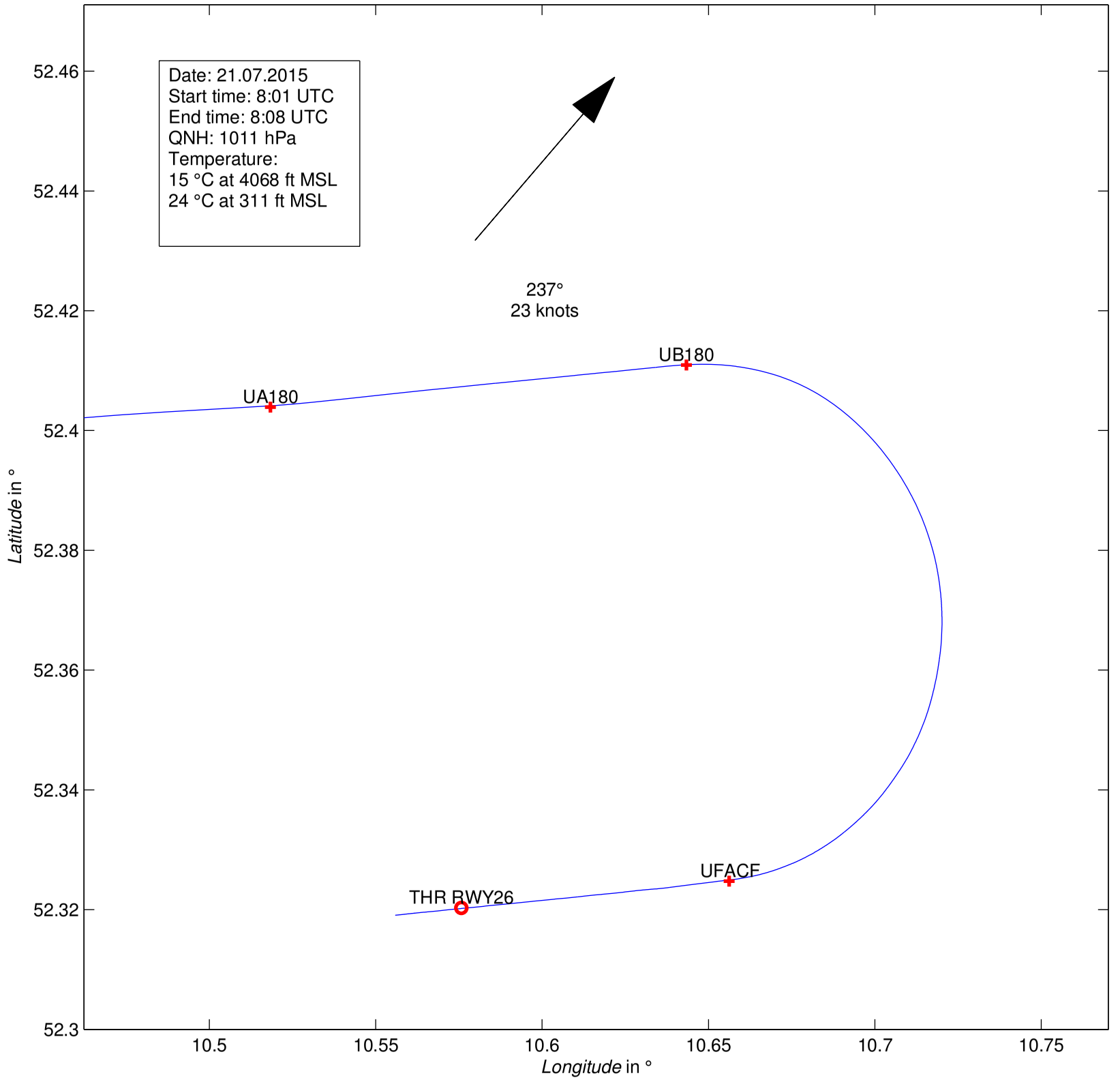

DLR Institut für Flugführung

#9 ILS T 90°

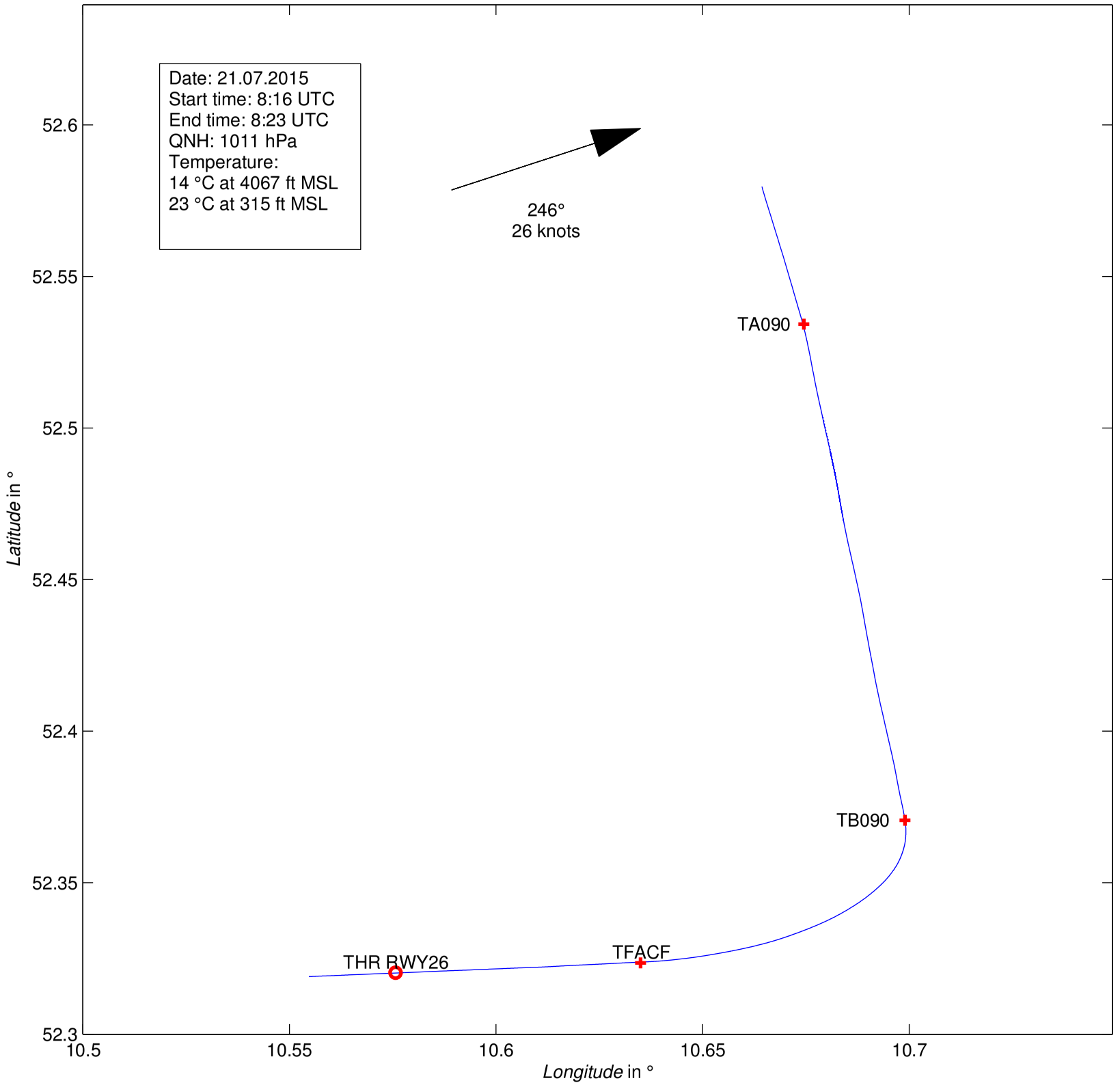

DLR Institut für Flugführung

#10 ILS W 180°

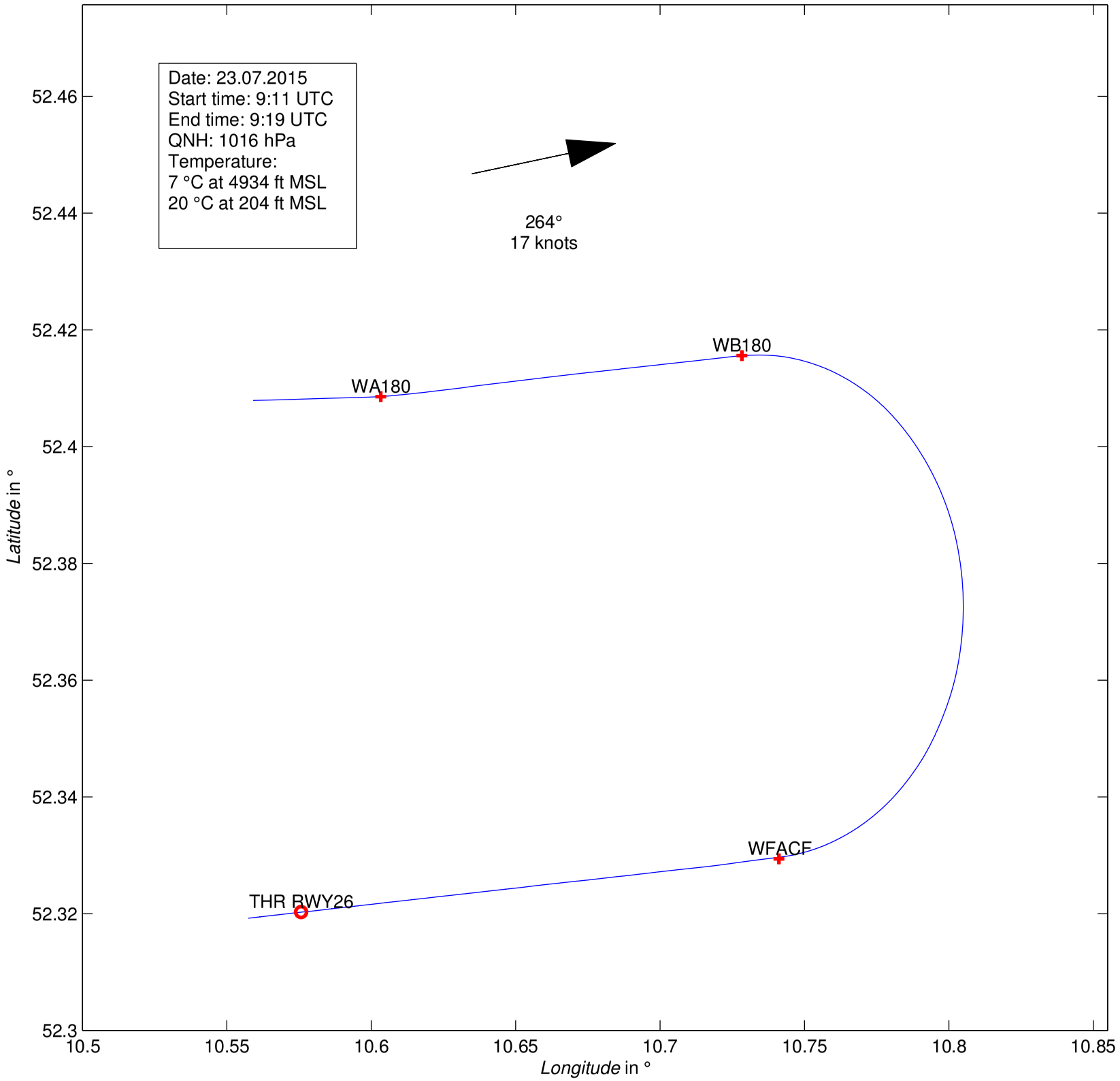

DLR Institut für Flugführung

#11 ILS T 90°

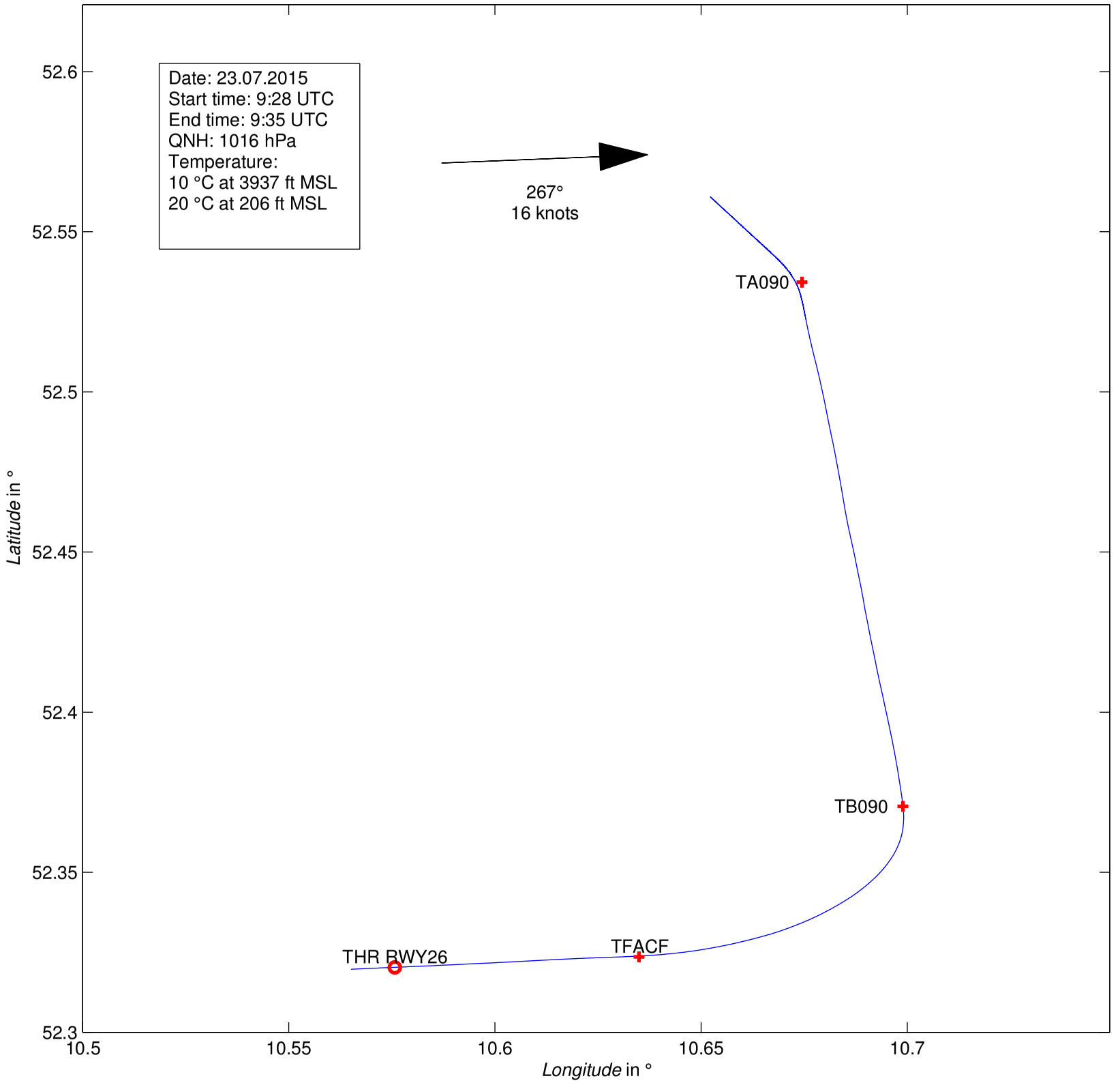

DLR Institut für Flugführung

#12 ILS S 90°

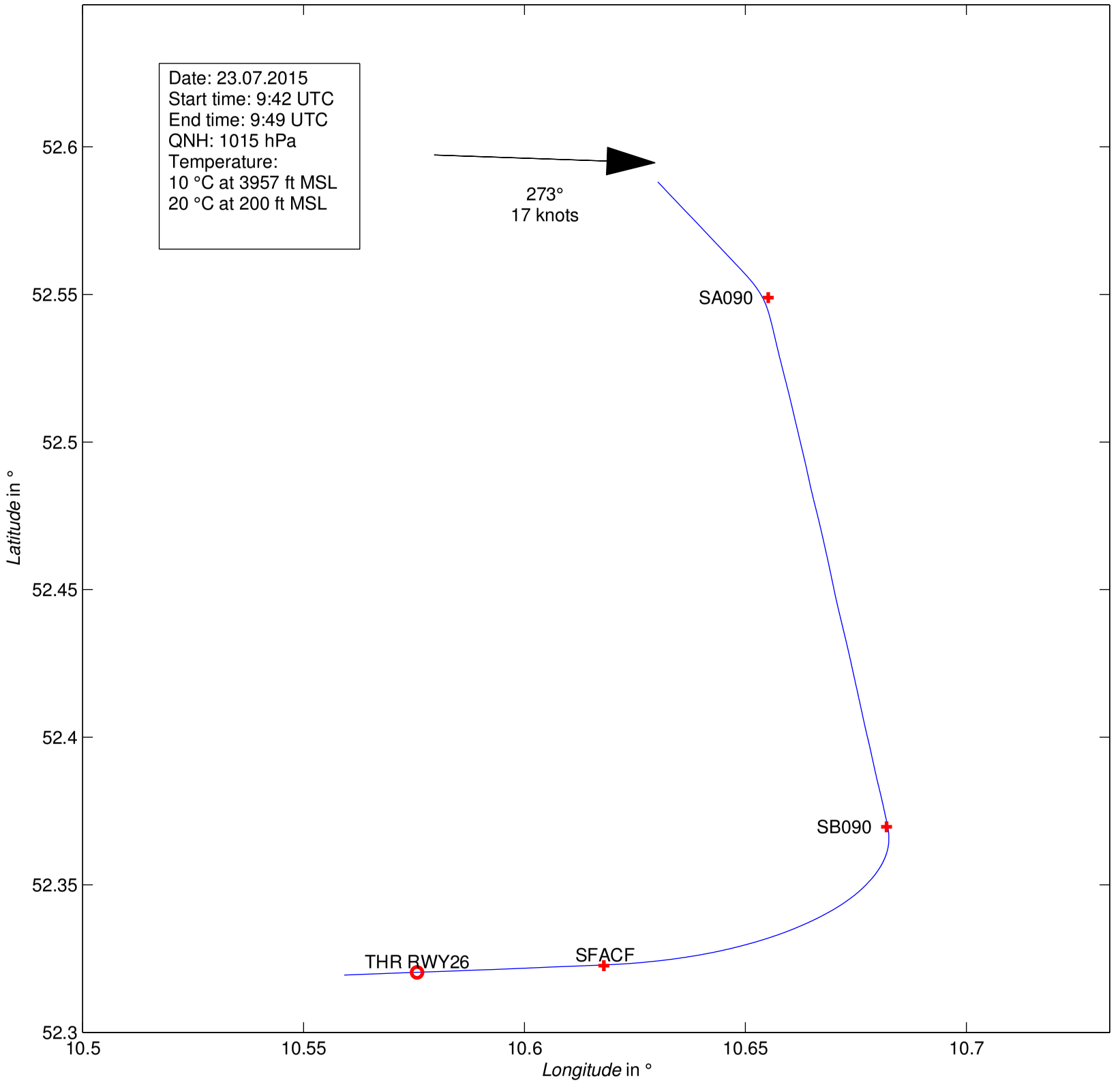

DLR Institut für Flugführung

#13 ILS V 90° APPR

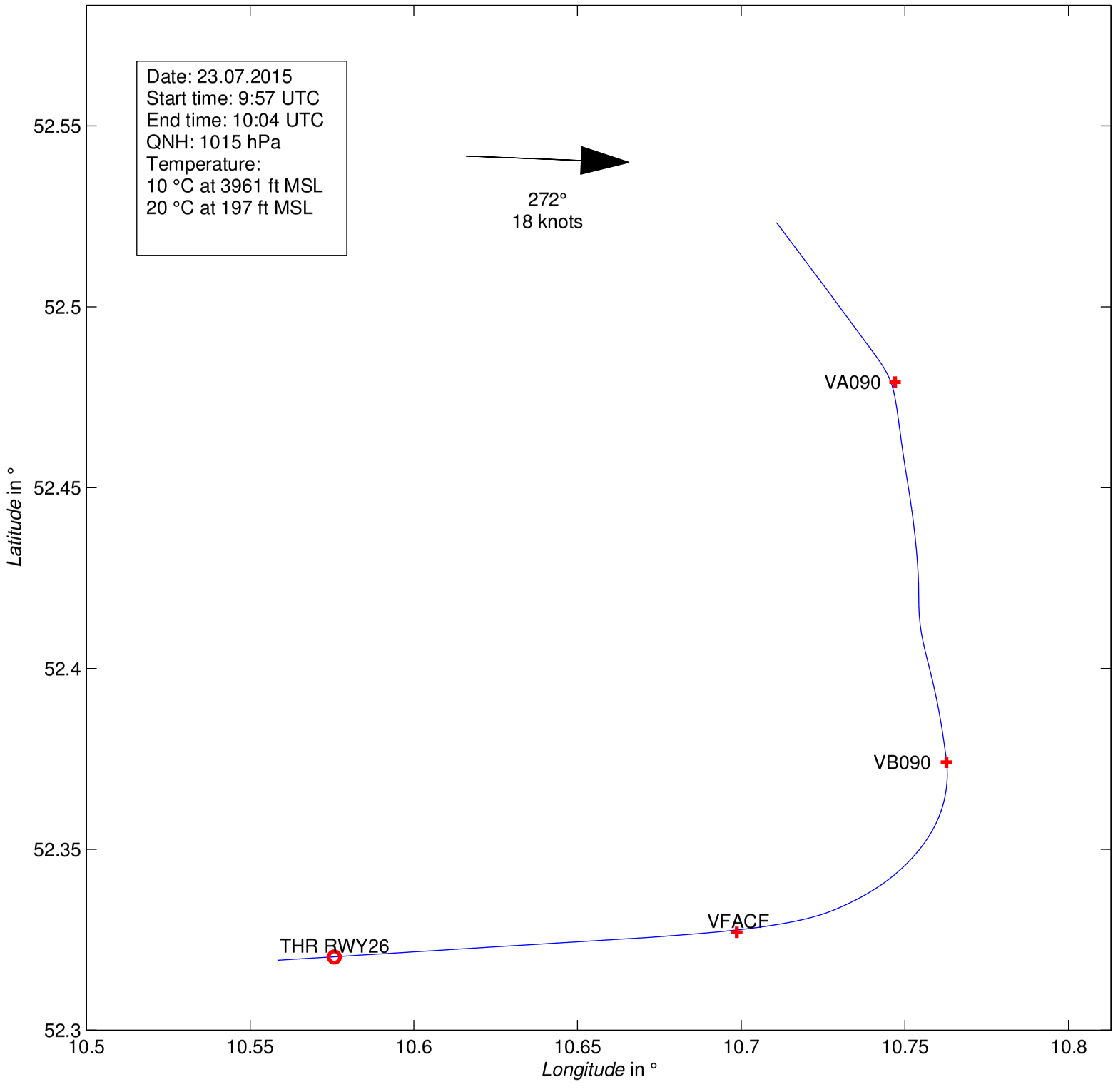

DLR Institut für Flugführung

#14 ILS U 90°

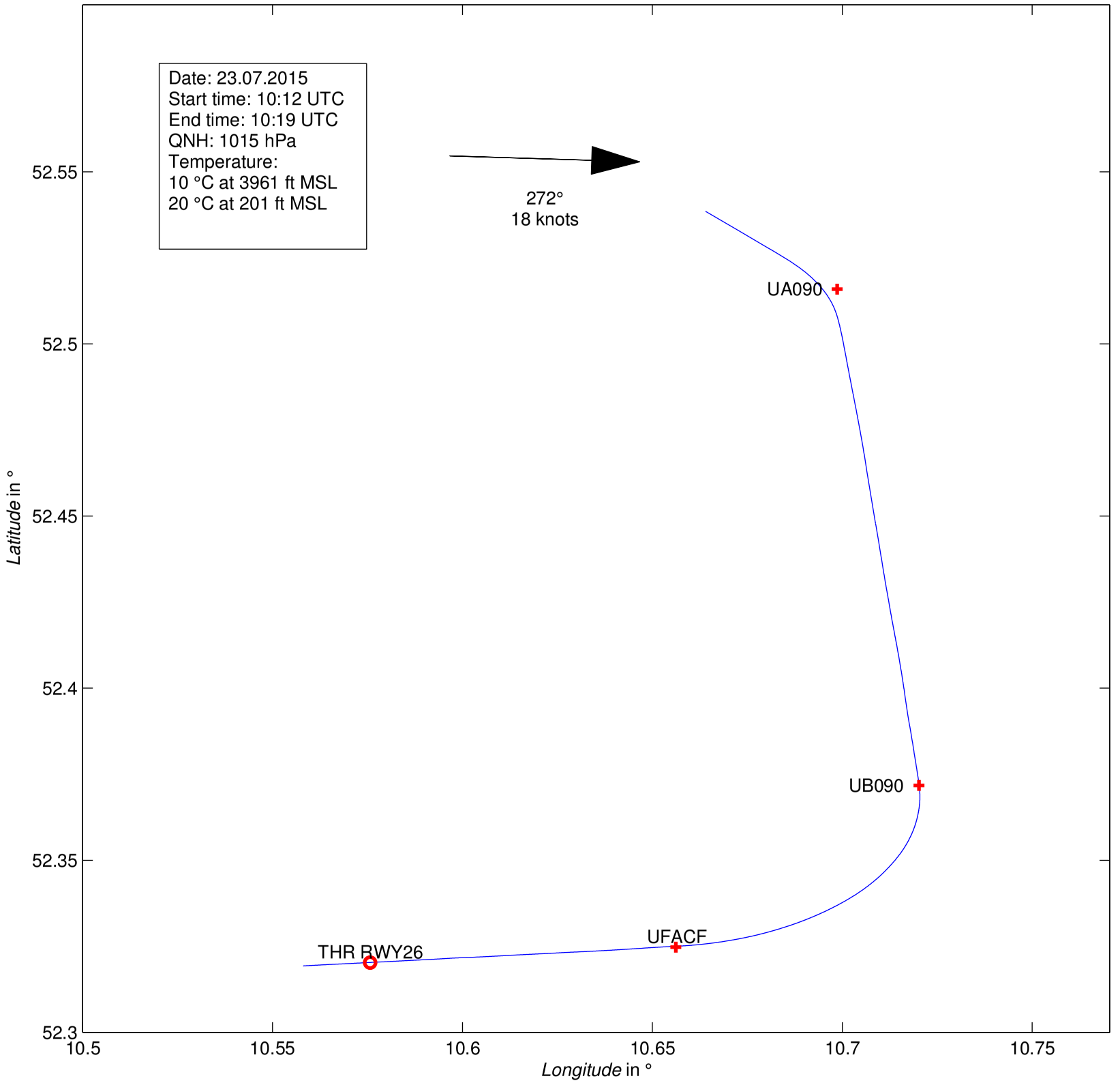

DLR Institut für Flugführung

#15 ILS V 180° APPR

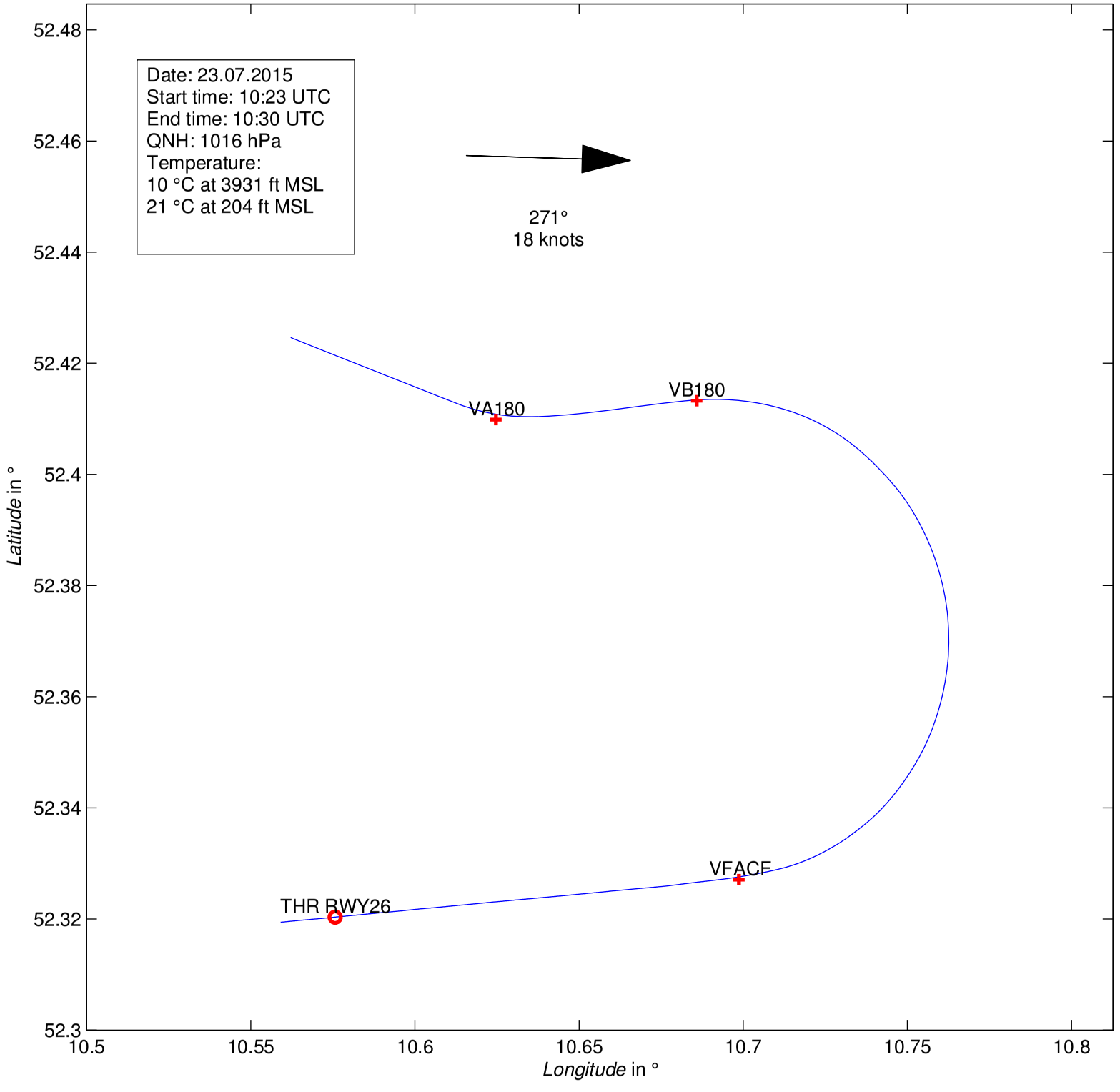

DLR Institut für Flugführung

#16 ILS S 90°

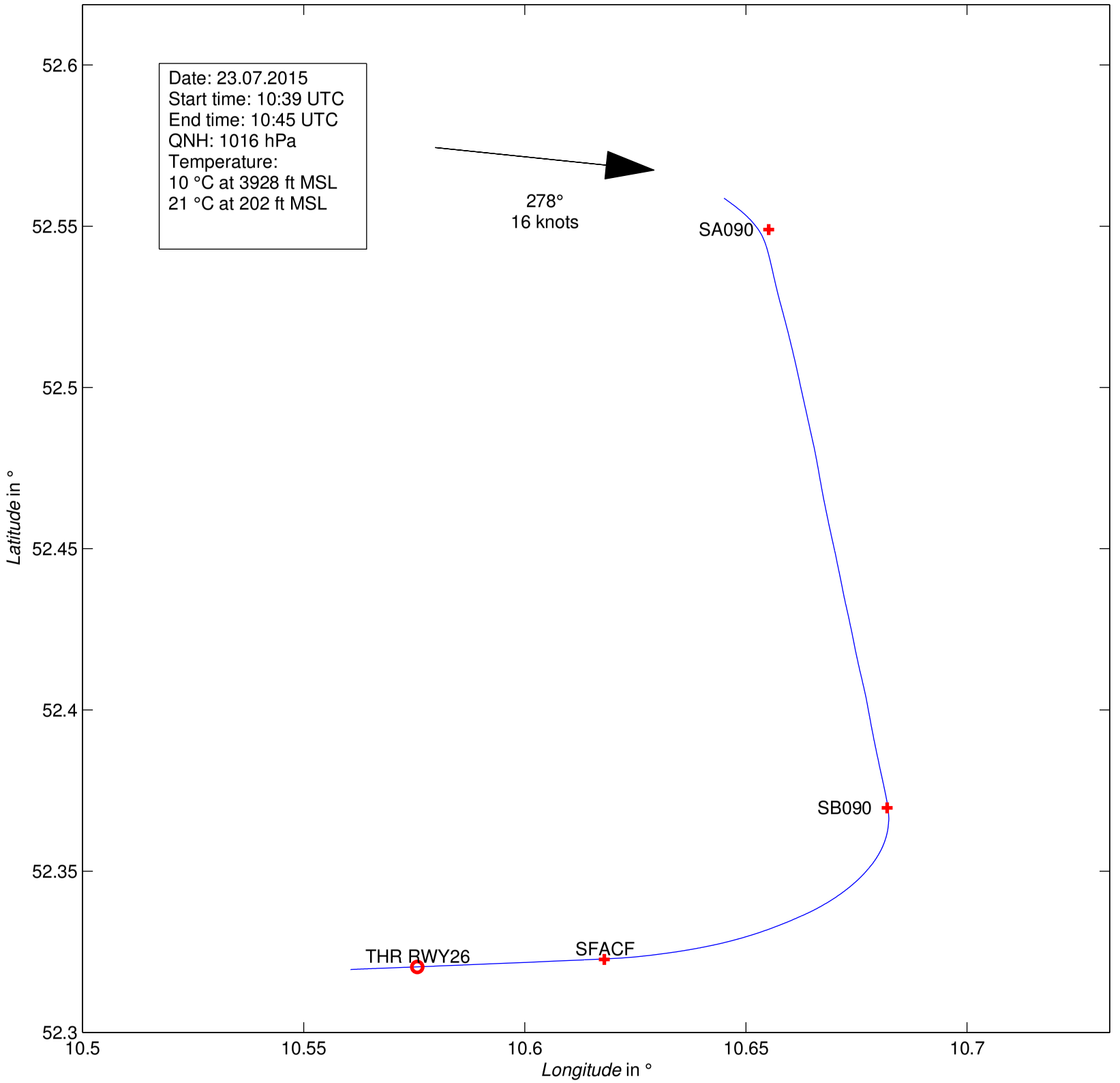

DLR Institut für Flugführung

Appendix C – Lateral and Vertical Flight Technical Error

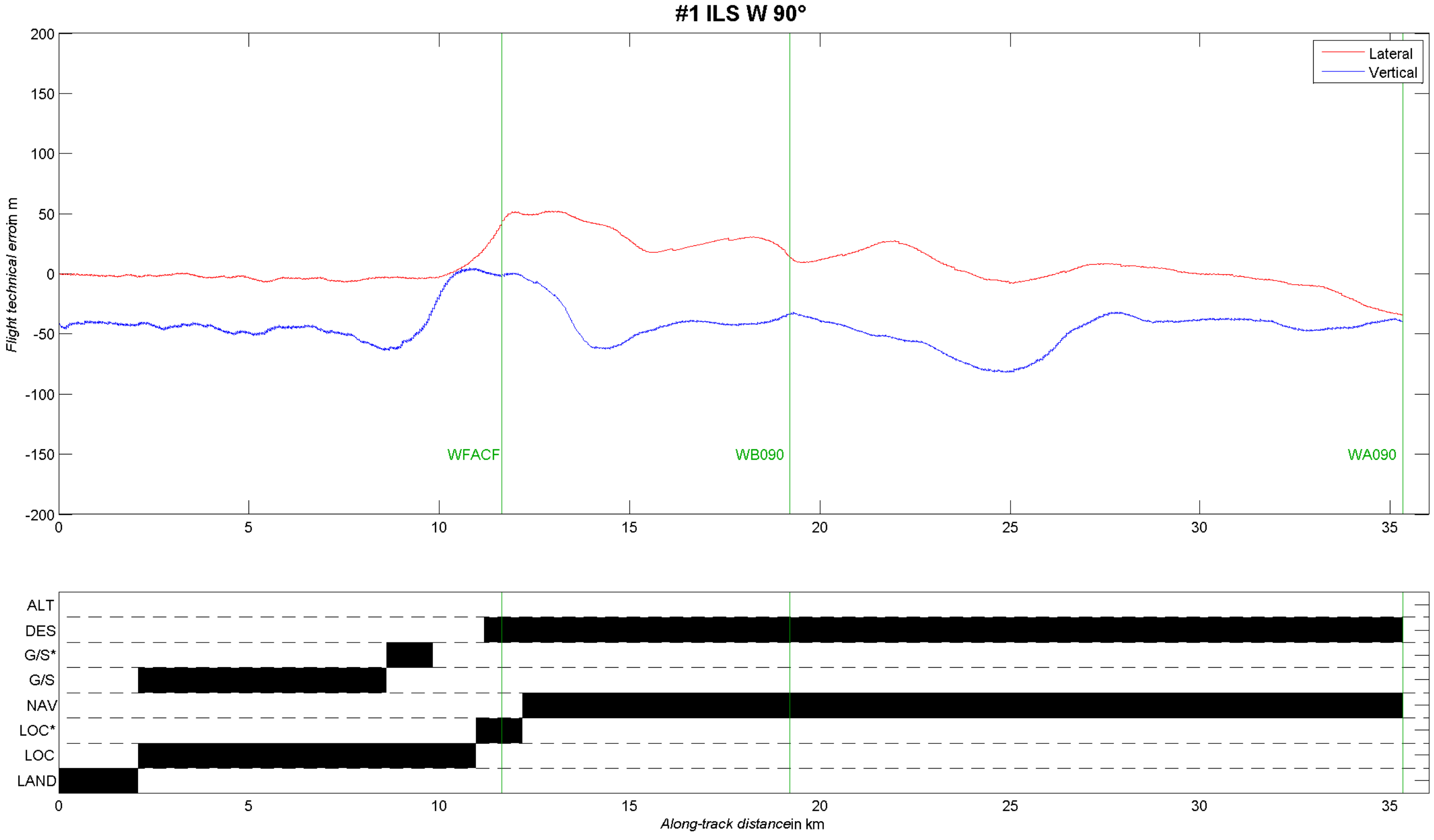

DLR Institut für Flugführung

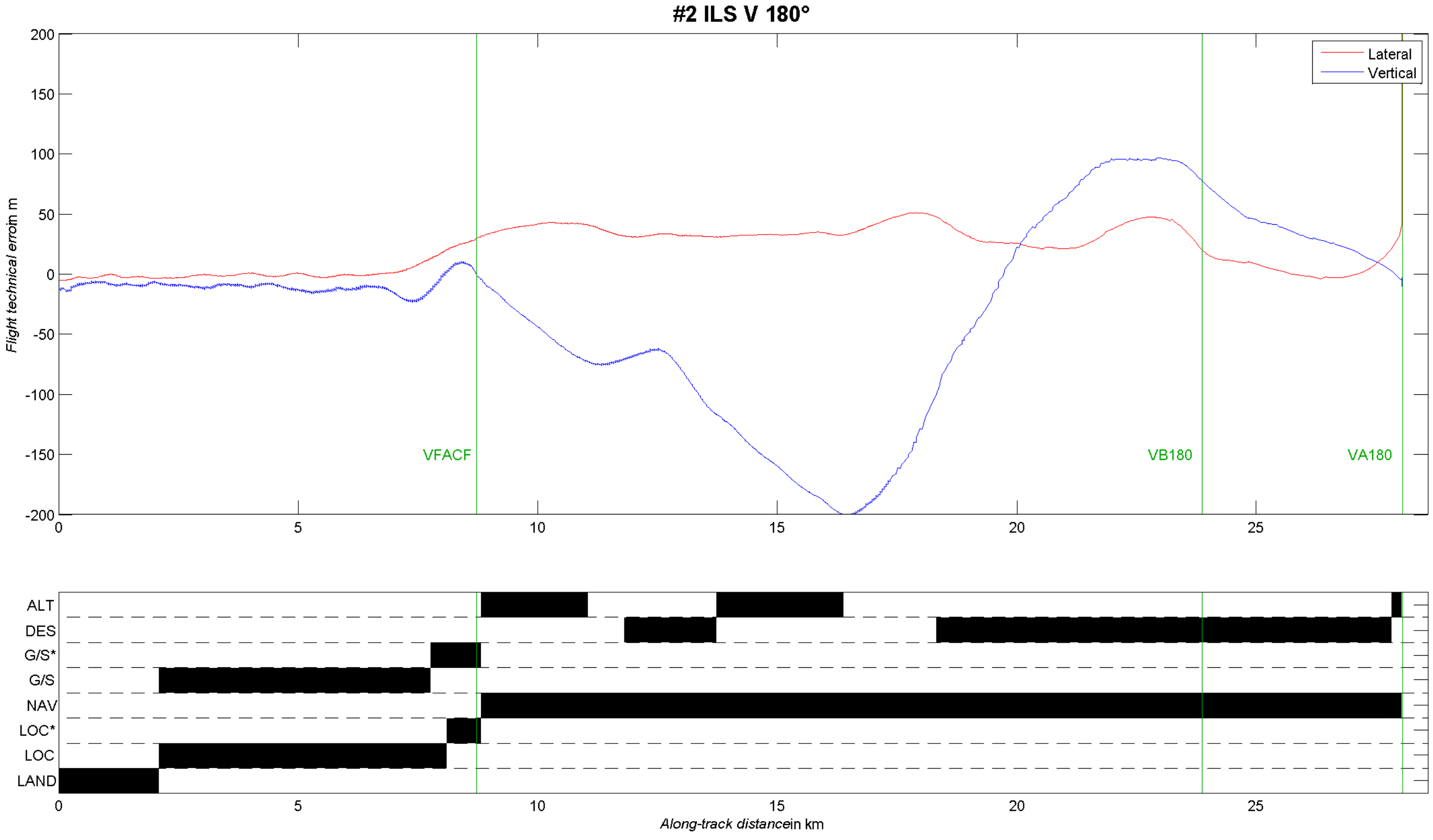

DLR Institut für Flugführung

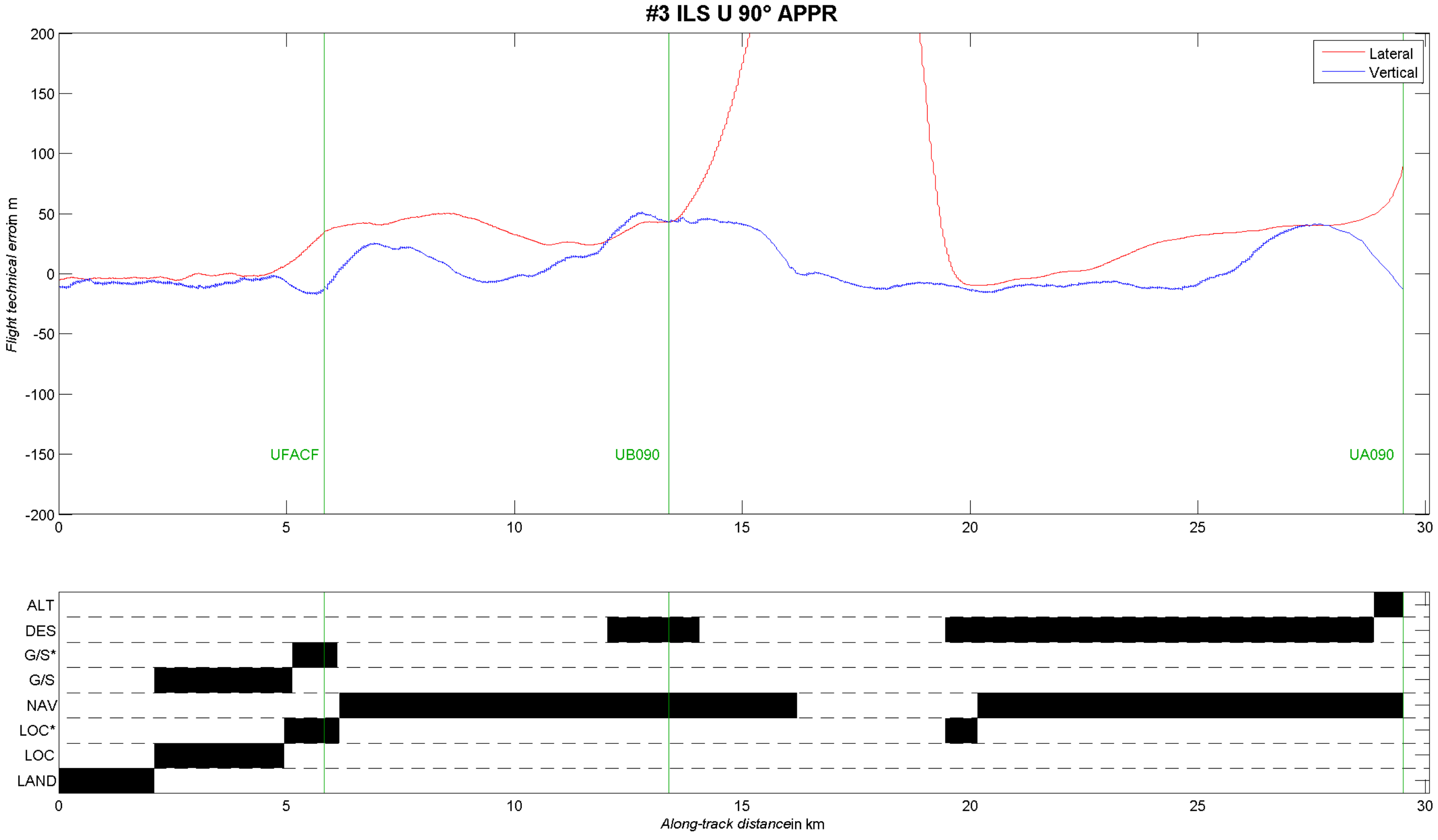

DLR Institut für Flugführung

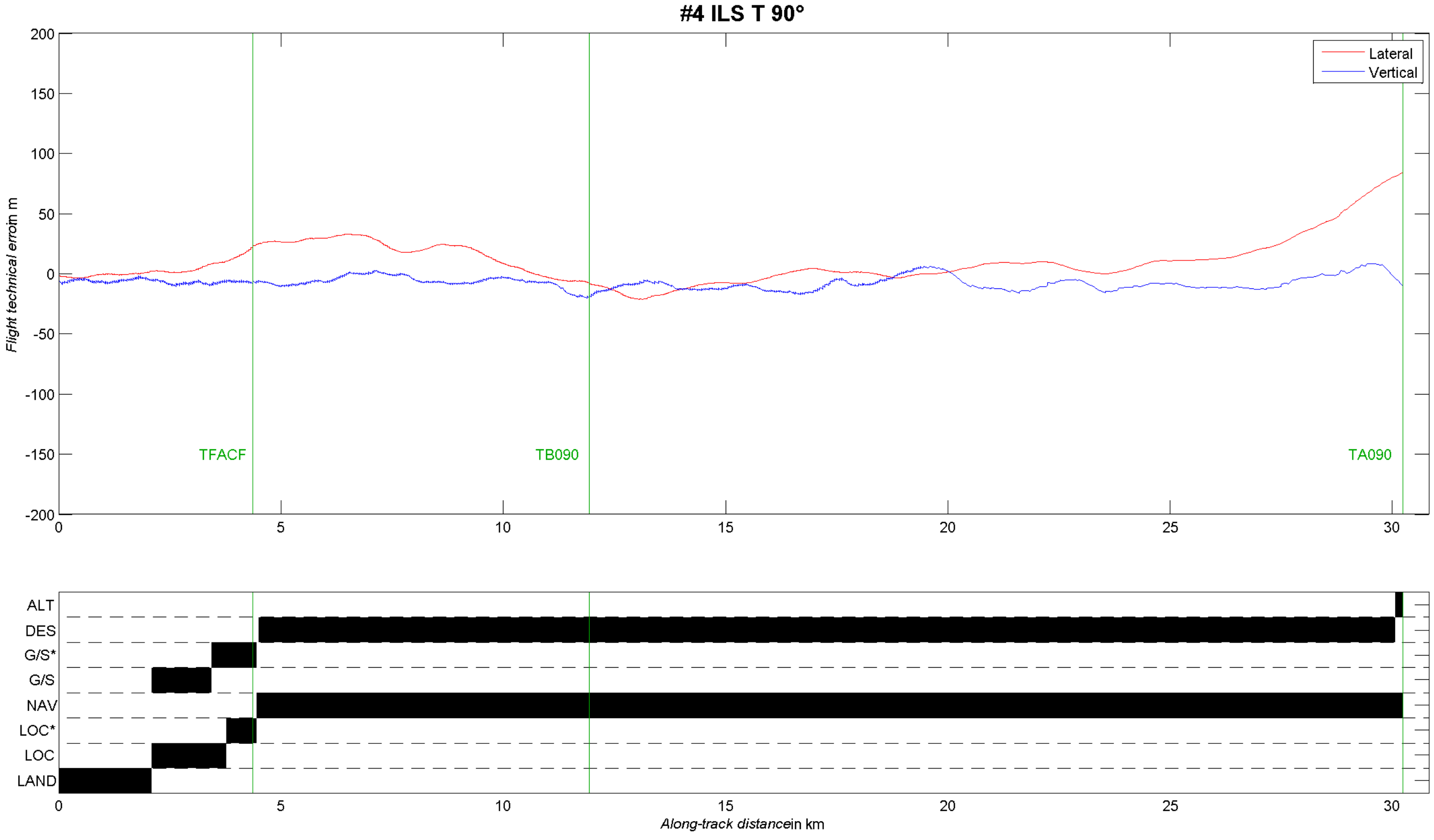

DLR Institut für Flugführung

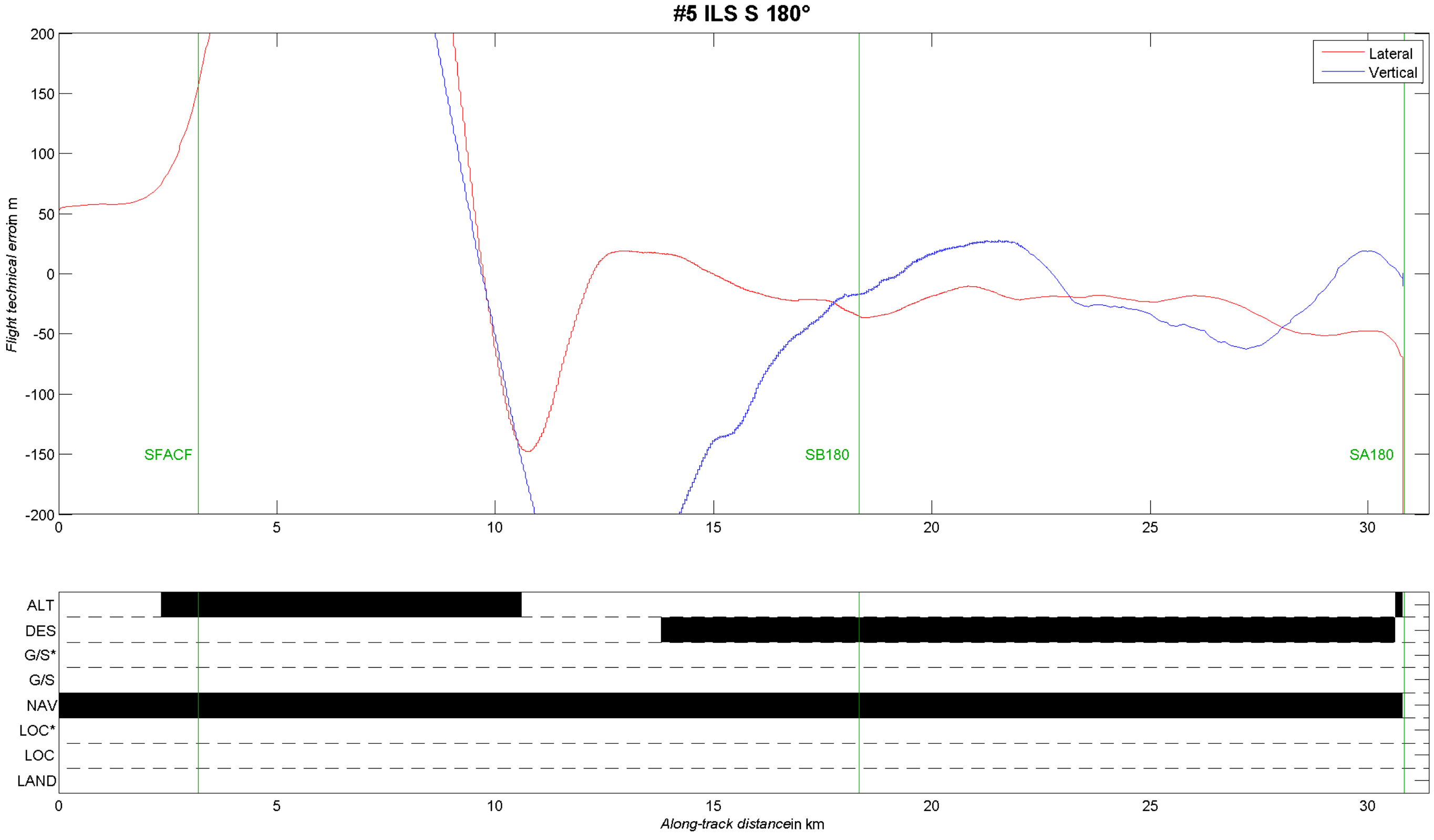

DLR Institut für Flugführung

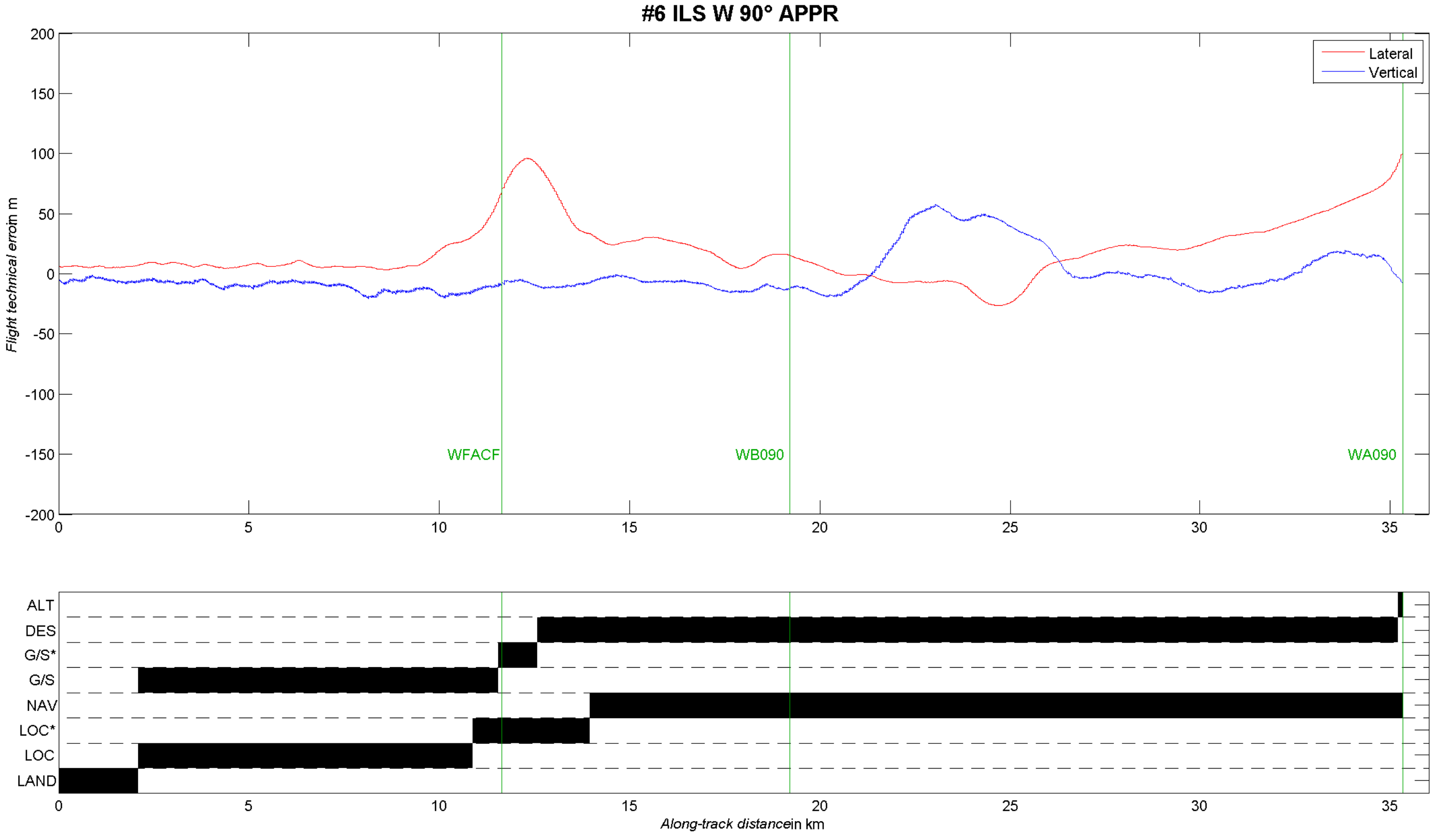

DLR Institut für Flugführung

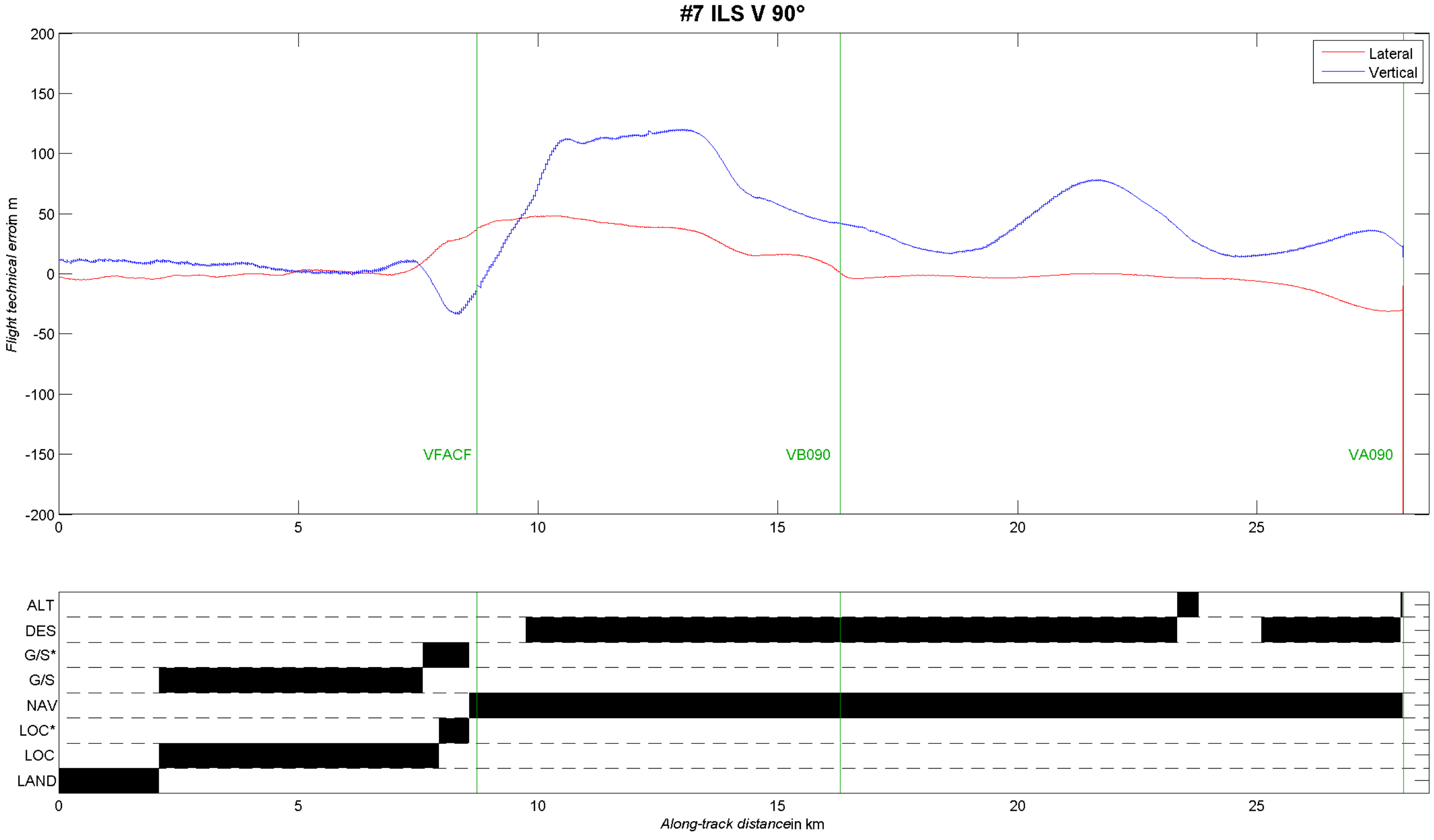

DLR Institut für Flugführung

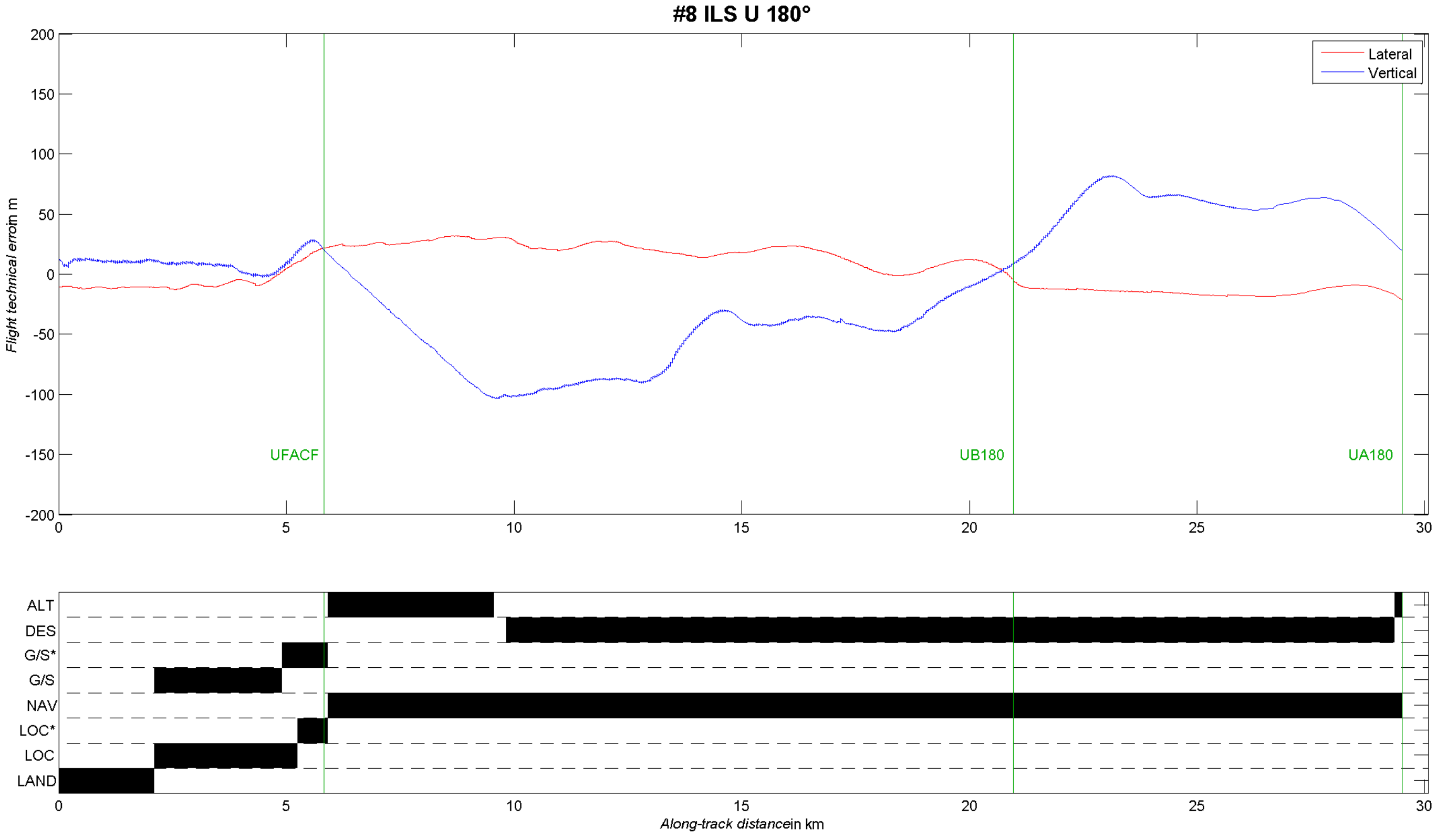

DLR Institut für Flugführung

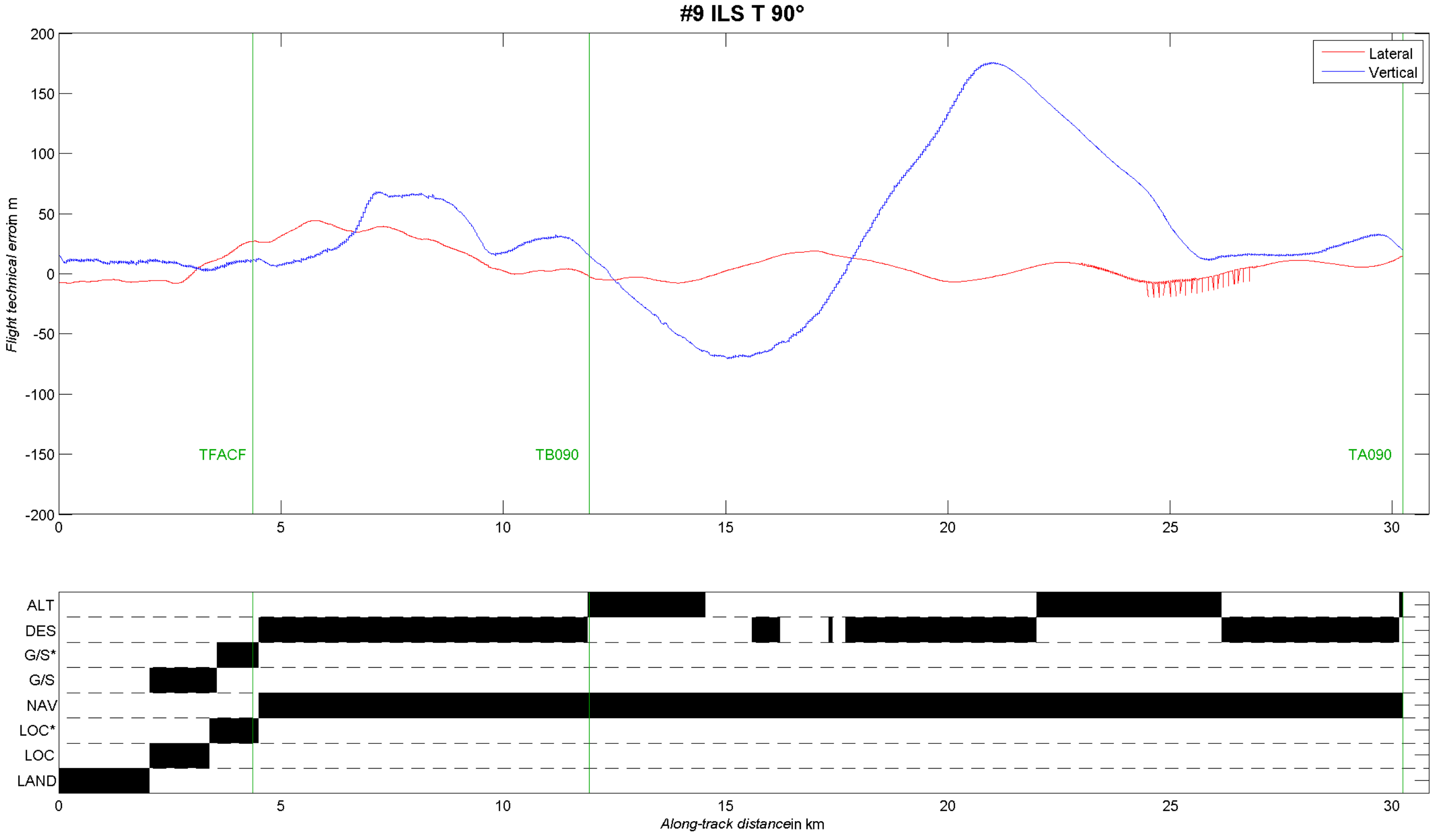

DLR Institut für Flugführung

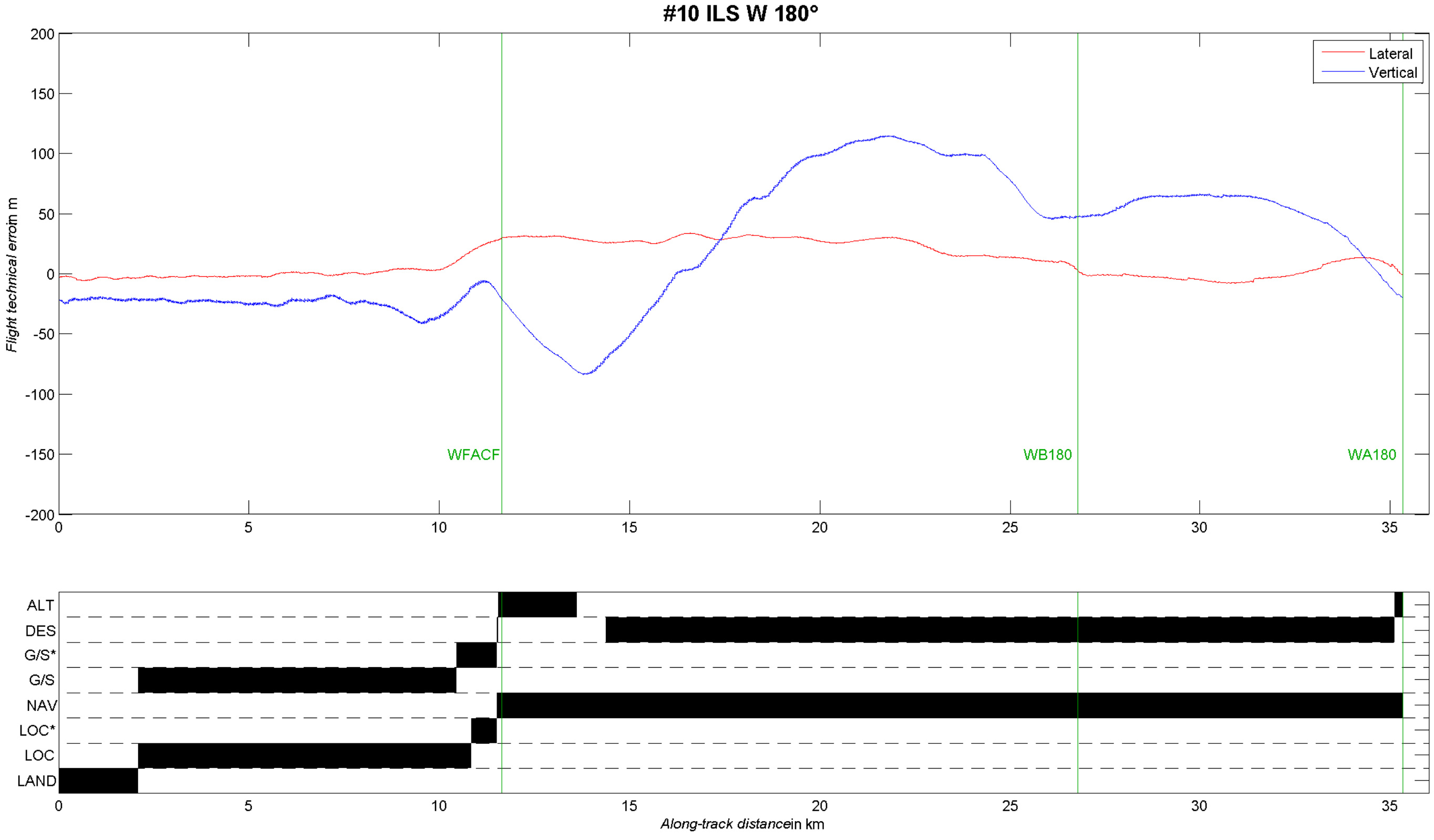

DLR Institut für Flugführung

#11 ILS T 90°

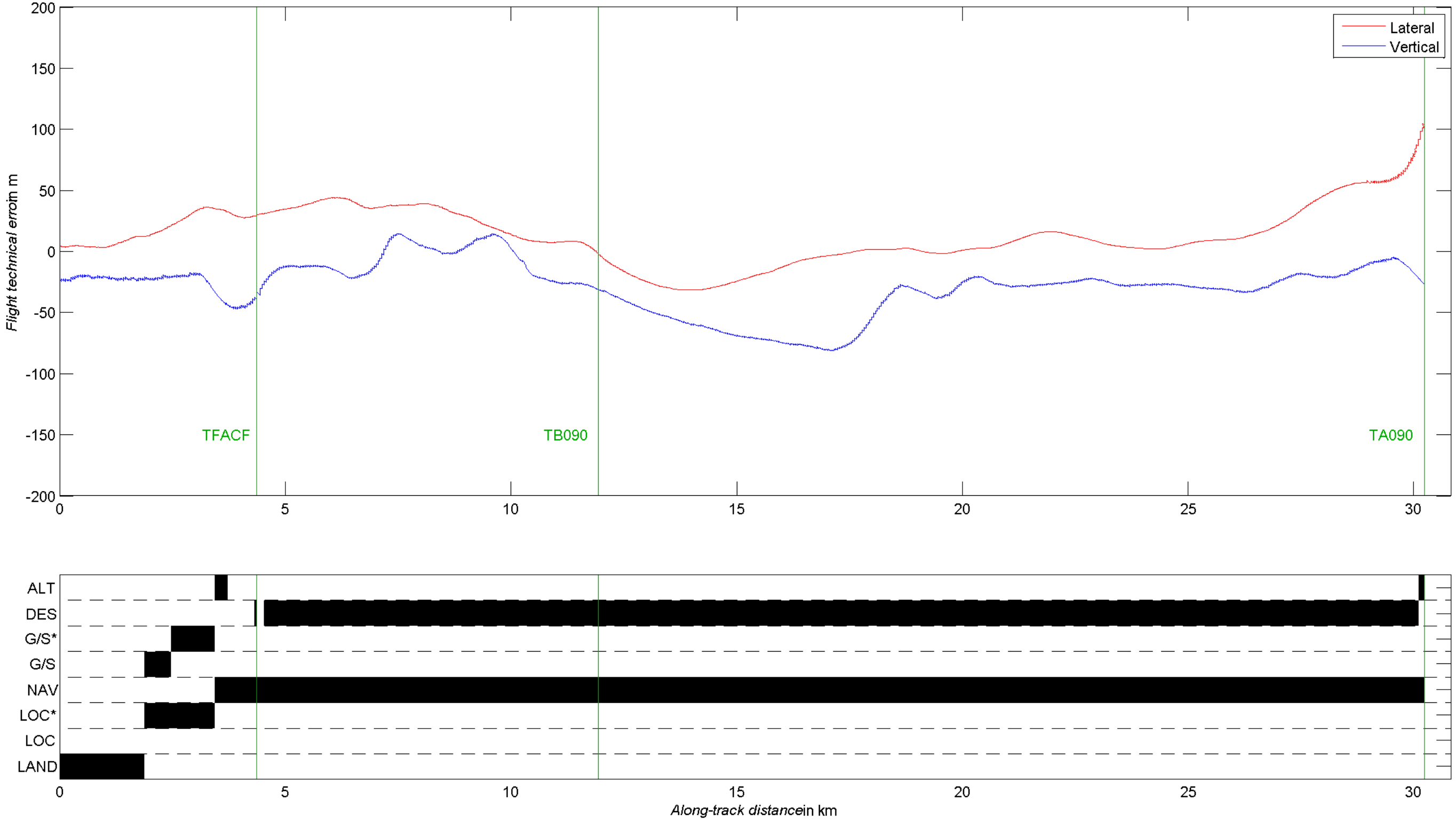

DLR Institut für Flugführung

#12 ILS S 90°

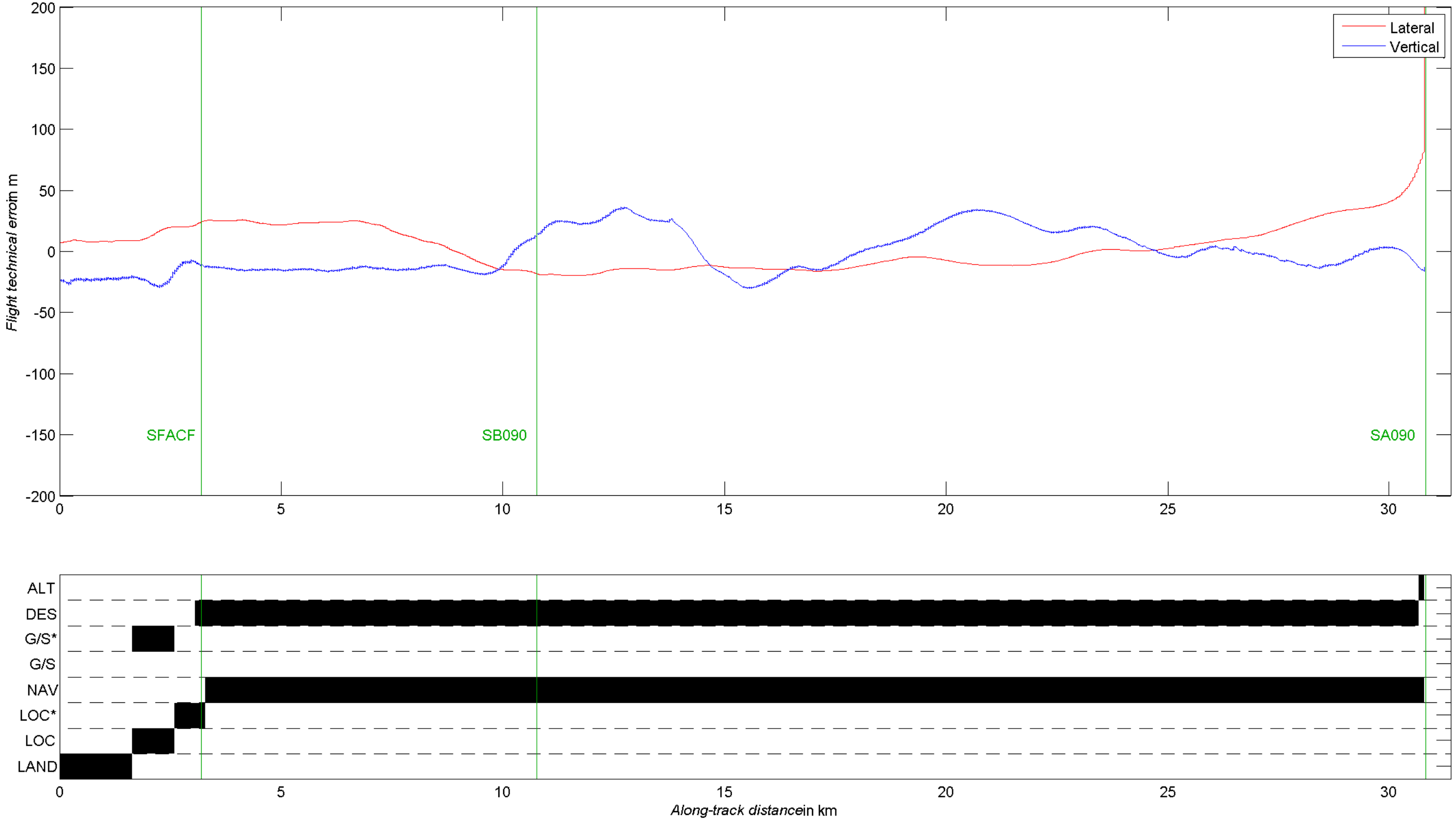

DLR Institut für Flugführung

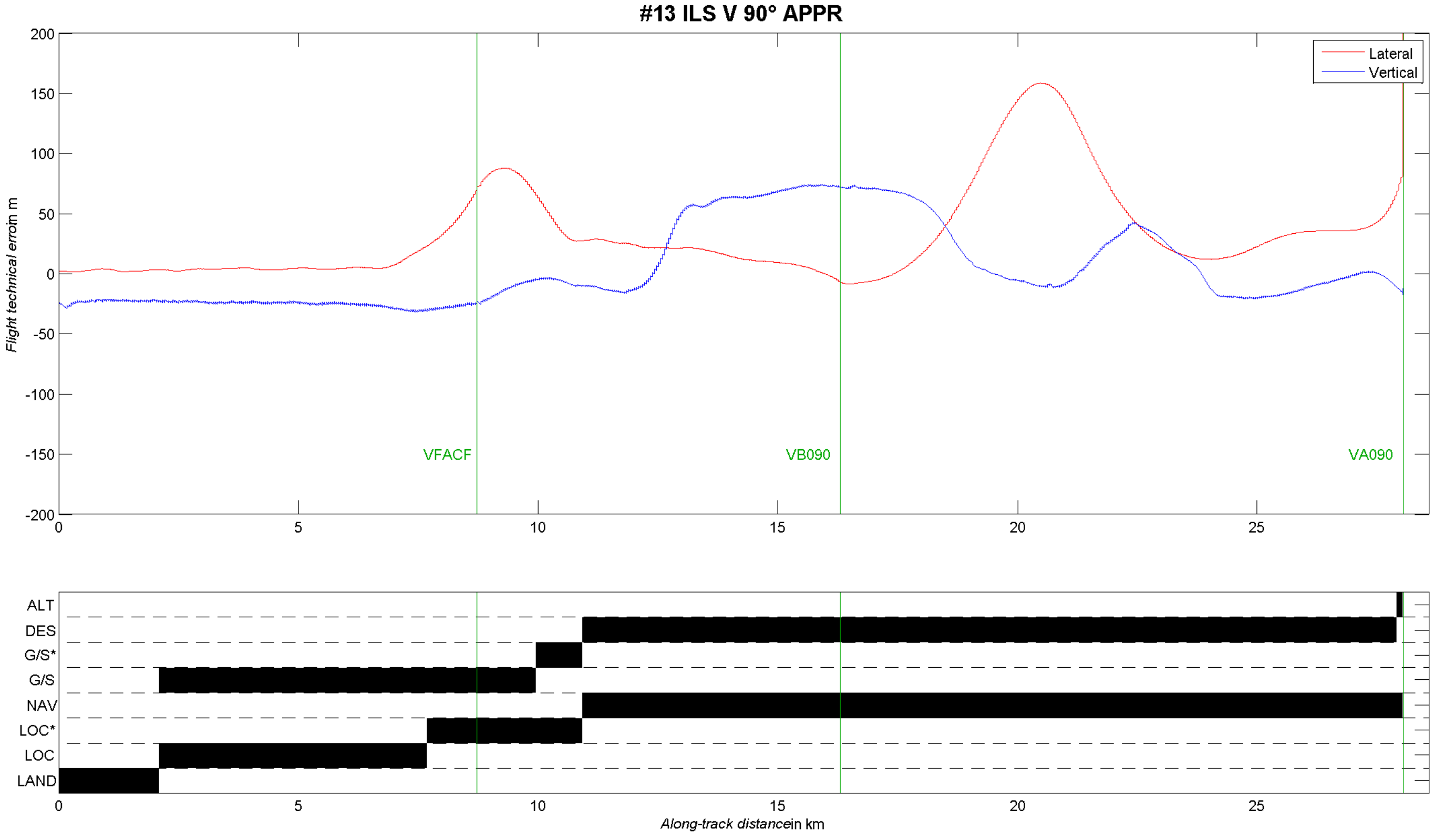

DLR Institut für Flugführung

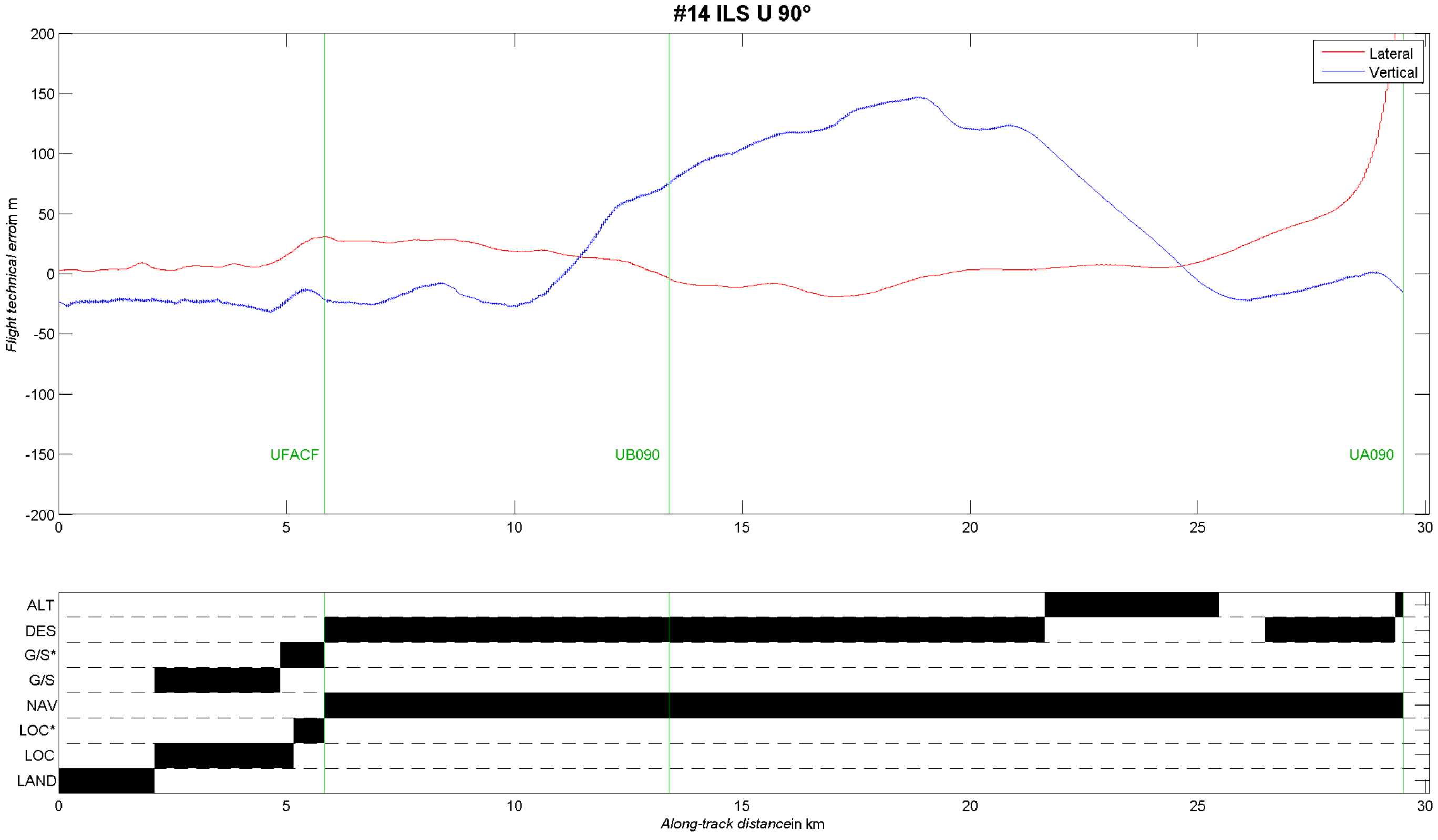

DLR Institut für Flugführung

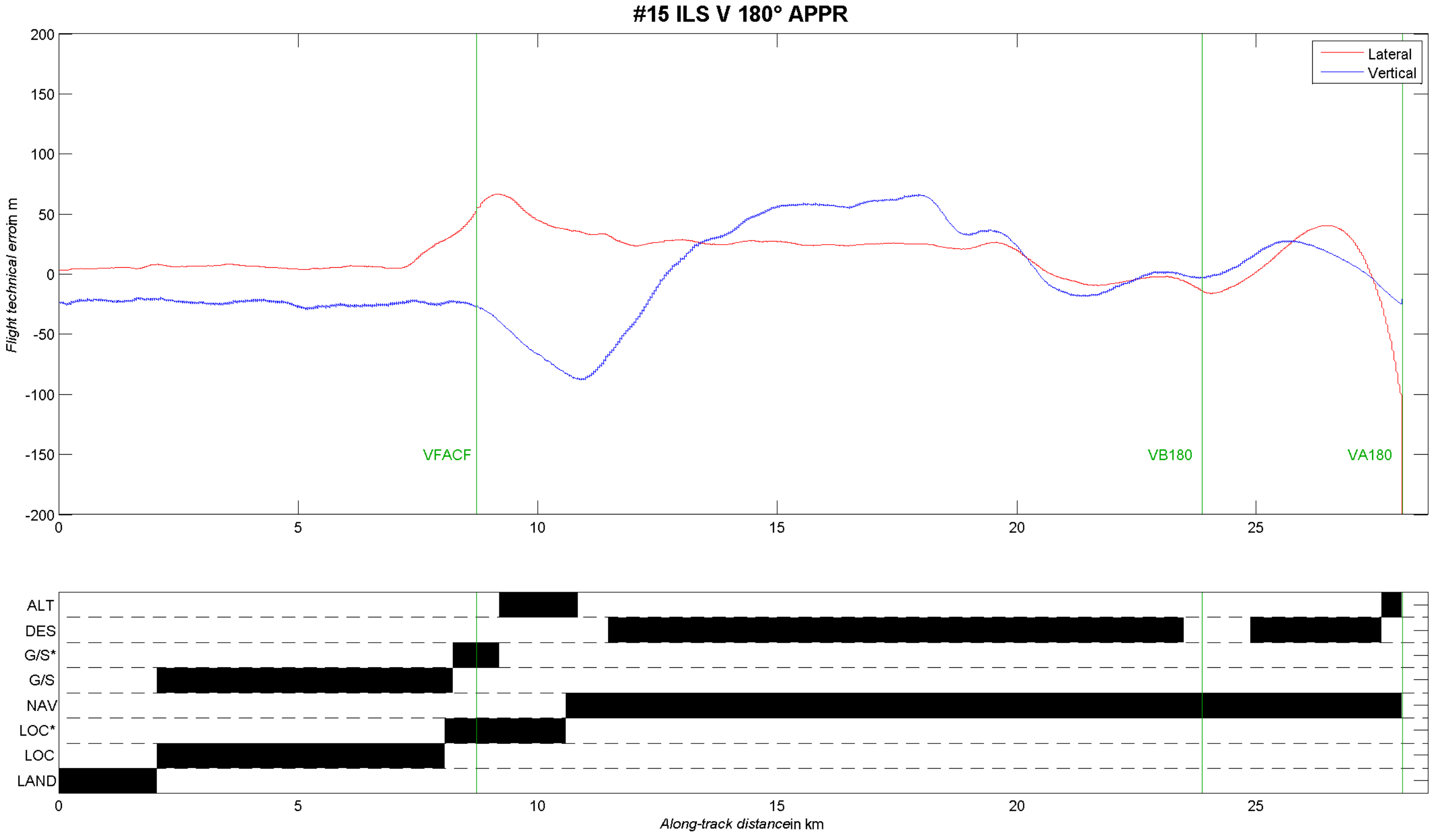

DLR Institut für Flugführung

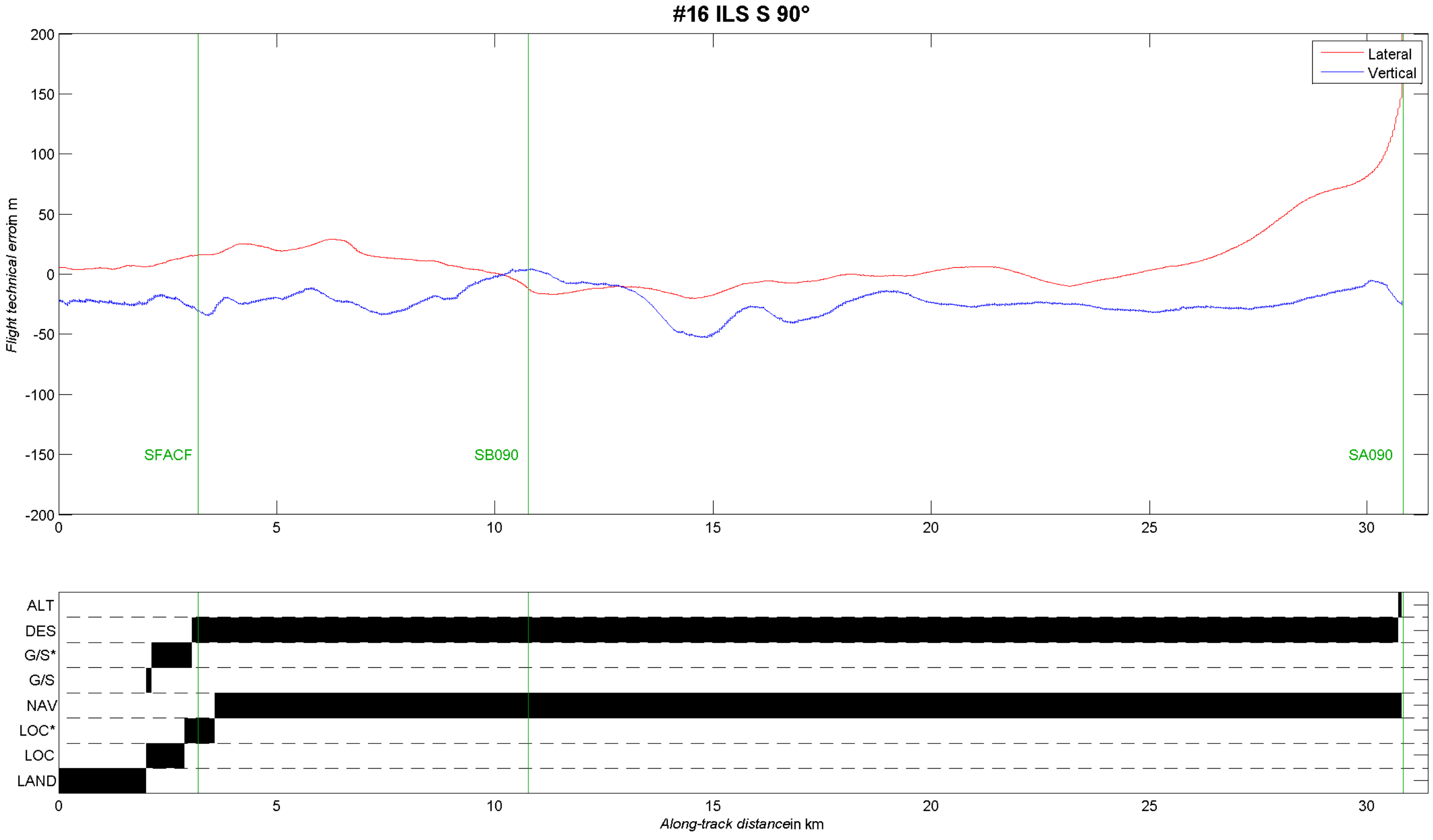

DLR Institut für Flugführung

Appendix D – Lateral Navigation System Error

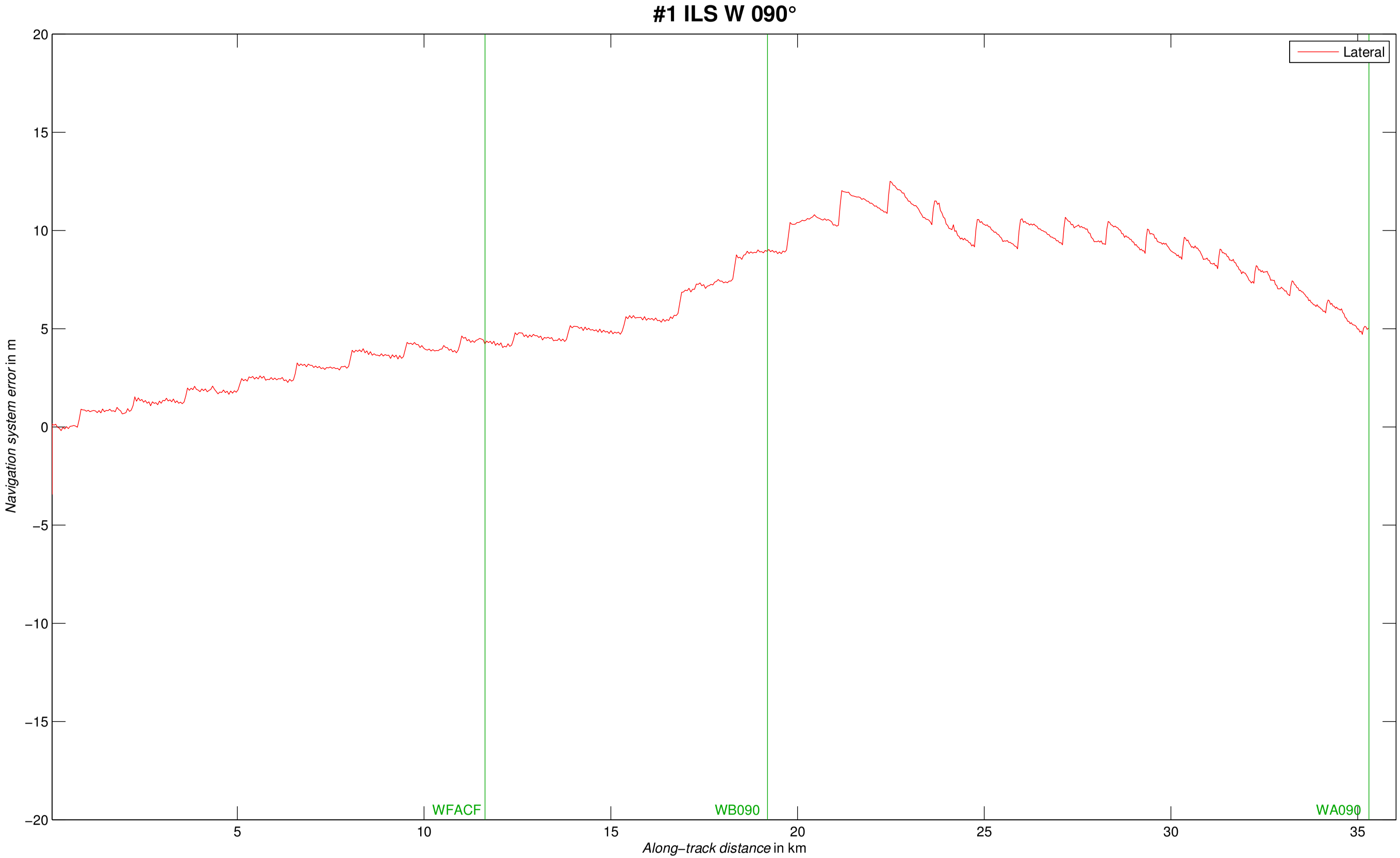

DLR Institut für Flugführung

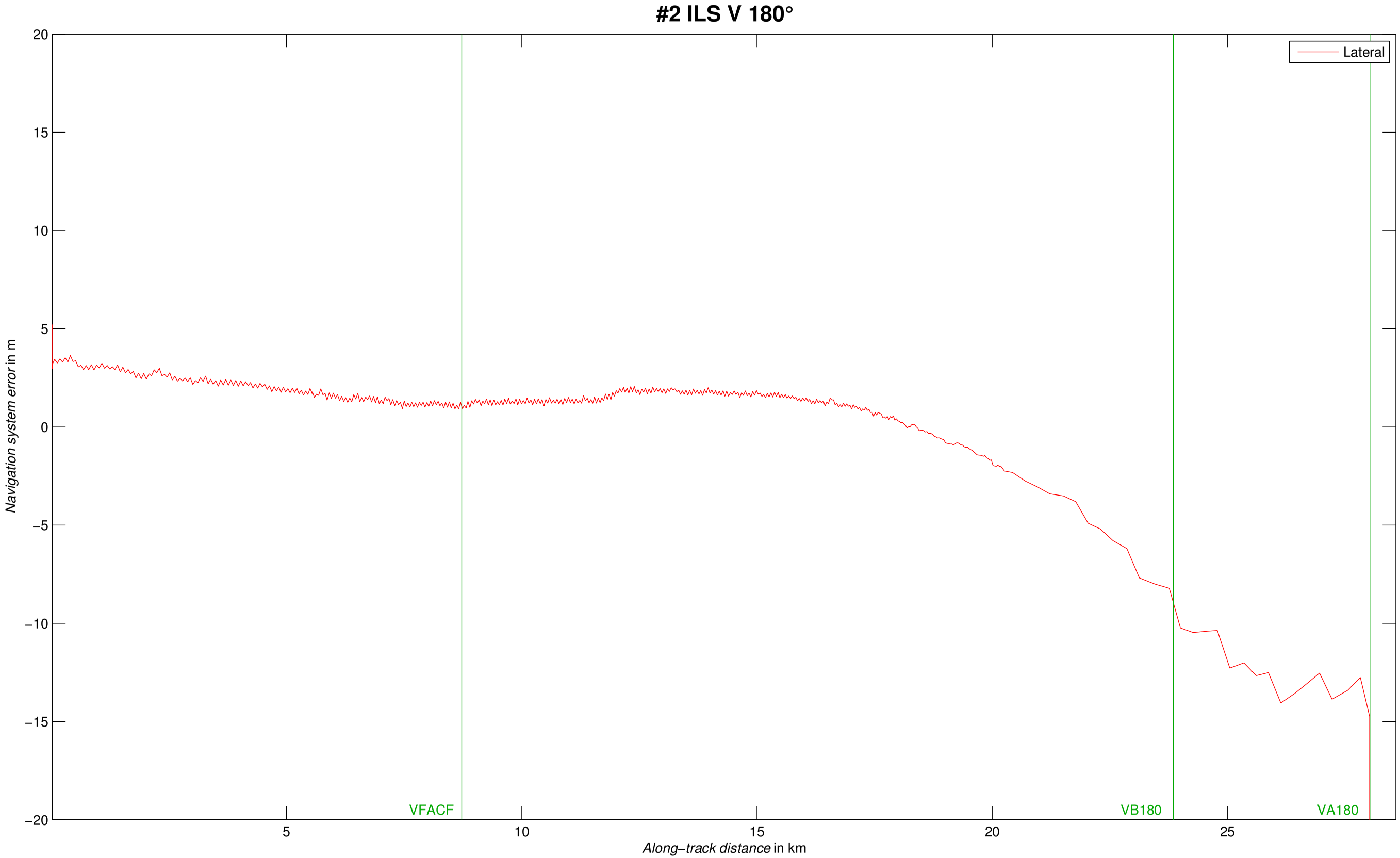

DLR Institut für Flugführung

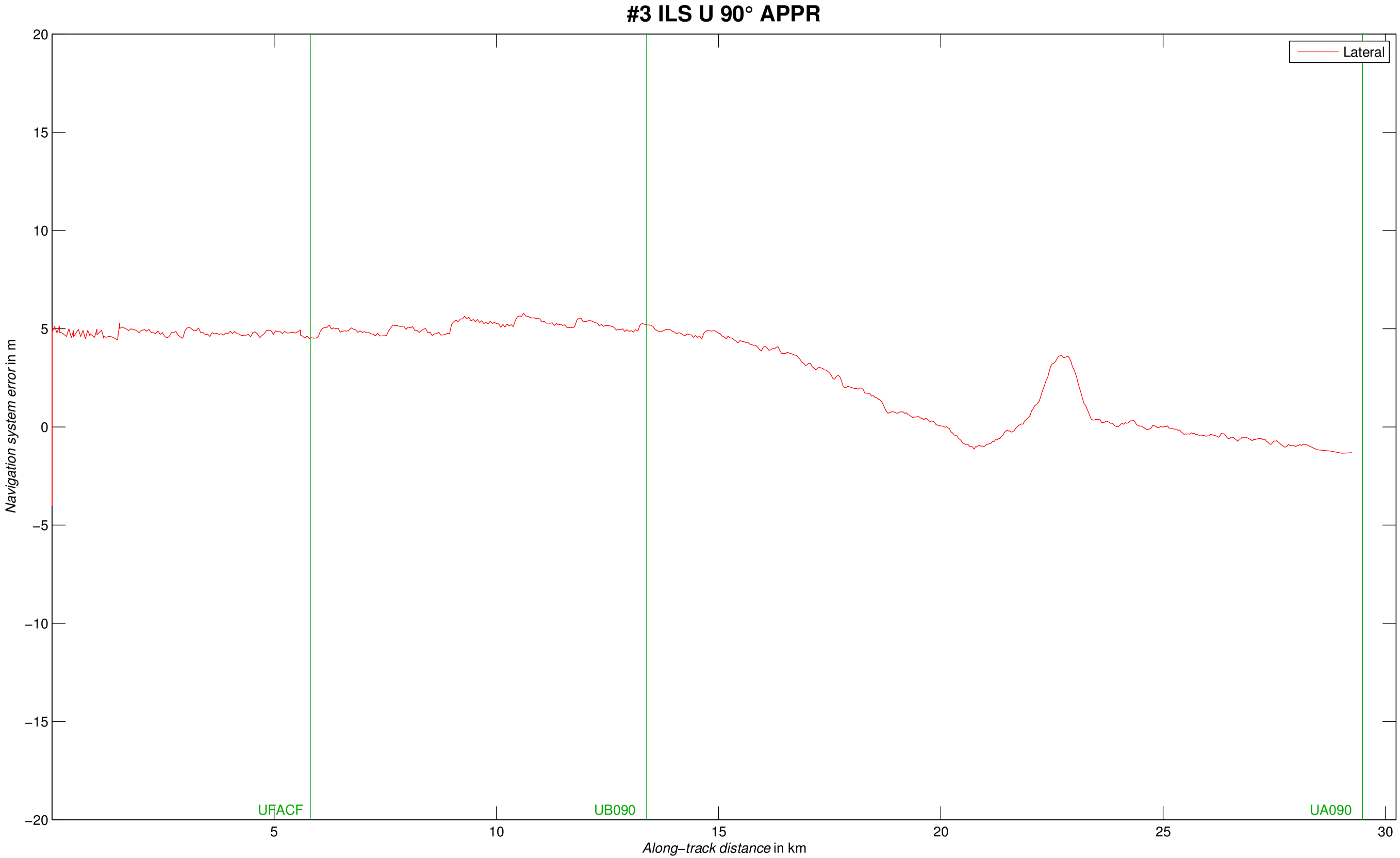

DLR Institut für Flugführung

#4 ILS T 90°

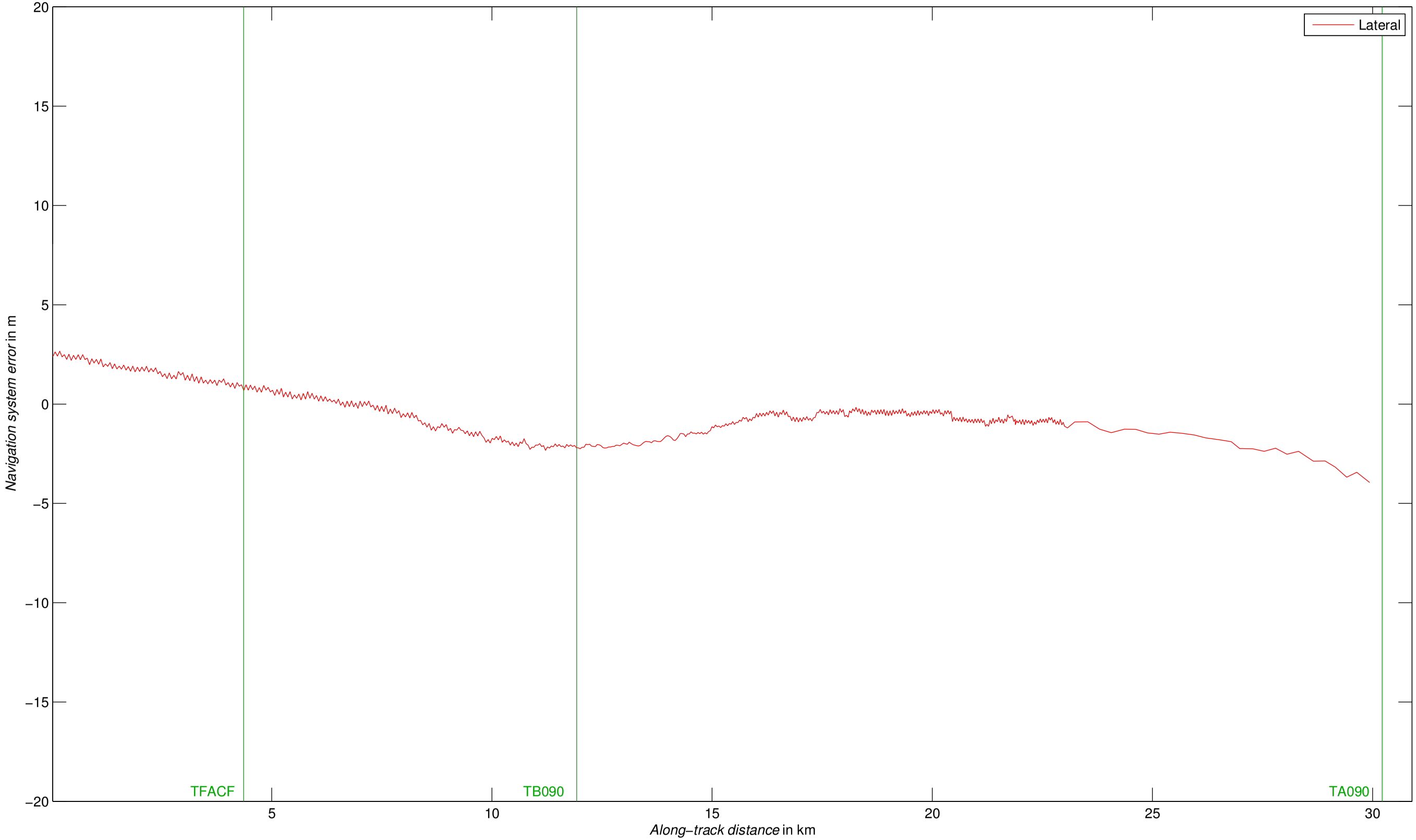

DLR Institut für Flugführung

#5 ILS S 180°

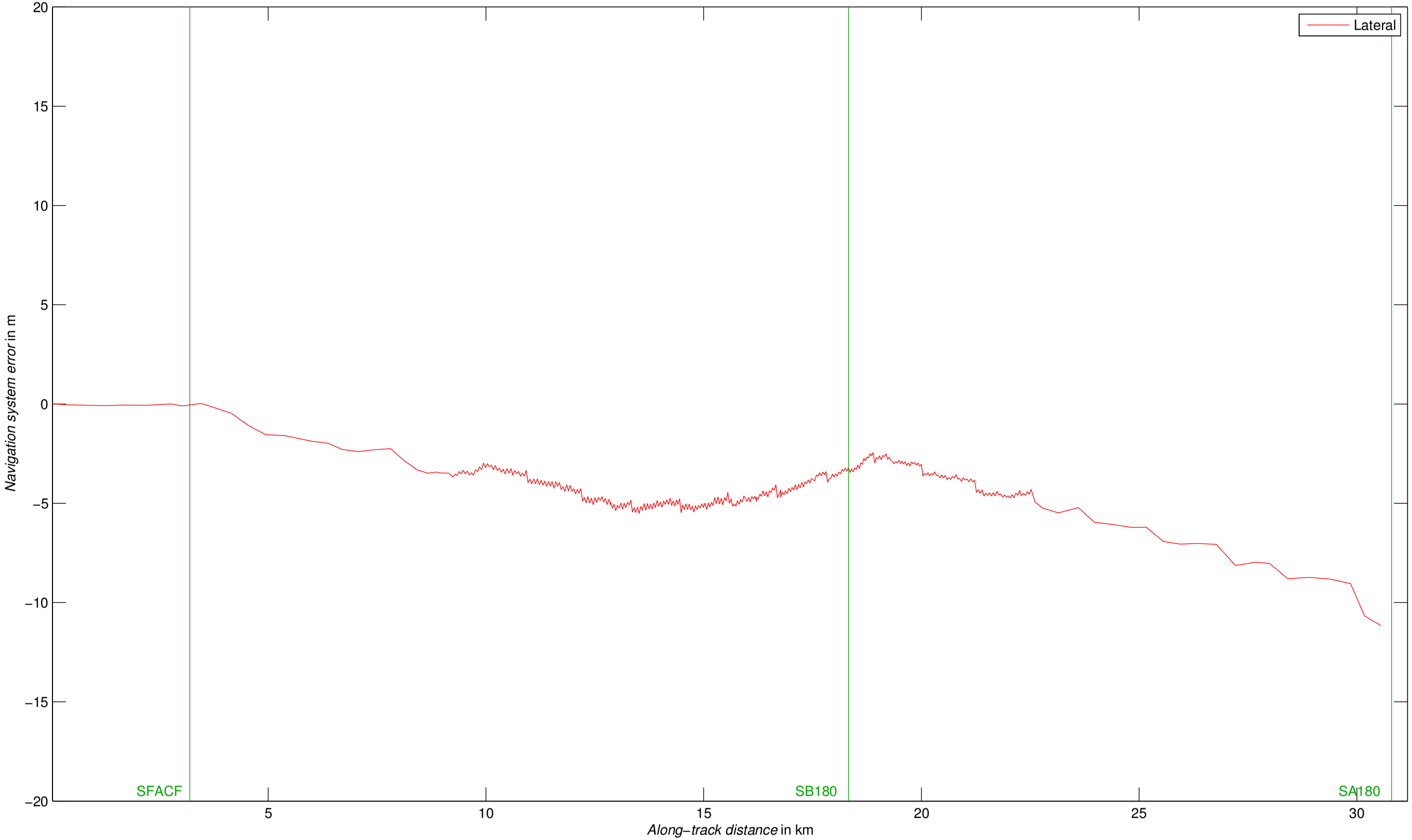

DLR Institut für Flugführung

#6 ILS W 90° APPR

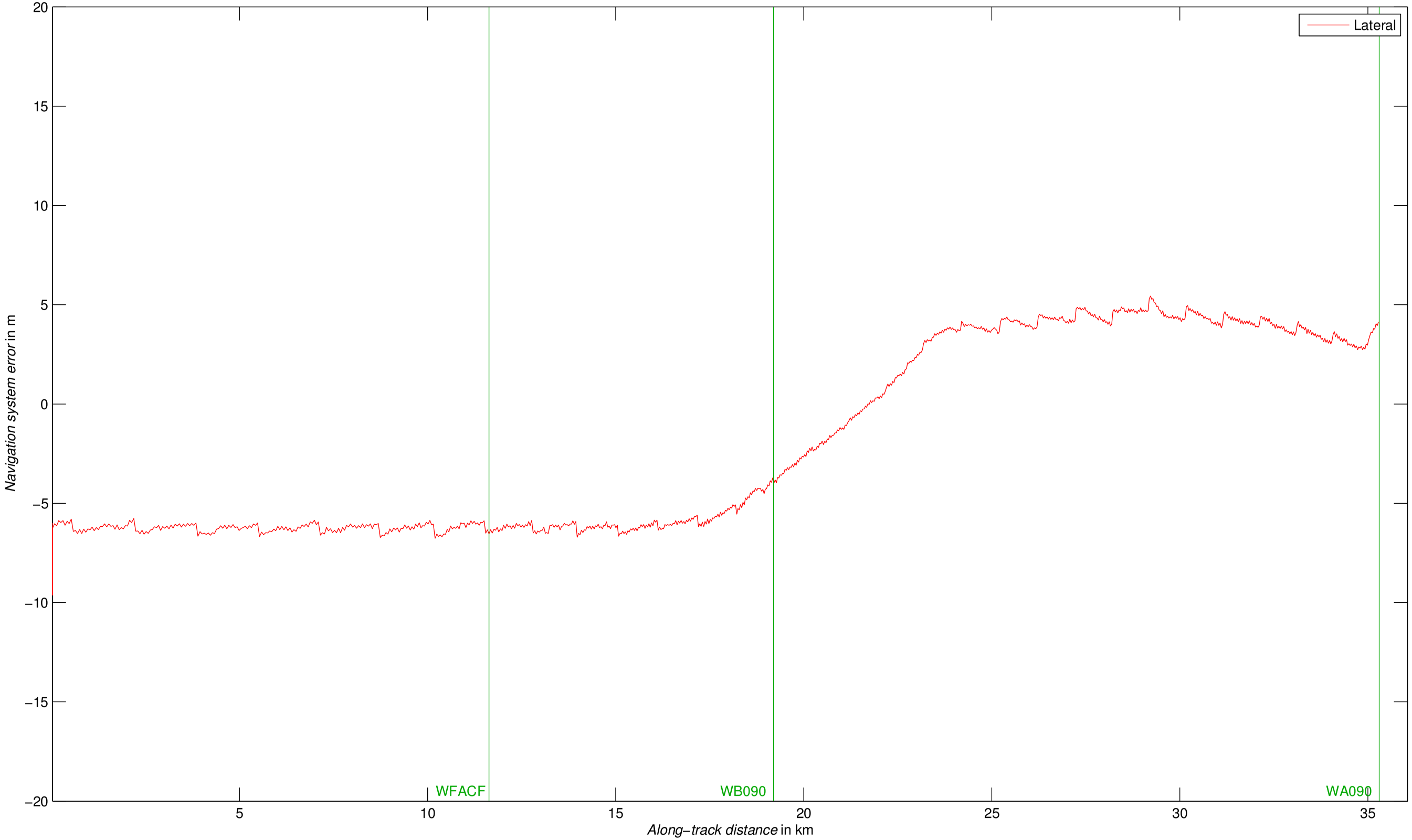

Institut für Flugführung
DLR

#7 ILS V 090°

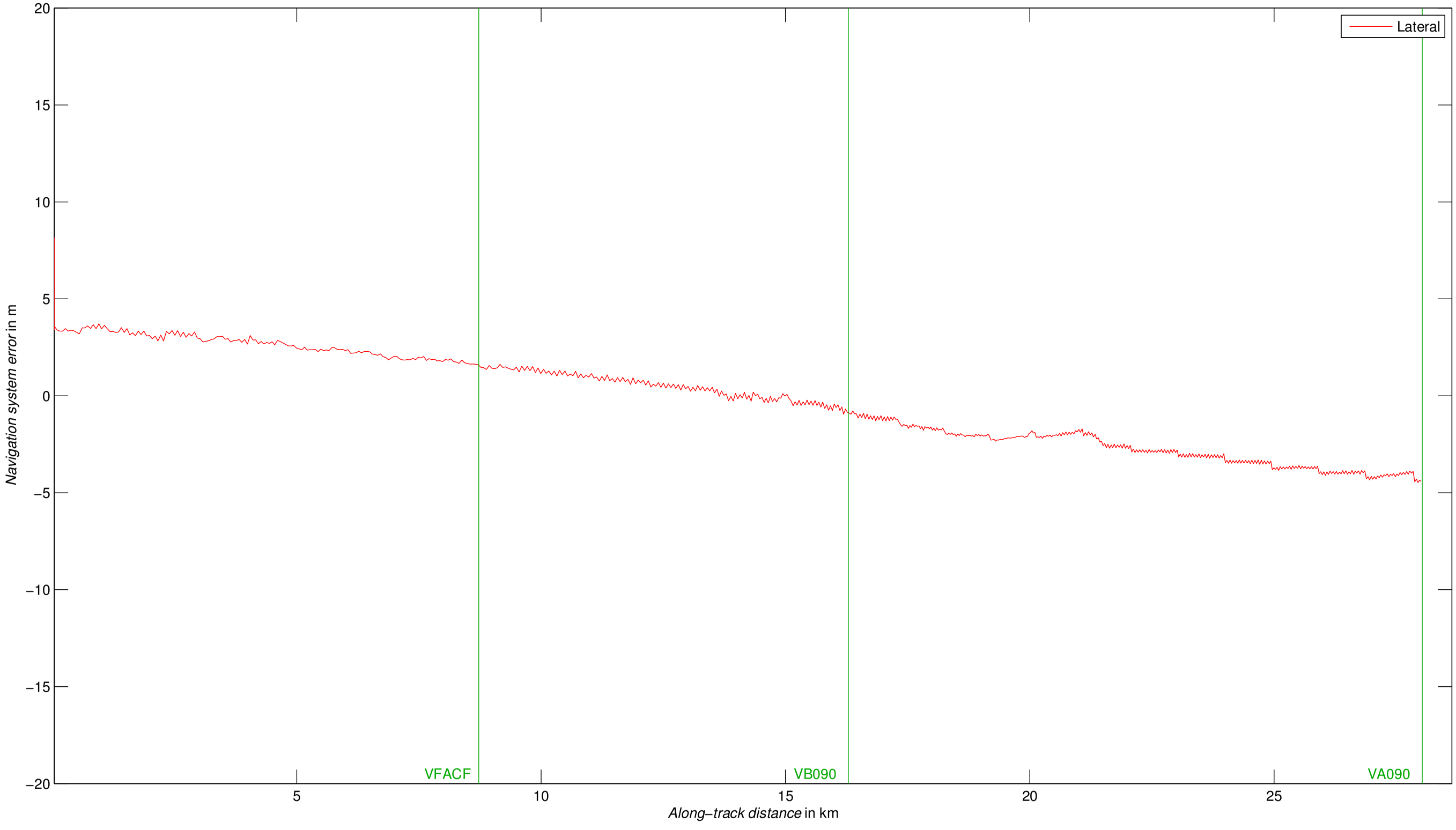

DLR Institut für Flugführung

#8 ILS U 180°

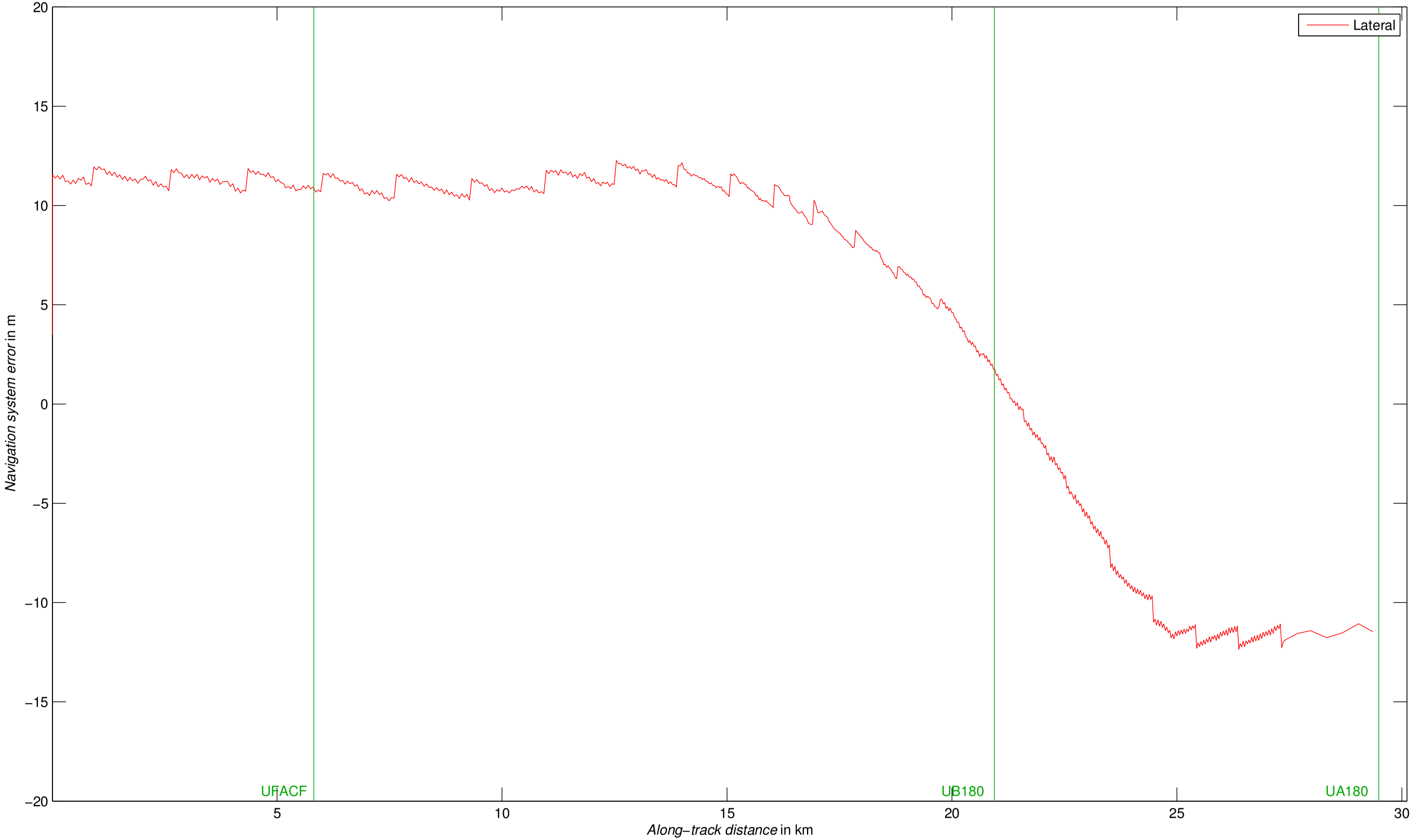

DLR Institut für Flugführung

#9 ILS T 90°

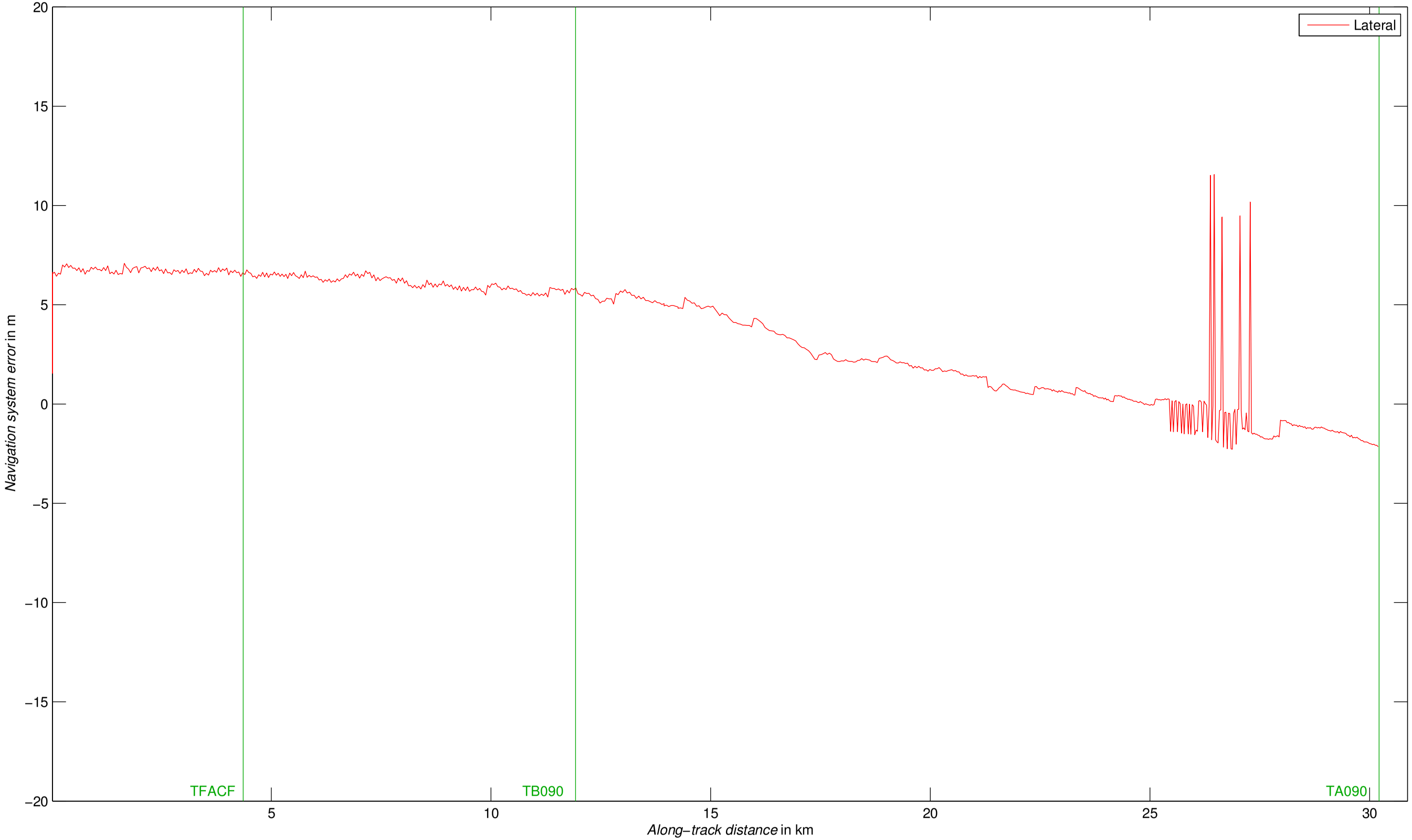

DLR Institut für Flugführung

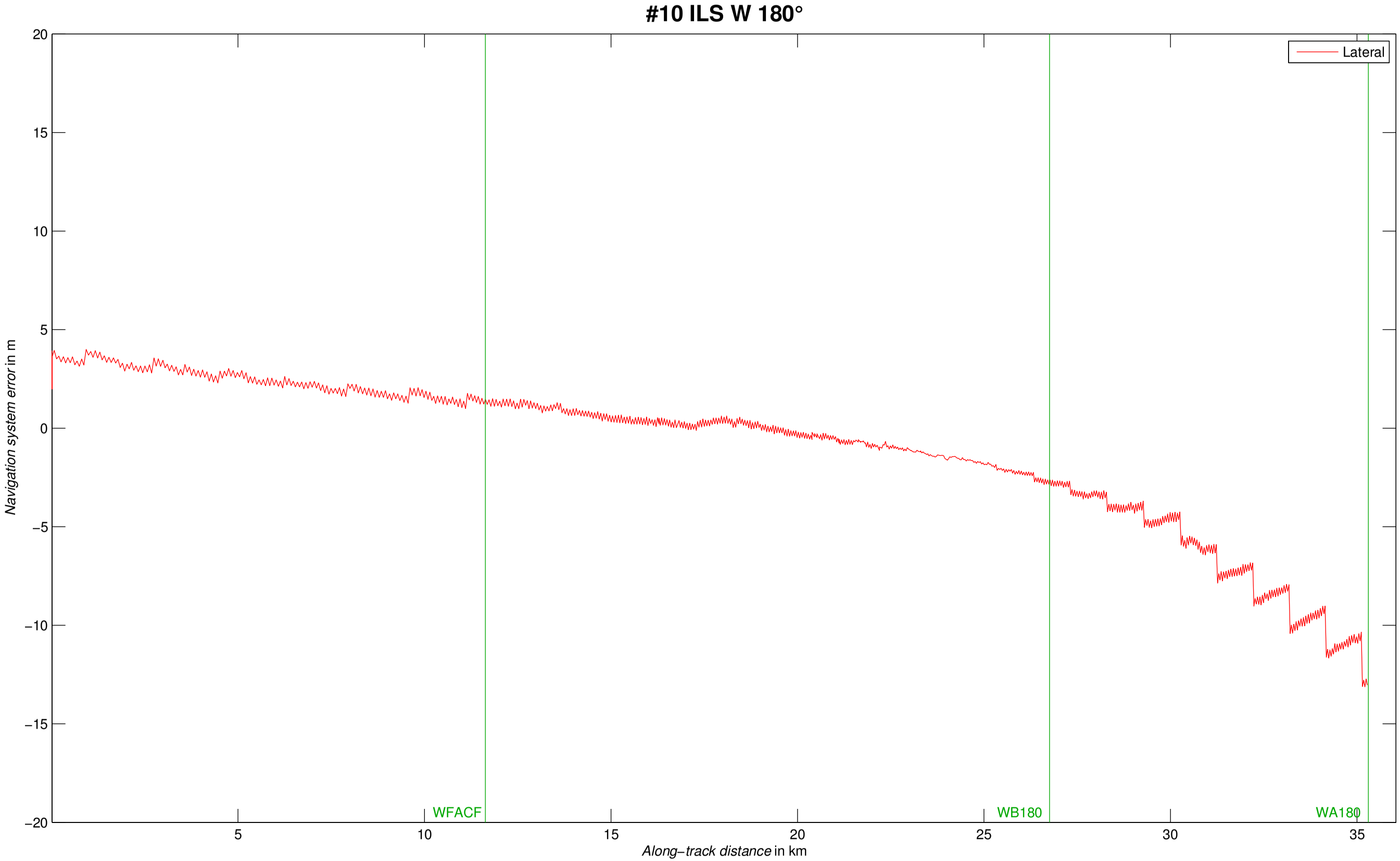

DLR Institut für Flugführung

#11 ILS T 90°

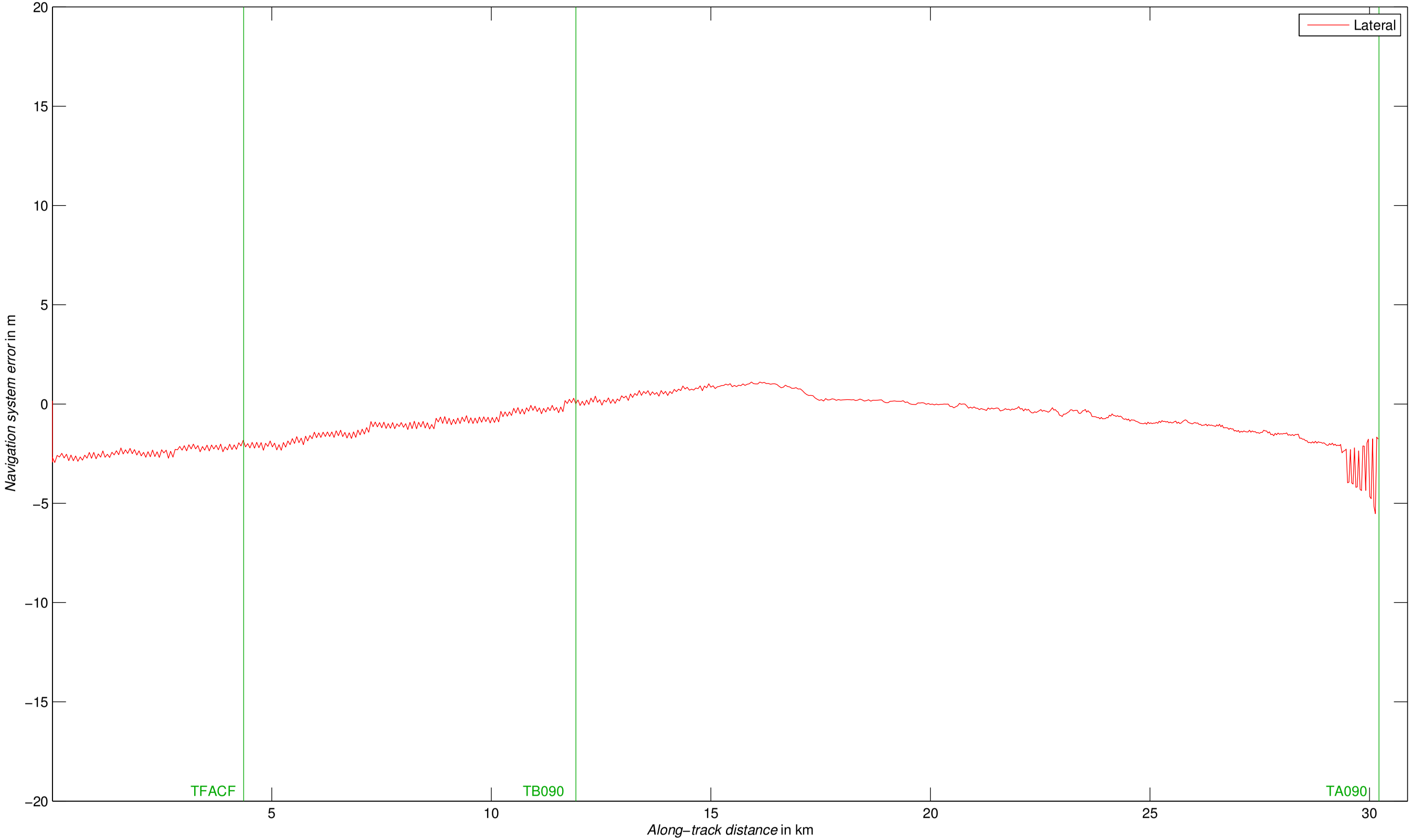

DLR Institut für Flugführung

#12 ILS S 90°

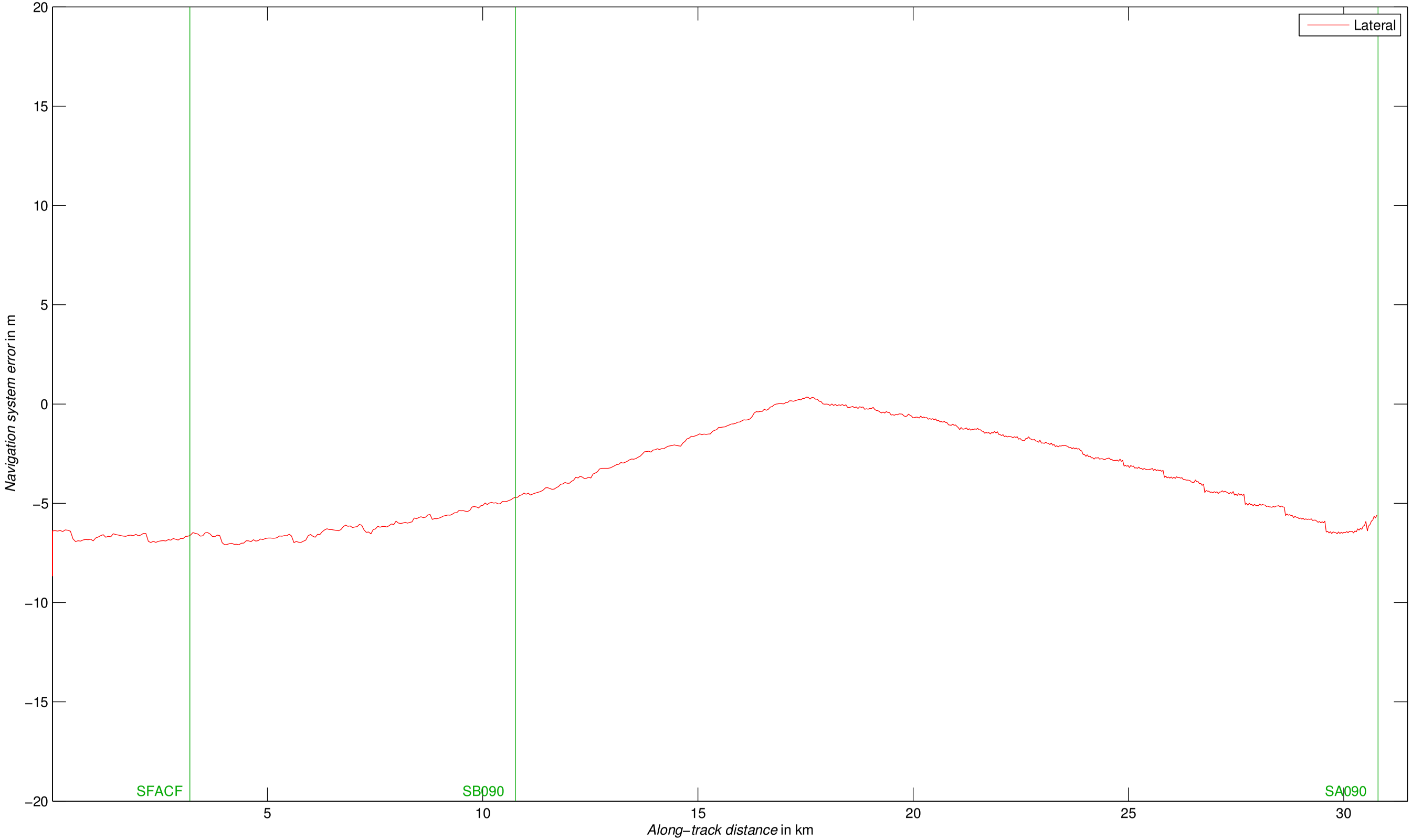

Institut für Flugführung
DLR

#13 ILS V 90° APPR

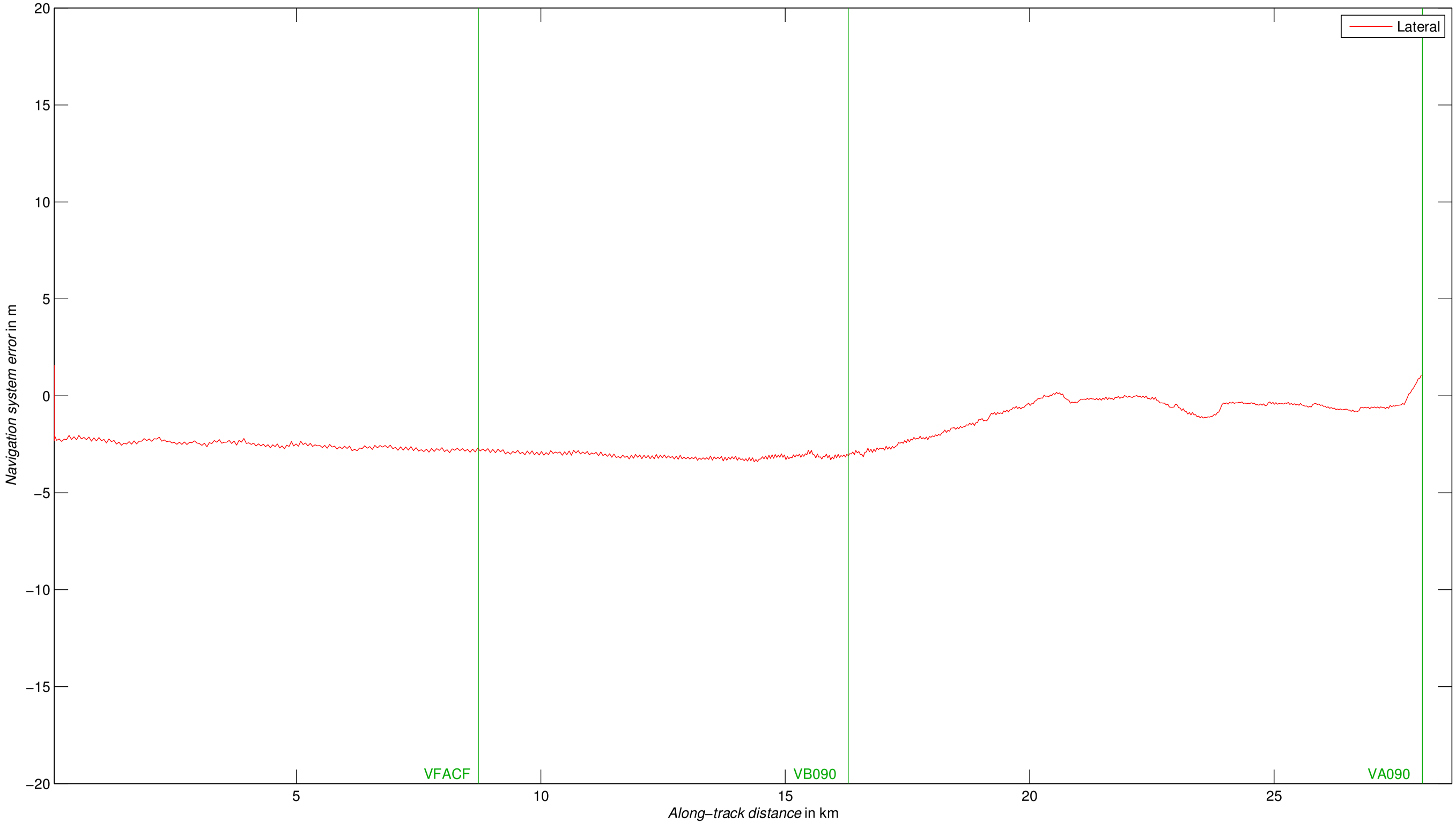

DLR Institut für Flugführung

#14 ILS U 90°

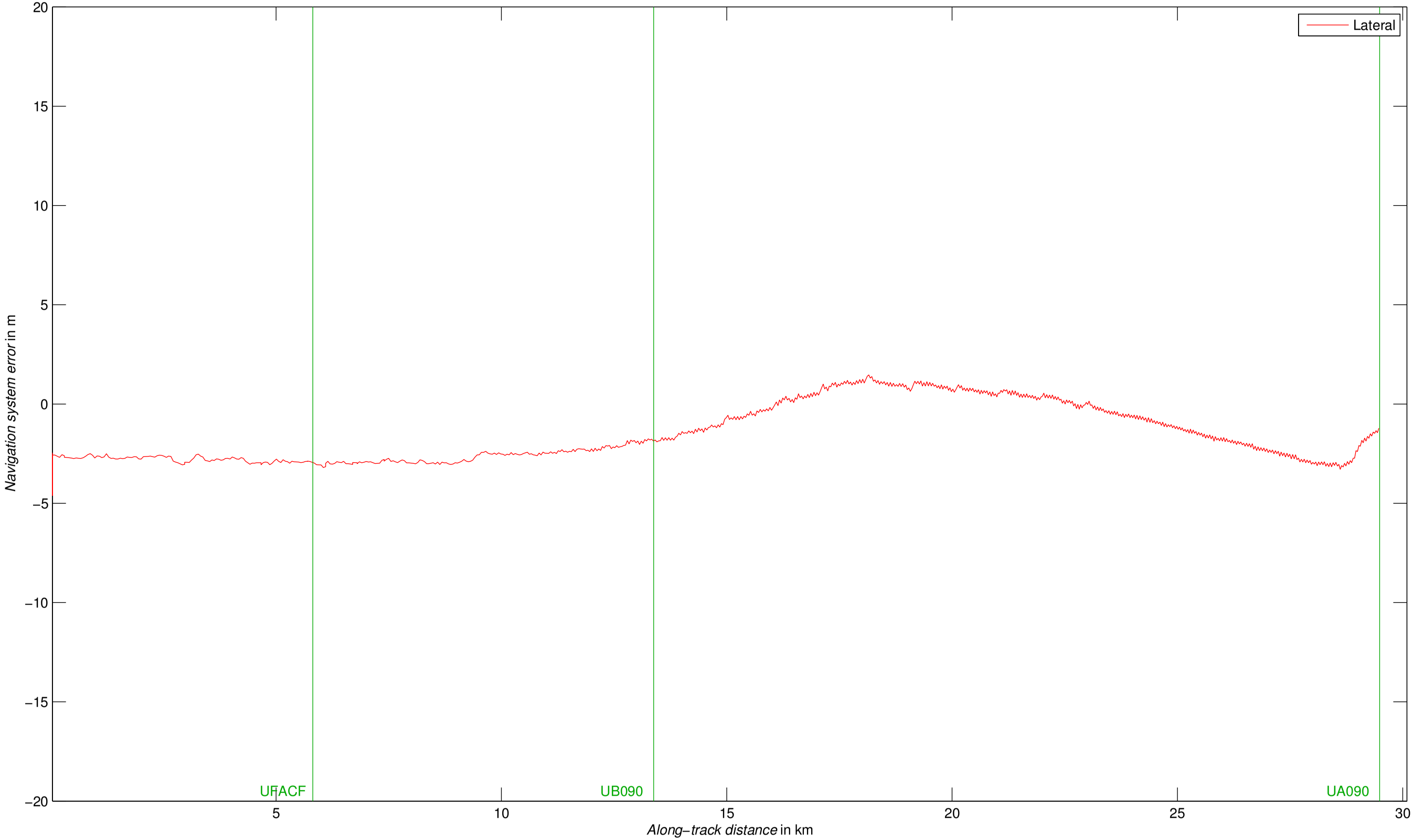

DLR Institut für Flugführung

#15 ILS V 180°

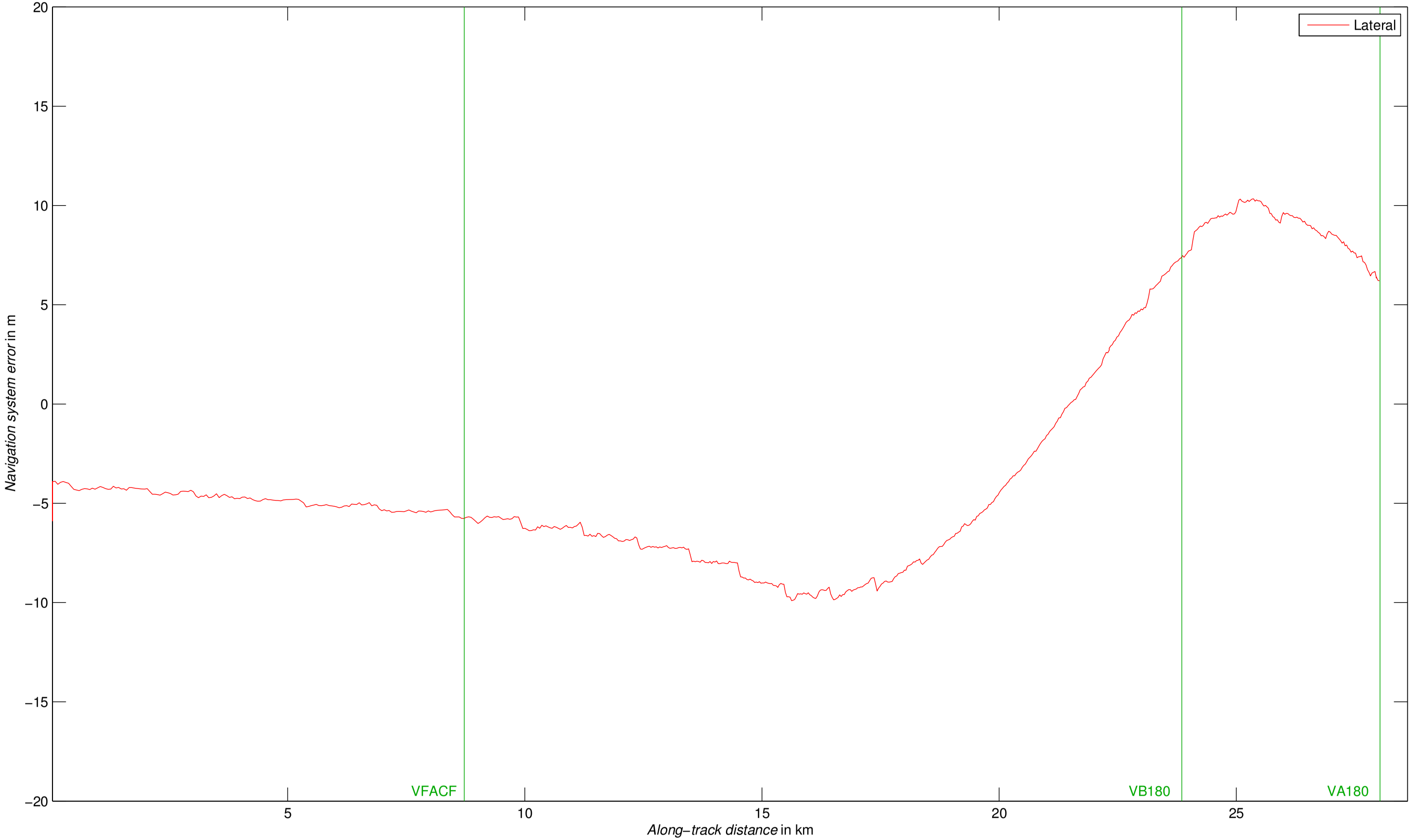

DLR Institut für Flugführung

#16 ILS S 090°

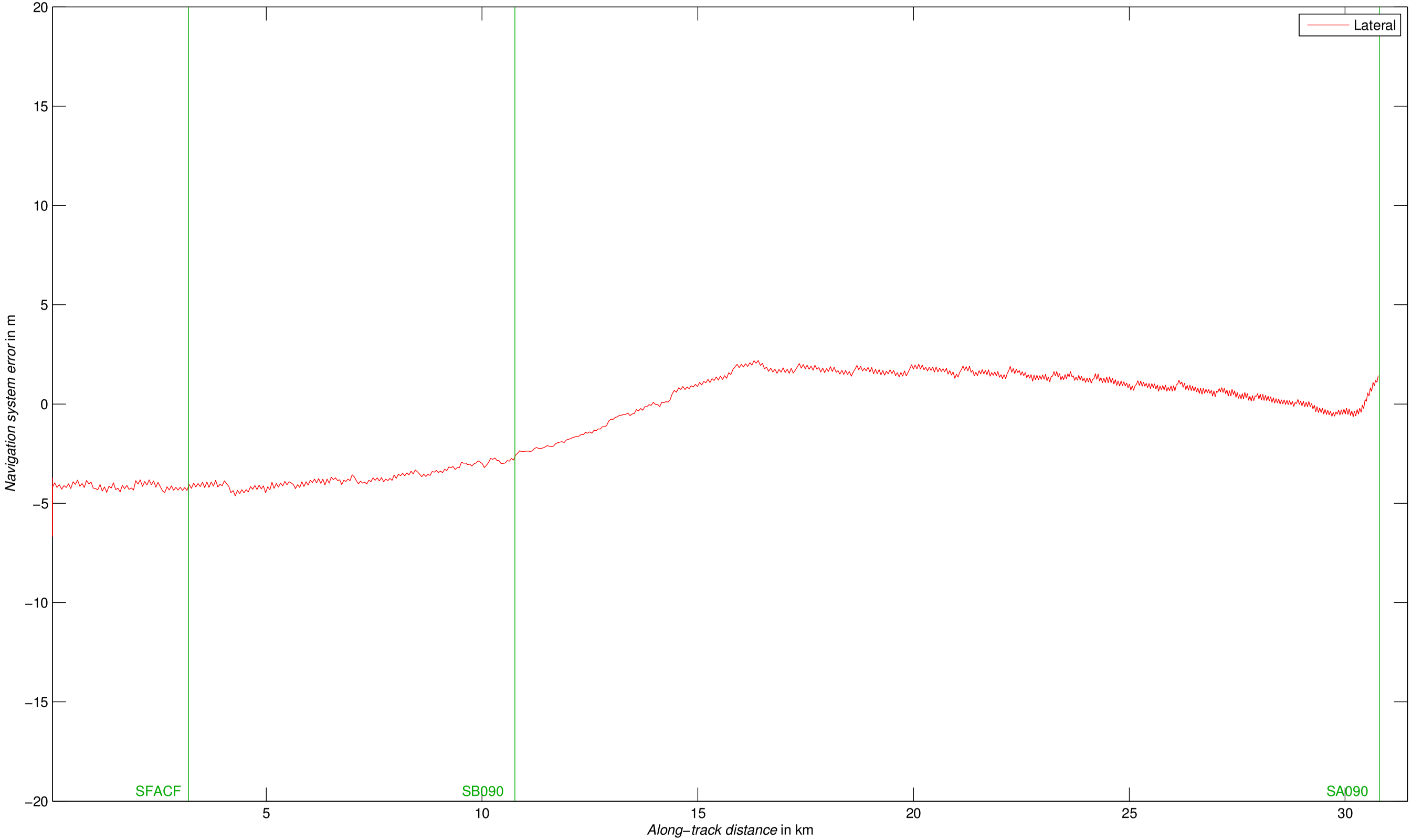

DLR Institut für Flugführung

Appendix E – Flight Path Angle

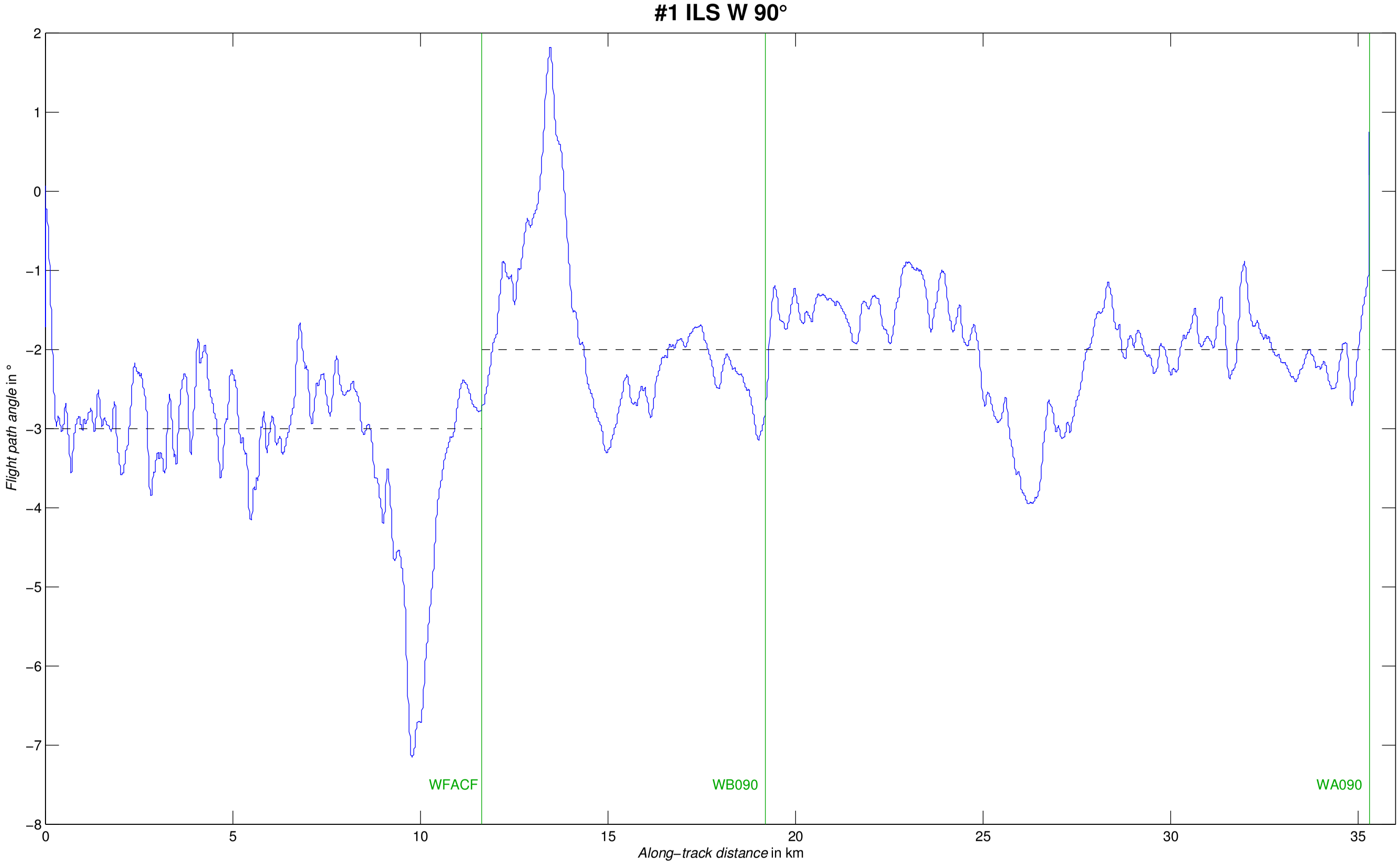

DLR Institut für Flugführung

#2 ILS V 180°

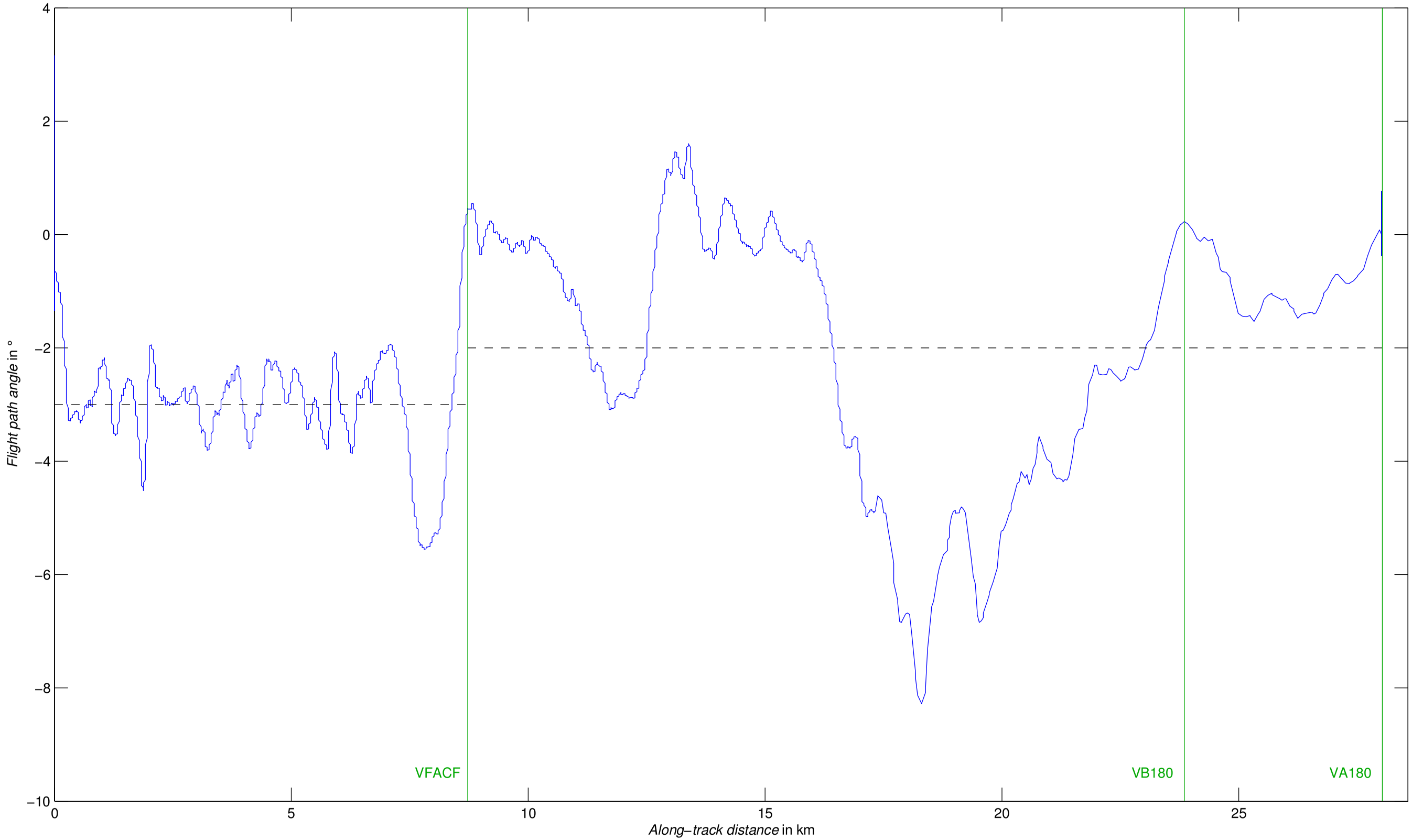

DLR Institut für Flugführung

#3 ILS U 90° APPR

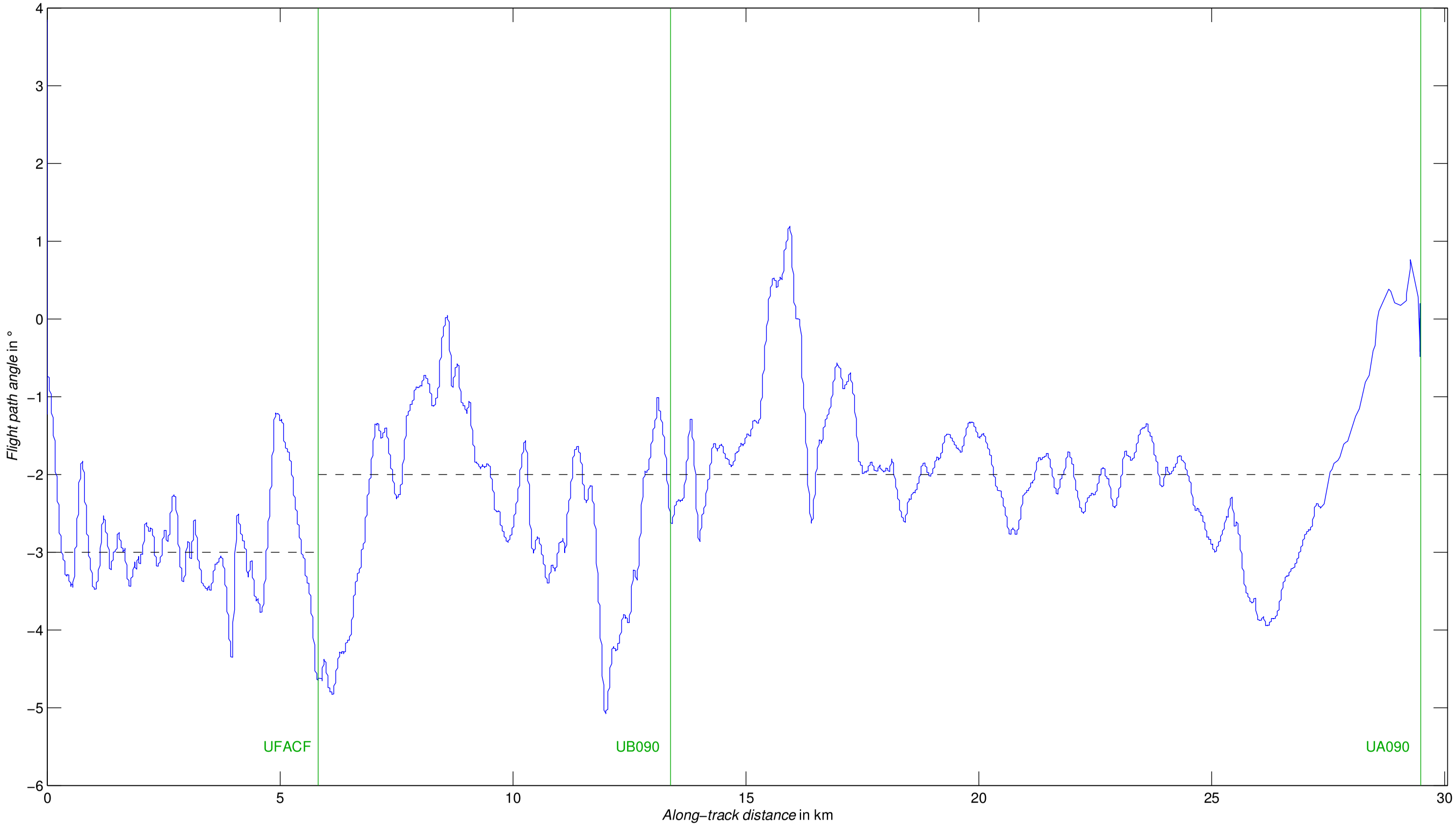

DLR Institut für Flugführung

#4 ILS T 90°

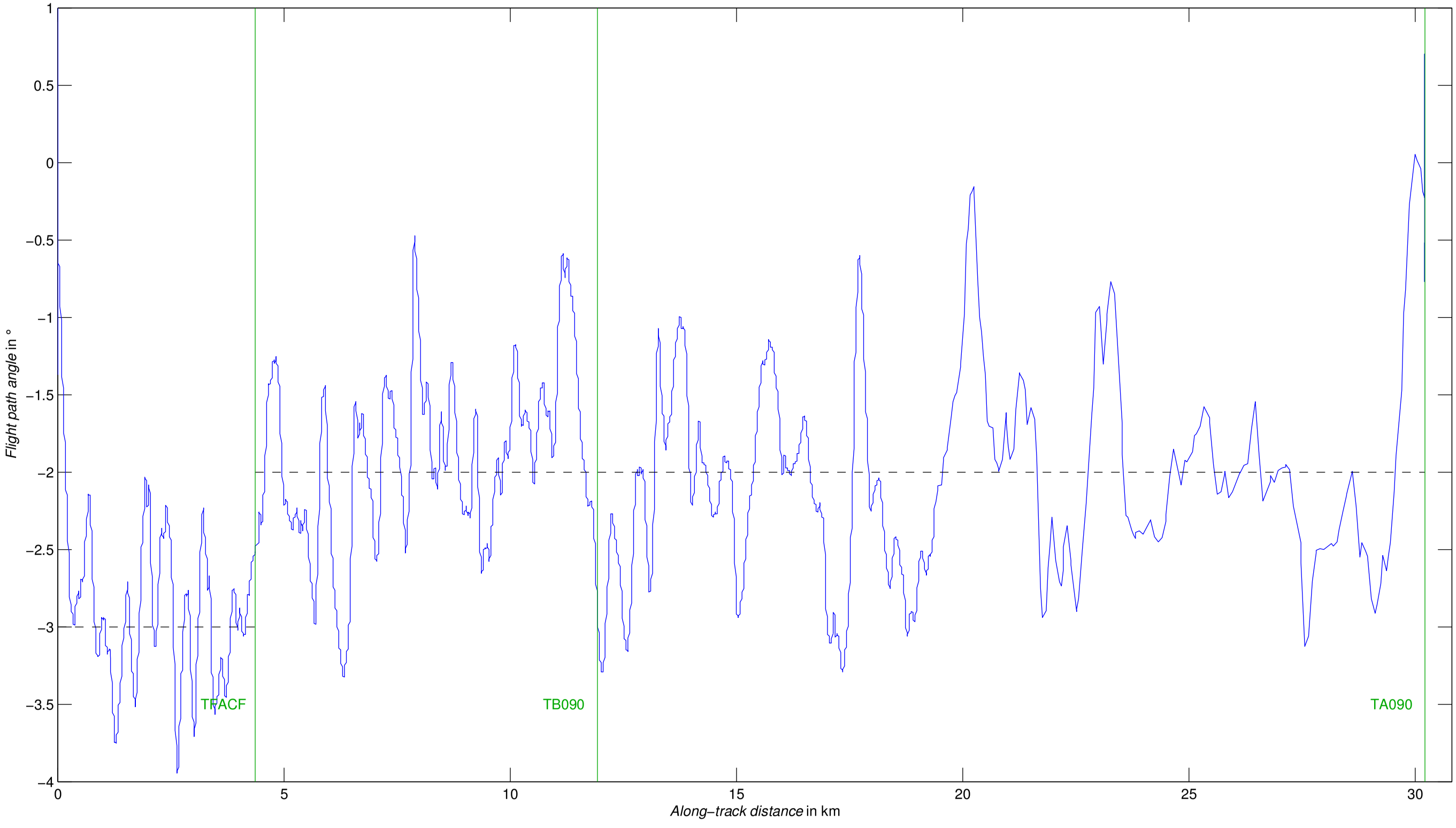

DLR Institut für Flugführung

#5 ILS S 180°

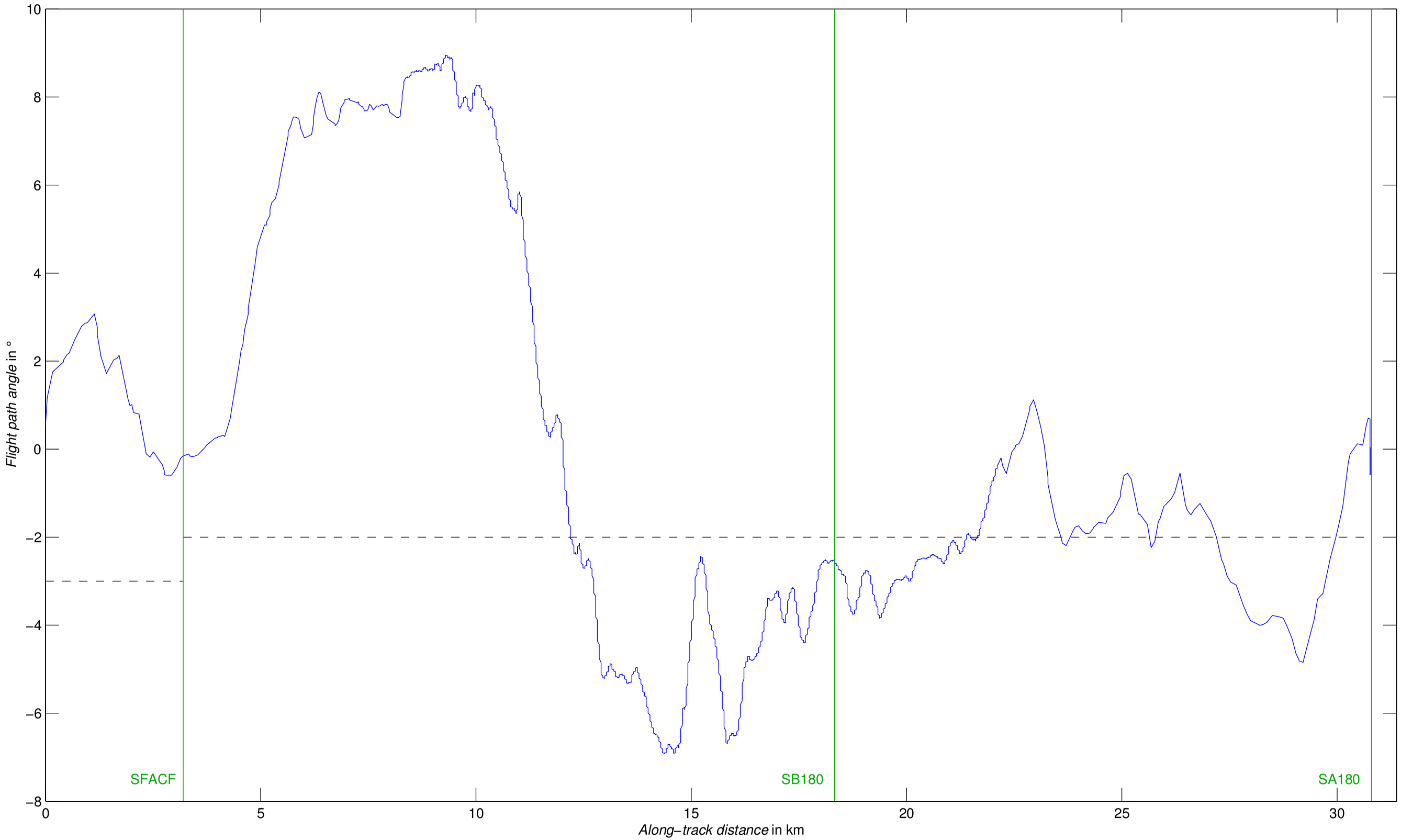

DLR Institut für Flugführung

#6 ILS W 90° APPR

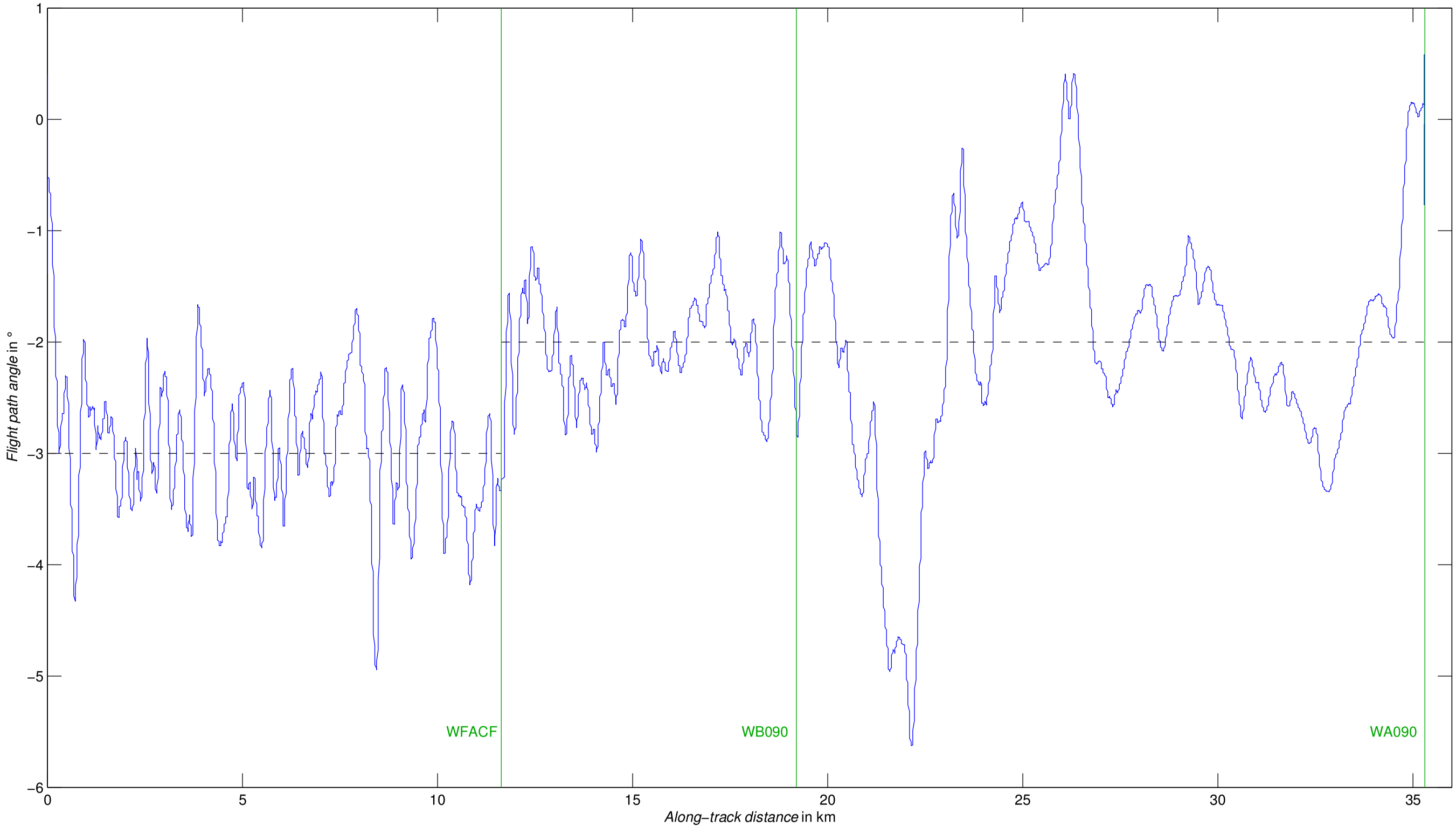

DLR Institut für Flugführung

#7 ILS V 90°

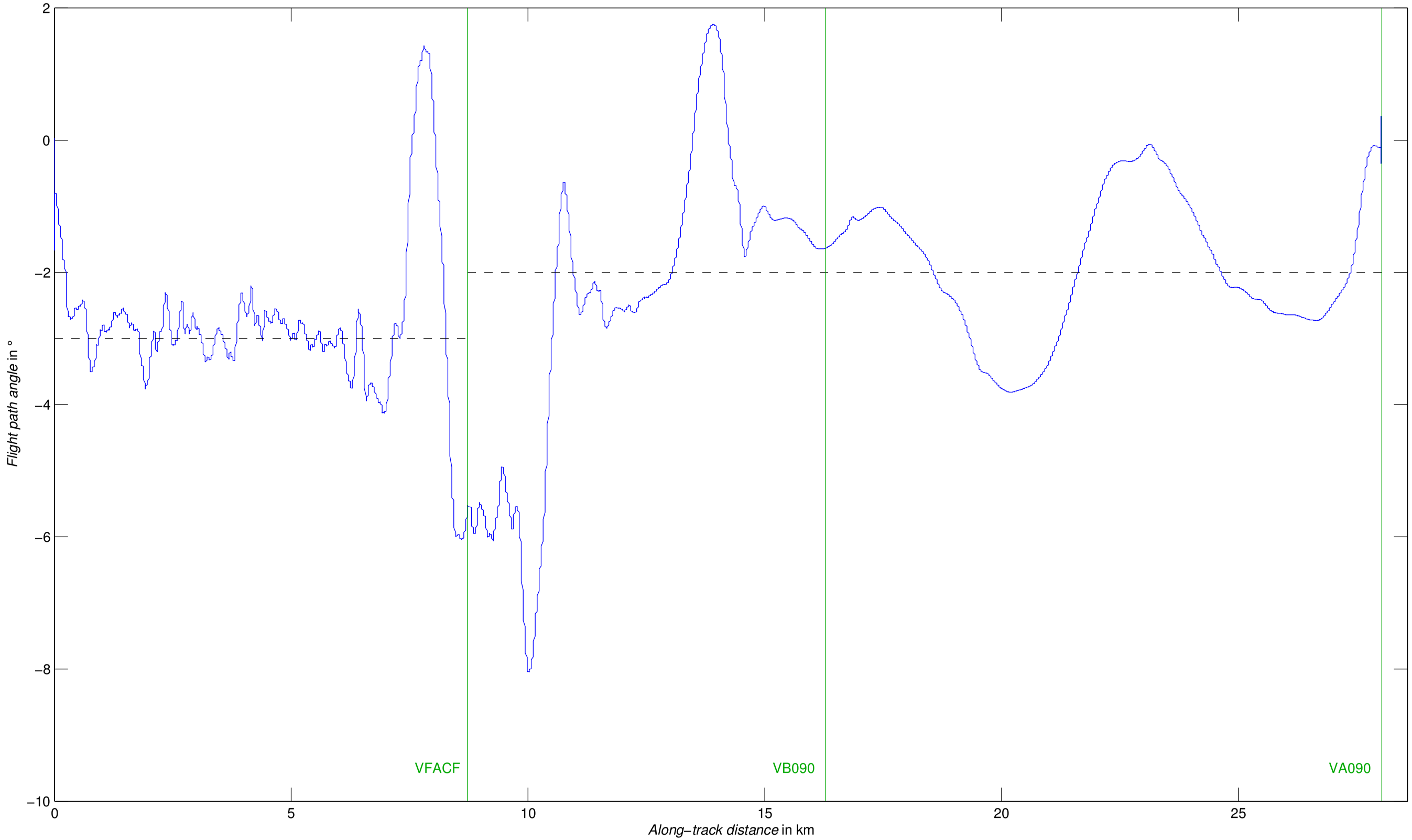

DLR Institut für Flugführung

#8 ILS U 180°

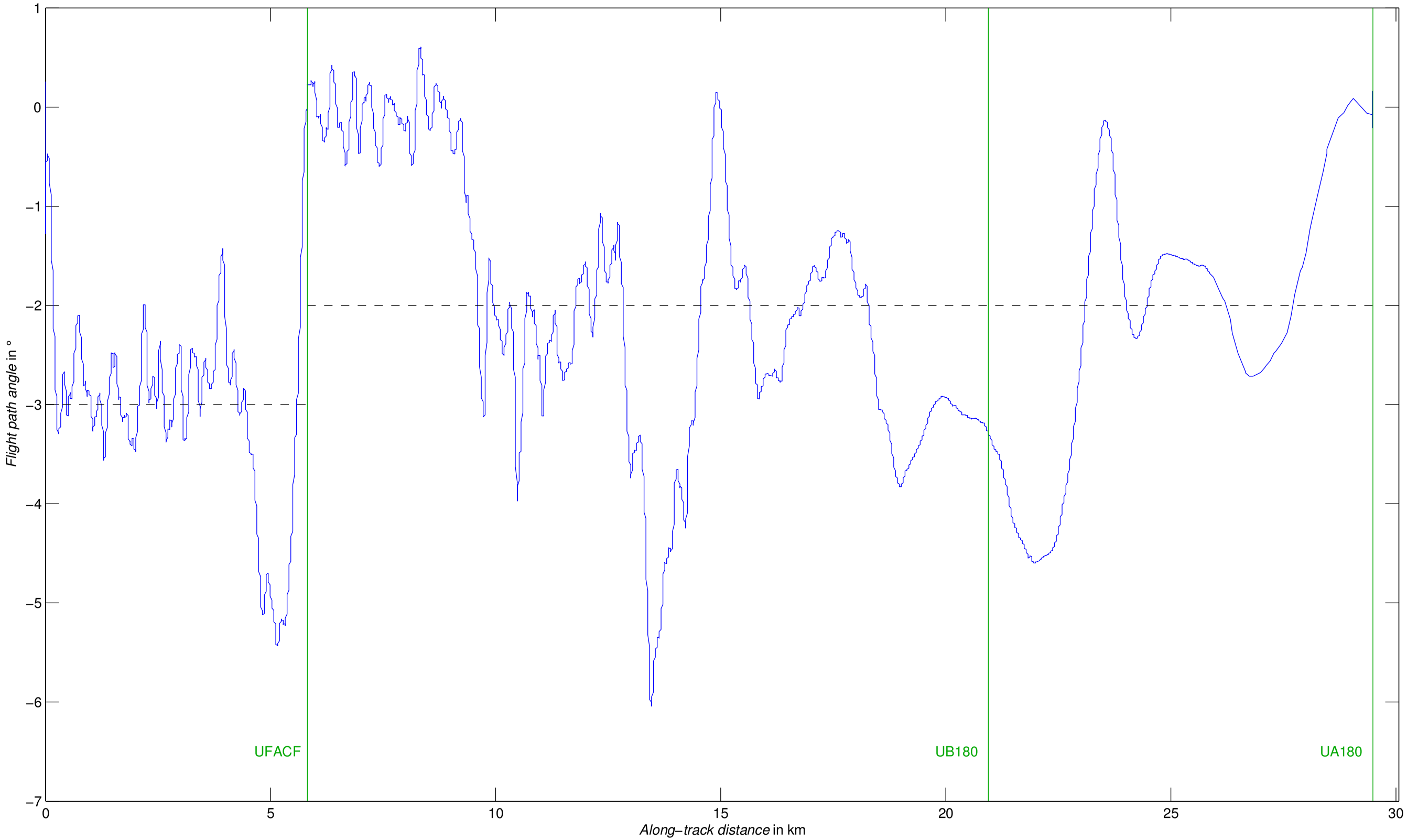

DLR Institut für Flugführung

#9 ILS T 90°

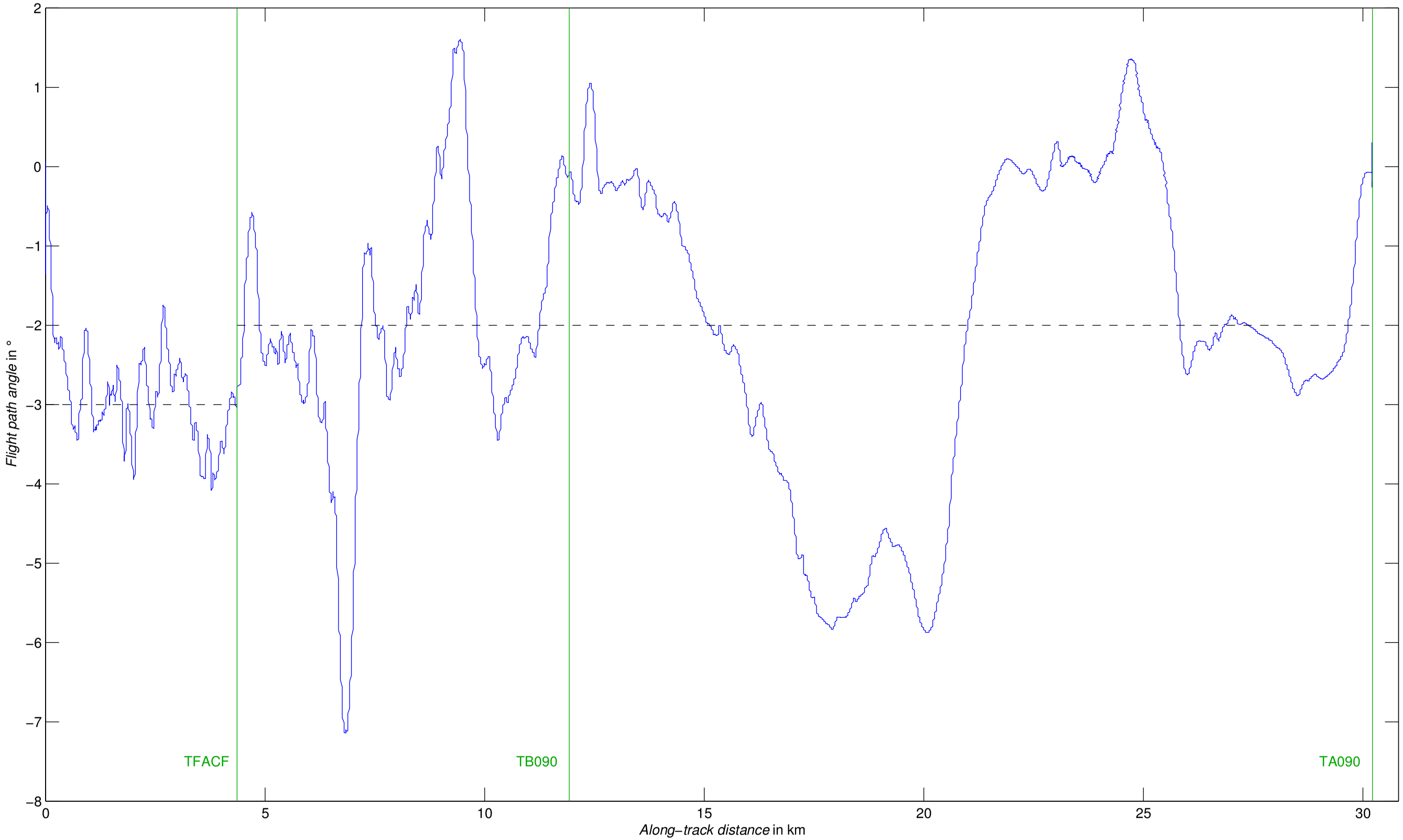

DLR Institut für Flugführung

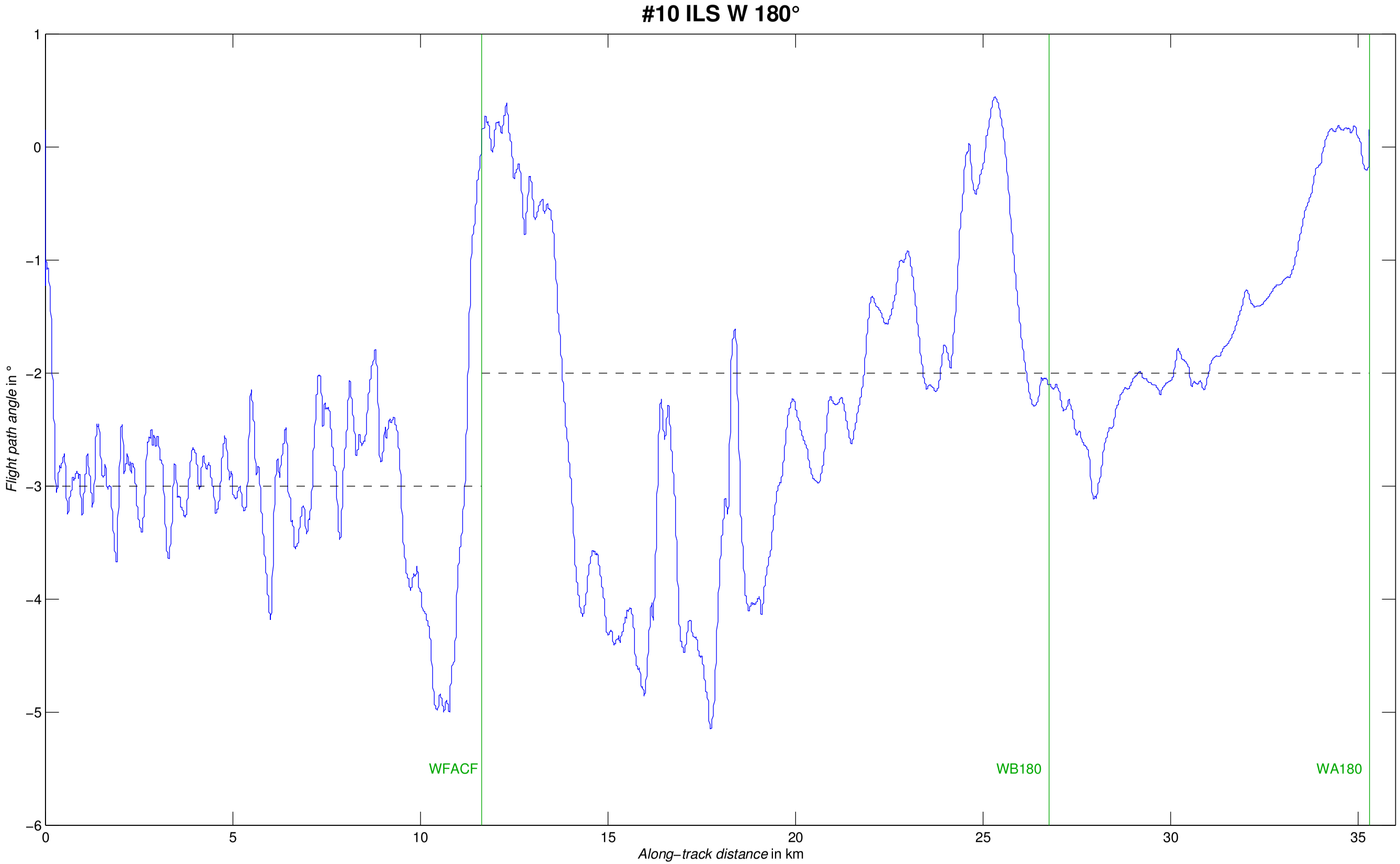

DLR Institut für Flugführung

#11 ILS T 90°

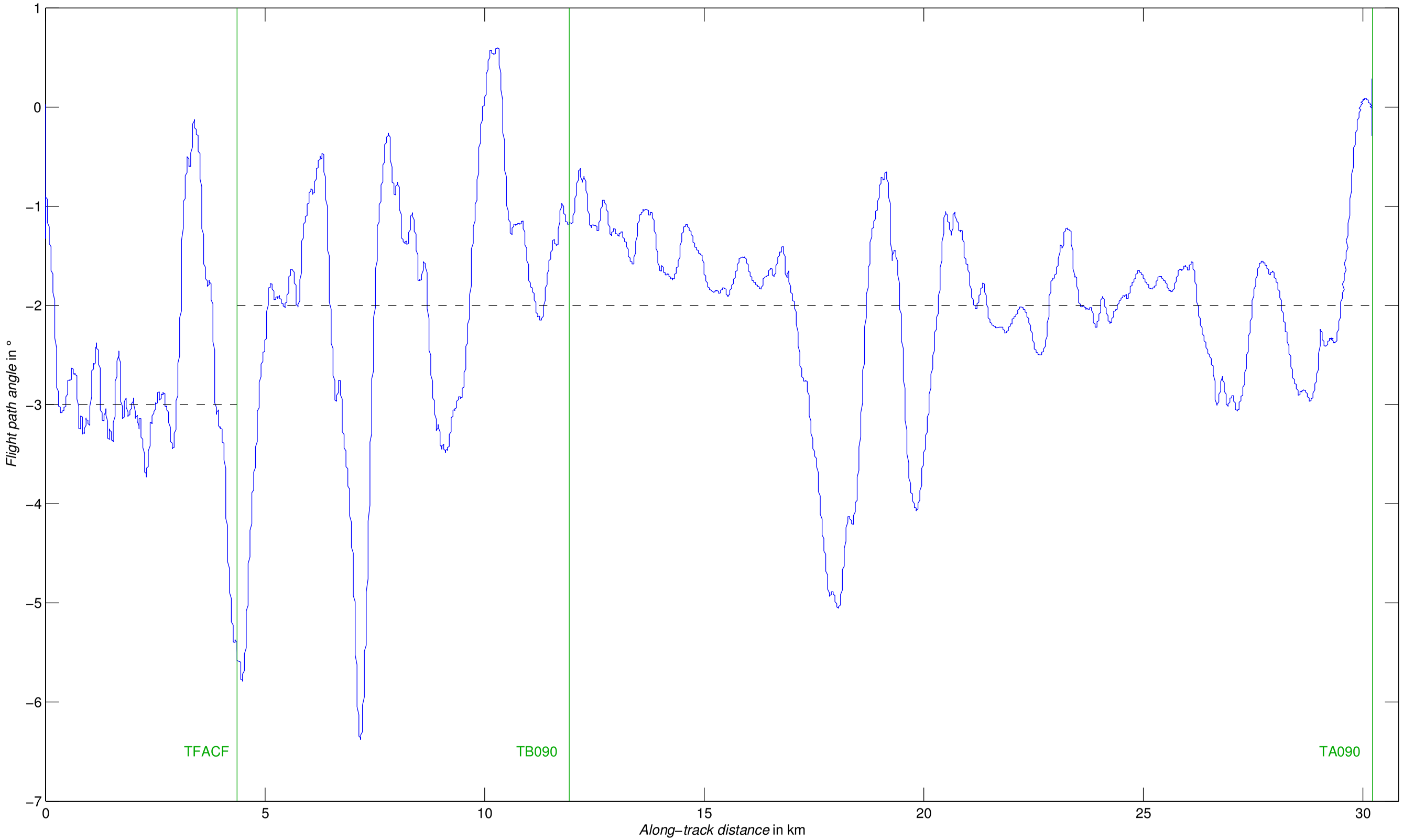

DLR Institut für Flugführung

#12 ILS S 90°

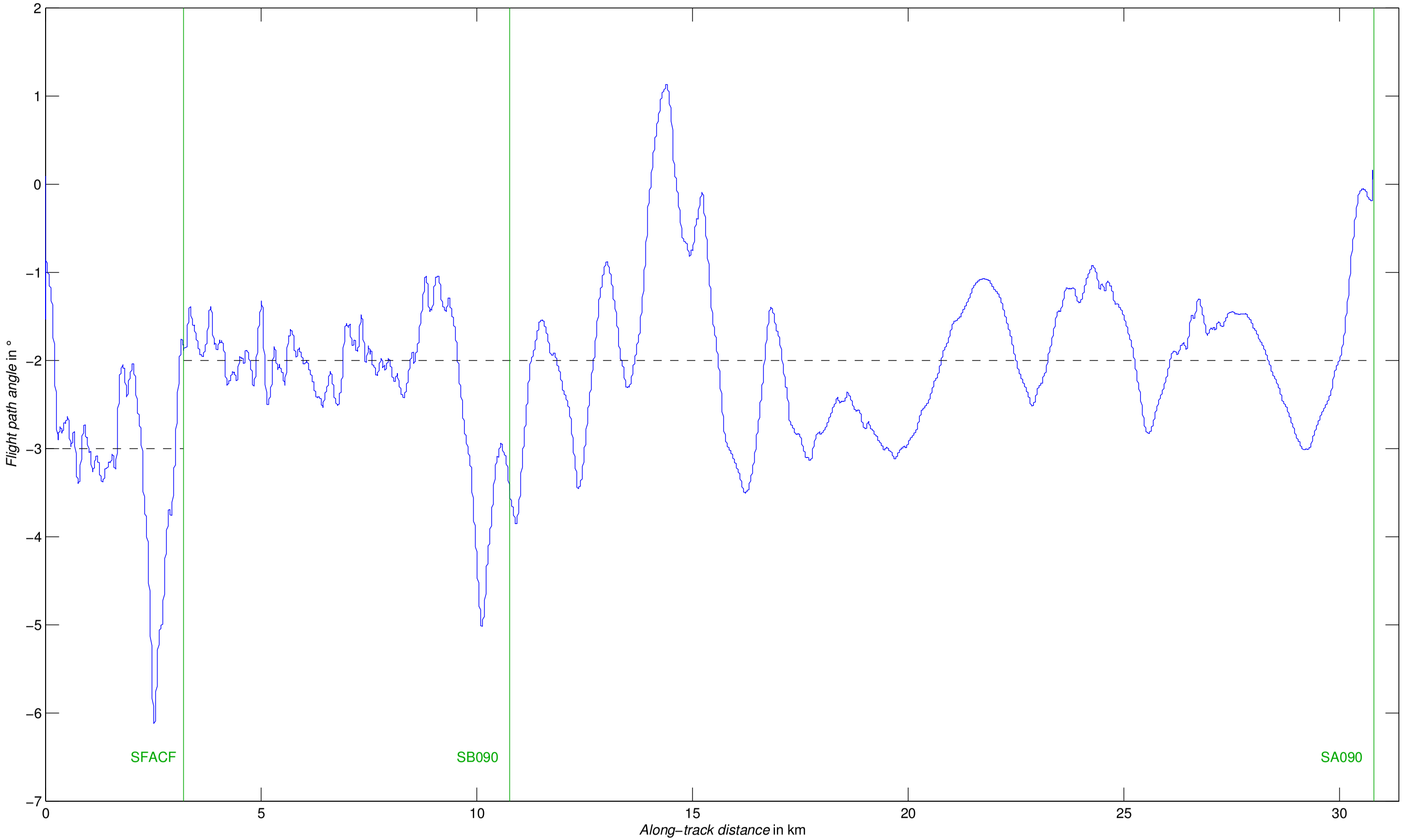

DLR Institut für Flugführung

#13 ILS V 90° APPR

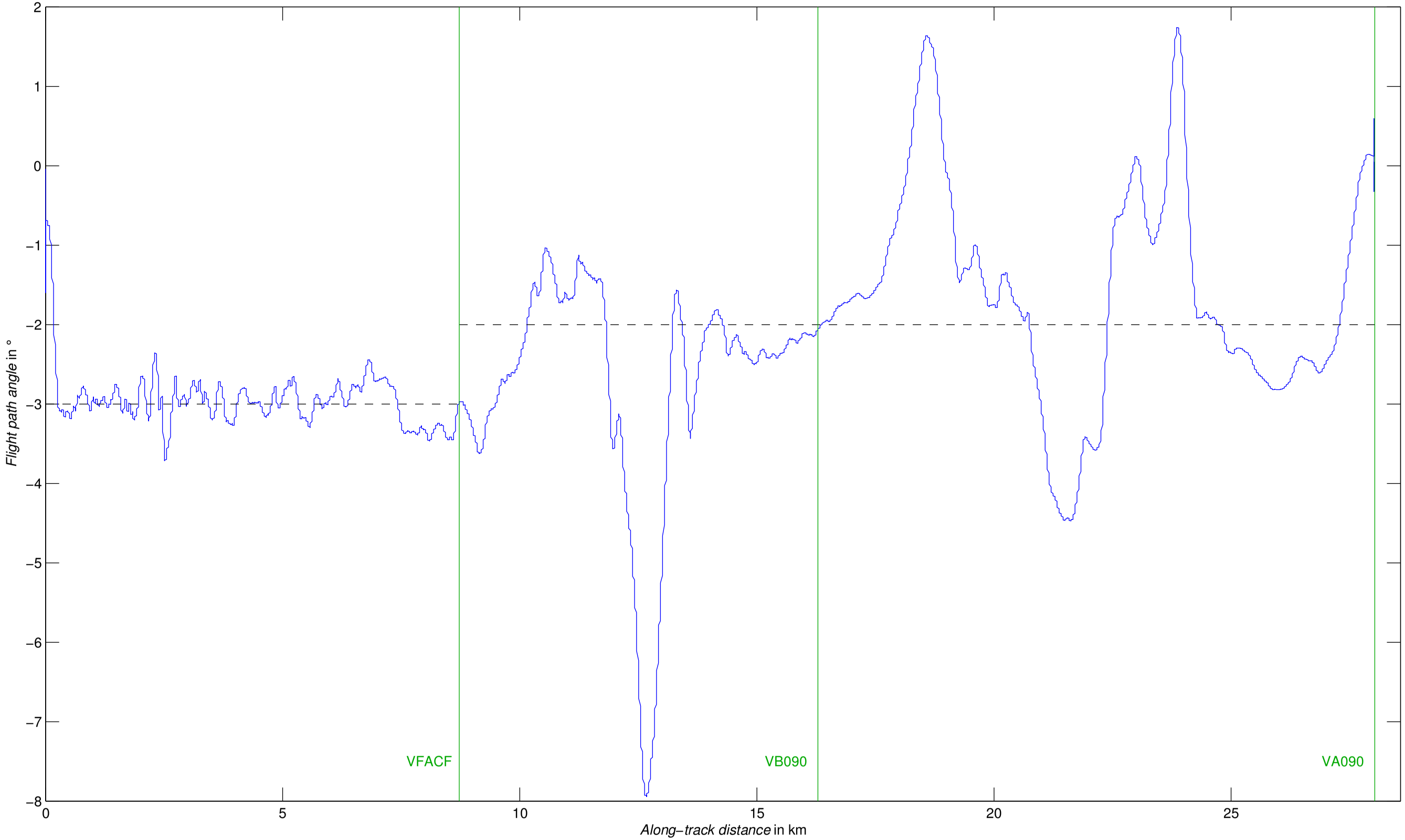

Institut für Flugführung
DLR

#14 ILS U 90°

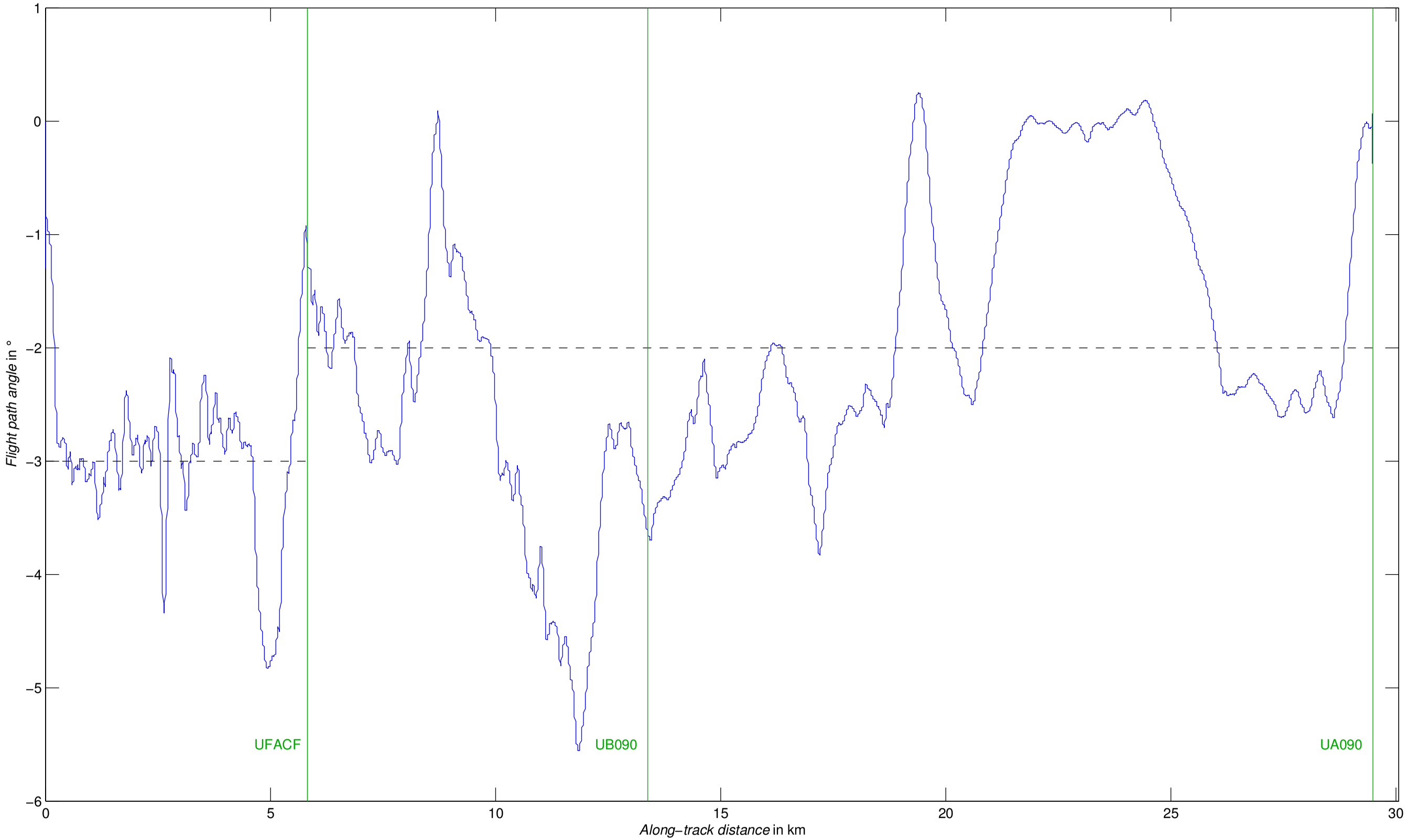

DLR Institut für Flugführung

#15 ILS V 180° APPR

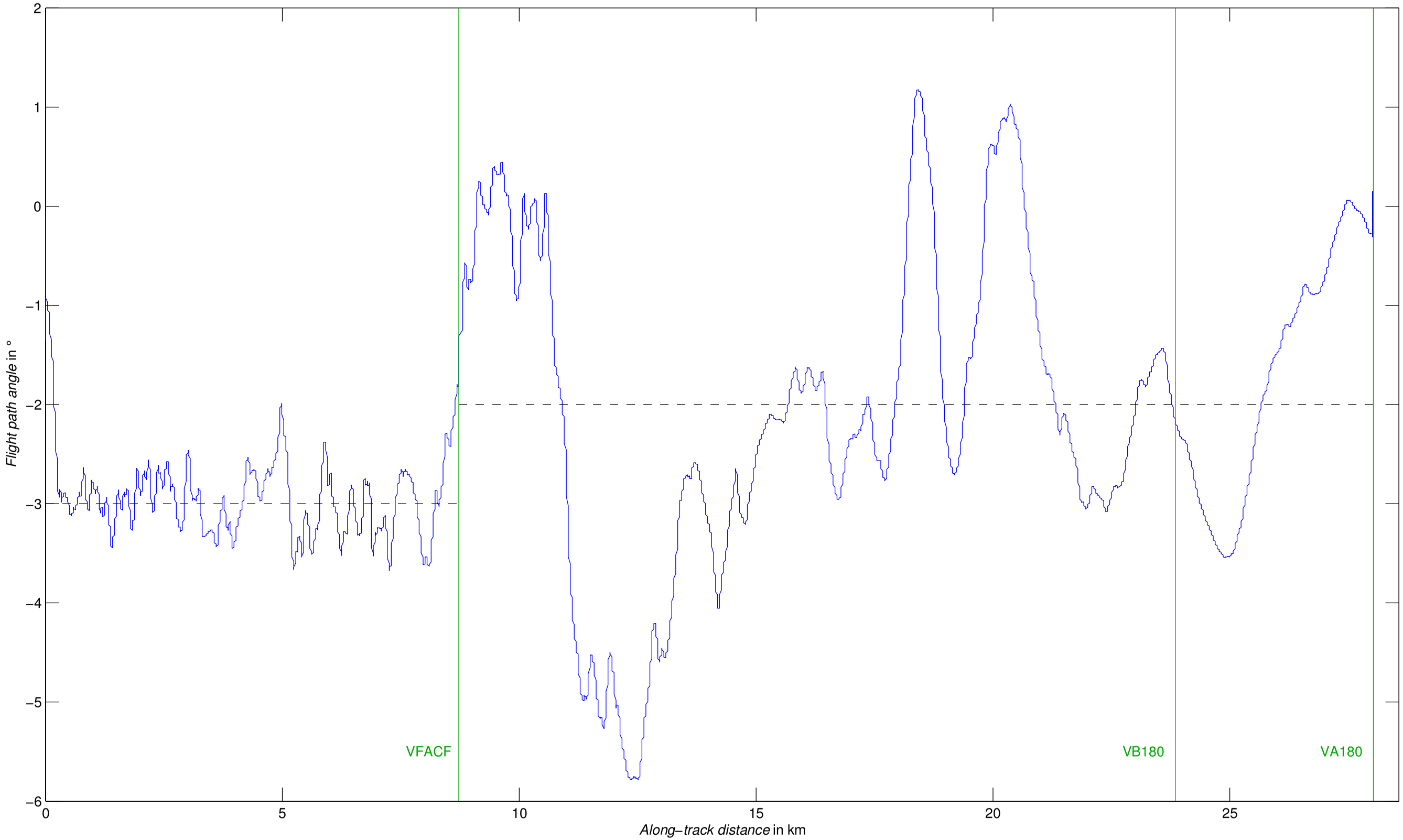

Institut für Flugführung
DLR

#16 ILS S 90°

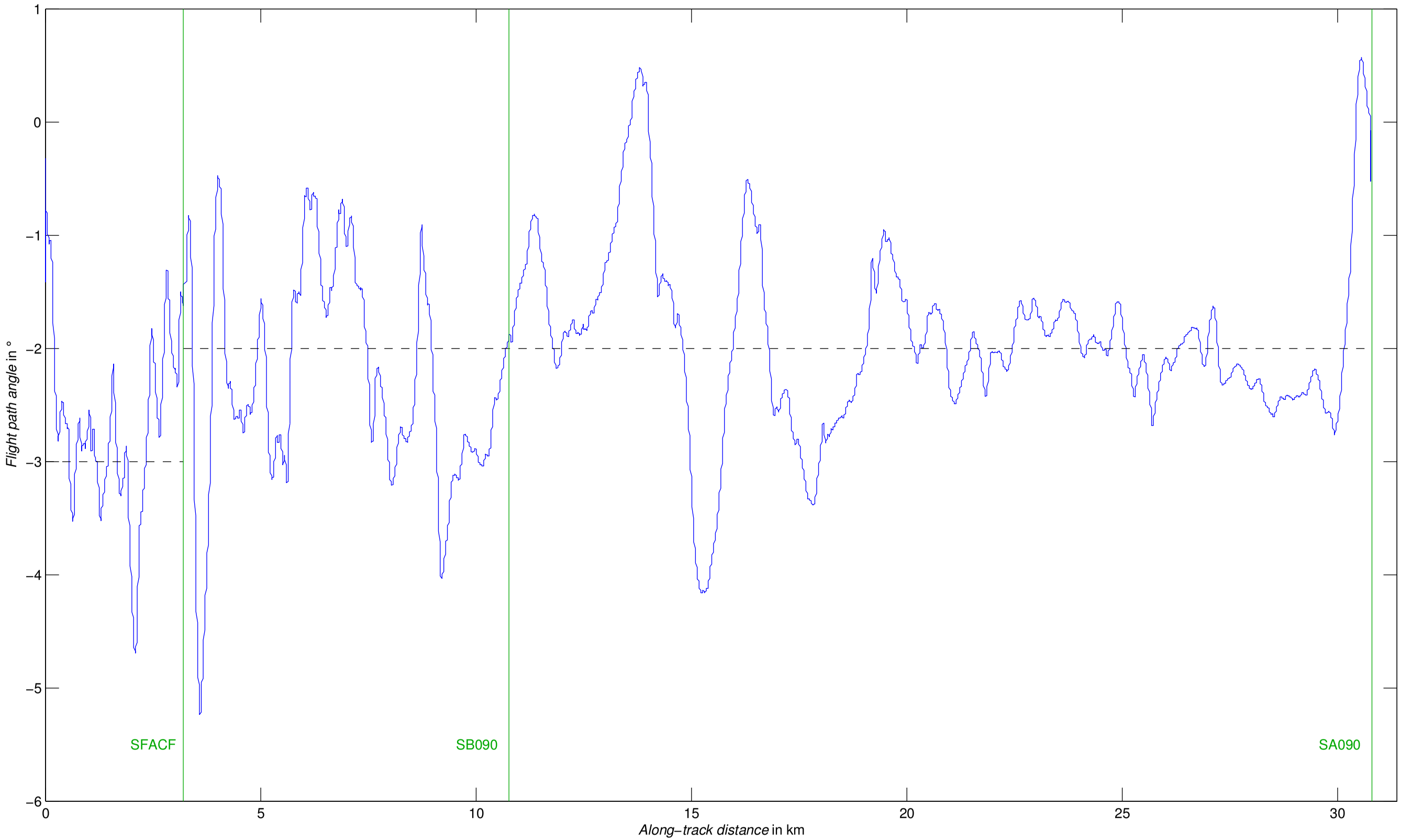

DLR Institut für Flugführung

Appendix F – Localizer and Glideslope Deviations

#1 ILS W 90°

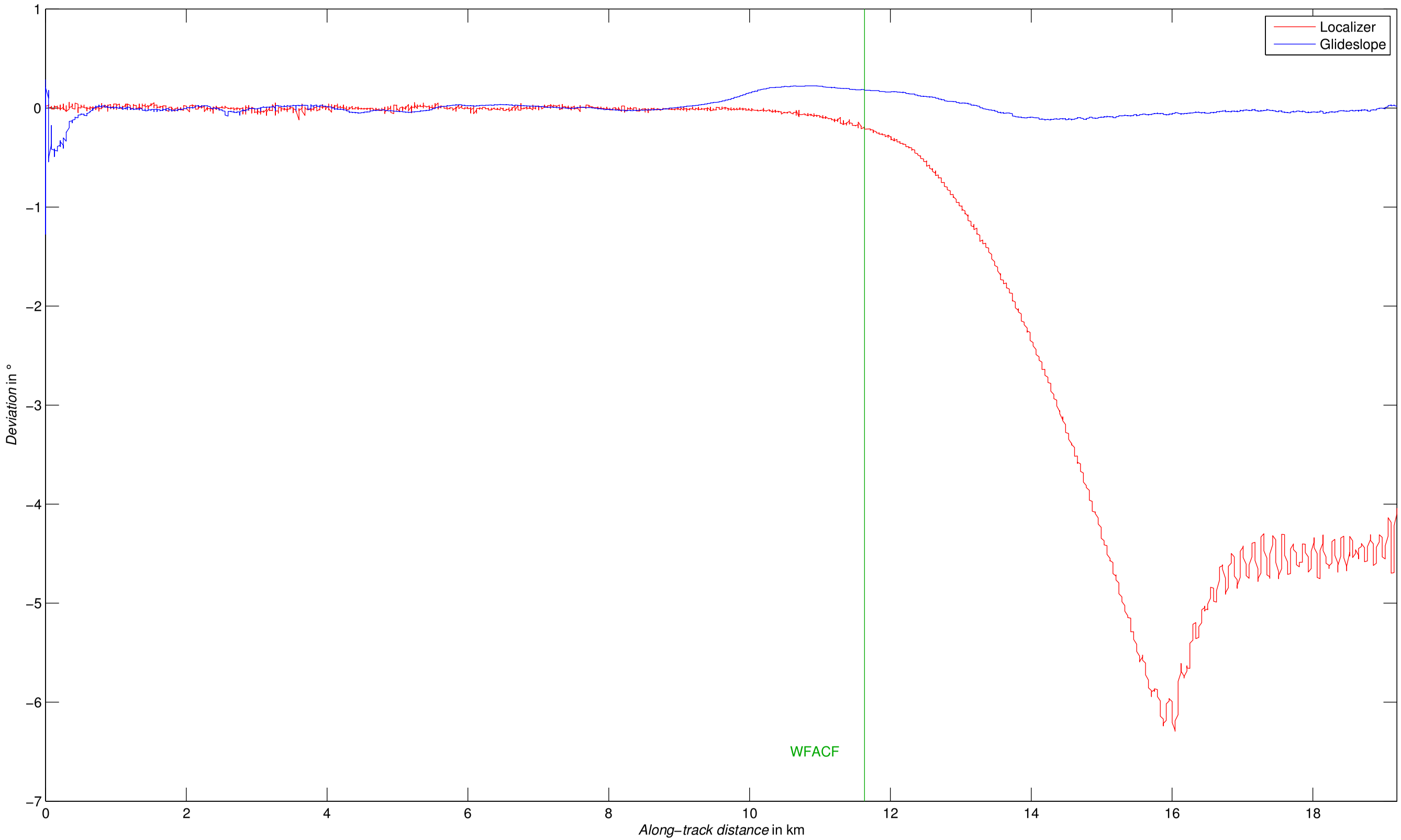

DLR Institut für Flugführung

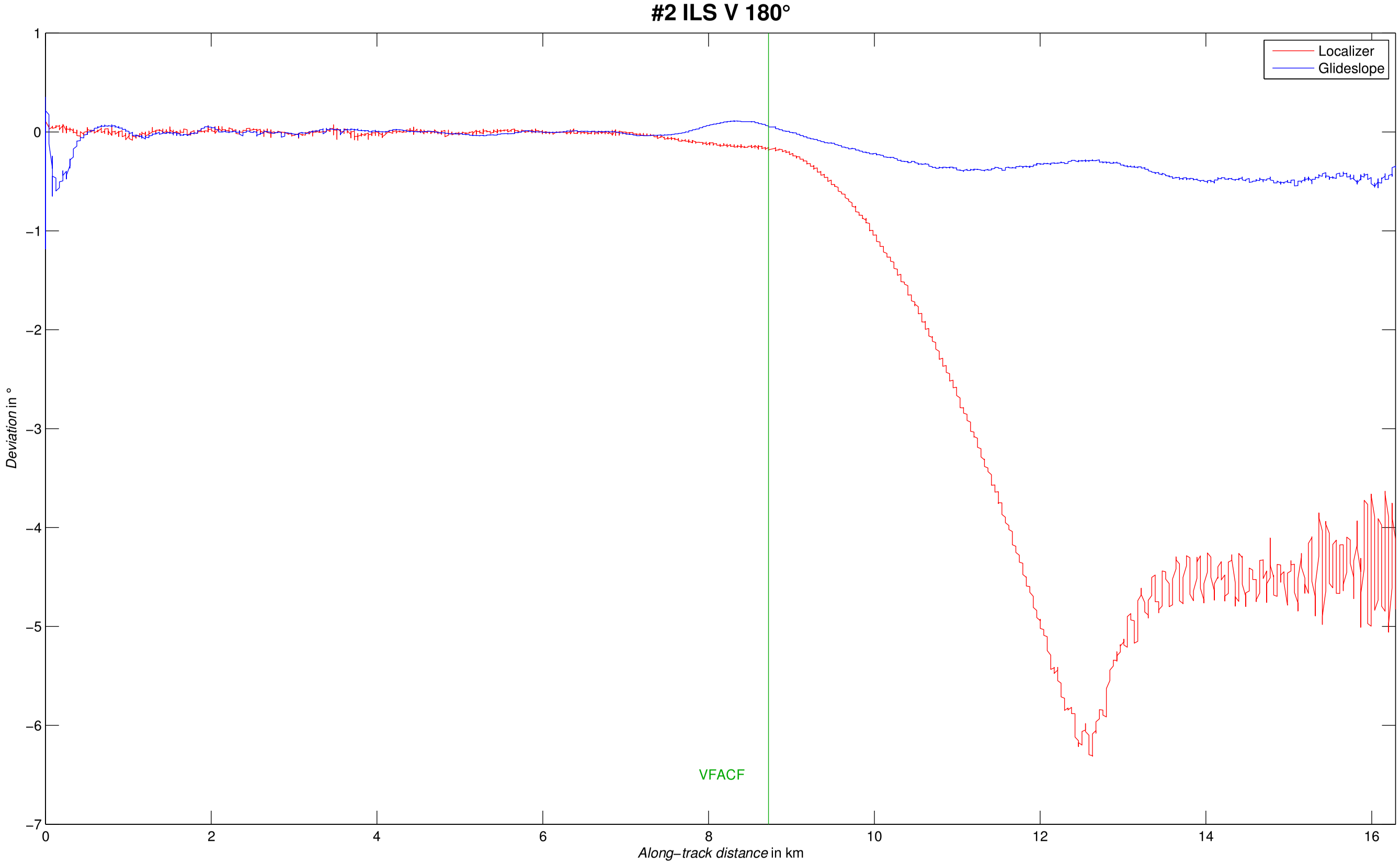

DLR Institut für Flugführung

#3 ILS U 90° APPR

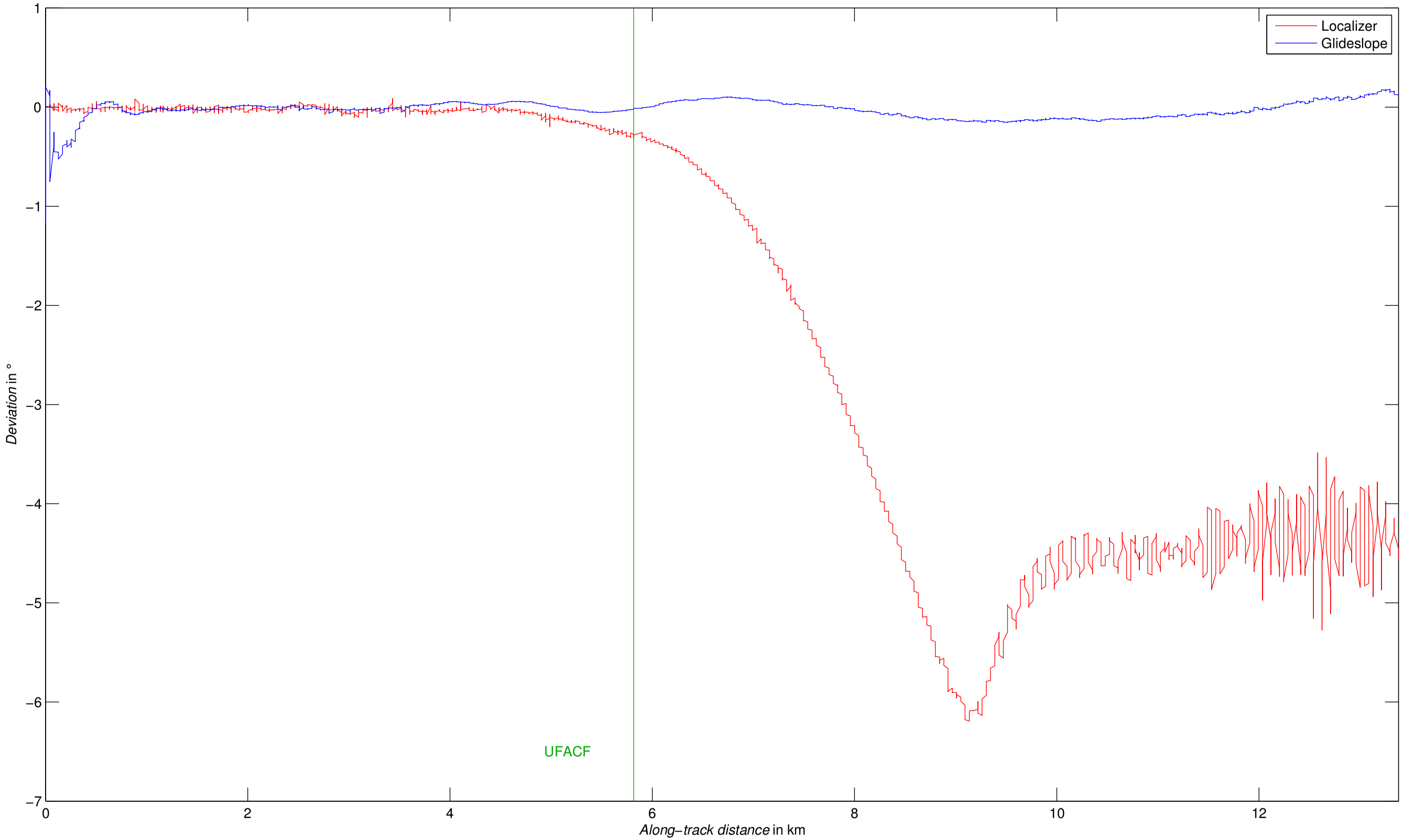

DLR Institut für Flugführung

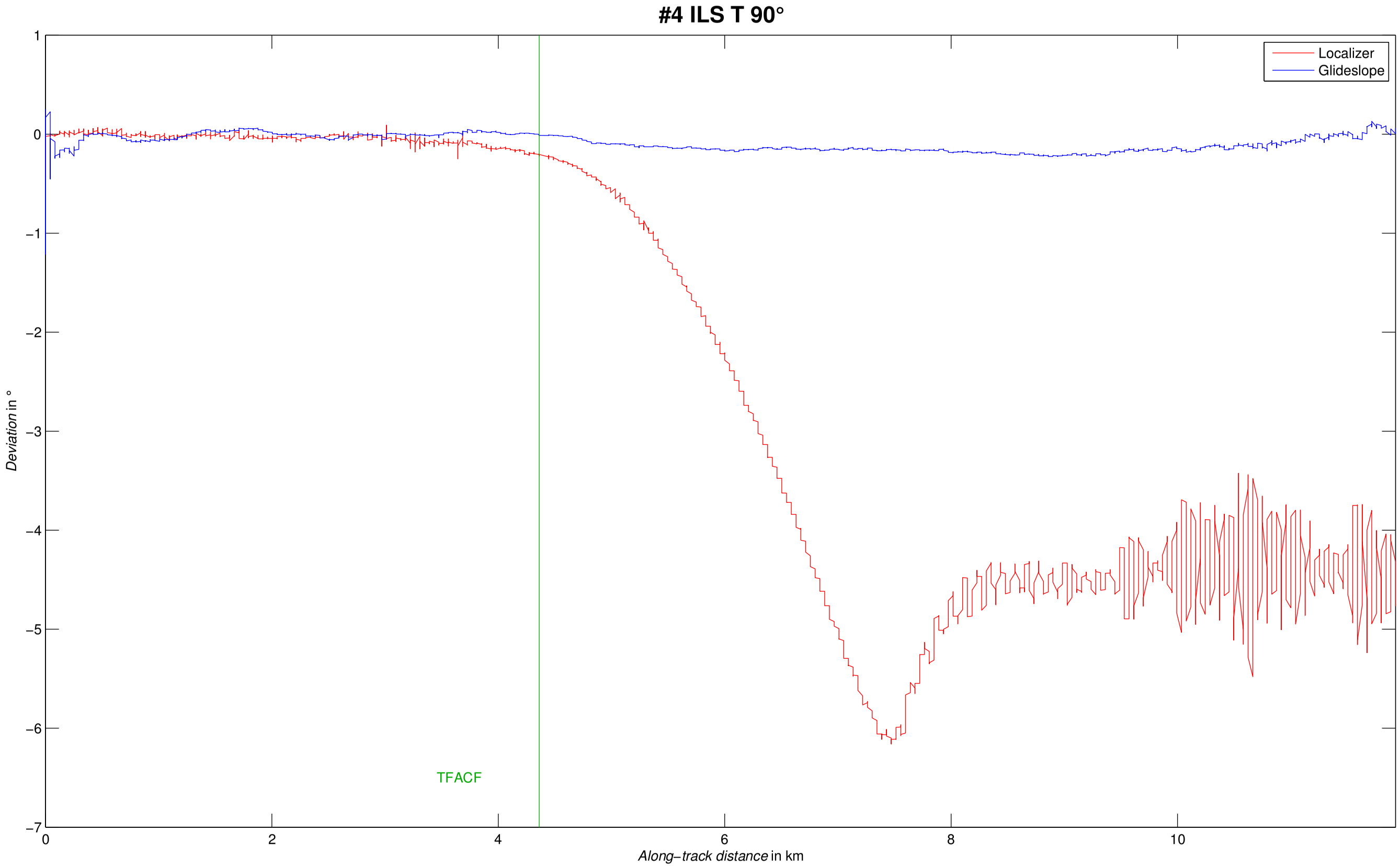

DLR Institut für Flugführung

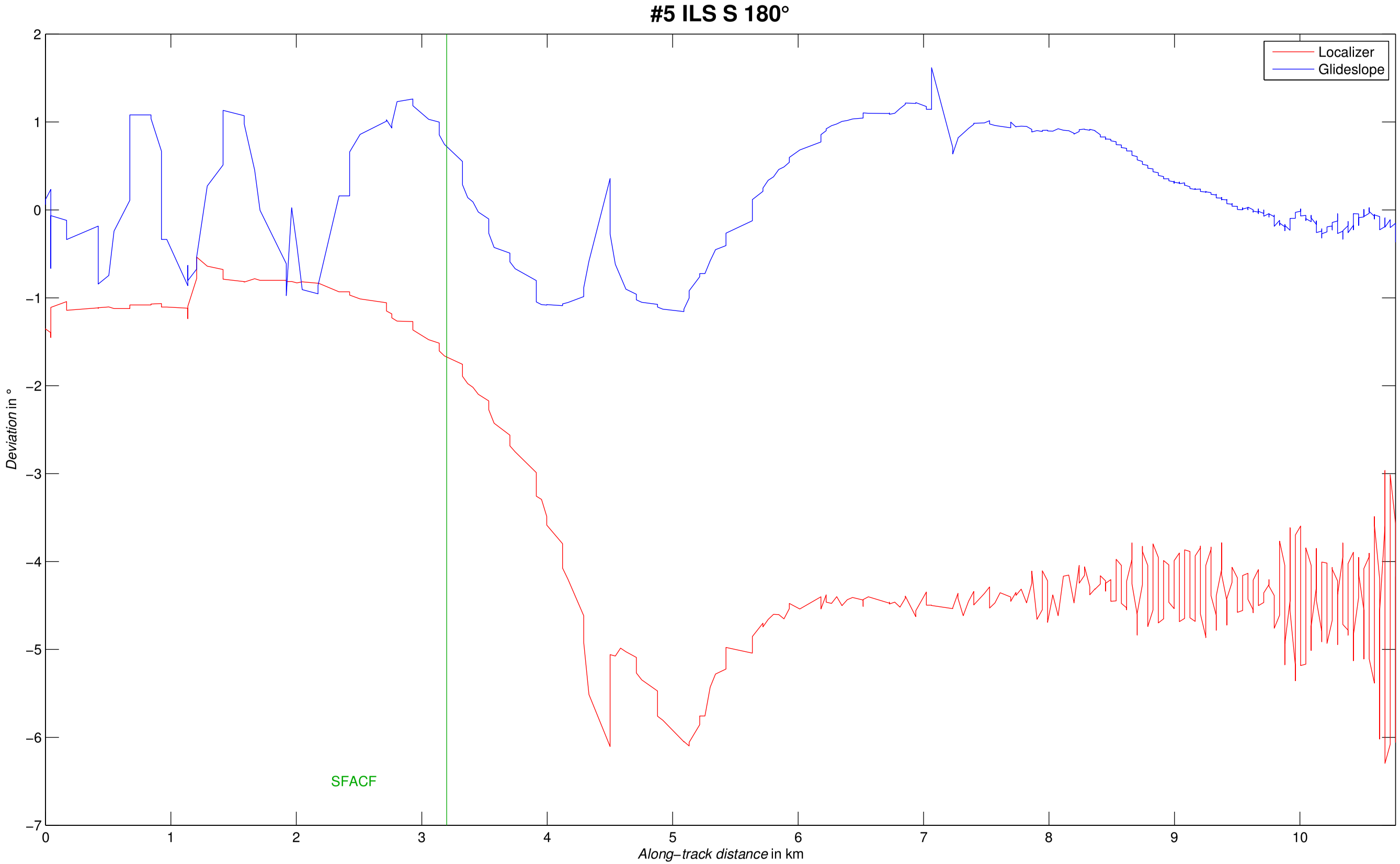

DLR Institut für Flugführung

#6 ILS W 90° APPR

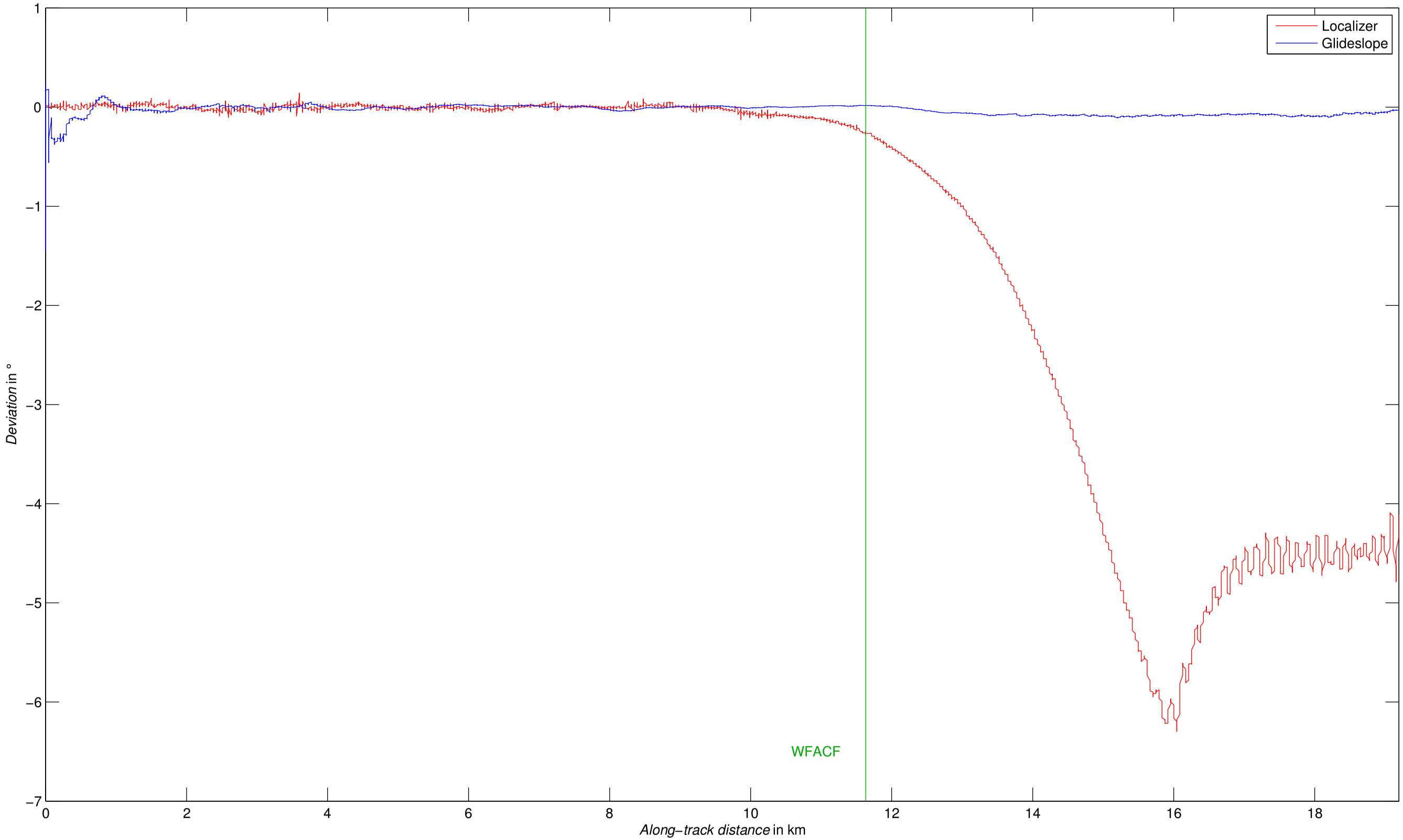

DLR Institut für Flugführung

#7 ILS V 90°

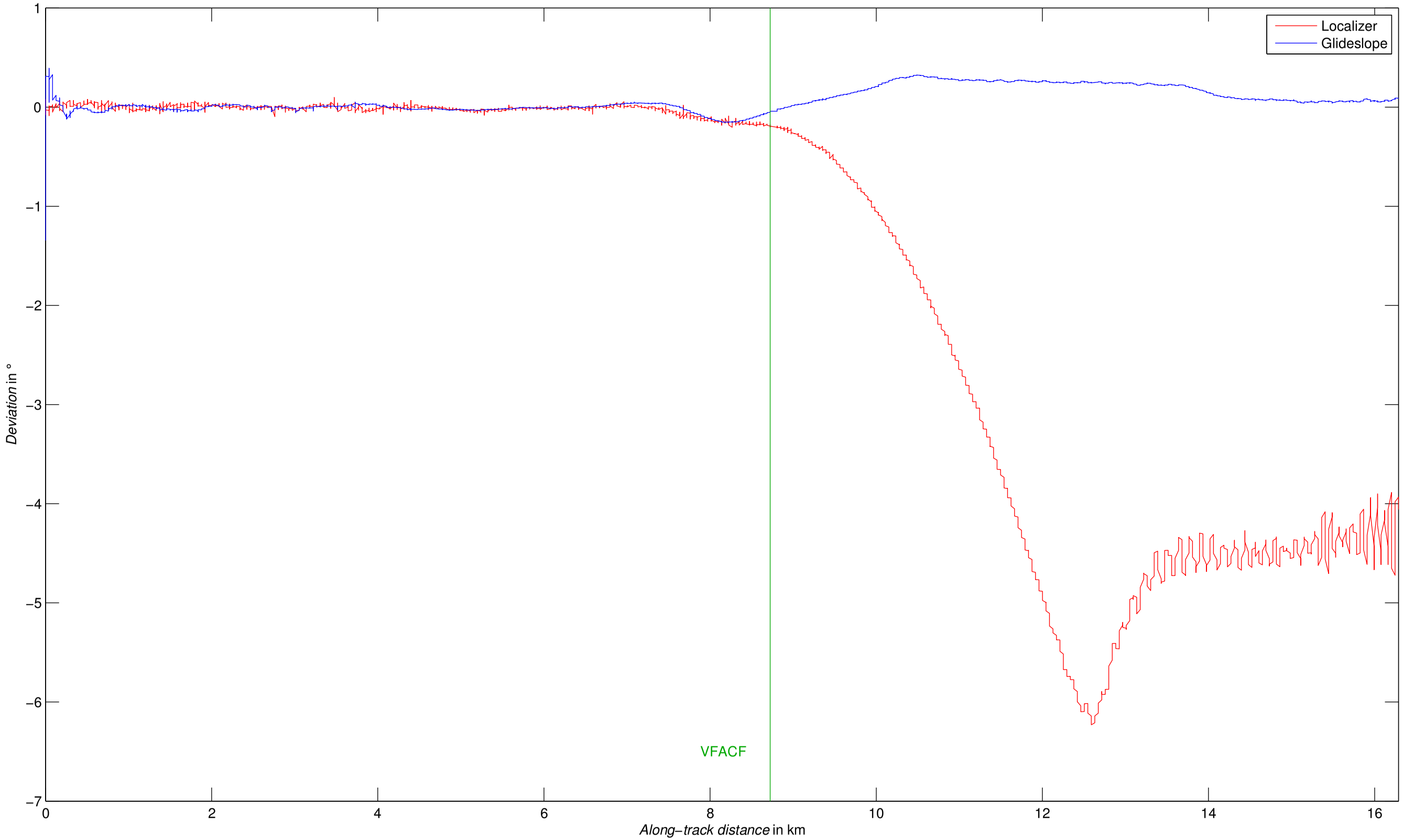

DLR Institut für Flugführung

#8 ILS U 180°

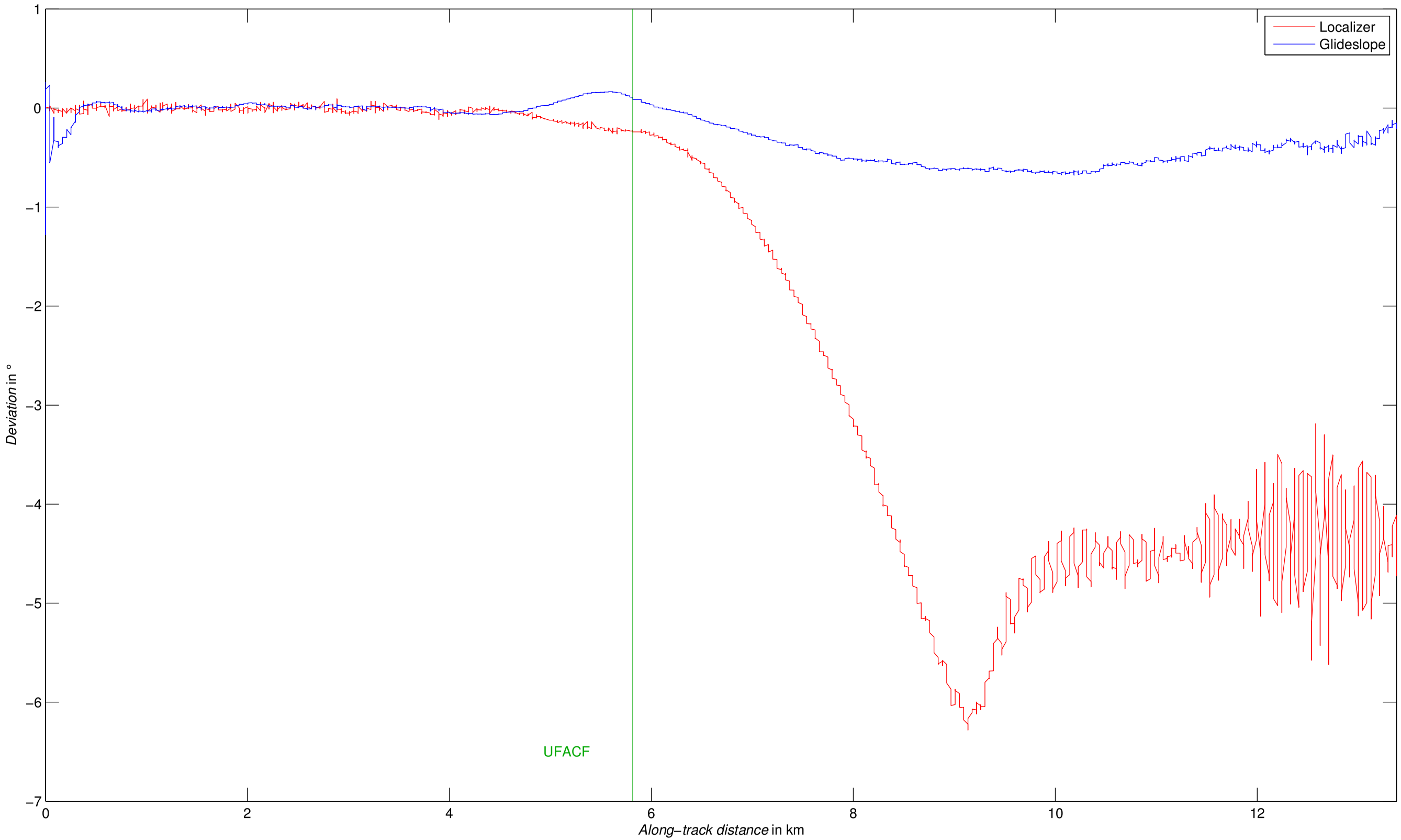

DLR Institut für Flugführung

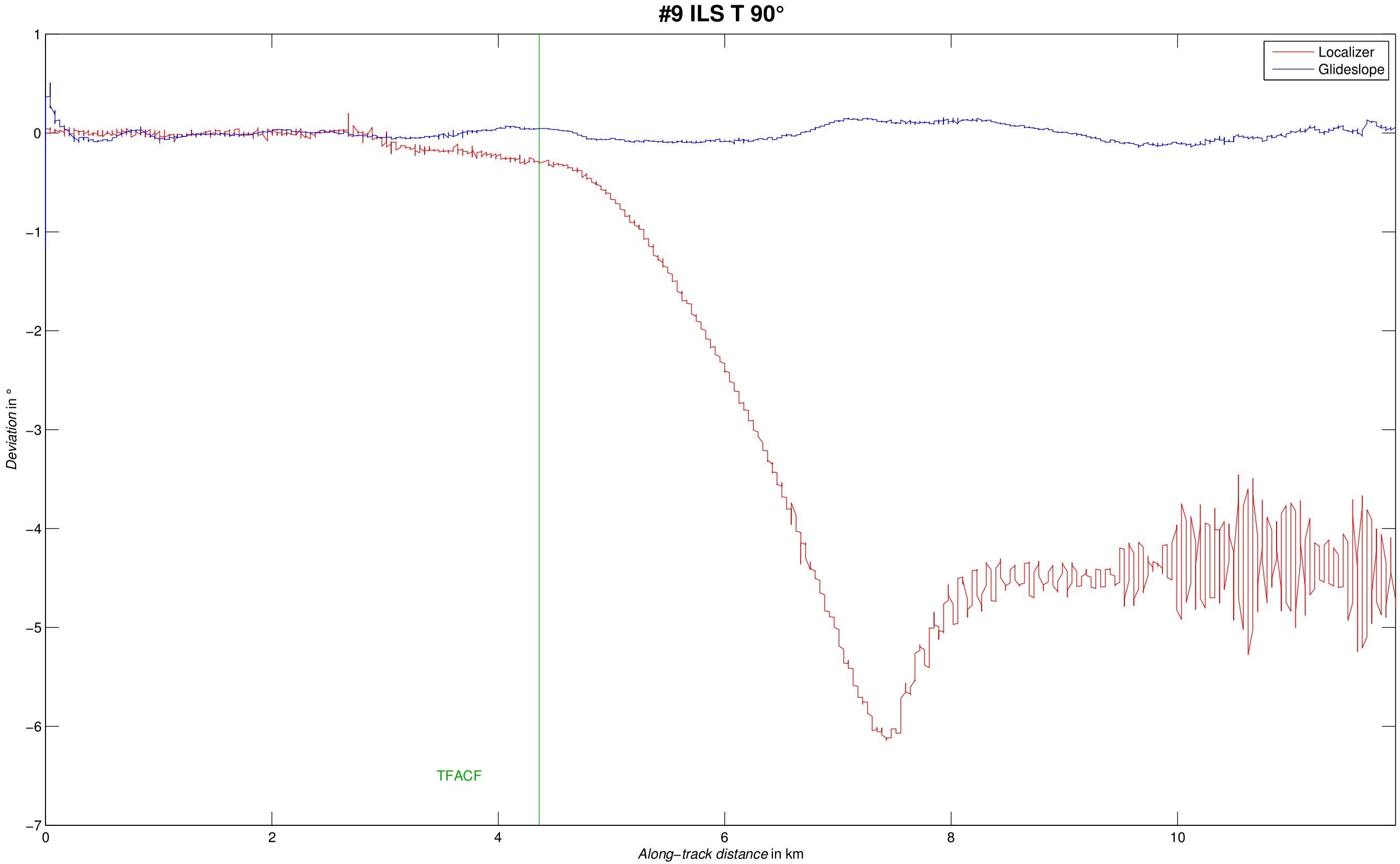

DLR Institut für Flugführung

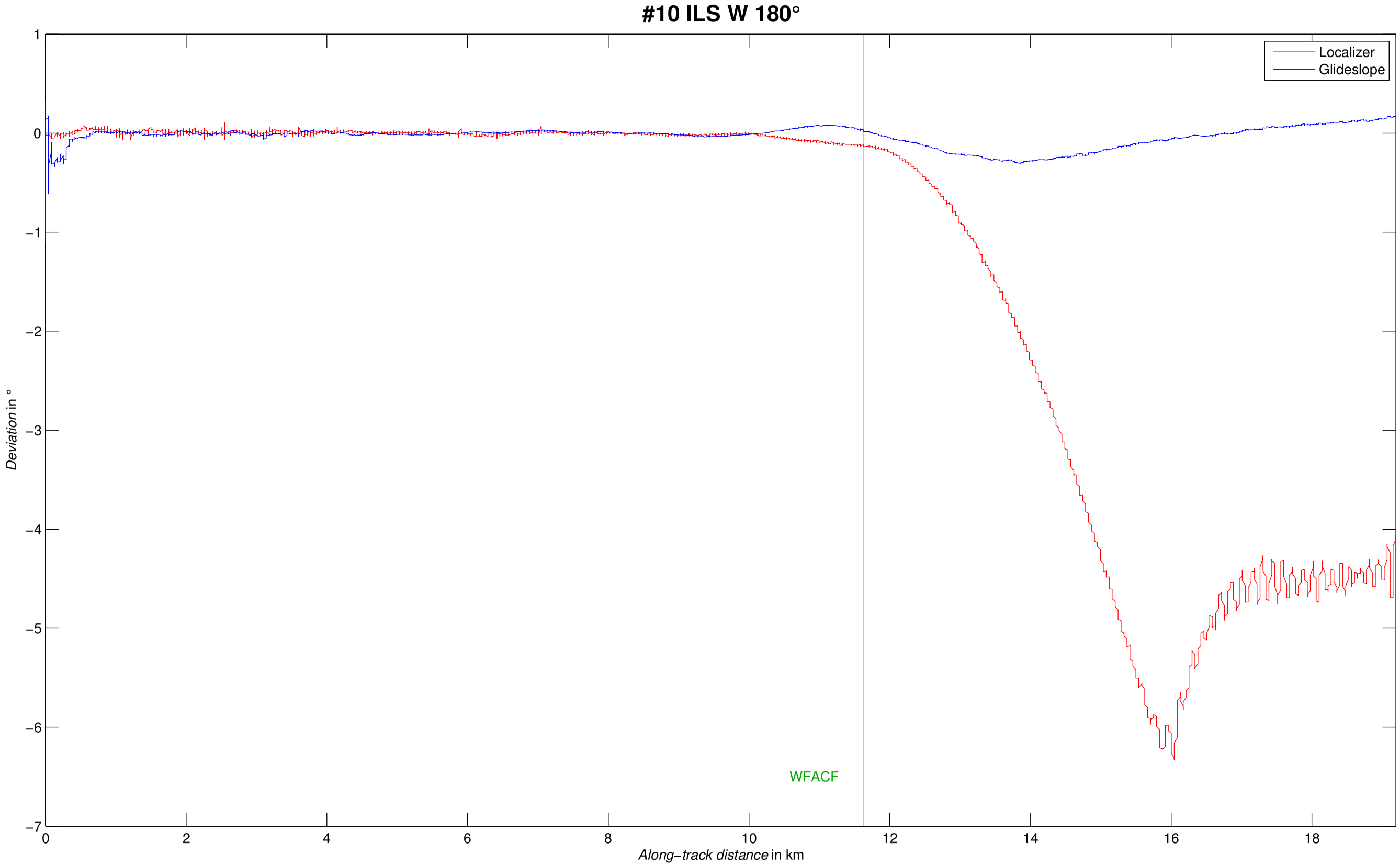

DLR Institut für Flugführung

#11 ILS T 90°

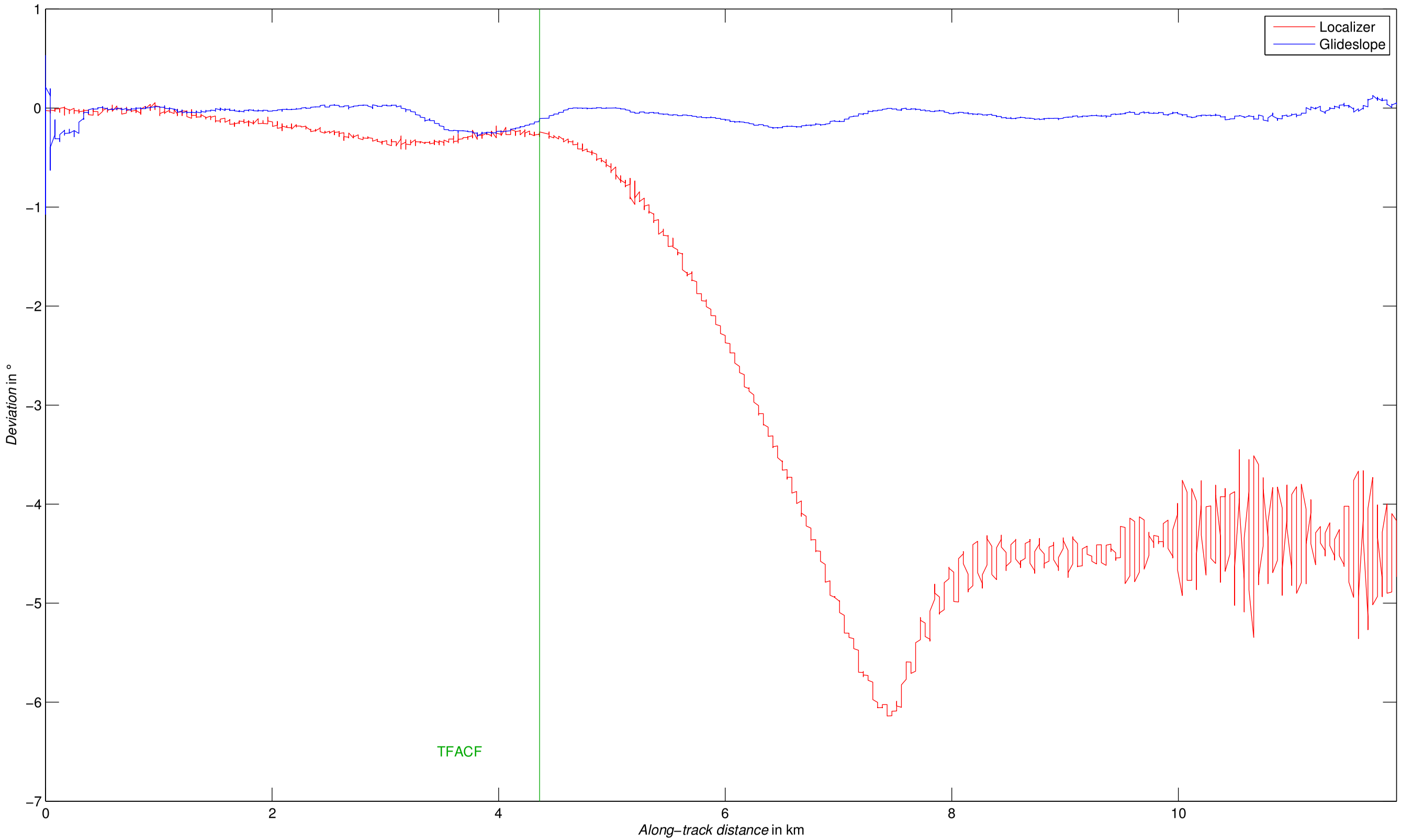

DLR Institut für Flugführung

#12 ILS S 90°

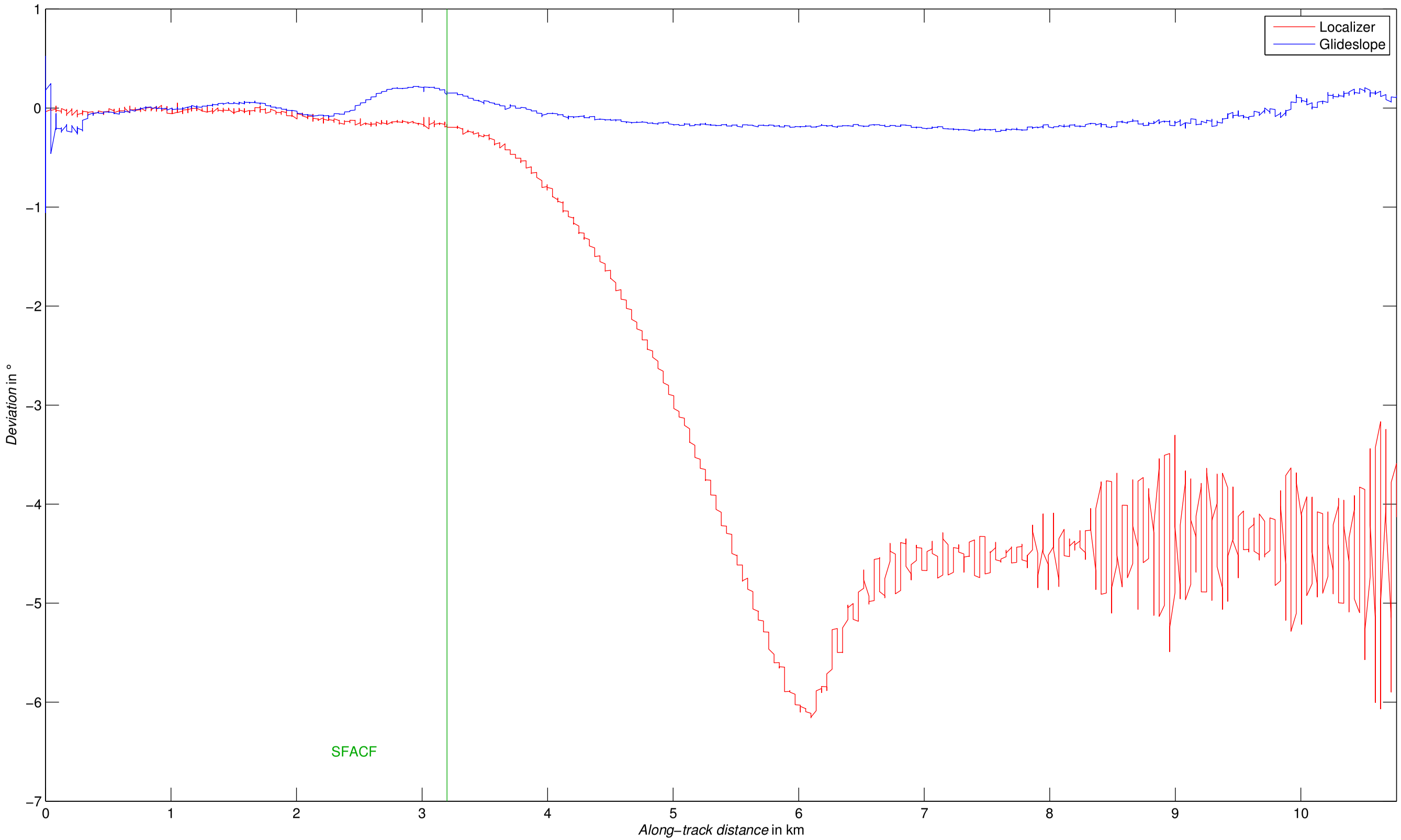

DLR Institut für Flugführung

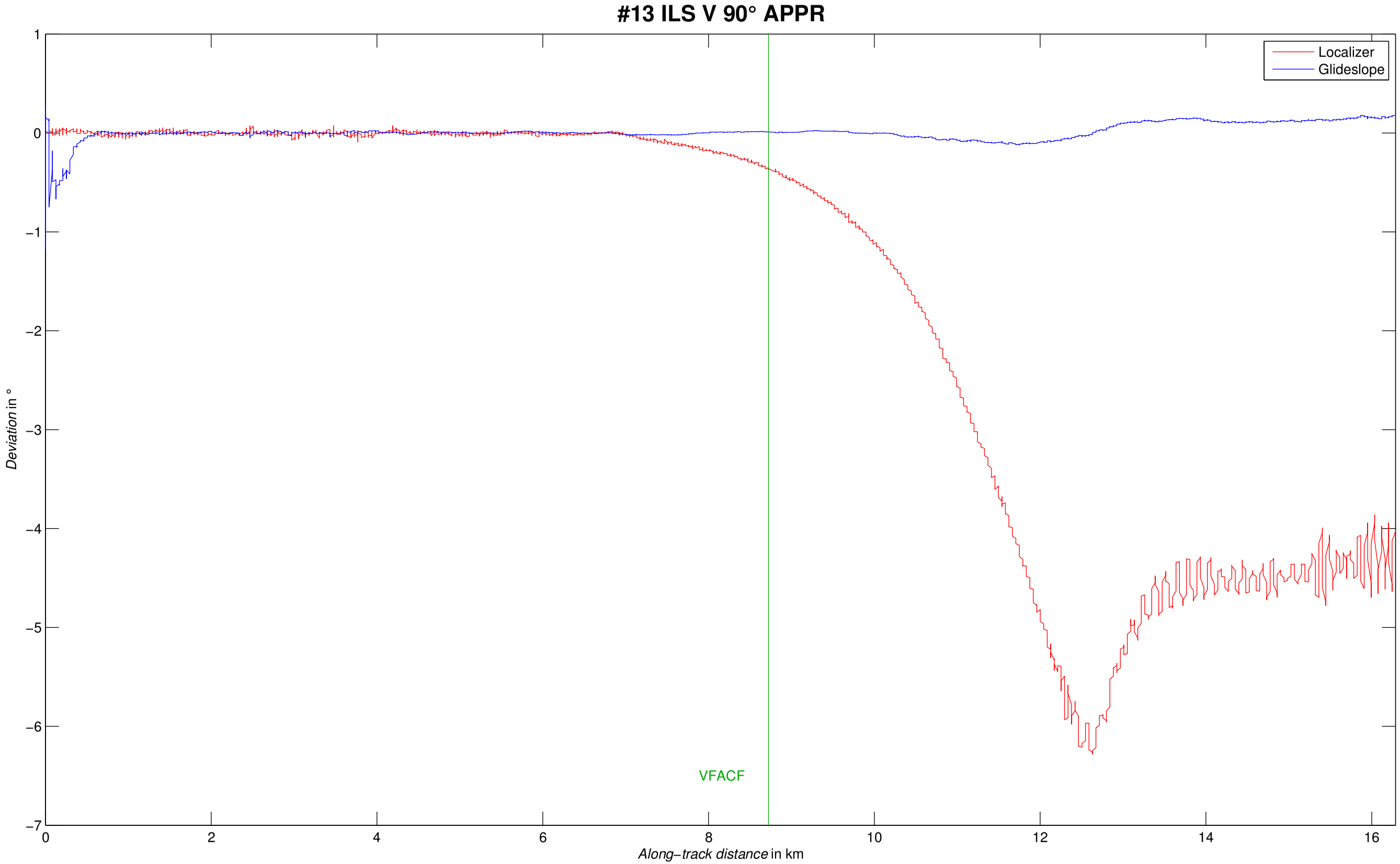

DLR Institut für Flugführung

#14 ILS U 90°

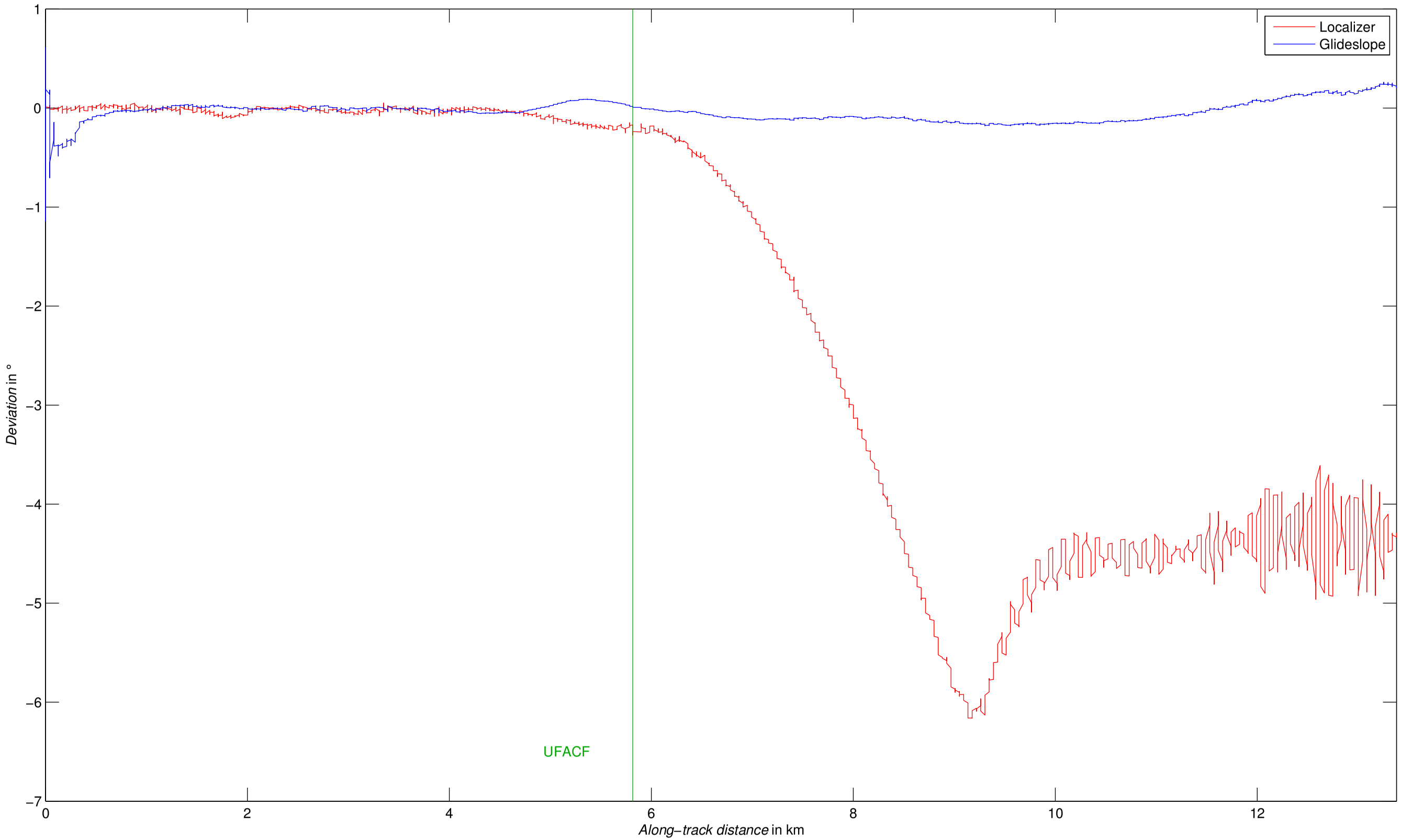

DLR Institut für Flugführung

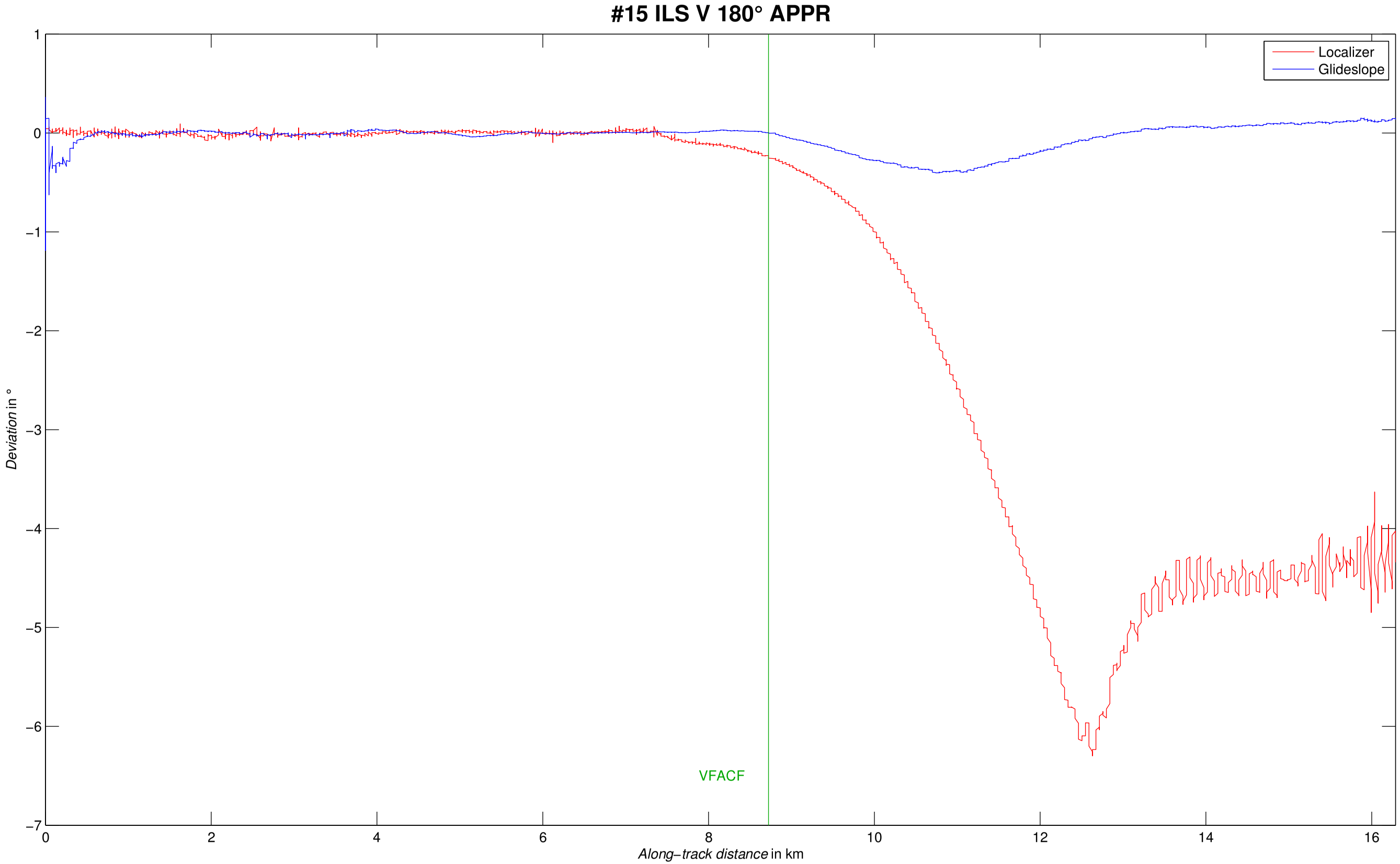

DLR Institut für Flugführung

#16 ILS S 90°

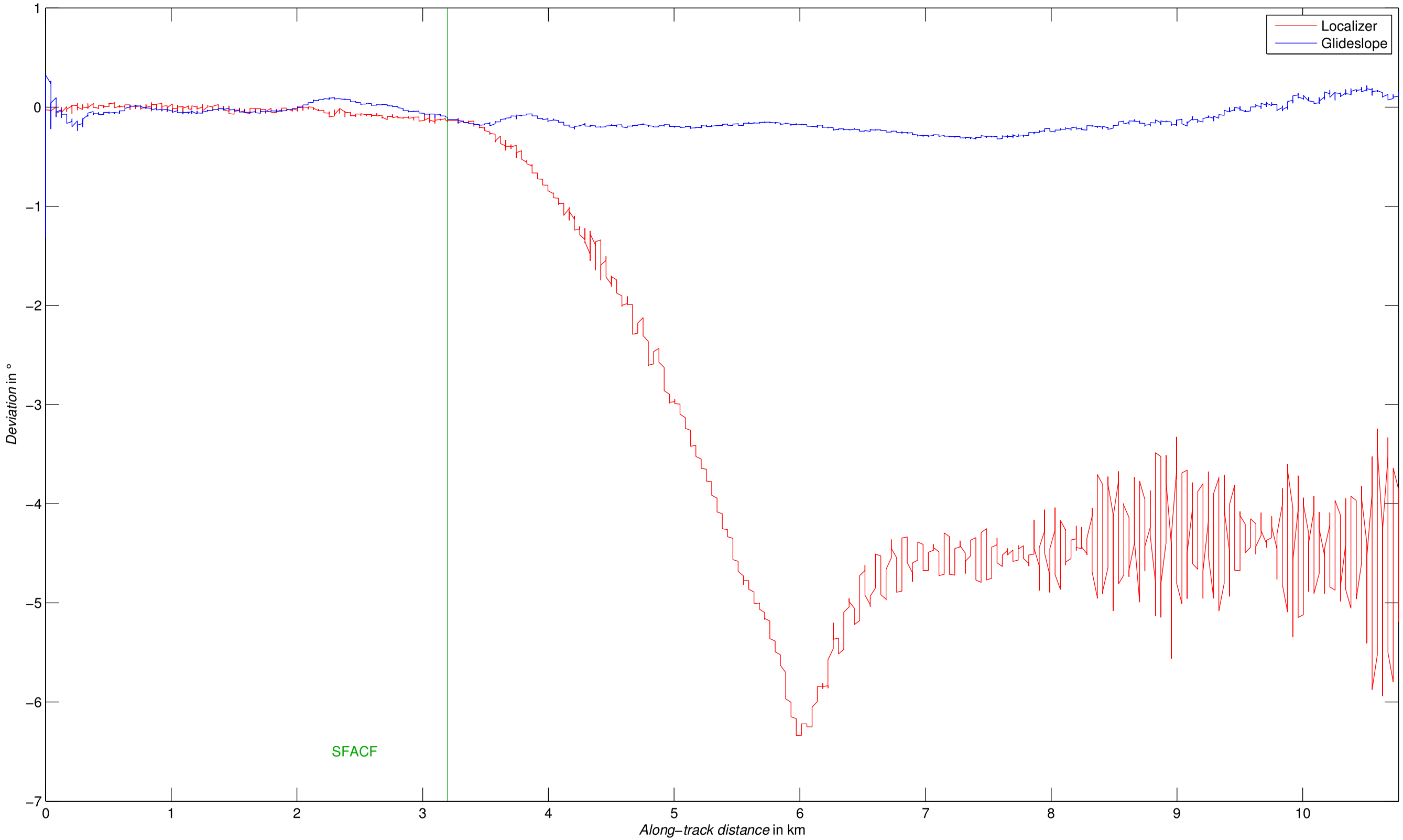

DLR Institut für Flugführung